THE RELATIONSHIP BETWEEN GEOLOGICAL STRUCTURES AND DOLERITE INTRUSIONS IN THE WITBANK HIGHVELD COALFIELD, SOUTH AFRICA

By

GIDEON PETRUS DU PLESSIS

Supervisor

DR. H.E. PRAEKELT

Submitted in fulfilment of the requirements for the degree of MAGISTER SCIENTIAE in the Faculty of Natural and Agricultural Sciences, UNIVERSITY OF THE FREE STATE, BLOEMFONTEIN.

MAY 2008

DECLARATION

"I declare that this dissertation is my own, unaided work. It is being submitted by me for the degree of Master of Science in the University of the Free State, Bloemfontein. It has not been submitted before for any degrees or examination in any other university or faculty, nor has it been prepared under the aegis or with assistance of any other body or organisation or person outside the University of the Free State. I further more cede copyright of the dissertation in favour of the University of the Free State."

……..
Gideon Petrus du Plessis

……...
Date

I dedicate this work to my wife, Lerika du Plessis, and son, Gian du Plessis.

ABSTRACT

The study forms part of the COALTECH 2020 research program, a collaborative study which aims to ensure the continued viability of the South African Coal Mining Industry well beyond the year 2020. It participates in the Geology and Geophysics Technology Area of the COALTECH 2020 Technology Wheel. The mission statement of this Working Group is to facilitate applied research to identify, quantify and qualify the remaining Coal Resources, starting with the Witbank-Highveld Coalfield, to enable informed decisions when defining and extracting Coal Reserves. The structural investigation of dolerites in the south-eastern part of the Witbank Coalfield contributes to Task 1.1.1; Sedimentological and Structural Model of the Witbank-Highveld Coalfield.

The Witbank Coalfield in the Mpumalanga Province of South Africa is situated on the northern sector of the main Karoo basin. The main Karoo basin is described as an asymmetric depository with a stable, passive cratonic platform (Kaapvaal Craton) in the northwest and a foredeep to the south with the Cape Fold Belt on its southern margin.

The study area is situated south of the prominent ± 15m thick Ogies Dyke, which strikes from Ogies in the west to Optimum Colliery in the east. The east-west trending pre-Karoo Smithfield Ridge, consisting of Rooiberg Felsites, bounds the study area to the south and also separates the Witbank Coalfield from the adjacent Highveld Coalfield to the south. The study was conducted on four collieries, namely Bank, Goedehoop, Koornfontein and Optimum Collieries in the south-eastern part of the Witbank Coalfield.

The objective of the study is to investigate the intrusion mechanism of the dolerites and the metamorphic effect the dolerite intrusions had on the coal in order to quantify the impact on mining and coal utilisation in the south-eastern part of the Witbank Coalfield.

The most important effects of dolerites on mining with a decreasing order of importance are:

1. Decrease in the safety conditions and an increase in the risk of roof failures, pillar and floor stability.
2. Increase in the overall production and mining costs with a decrease in the potential profit.
3. Decrease in saleable tonnages with a decrease in the profit margin.
4. Increase in waste product generation and an increase in the environmental risk.

From the objective two separate studies were identified: the first study (A) focuses on the relationship between geological structures and dolerite intrusions and the second study (B) determines the metamorphic effect the dolerite intrusions had on the coal. The structural investigation of the relationships between geological structures and the dolerites is contained in this document.

Regional scale information was acquired by using various remote-sensing techniques. The CSIR Miningtek through the COALTECH 2020 Research Program provided this state of the art information. In conclusion to the regional scale study probable relationships between certain Karoo-age dyke, sill and lineament trends that are associated with the northern main Karoo basin and surroundings could possibly provide insight into better understanding of the intrusion mechanism of dolerites in the south-eastern Witbank Coalfield. It is therefore probable that some of the Karoo-age intrusives in the south-eastern Witbank Coalfield followed older basement structures inherited by the Karoo strata and/or syn-tectonic structures related to Gondwana fragmentation which was synchronous with dolerite intrusion (Encarnación et al., 1996).

The EW striking Ogies Dyke, which is the main structure in the Witbank Coalfield, most probably pre-dates its associated smaller scale dykes and sills. Conclusions for this relative age difference are summarised as being the following:

- Its association with EW basement Pre-Karoo diabase, which probably acted as a plane of weakness and might have triggered its earlier intrusion.
- Difference in geochemical and mineralogical characteristics.
- Absence of sills immediately to its north.
- Should the NS striking dykes north and south of the Ogies Dyke be favoured by cooling joints which developed as a result of its earlier intrusion, the age difference is evident.

Comparing the physical appearance of the ± 20m sill (main sill) in the Witbank Coalfield with the B8 sill in the Secunda Coalfield, the two sills have a number of properties in common. However, these physical property comparisons are not precise and it is therefore suggested a detailed geochemical analysis be undertaken focussing on the mineralogy, major and trace elements.

The sedimentary sequence is reconstructed by removing the main sill from the stratigraphy. The reconstruction is aimed at determining if a spatial relationship exists between the coal seams, the intra-seam strata and the main sill prior to the intrusion event. Borehole information on the

elevation of the pre-Karoo basement is sparse as borehole penetration was terminated at the bottom of the coal seam of interest. The removal of the dolerite convincingly reveals the pre-Karoo basement topography, palaeo-floor and -roof morphology, as well as the width distribution of the sedimentary units.

The following reconstructed sedimentary units were examined individually:

- No. 2 Coal Seam;
- Facies between the No. 2 Coal Seam and No. 4L Coal Seam;
- No. 4L Coal Seam;
- Facies between No.4L and No. 5 Coal Seam;
- No. 5 Coal Seam.

The examination process of the data of each unit starts with the statistical analyses thereof which includes histogram and probability plots of the palaeo floor, width and palaeo roof.

The investigation resulted in nearly direct linear correlation curves which disclose the existing relationships between the palaeo floor elevations of the No.2, No.4L and No.5 Coal Seams. Considering the range of correlation coefficient values of 0.81 to 0.99 for the palaeo floor elevations it convincingly reveals the co-existing relationship in the geometry of elevations throughout the entire stratigraphy of the sedimentary sequences. Several sedimentological factors contributed to the present day geometries and widths of coal and associated clastical sedimentary rocks of sequence of succession. The evidence in the relationship of the geometries of the palaeo floor and roof elevations concludes that irrespective of variable intra-seam strata and coal seam widths the pre-Karoo topography is reflected throughout the entire stratrigraphic sequence.

Prior to sediment burial, plant growth took place most probably on similar structural relief of gentle attitudes. To conclude, a four-stage model is proposing how burial could have influenced widths and aerial distribution of peat and intra-seam clastic sedimentary rocks of sequence of succession. At the time of peat formation, the unconsolidated sediments had not yet undergone a great deal of lithification in that the floor structure of the peat might have been without undulations.

Therefore the present day coal and intra-seam strata are not displaying the syndepositional widths or aerial distribution, but rather reflect the result of subsidence which was probably contemporaneous with basin development. Hence the uneven, non-compactable pre-Karoo basement topography had major influence in the control of the present day geometry of the coal and intra-seam strata.

In conclusion, a reasonable inverse relationship between the net width of the stratigraphic sequence from the palaeo floor of the No. 2 Coal Seam to the palaeo roof of the No.5 Coal Seam and the floor elevation of the main sill exists. A Quantile-Quantile-plot and the regression slope analysis of the data sets convincingly conclude the inverse relationship that exists between the floor elevation of the main sill and the net width of the almost entire sediment sequence. In this context the reasonable negative correlation coefficient of -0.57 is good.

This negative correlation implies that where the main sill is present in the lower stratigraphic levels it underlies thicker sedimentary sequences and conversely where the sill had stepped up to higher stratigraphic levels it underlies the thinner sedimentary sequences. In conclusion the differential compaction of the sedimentary strata was in the main controlled by the the Pre-Karoo basement topography. This in turn resulted in the fracturing and jointing of the sedimentary rocks over the flanks of the pre-Karoo basement topography which to a large extent controlled the propagation path of the main sill.

Evidence established in this study suggests the effect of basin tectonics to be the overriding controlling factor of the stratigraphic position of the main sill in the Vryheid Formation sedimentary rocks of sequence of succession of the south-eastern Witbank Coalfield. Other factors i.e. the influence of the Ogies Dyke and syn-tectonic related regional scale structures seem to have had some control in the propagation paths of the associated offshoots of the main sill.

UITTREKSEL

Hierdie studie vorm deel van die Coaltech 2020 navorsingspogram wat `n samewerkende ondersoek is met die doelwit om die voortbestaan van die Suid-Afrikaanse steenkool mynbou-industrie na 2020 te verseker. Die studie vorm ook deel van die Geologiese en Geofisiese Tegnologiese gebied van die Coaltech 2020 Tegnologie-kring. Die missie van die Werkgroep is om toegepaste navorsing te fasiliteer vir die identifisering, kwantifisering en kwalifisering van die oorblywende steenkoolhulpbronne. Dit behels die ondersoek van die Witbank-Hoëveldsteenkoolveld, ten einde behulpsaam te wees met die definiëring en ekstraksie van steenkoolreserves om ingeligte besluite ten opsigte van bogenoemde te kan neem. Die struktuurondersoek van die doleriete in die suid-oostelike gedeelte van die Witbanksteenkoolveld maak `n bydrae tot Taak 1.1.1: Sedimentologiese en Strukturele model vir die Witbank-Hoëveldsteenkoolveld.

Die Witbanksteenkoolveld in die Mpumalangaprovinsie van Suid-Afrika is geleë op die noordelike gedeelte van die hoof Karookom. Die Karookom word beskryf as `n assismetriese afsetting met `n stabiele, passiewe kratoniese platvorm (die Kaapvaalkraton) in die noordweste en `n voorlandkom in die suide met die Kaapse plooigordel wat die suidelike grens vorm.

Die studiegebied is suid van die prominente ± 15m dik Ogiesgang geleë en strek van Ogies in die weste tot by Optimumsteenkoolmyn in die ooste. Die oos-wes neigende voor-Karoo Smithfieldrug wat hoofsaaklik uit Rooibergfelsiete bestaan, vorm die suidelike grens van die studiegebied, maar vorm ook die grens tussen die Witbanksteenkoolveld en die Hoëveldsteenkoolveld wat verder suid voorkom. Hierdie studie is op vier steenkoolmyne, naamlik Bank, Goedehoop, Koornfontein en Optimum gedoen wat in die suid-oostelike gedeelte van die Witbanksteenkoolveld geleë is.

Die oogmerk van die studie was om ondersoek in te stel wat betref die inplasingsmeganisme van die doleriete asook die metamorfe effek wat die dolerietintrusies op die steenkool gehad het om die impak op die mynbou en die benutting van die steenkool te kwantifiseer.

Die belangrikste effekte, in afnemende orde van belangrikheid, wat doleriete op steenkoolmynbou het, is as volg:

1. `n Afname in veiligheidsomstandighede en `n toename in die risiko van dakineenstortings asook pilaar- en vloerstabiliteit.

2. `n Toename in die produksie- en mynboukoste, en daarenteen `n afname in potensiële wins.
3. `n Afname in verkoopbare tonnemaat wat gepaard gaan met die afname in winsgrense.
4. `n Toename van afvalprodukte asook `n toename in die risiko op die omgewing.

Op grond van bogenoemde oogmerk het twee afsonderlike studies voortgespruit: die eerste studie (A) fokus op die verwantskap tussen die geologiese strukture en die dolerietintrusies en die tweede studie (B) bepaal die metamorfe-effek van die doleriete op die steenkool. Die strukturele ondersoek op die verwantskap tussen die geologiese strukture en die doleriete is in hierdie dokument saamgevat.

Inligting van regionale omvang is ingewin deur van verskillende afstandwaarnemingstegnieke gebruik te maak. Hierdie nuwe inligting is beskikbaar gemaak deur die WNNR Miningtek met behulp van die Coaltech 2020 Navorsingsprogram. Die gevolgtrekking tot die regionale studie van moontlike verwantskappe tussen sekere Karoo-ouderdom gange, plate en lineamentneigings wat verband hou met die noordelike hoof Karoo-kom en omgewing, het aanleiding gegee tot die beter begrip van die implasingsmeganisme van die doleriete in die suid-oostelike Witbanksteenkoolveld. As gevolg hiervan bestaan die moontlikheid dat sekere Karoo-ouderdom gange in die suid-oostelike Witbanksteenkoolveld ouer geërfde vloerstrukture in die Karoostrata en/of sin-tektoniese strukture is. Dit hou verband met die opbreek van Gondwana, wat gepaardgaande dolerietintrusies (Encarnación et al., 1996).

Die oos-wesstrekkende Ogiesgang, wat die hoofstruktuur in die Witbanksteenkoolveld is, is heel waarskynlik ouer as die verwante ondergeskikte gange en plate. Gevolgtrekkings vir hierdie relatiewe ouderdomsverskil word as volg opgesom:

- Die verwantskap met die oos-wes strekkende voor-Karoovloer diabaas, wat moontlik `n swak sone gevorm het waarlangs die inplasing van die vroeëre intrusies kon plaasvind.
- `n Verskil in die geochemiese en mineralogiese eienskappe van die intrusies.
- Die afwesigheid van plate direk noord van die Ogiesgang.
- Sou die noord-suidstrekkende gange wat noord en suid van die Ogiesgang voorkom, `n voorkeur vir die afkoelingsnate gehad het, is `n ouderdomsverskil onafwendbaar.

`n Vergelyking van die fisiese voorkoms van die ± 20m dik plaat (hoofplaat) in die Witbanksteenkoolveld met die B8 plaat in die Sekundasteenkoolveld, bewys dat die twee plate sekere eienskappe in gemeen het. Die vergelyking in hierdie fisiese eienskappe is nie presies nie

en daarom word voorgestel dat gedetailleerde geochemiese analises op die mineralogie asook hoof- en spoorelemente gedoen moet word.

Die sedimentêre gesteentes is geherkonstrueer deur die verwydering van die hoofplaat uit die stratigrafie. Die herkonstruksie se hoofdoel was om te bepaal of `n ruimtelike verwantskap tussen die steenkoollae, die intra-steenkoollaagstrata en die hoofplaat bestaan. Boorgatinligting van die elevasie van die voor-Karoovloer is skaars as gevolg van `n gebrek aan data wat toegeskryf kan word aan die feit dat boorgate aan die onderkant van die steenkoollaag gestop is. Deur die dolerietplaat te verwyder, is voor-Karoovloertopografie ooglopend sigbaar in die paleo-vloer- en -dakmorfologie, sowel as die dikte-verspreiding van die sedimentêre eenhede.

Die volgende geherkonstueerde sedimentêre eenhede is afsonderlik ondersoek:

- No. 2 steenkoollaag;
- Strata tussen die No. 2 steenkoollaag en die No. 4L steenkoollaag;
- No. 4L steenkoollaag;
- Strata tussen die No. 4L steenkoollaag en die No. 5 steenkoollaag;
- No. 5 steenkoollaag.

Die ondersoekproses van elke eenheid begin met `n statistiese analise van die data wat histogramme, waarskynlikheidskurwes van die paleo-vloer en paleo-dak en dikte insluit.

Die resultate van hierdie ondersoek dui op bykans direkte lineêre korrellasie kurwes wat die bestaande verwantskappe tussen die paleo-vloerelevasies van die No. 2, No. 4L en No. 5 steenkoollae aandui. Inaggenome die korrelasiekoeffisiënt-waardes, wat wissel tussen 0.81 tot 0.99 vir die paleo-vloerelevasies, word die onderlinge verwantskap in die geometrie van die elevasies deur die totale sedimentêre opeenvolging ontbloot. Heelwat sedimentologiese faktore dra tot die hedendaagse geometrie en diktes van die steenkool asook die verwante klastiese sedimentêre gesteentes by. Bewyse van die verwantskap tussen die geometrie van die paleo-vloer- en –dakelevasies, bevestig dat selfs met variërende intra-steenkoollaagstrata en steenkoollaagdiktes, die voor-Karoo topografie steeds deur die totale stratigrafiese opeenvolging gereflekteer word.

Voordat sedimentbegrawing plaasgevind het, het plantegroei waarskynlik op soortgelyke, gematigde topografie plaasgevind. `n Vier-stadium-model stel voor hoe begrawing die dikteverspreiding van die veen en intra-steenkoollaag klastiese sedimente beïnvloed het. Tydens

veenvorming, het die sedimente minimale litifikasie ondergaan, sodat die vloerstruktuur waarop die veen ontstaan het, waarskynlik reëlmatig was.

Hedendaagse steenkool- en intra-steenkoolstrata stel nie die sin-afsettingsdikte en ruimtelike verspreiding tentoon nie, maar eerder die resultaat van versakking is wat moontlik met die hoofkom se ontwikkeling gepaardgegaan het. Dus het die onewe, nie-kompakteerbare voor-Karoovloer-topografie die oorhoofse invloed in die beheer van die hedendaagse geometrie van die steenkoollae en die intra-steenkoolaagstrata gehad.

`n Omgekeerde verwantskap bestaan tussen die netto dikte van die stratigrafiese opeenvolging van die paleo-vloer van die No. 2 steenkoollaag met die paleo-dak van die No. 5 steenkoollaag en die vloerelevasie van die hoofplaat. `n Kwantiel-kwantiel stip asook die regressiegradiënt-analise van die datastelle bewys hierdie sogenaamde omgekeerde verwantskap tussen die vloer van die hoofplaat en die netto dikte van die totale sedimentêre opeenvolging. In hierdie konteks gesien, is die korrellasiekoeffisiënt van -0.57 baie goed.

Hierdie negatiewe korrellasie impliseer dat waar die hoofplaat in die laer stratigrafiese eenhede voorkom, die plaat oorlê word deur dikker sedimentêre opeenvolgings terwyl omgekeerd, waar die plaat in die hoër stratigrafiese eenhede voorkom, onderlê die plaat dunner sedimentêre opeenvolgings. Gevolglik is die differensiële kompaksie van die sedimentêre strata hoofsaaklik deur die voor-Karoovloer topografie beheer. Daarvolgens het die nate en krake van die sedimentêre gesteentes wat op die flanke van die voor-Karoovloer topografie voorkom, tot `n groot mate die beherende rol in the meganisme, wat die indringingsvlak van die hoofplaat bepaal het, gespeel.

Hierdie studie het bewys dat die effek van komtektoniek die beherende faktor in die stratigrafiese posisionering van die hoofplaat, in die sedimentêre gesteentes van die Vryheidformasie van die suid-oostelike Witbanksteenkoolveld, is. Ander faktore, insluitende die invloed van die Ogiesgang en die sin-tektoniese verwante regionale strukture, kon moontlik beheer uitgeoefen het op die ontwikkeling van die indringingsvlak van die verwante vertakkings van die hoofplaat.

TABLE OF CONTENTS

LIST OF FIGURES

LIST OF TABLES

CHAPTER 1

1. INTRODUCTION

1.1 DEFINITION AND OBJECTIVES

The flow diagram in Figure 1.1 shows from where this study has emerged and how it was defined and its objectives identified. It forms part of COALTECH 2020, a collaborative research program, which aims to ensure the continued viability of the South African Coal Mining Industry well beyond the year 2020. This study participates in the Geology and Geophysics Technology Area of the COALTECH 2020 Technology Wheel. The mission statement of this Working Group is to facilitate applied research to identify, quantify and qualify the remaining Resources, starting with the Witbank-Highveld Coalfield, to enable informed decisions when defining and extracting Reserves. Structural investigation of dolerites in the south-eastern part of the Witbank Coalfield contributes to Task 1.1.1; Sedimentological and Structural Model of the Witbank-Highveld Coalfield.

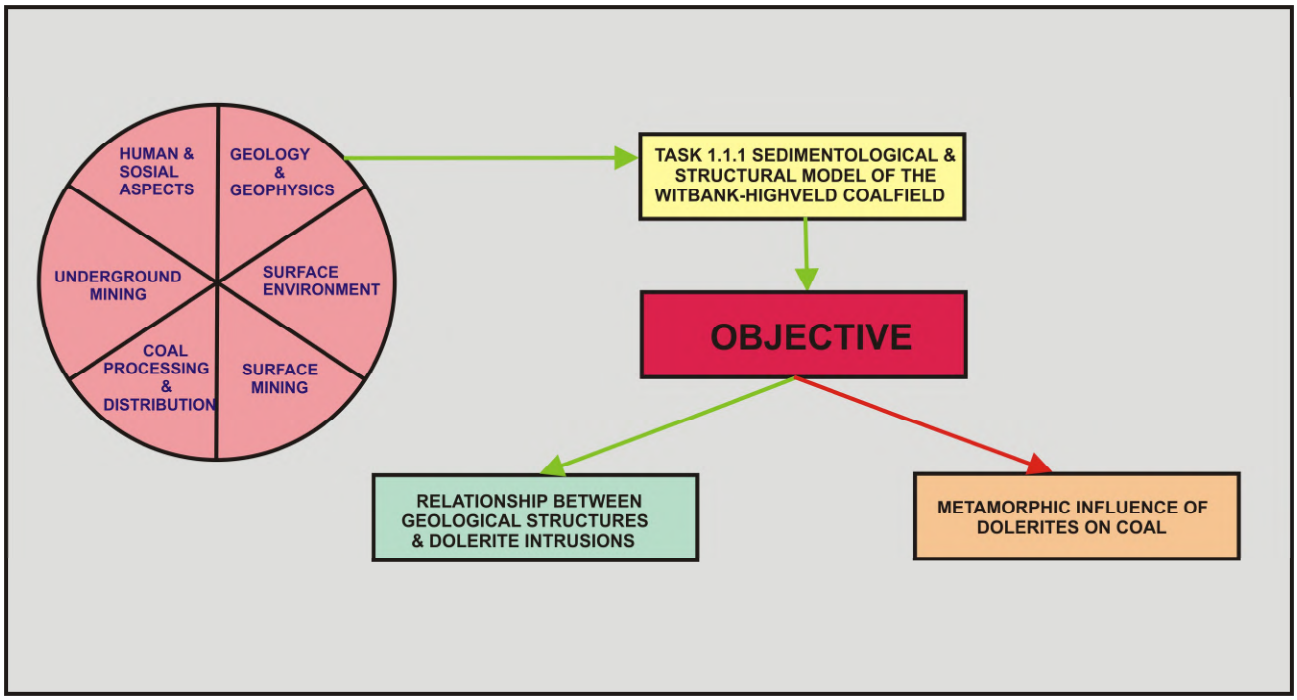

Figure 1.1: ***Flow diagram explaining how this study emerged, how it was defined and identifying its objectives.***

The objective, as defined by the industry and COALTECH 2020 is to investigate the dolerite structure, its intrusion mechanism and the metamorphic effect the dolerite intrusions had on the coal in order to quantify the impact on mining and coal utilisation in the south-eastern part of the Witbank Coalfield. From the objective two separate studies were identified: study A focuses on the relationship between geological structures and dolerite intrusions and study B determines the metamorphic effect the dolerite intrusions had on the coal. The structural investigation of the relationships between geological structures and the dolerites is contained in this thesis.

1.2 GENERAL GEOLOGY AND STUDY AREA

The Witbank Coalfield in the Mpumalanga Province of South Africa is situated on the northern sector of the main Karoo basin (Figure 1.2A and 1.2B). The main Karoo basin is described as an asymmetric depository with a stable, passive cratonic platform (Kaapvaal Craton) in the northwest and a foredeep to the south with the Cape Fold Belt on its southern margin (Cadle et al., 1990). A simplified stratigraphic column of the Karoo Supergroup in Table 1.1 introduces the general geology of the basin.

Table 1.1: Simplified stratigraphic column of the Karoo Supergroup in the northern portion of the Karoo basin (after SACS, 1980).

PERIOD (AGE)	GROUP	FORMATION	ROCK TYPES
Jurassic (150 my)		Drakensberg	Basaltic lava
Triassic (195 my)		Clarens	Fine-grained sandstone
		Elliot	Red sandstone, mudstone
		Molteno	Sandstone, sub-ordinate coal
Permian (225 my)	Beaufort	Tarkastad	Sandstone, shale
		Estcourt	Sandstone, shale, sub-ordinate coal
	Ecca	Volksrust	Shale, sandstone, sub-ordinate coal
		Vryheid	Sandstone, shale, coal
		Pietermaritzburg	Shale
Upper Carboniferous (285 my)		Dwyka	Tillite, varved shale

Pre-Karoo basement topography reveals predominantly north-south trending valleys sculptured by the Permo-Carboniferous Dwyka glaciers and continental ice sheets. After the northward retreat of the ice sheets these valleys were filled with glaciogene strata of the Dwyka Formation, consisting of a variety of glacial to periglacial sedimens which today occupy the base of the Karoo Supergroup (Snyman, 1998). An intracratonic basinal and marine phase (Ecca Group) and eventually a period of terrestrial sedimentation with increasing aridity (Beaufort Group, Molteno, Elliot and Clarens Formations) followed (Snyman and Barclay, 1989 and Falcon 1989). Karoo basin development was terminated during the outpouring of Drakensberg basaltic lava fed by abundant post-Karoo (183 ± 1 Ma after, Duncan et al., 1997) dolerite dykes and sills prior to the Mesozoic break-up of the Gondwana supercontinent (Uken and Watkeys, 1997). The Drakensberg Basalt Formation forms the top of the Karoo succession.

The stable Kaapvaal Craton in the northern sector of the basin is reflected by the sedimentary depositional style of the Ecca Group of rocks (Cadle et al., 1990) and the Permian peat (coal) accumulated exclusively on parts of this stable shelf area (Holland et al., 1989). These sedimentary rocks have never been subjected to deep burial, intense tectonic stresses or high geothermal gradients (Cadle et al., 1990 and Van Niekerk, 1995). Stratigraphically the Ecca Group consists of the basal Pietermaritzburg Formation conformably overlying the Vryheid and Volksrust Formations. The proximal coarse fluvio-deltaic sandstones of the Vryheid Formation, mainly derived from a northern source, thin towards and wedge southwards into the siltstones and mudstones of the Pietermaritzburg and Volksrust Formations, deposited in the intracratonic Ecca Sea (Cadle et al., 1990). Coal seams developed in the Witbank Coalfield are contained within the Vryheid Formation, which ranges in thickness between 80m and 200m (Cairncross and Cadle, 1988). Five mineable bituminous coal seams are present from No.1 at the base to No.5 at the top.

Dolerite dykes and sills outcrop over two thirds of South Africa (Chevallier and Woodford, 1999). The structural complexity of these intrusives is phenomenal and has not received much attention in the past published literature. These intrusives form a complex network within the coal bearing Vryheid Formation of the Ecca Group, leaving these sedimentary rocks of sequences of succession structurally and metamorphically disturbed. The structural disruptions of the coal seams in the Witbank Coalfield are mainly due to the intrusion of dolerite dykes and sills. However, small-scale graben type faulting and fracturing within the coal seams also occur.

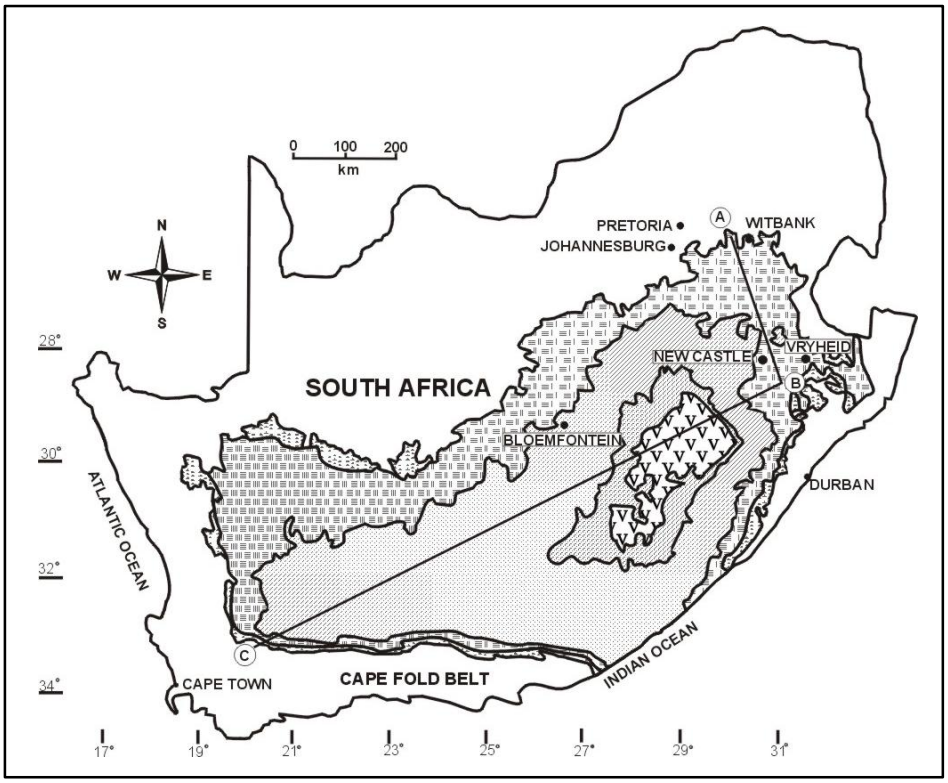

Figure 1.2: ***A) Plan view of the Karoo basin showing the stratigraphy of the Karoo Supergroup (after Cadle et al., 1990).***

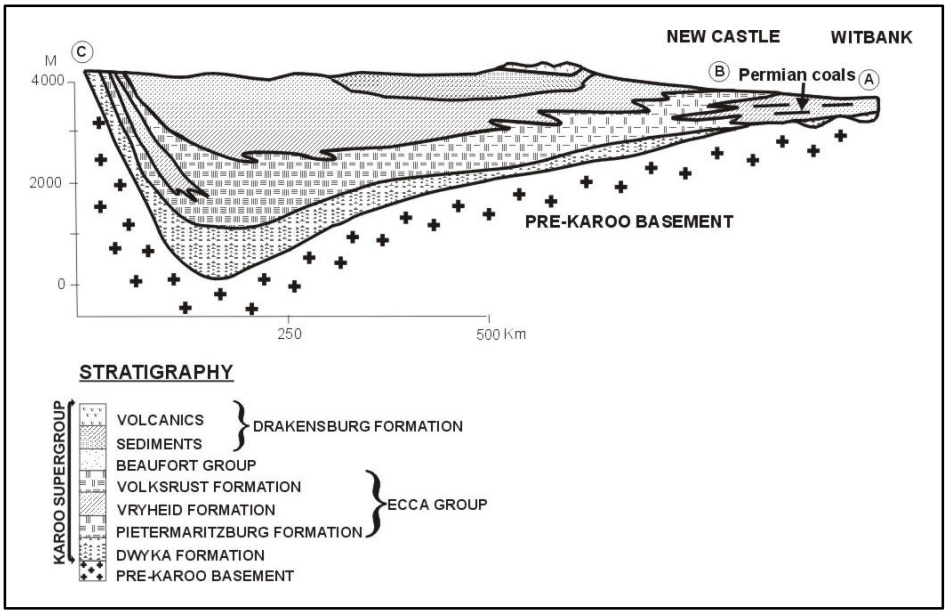

Figure 1.2: ***B) Cross-section through the Karoo basin illustrating the tectonic and stratigraphic position of the coal bearing Vryheid Formation (after Cadle et al., 1990).***

The study area (Figure 1.3) is situated south of the prominent ± 15m thick Ogies Dyke, which strikes from Ogies in the west to Optimum Colliery in the east. The east-west trending pre-Karoo Smithfield Ridge, consisting of Rooiberg Felsites, bounds the study area to the south and also separates the Witbank Coalfield from the adjacent Highveld Coalfield to the south. The study was conducted on four collieries, namely Bank, Goedehoop, Koornfontein and Optimum Collieries in the south-eastern part of the Witbank Coalfield. The former three collieries have underground as well as opencast operations while the latter mainly exploits the coal seams using opencast methods.

The area is characterised by extensive overburden with an average width of ± 10m and consequently surface outcrop of the rocks is sparse. The majority of geological information available for research is in the form of vertical, sub-surface lithological borehole logs. Exposure of the dolerites is limited to where it intersects the coal seams in underground and opencast mines. Information on the pre-Karoo rocks in this area is also sparse, as it is not the intention of exploration and mining companies to penetrate the pre-Karoo basement during drilling of boreholes, but rather to terminate penetration beneath the coal seam of interest. In the underground mines the coal pillars are generally stone dusted or covered with gunnite, obscuring the strata. Thus, in the main, this investigation relies on diamond drilled core that has been logged over the lifetime period of the mines by several different geologists.

1.3 THE EFFECT OF DOLERITES ON COAL MINING

Dolerite intrusions can have a number of deleterious effects on coal and coal mining (pers. comm. Veldsman and Esterhuisen, 2000). The points below detail some of the effects.

a. Different sills have different thermal effects on the coal. A thin younger sill can have a more severe metamorphic effect than a thicker older sill with the same interburden thickness between the sill and the coal seam.

b. In general, the thermal effect of intersecting dolerite sills is more severe than that of dolerite dykes.

c. Devolatilised coal has the tendency to degrade rapidly during and after mining resulting in an excess of fine coal associated with the following:

- Transportation and screening problems (wet and dry screens, but more severe when wet screens are used).
- Effects on the relative density in a beneficiation plant, positive or negative, depending on the type of plant.
- Increases in coal waste generation and environmental problems (i.e. pollution).
- Excess coal dust in underground mines necessitating an increase in ventilation requirements resulting in air pollution.
- Decrease in “usable” coal tonnages and an increase in Rand per tonnage production costs.
- Decrease in plant yield resulting in a decrease in saleable tonnages and an increase in beneficiation costs.
- Decrease in coal quality, mainly the volatile matter content; the coal product may not be acceptable to the client due to utilisation constraints.

d. The higher frequency of joints and faults where a dolerite sill intersects the coal seam result in unfavorable mining conditions and an increase in roof support requirements and costs. The working environment may be unsafe and unhealthy.

e. Higher methane concentrations may occur, which increases the risks of methane and coal dust explosions.

f. The floor structure of the sills, sill thickness and interburden coal seams thickness affects mine design and layout and is critically important in high extraction areas.

g. Floor stability tends to decrease in the areas due to the thermal effect of dolerites, mainly in the areas where the floor material contains mica on the bedding planes.

h. Induced stresses occur at the face of longwall panels if the sill does not collapse/break over the goaf area. The face can collapse, causing severe problems with a high financial implication.

i. Groundwater flow is compartmentalised in the areas where sills are frequently transgressive. Dykes can have a similar effect.

j. The different sills collapse in unlike manners over high extraction mining areas due to dissimilar joint patterns.

k. The potential reserves in the coal bearing area are compartmentalised, which affects the following:

- Optimal coal exploitation.
- Mine design and layout, mining methods and possibly additional shaft construction.
- The higher costs of mining dolerite in a development section to access adjacent coal reserves and an increase in waste material that must be transported and stored, resulting in a loss in effective production rate.
- "Reserves" are lost in the areas where the tonnages contained in specific resource blocks do not justify the costs to access the coal.

l. The thickness and physical blasting or cutting characteristics can have a severe implication on shaft construction costs.

m. Swell clays are the degradation products of dolerite sills that occur near the surface, which will effect the construction and costs of the surface infrastructure.

n. The top portion of a coal seam, approximately 0.50m, can be highly fractured where dolerite sills occur above the coal seams, with an increase in roof support cost and a higher safety risk.

o. Dolerite dykes and intersecting sills can have a severe effect on the planned mine layout in an opencast mine and will contaminate the coal product if the material is not separated from the product.

p. Sills overlying coal in an opencast mine results in an increase in the drilling and blasting cost and can damage truck tyres. In the case of excessive thick overlying sills, the underlying coal might only be accessible with underground methods, which increase mining costs and a potential loss of coal Reserves.

q. Where dolerite material is present a special pad as a platform is often required for the dragline.

r. Secondary blasting or breaking is often required to reduce the size of large dolerite fragments in opencast mines, which results in costs increases.

1.4 THE MOST IMPORTANT EFFECTS OF DOLERITES ON MINING WITH A DECREASING ORDER OF IMPORTANCE

1. Decrease in the safety conditions and an increase in the risk of roof failures, pillar and floor stability.

2. Decrease in saleable tonnages with a decrease in the profit margin.

3. Increase in waste product generation and an increase in the environmental risk.

4. Increase in the overall production and mining costs with a decrease in the potential profit.

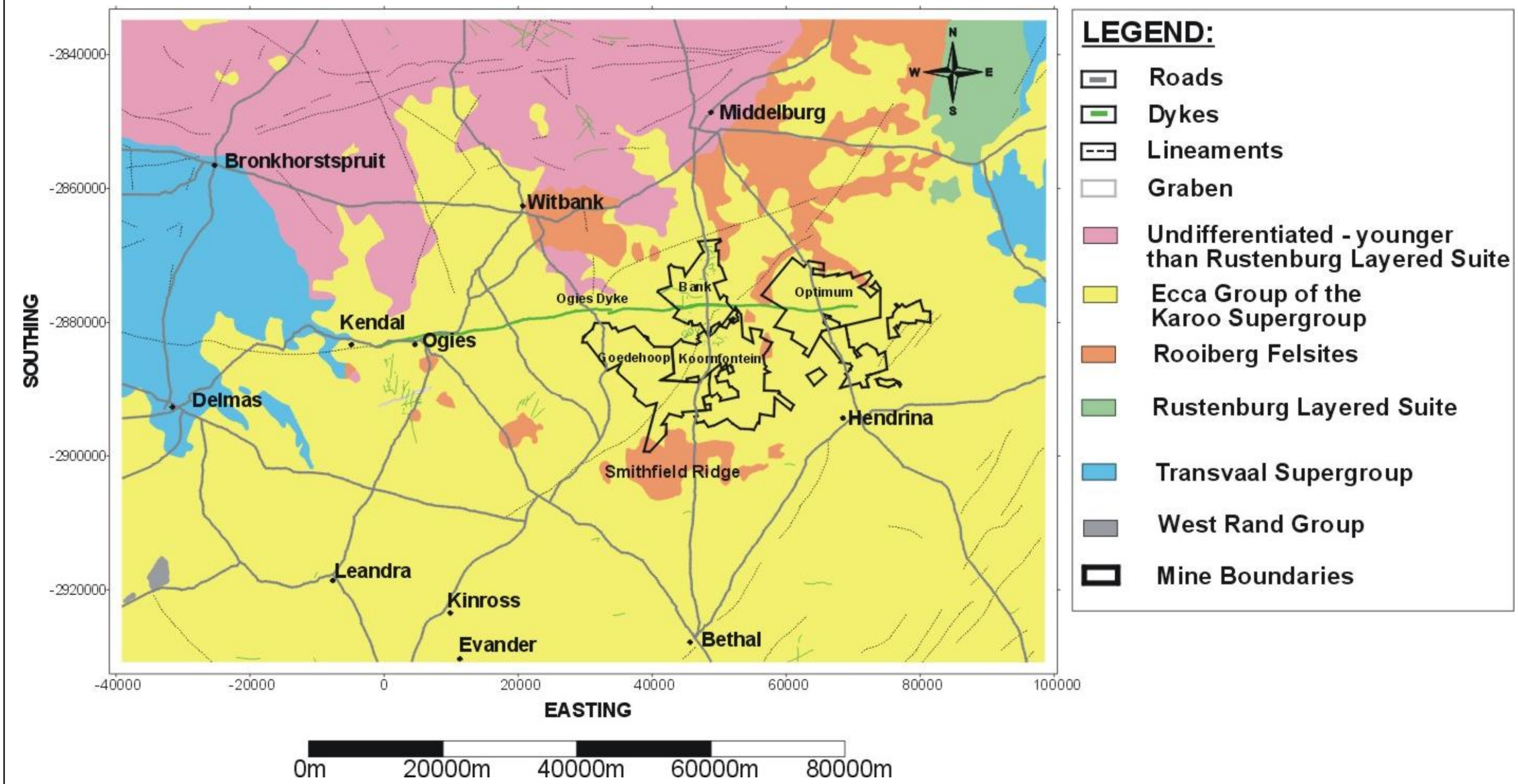

Figure 1.3: ***Map showing the locality and general geology of the study area (modified after pers. comm. Henckel, 2001).***

1.5 SEDIMENTOLOGICAL BACKGROUND ON THE COAL BEARING VRYHEID FORMATION

The coal bearing Vryheid Formation of the Ecca Group has been extensively investigated in the twentieth century by various authors of which some are Le Blanc Smith (1980), Falcon (1981, 1988), Winter (1985), Cadle (1986) and Cairncross (1986). The Pietermaritzburg Formation shales, the basal part of the Ecca Group, are absent in the Witbank Coalfield thus the Vryheid Formation either conformably overlies the glaciogenic Dwyka Formation or unconformably overlies the pre-Karoo basement (Cairncross, 1987). This background discussion focuses primarily on the palaeo depositional environments and stratigraphy of the Vryheid Formation in the Witbank Coalfield. However, broad similarities and contrasts between the latter and the adjacent Highveld Coalfield have been found and comparatively compiled by Jeffrey (2001). A generalised stratigraphic column of the Vryheid Formation in the Witbank Coalfield is shown in Figure 1.4 with lithologies, coal seams and interpreted depositional environments.

In the Witbank Coalfield the pre-Karoo rocks pre-dominantly consist of Rooiberg felsites of the Proterozoic Bushveld Complex forming palaeo topographic ridges and valleys. The pre-Karoo basement owes its rugged topographical character to the scouring effect of the Permo-Carboniferous Dwyka glaciers and continental ice sheets prior to the deposition of the coal bearing Vryheid Formation sediments (Snyman, 1998). According to the work of Cairncross (1989), the sediment dispersal and distribution of the coal seams was largely controlled by the undulating pre-Karoo topography.

Extensive deposits of glacial moraines and glaciolucastrine varved sediments are evidence of glaciation dominated sedimentary processes. Subsequently to those a reworked glaciofluvial outwash plain emanated from the northward retreating ice sheets as a consequence of climatic amelioration. Immediately after this active sedimentation took place, peat accumulated on the glaciofluvial sedimentary platform (Cadle et al., 1990). Deposition of the lower most coal seams (No's 1 and 2 Coal Seams) and associated sediments was contemporaneous with the northward retreat of the glaciers and ice sheets (Holland et al., 1989) and is confined mainly to the reworked glaciofluvial outwash plain (Cadle et al., 1990). Large-scale climatic changes from cold to cool to ultimately warm (late Permian) and finally hot, dry arid conditions (late Triassic) are characterised by macrofloral and microfloral evidence (Falcon, 1989). Vegetation of the Ecca coal swamps during early Permian stages constituted diversified *Glossopteris-Gangamopteris* flora suggesting post-glacial and cool temperate climatic conditions (Falcon, 1986). Various peat (coal)

accumulating stages occurred over a long period of climatic and vegetational change such as temperature, moisture and parent vegetation (Falcon, 1989).

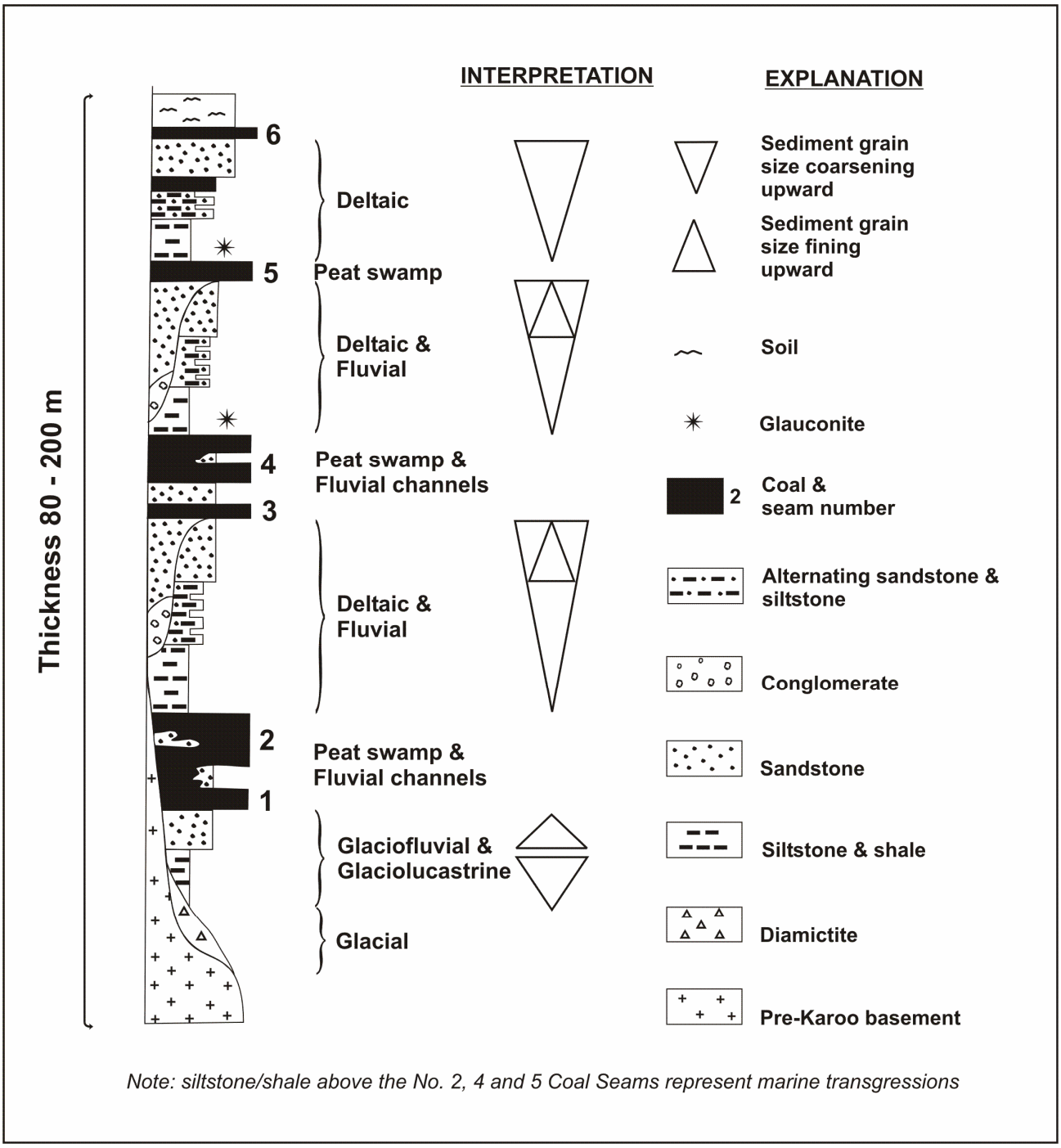

Figure 1.4: ***Generalised stratigraphic column for the Vryheid Formation in the Witbank Coalfield showing lithologies, coal seams and interpreted depositional environments (after Cairncross et al., 1990).***

The Vryheid Formation in the Witbank Coalfield contains five mineable coal seams (rarely the sixth seam is present) interbedded with an 80-200m thick coarse fluvio-deltaic sequence of sandstone, conglomerate and minor shale and siltstone (Cairncross, 1989). Depositional increments of strata (Le Blanc Smith, 1980) or depositional sequences (Cairncross, 1986) have been recognised, allowing for description and interpretation of widespread genetically related sedimentary units in the Vryheid Formation. These are briefly described as progradational sequences (progradation to abandonment to quiescence and peat accumulation and eventually marine transgression), each ending with the formation of a coal seam (Cairncross and Cadle, 1988). Basin evolution can be understood in terms of these sedimentological units that are based on their facies characteristics. A regional 3D geological model of the Witbank Coalfield (Grodner, 2002) has been constructed according to the equivalent facies associations of Le Blanc Smith (1980) and Cairncross (1986).

In his 3D model Grodner (2002) divides the pre-Karoo basement to the No. 2 Coal Seam succession into two sequences termed the Basement to Dwyka Sequence and the Top of Dwyka to Floor of No. 2 Seam Sequence. The rocks in the Basement to Dwyka Sequence are characteristically siltstones and diamictites. Between the Dwyka Formation diamictites and the No. 2 Coal Seam in the central and southern Witbank Coalfield a coarsening-upwards succession is present, resulting from initially glaciolucastrine processes (varved rhythmites) followed by glaciodeltaic and finally glaciofluvial/braided river deposits described as multiple upward fining units of mainly sandstone and conglomerate (Le Blank Smith, 1980). These include upward fining syn-depositional bedload channel deposits (Cairncross, 1980) of coarse-grained sandstone and granulestone that occur below and within the No. 2 Coal Seam and are responsible for seam splitting (Cadle et al., 1990). These occurred within the peat swamps during accumulation of the lower most coal seams (No. 1 and 2 Coal Seams) described as anastomosing river deposits (Cairncross, 1980) that transported sediment from a northern, predominantly granitic source (Cairncross et al., 1990).

A basin wide transgression terminated the No. 2 Coal Seam development followed by shallow water deltas that prograded into the basin providing a stable platform upon which the No. 4 Coal Seam peats could establish (Holland et al., 1989 and Cadle et al., 1990). This facies, refer to as Roof of No. 2 Coal Seam to Floor of No. 4 Coal Seam Sequence (Grodner, 2002), contains clastic material of carbonaceous siltstone, bioturbated siltstone/sandstone, interlaminated siltstone as well as sandstone and coal (intermittently No. 3 Coal Seam). Cadle et al. (1992) interpreted a braided/bed-load channel system deposited between the No. 3 and 4 Coal Seams in the Witbank Coalfield. At certain localities sandbodies incise through the underlying No. 3 Coal Seam and appear to rest either close to or directly on the roof of No. 2 Coal Seam. Texturally these

sandbodies comprise of coarse to very coarse-grained sandstone and granule-grade conglomerate and range in width between 1km to 12km and have a thickness variation of 12m to 22m. Embayment formation and minor braided channels were active in the peat swamp during No. 4 Coal Seam formation that explains the splitting of the No. 4 Coal Seam into No. 4 Lower, Upper and Upper A Seams (Holland et al., 1989).

The formation of the No. 4 Coal Seam was interrupted by a transgression event of laterally extensive glauconitic sandstones (Cadle, 1982) suggesting brackish water conditions (Selley, 1976). This sequence is termed the Roof of No. 4 Seam to the Floor of No. 5 Seam Sequence after Grodner (2002), which ranges in thickness between 25 – 30m over much of the Witbank Coalfield (Le Blanc Smith, 1980). Lobate, high-constructive shallow water deltas (Cairncross et al., 1984) prograded into the Ecca sea to form a stable platform onto which the No. 5 Coal Seam peats grew. Torbanite deposits within the No. 5 Coal Seam are explained by Cadle et al. (1990) as low-lying embayments where a proliferation of algae occured.

The relatively thin No. 5 Coal Seam reveals a short period of peat accumulation in a relatively unstable basin that consequently was flooded by another transgressive event which, as previously, halted peat accumulation (Cadle et al., 1990). The present-day erosion surface of the Witbank Coalfield is slightly undulating leaving patchy remains of these sedimentary rocks. Grodner's (2002) model terms these siltstone and sandstone facies as Above Roof of No. 5 Coal Seam Sequence that sporadically contains the No. 6 Coal Seam as well.

1.6 PREVIOUS WORK ON STRUCTURAL ASPECTS OF KAROO DOLERITES

The dolerite intrusions in the south-eastern part of the Witbank Coalfield that form a complex network within the coal bearing Vryheid Formation on the northern sector of the main Karoo basin, accompanied the Mesozoic fragmentation of the Gondwana supercontinent (Duncan et al., 1997), and formed the intrusive phase of the mainly extrusive Drakensberg Formation (Chevallier and Woodford, 1999). Chevallier and Woodford (1999) believe that the main Karoo basin contains a much larger proportion of intrusive dykes and sills as opposed to the extrusive lavas. During the blanketing by the Karoo volcanics over a vast area of probably 1 million km^2 (Cox, 1970; Cox, 1972), much of the southern African continent was covered by sediments of the Karoo Supergroup (Smith et al., 1993). These predominantly continental sediments persisted for over 100Ma, from the Permian through to the Early Jurassic times.

In southern Africa, associated remnants of thick volcanic successions of lava flows and extensive arrays of dyke and sill complexes that are similar in composition have been grouped together and in this particular instance were termed the Karoo Igneous Province (KIP) (Duncan et al., 1997). The KIP is regarded as one of the largest flood basalt provinces in the world (Duncan et al., 1997) with a total original volcanic volume probably in the order of 5 million km^3 (Coffin and Eldholm, 1994; White and Mkenzie, 1995).

Much of the remains of the KIP that outcrop over the undisturbed Archaean Kaapvaal Craton reveal no evidence of rifting during the extrusion of the Karoo volcanics. Smaller sets of dykes occurring in the KIP have more random orientations, which most probably reflect control by local geological structure. In addition, clear indications from subsequent Cretaceous and younger kimberlites that are emplaced in the Kaapvaal Craton, show relatively little thermal perturbation during the intrusion of the Karoo volcanics. After the Karoo volcanism took place, the Kaapvaal Craton has remained elevated as the crust has been thickened by the addition of a large amount of igneous material (White, 1997).

In terms of continental scale rifting Uken and Watkeys (1997) interpreted mafic dyke swarms in relation to magmatic and volcanic events on the Kaapvaal Craton margins and Limpopo Belt. Three major trends are recognised in the pre-Karoo diabase intrusions, which are NW, EW, and NE. The NW trending dykes are associated with the ~ 3.0 Ga Pongola rift system re-utilised by the Usushwana Complex at ~ 2.8 Ga, during Bushveld Complex times at ~ 2.0 Ga, and by some ~ 1.4 Ga post-Waterberg Group dykes. Dyke trends also coincide with the NE main axis of the ~2.7 Ga Ventersdorp rift systems. During the emplacement of Karoo igneous rocks this NE Ventersdorp

trend was re-utilised in the basement with a marked southerly trend change in the overlying Transvaal Supergroup and Bushveld Complex. The east-west trending diabase dykes resemble the Bushveld Complex axis, which is associated with a craton wide east-west compression. Along the northern and eastern margin of the Kaapvaal Craton the Karoo dykes have major trends such as NNW, NE and NS.

As scant attention has previously been paid to Karoo structural geology, it was felt necessary to review some basic theory on the intrusion of dykes and sills in general. Rubin (1995) and Park (1997) mentioned that the propagation paths of dykes and sills tend to be poorly understood but are indeed a very important aspect of these igneous bodies.

Considering ideal elastic crustal rocks, the horizontal stress is three times the vertical stress ($\sigma_h = 3\sigma_v$), therefore dyke emplacement will take place where the magma pressure (MP) exceeds the horizontal stress plus the tensile strength (TS) that is perpendicular to the bedding of the country rocks (Dyke Emplacement > σ_h + TS $\perp$ to bedding) (Gold et al., 2001). Thus, in structurally homogeneous rocks, dyke emplacement is enhanced in regions of crustal tension, where low horizontal stress (σ_h) in the rocks is expected (Gold et al., 2001). Dyke emplacement is ideally perpendicular to the horizontal stress (σ_h) (see Figure 1.5). In practice though, dyke emplacement favours pre-existing fracture planes (Tokarski, 1990) given that the magma pressure is larger than the compressive stress along the plane (Park, 1997). It is indeed likely that planes making a relatively large angle to σ_3 are preferred propagation paths of dykes (Delaney, et al., 1986).

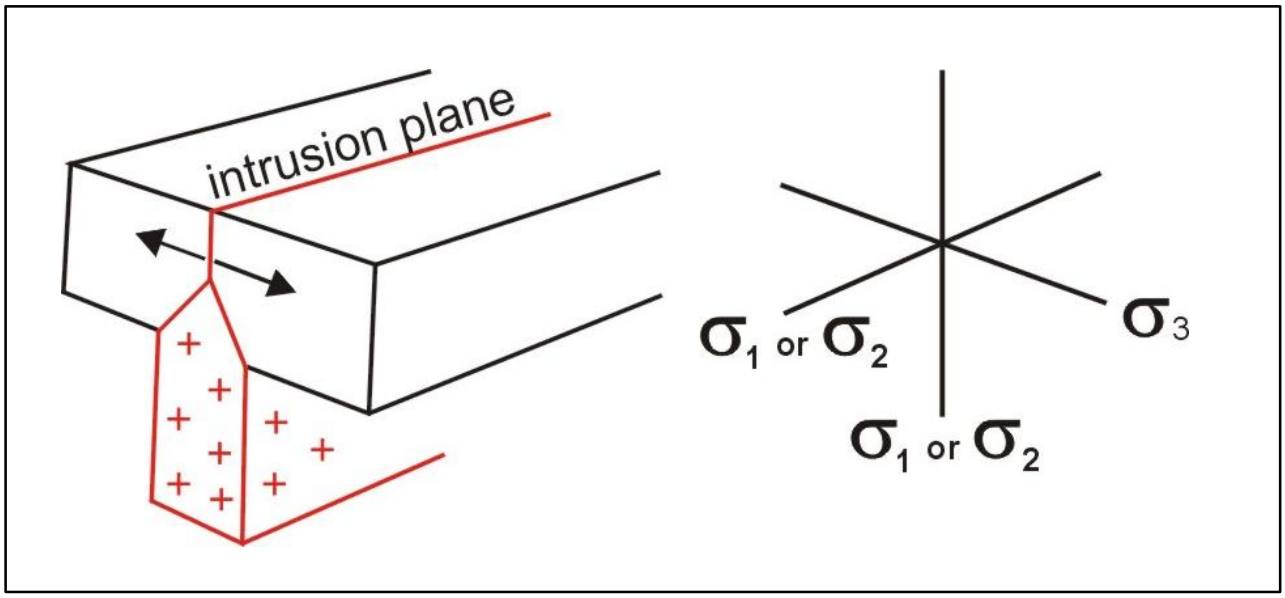

Figure 1.5: Dyke intrusion in homogeneous country rock (Park, 1997).

On the other hand, sills will dominate in areas where MP is larger than the vertical stress or load pressure of overlying strata plus TS parallel to bedding of the country rocks (Sill Emplacement > σv + TS parallel to bedding) (Gold et al., 2001). Figure 1.6 shows sill intrusion in homogeneous country rocks. As opposed to dykes, sills would preferentially intrude into terrains of crustal compression (Gold et al., 2001). The Stirling Castle Sill in the Midland Valley of Scotland provides a good example where the geometry of the sill is a direct result of the pre-existing faults and bedding planes in the country rock (Park, 1997).

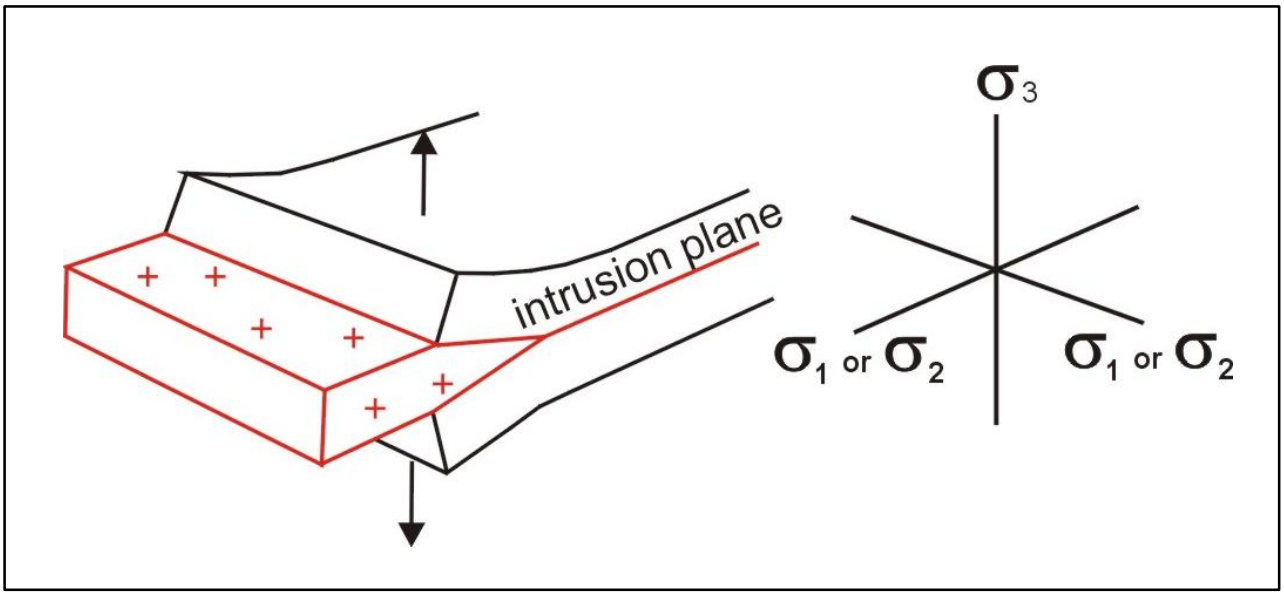

Figure 1.6: Sill intrusion in homogeneous country rock (Park, 1997).

Karoo dolerite dykes, sills and rings in the Western Karoo were spatially analysed and their intrusion mechanism proposed (Chevallier and Woodford, 2001). Dykes propagated laterally within the Karoo sedimentary rocks of sequence of succession, and at certain lithostratigraphic boundaries, they changed into curved inclined sheets where they act as feeders for rings and sills.

Van Niekerk (1995) reports on the intrusion mechanism of two major sills (referred to as B4 and B8) in the Secunda Coalfield situated in the greater Highveld Coalfield. His work concludes that the intrusion of the B4 dolerite sill could have been controlled by a compensation surface, which is the intersection of equal isopiestic surfaces (gravity equipotential surfaces) of rock pressure (overlying strata) and magma pressure. Thus, a negative relationship between the B4 sill's geometry and surface topography at the time of intrusion is proposed. Regional joint patterns controlled the undulating B8 sill, which has near vertical intrusion angles and bifurcates in the form of offshoots.

An altered stress field caused by the intruding sill led to bifurcation. The structural influence of the sill on the host rock is variable as is the deformation associated therewith. Lateral compression of the host rock caused by the sill is the main consequence for structural deformities. These deformities are faults, systematic joints, small folds and bedding plane slip. Irregularities in siltstone would lead to an alteration in the propagation path as its tensile strength exceeds its magmatic overpressure. Comparable tensile strength and magmatic overpressure in sandstone occasionally caused the magma to create its own intrusion direction.

Snyman and Barclay (1989) investigated the metamorphic effect Karoo-age dolerite dykes and sills had on South African coal. It is reported that only narrow contact aureoles are associated with these intrusives and their contribution to regional increase in the rank of South African coal is negligible. However, the rank of coal is exponentially related to the ratio D/T, where D is the distance between the coal and the intrusion contact and T the thickness of the intrusion. In general, the distance of metamorphism is 0.6 to 2 times the thickness of the intrusive.

Blignaut (1952) investigated field relationships of dolerite intrusions in the Natal Coalfields. Dolerite sills displaced and uplifted coal seams in the direction of dip approximately equal to the intersecting sill in the Natal Coalfields. Dolerites are found to be the most common structural features you would get, although small scale normal faulting happens to exist as well. Blignaut (1952) also stated that no supportive evidence of dolerites exploiting pre-existing fault planes exists. In conclusion, Blignaut (1952) considered geostatic pressure caused by the outpouring of Drakensberg lavas resulted in sufficient hydrostatic pressure in the magma to be forced into joints and bedding planes of the country rock. It is also argued that it is apparent that dykes are younger in age as opposed to the sills as the sills created tensional stresses produced by their associated cooling and contraction for dyke emplacement to be favoured. In some cases, sills tend to adopt a vertical dyke-like geometry, but there is always associated displacement involved and the sills always complete its domal or basin circuit irrespective of the degree of undulation.

CHAPTER 2

2. METHODOLOGY

The process flow diagram in Figure 2.1 explains the methodology that was undertaken in this study. The regional scale structure of the Witbank Coalfield forms an integral part of the investigation of geological relationships that controlled the intrusion mechanism and morphology of the dolerite structures in the study area. Regional scale information was obtained using various remote-sensing techniques. Such information includes regional geology and lineaments interpreted from Aeromagnetic, Landsat TM and MSS images. Regional scale trends were analysed using rose diagram plots to determine the preferred and sub-ordinate strike directions of the interpreted lineaments and dolerite dykes.

The regional scale geological and lineament maps were geo-referenced and digitised. The goal is to enable the integration and comparisons with the mine scale structural trends to examine if relationships exist. The regional scale geology and the associated interpretations are discussed in Chapter 3.

Chapter 4 deals with the analysis of the local geological structure determined from dolerite interpretations on a mine scale basis followed by sedimentological interpretations. Investigating the local structure constitutes three main tasks: data acquisition (database construction), data analysis, and data interpretation and integration. Dolerite interpretations have been carried out on a mine scale basis on the Bank Colliery in the Witbank Coalfield. Findings at the Colliery are assumed to be applicable on the other mines with similar geological conditions and where the same main sill is present.

Principal study areas within the mine lease areas were selected on the basis of their association with complex dolerite structure (Figure 2.2). These areas are partly mined out as well as containing virgin resources. Sub-surface geological data and air dried raw coal analyses of more than 1500 boreholes from Bank, Goedehoop, Koornfontein and Optimum Collieries were acquired, as were mine plans containing structural information. The LO29 (Clark 1880 Survey System) coordinates of the borehole collars are transposed and a constant of –1 applied to the X and Y values.

In order to understand the geometry of the dolerites and their associated controls of intrusion, construction of hand-drawn geological cross-section interpretations were necessitated. The vertical and horizontal scales that were used for the geological cross-sections are 1: 1000 and 1: 1667,

respectively. These geological cross-sections were drawn north-south, east-west and zig-zag over the principal study areas. Volatile matter (daf), calorific value (CV) and ash content as well as the displacement of the coal seams supplemented the interpretation of the main sill as part of the geological cross-section construction.

Dolerite interpretations revealed the presence of a ± 20m thick, transgressive sill (hereinafter referred to as the main sill), as well as an upper ± 9m thick, non-transgressive sill. The ± 20m thick sill tends to bifurcate fairly regularly. However a consistent average thickness of ± 20m for the main sill was estimated. The transgressive mode of the main sill facilitated interpretation of intersection points or the contacts between the sill and laterally persistent coal seams. A map depicting the intersection lines (*syn:* apparent strike) between the main sill and the No. 2, 4L and 5 Coal Seams was compiled using information transferred from geological cross-sections to structure plans. These structure plans containing the intersection lines between the sill and the coal seams in fact represent the third dimension of the two dimensional geological cross-section interpretations. The intersection lines were digitised and overlain onto isopach maps of various parameters as calculated from the borehole information. After the main sill structure was interpreted, its floor elevation could be estimated by reading the floor elevation values off the geological cross-sections and capture of the data into the database.

Underground maps portraying dolerite offshoot intersections and fractures in the No. 2 Coal Seam are included. Determination of pre-dominant and sub-ordinate strike directions are undertaken with rose diagram plots.

The borehole information analysis is undertaken using SURFER Surface Mapping System Software (version 8.0) to generate various maps and 3D diagrams in order to visualise and interpret the disparate data sets. Point Kriging is selected as the appropriate gridding technique to generate interpolated grids by estimating values of the points at the grid nodes. The contouring method in the SURFER Software program uses a default algorithm which was considered appropriate for the trend analysis. Contour maps are generated from the interpolated grids to produce maps from irregularly spaced data for distribution analysis and visual comparisons.

Modelling of the sedimentology required the reconstruction of the coal seams and their associated interbedded strata by removing the main sill that displaced the strata. The palaeo floor elevations of the No. 2, 4L and 5 Coal Seams were calculated after subtracting the dolerite width associated

with each displaced coal seam from its floor elevation. A similar methodology is applied to the sedimentary unit widths in order to model the sedimentary sequences prior to the sill intrusion.

Classical statistics of the variables for each sedimentological unit is carried out with the aid of the GEMCOM SURPAC Mine Planning Software (version 6.0). Classical statistics is the calculation of the mean, standard deviation, skewness and kurtosis for raw data sets. Classical statistics of the palaeo-floor elevations, palaeo seam widths and facies widths allowed for the understanding of these sedimentary units and their geometrical relationship to one another. Depending on the homogeneity of the data sets, as determined in the classical statistics analyses, facies are defined on the basis of the normality in the data distribution.

Determination of the trends and relationships that exists in the sedimentary units is carried out with the aid of statistical analysis including Quantile-Quantile plots and Regression Slope Analysis. Correlation coefficients between the various sedimentary parameters were calculated from the regression curves to examine their spatial relationship to one another and finally between the reconstructed sedimentary units and the floor elevation of the main sill.

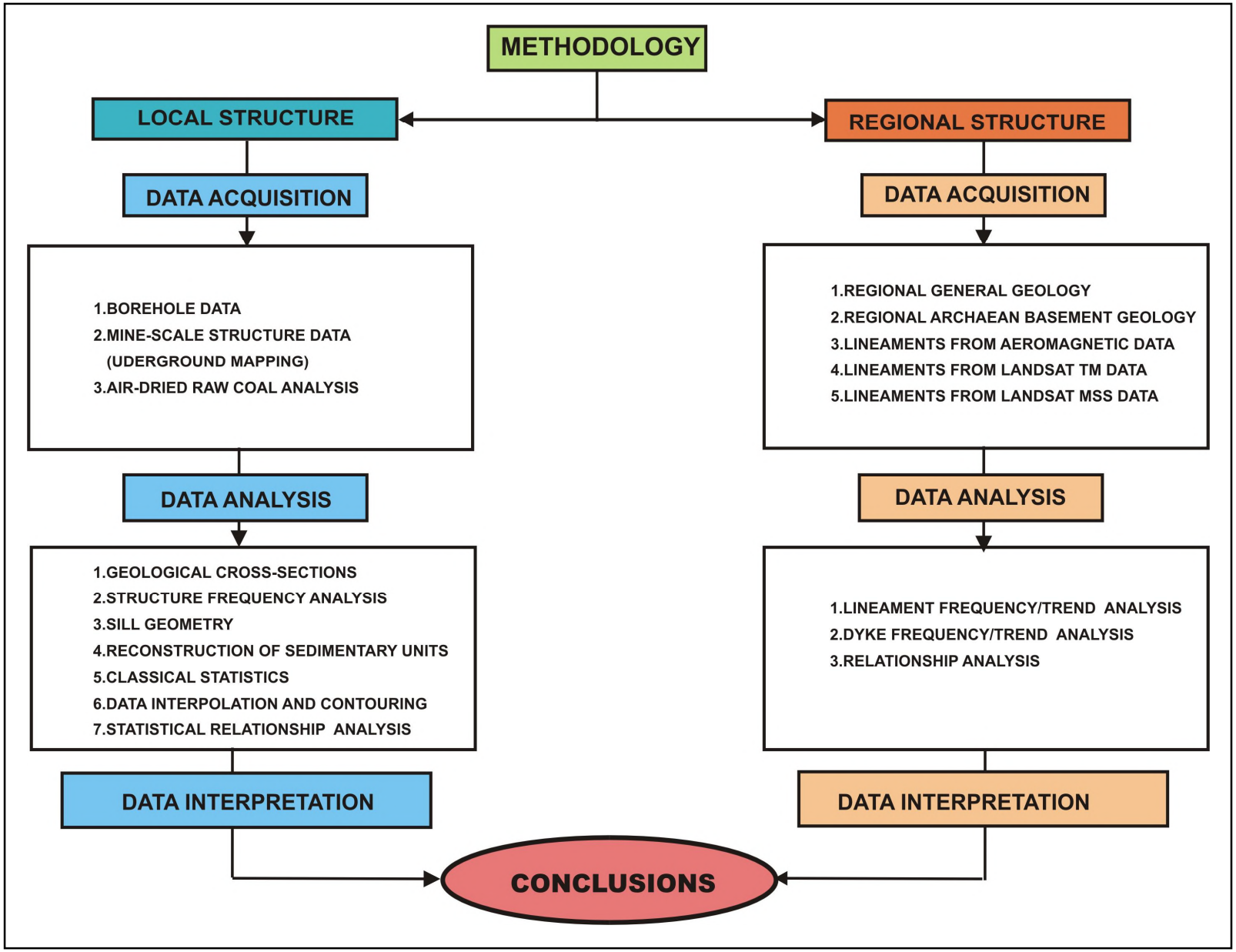

Figure 2.1: Process flow diagram showing the methodology of the study.

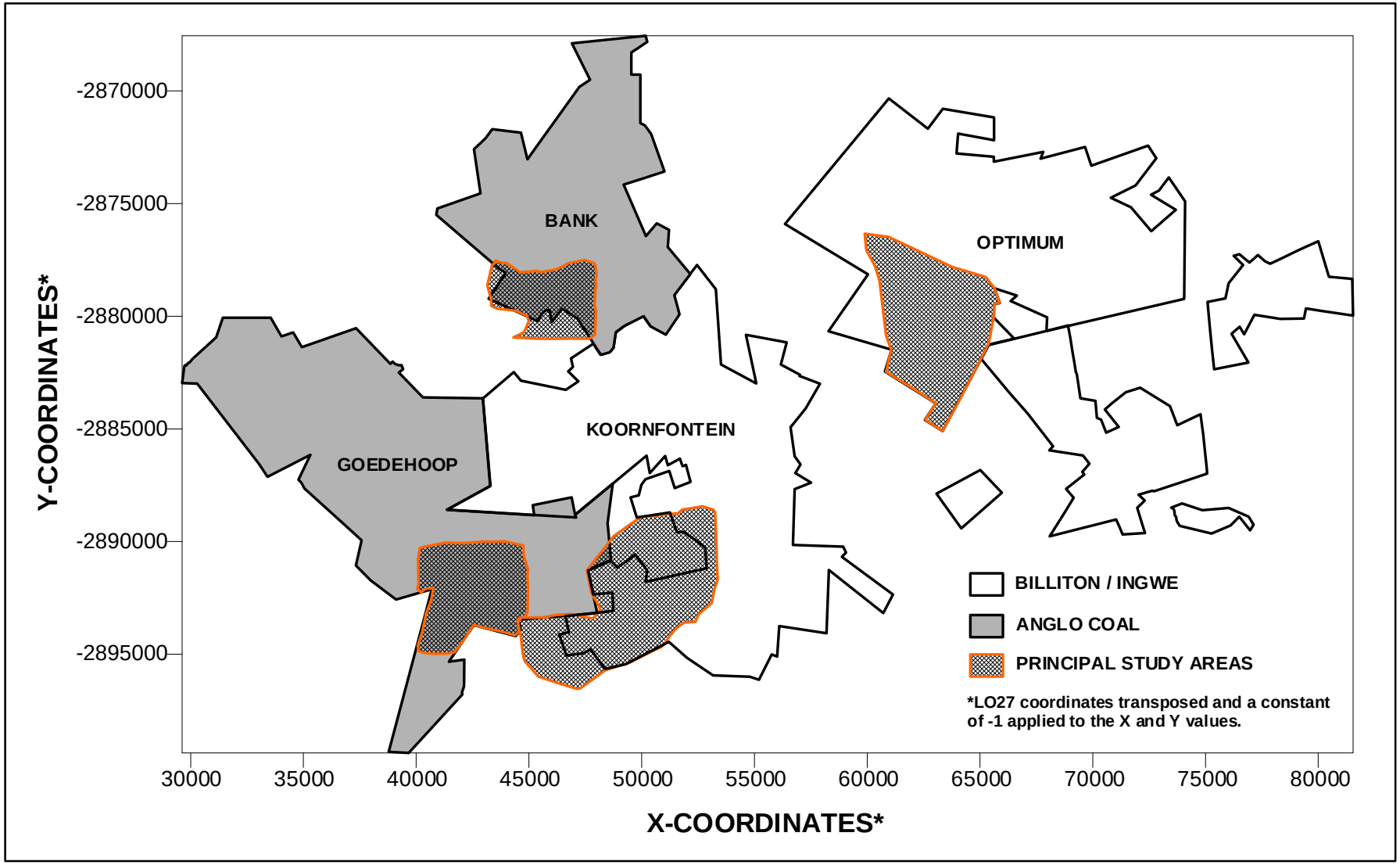

Figure 2.2: Selected principal study areas within the mine lease areas.

CHAPTER 3

3. REGIONAL STRUCTURE

Regional scale information was acquired by using various remote-sensing techniques. The CSIR Miningtek through the COALTECH 2020 Research Program provided this state of the art information. The maps were geo-referenced and the structural data digitised in order to overlay the disparate data sets for interpretation purposes.

3.1 DATA PRESENTATION AND DISCUSSION

3.1.1 ARCHAEAN BASEMENT

3.1.1.1 DATA PRESENTATION

Figure 3.1 presents the Archaean Basement of the Witbank Coalfield and its surroundings. The basement comprises covered greenstone (being the oldest) and granitic material, which is unconformably overlain by the Witwatersand Supergroup. In the immediate vicinity of the study area the basement mainly constitutes felsitic rocks of the Proterozoic Bushveld Complex. North of the study area felsites outcrop in areas surrounding the towns of Witbank and Middelburg. The Smithfield Ridge to the south forms along the topographical high of EW striking felsites. The ridge stretches from the south of Koornfontein Colliery to west of the town of Kendal. Here about the basement is unconformably overlain by glaciogene Dwyka sedimentary rocks deposited during the late Carboniferous period, which is in turn conformably overlain by Permain Vryheid Formation sedimentary rocks of sequence of succession.

3.1.1.2 DISCUSSION AND INTERPRETATION

Dykes in the Archaean basement have three predominant strike directions: NW (Pongola fabric), NE (Ventersdorp fabric) and EW (Uken and Watkeys, 1997). The NW trending, 100km wide diabase dyke swarm that intruded the Pongola fabric in the northeastern part of the Kaapvaal Craton is aeromagnetically quiet. In contrast, the NE trending 200km wide Ventersdorp related dyke swarm has a strong areomagnetic signature. For these dykes two main ages as well as compositional differences are distinguished: diabase dykes are restricted to the northern areas

whereas Karoo-age dolerite dykes occurring to the south re-utilised an older fracture fabric related to earlier diabase intrusions.

Prominent EW diabase dykes appear to be associated with a strong magnetic lineament transecting the Kaapvaal Craton and furthermore coincide with the long axis of the Bushveld Complex, suggesting that magnetic lineaments and EW striking dykes could be of Bushveld age.

Karoo strata unconformably cap the Archaean rocks in the Evander Goldfield, a structurally complex terrain that is situated approximately 70km southwest of the study area. Even so the overlying Karoo sedimentary sequences of succession do not show evidence of structures inherited from the largely faulted and folded rocks of the Witwatersrand and Ventersdorp Supergroups (Tweedie, 1986).

Three different ages of intrusions occur in the Evander Goldfield namely: Bushveld-age, Ventersdorp-age and Karoo-age intrusives (Tweedie, 1986). Near vertical, NS striking Ventersdorp-age intrusives dominate the Evander Goldfield while Bushveld-age intrusives consist of extensively altered diabases. Two different Karoo-age intrusions are also present. Non-porphyritic intrusives are older and intruded the Ecca rocks while the younger porphyrictic intrusives are emplaced in the older intrusions, as well as the Transvaal and Ventersdorp successions.

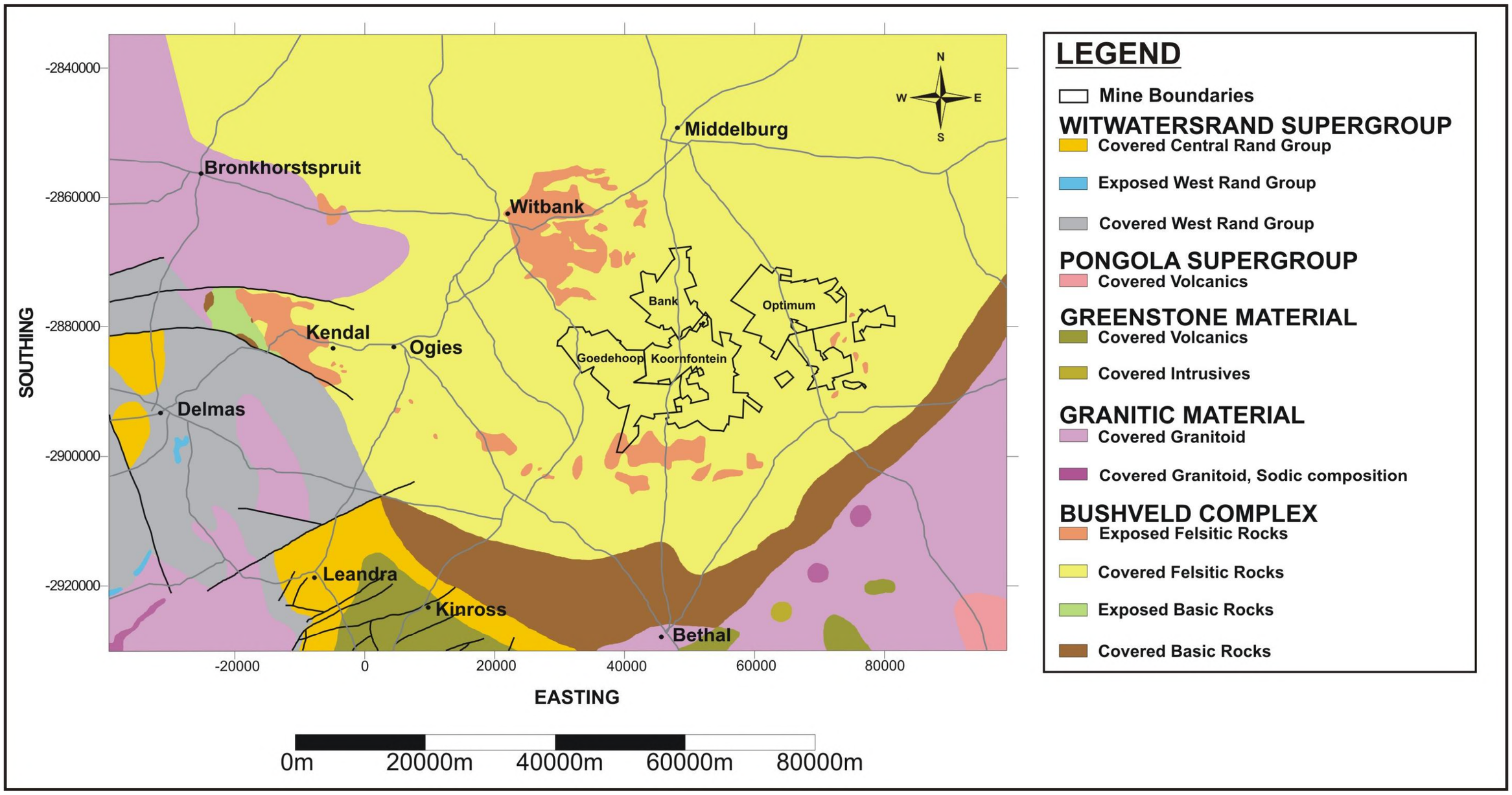

Figure 3.1: ***Archaean basement (modified after pers. comm. Henckel, 2001).***

3.1.2 GENERAL GEOLOGY

3.1.2.1 DATA PRESENTATION

Large-scale structures in the Witbank Coalfield are the ±15m thick Ogies Dyke, which strikes from Ogies in the west to Optimum Colliery in the east, as well as various prominent lineaments (Figure 3.2). The study area is transected by NE striking lineaments between the towns of Hendrina and Middelburg and a single NNW striking lineament between Witbank and Ogies developed across Bushveld and Ecca rocks. The lineament directly associated with the Ogies Dyke extends westwards into the Transvaal Supergroup rocks. Prominent EW trending lineaments are formed in the undifferentiated Bushveld sequence. NE striking lineaments occur in the Ecca in the lower right corner of Figure 3.2. These lineaments are predominantly orientated NE, EW and to a lesser extent NW and NS frequencies are observed (Figure 3.3).

Mine-scale structures of the Vryheid Formation sedimentary rocks comprise i.e. transgressive sills, dykes, faults with throws in the order of 1m and also differential compaction joints on the pre-Karoo valley flanks are commonly present. Smith (1990) reports small-scale graben type faulting at Optimum Colliery associated with the Ogies Dyke. It is generally observed (Smith, 1990) that dolerite sills north of the Ogies Dyke are absent. Strike information on the majority of dykes being studied is collated from mine plans which represent the intersections of the dykes with the coal seams.

Differences in dyke orientations and occurrences north and south of the Ogies Dyke are evident. These dykes, of which some are depicted in Figure 3.2, have been digitised and their strike directions measured to produce rose diagram plots for major trend analysis. The majority of the dykes south of the Ogies Dyke preferably strike NS and EW (Figure 3.4). Dykes north of the Ogies Dyke preferably strike EW, and sub-ordinate directions of WNW, ENE and NS were frequently intruded as well (Figure 3.5).

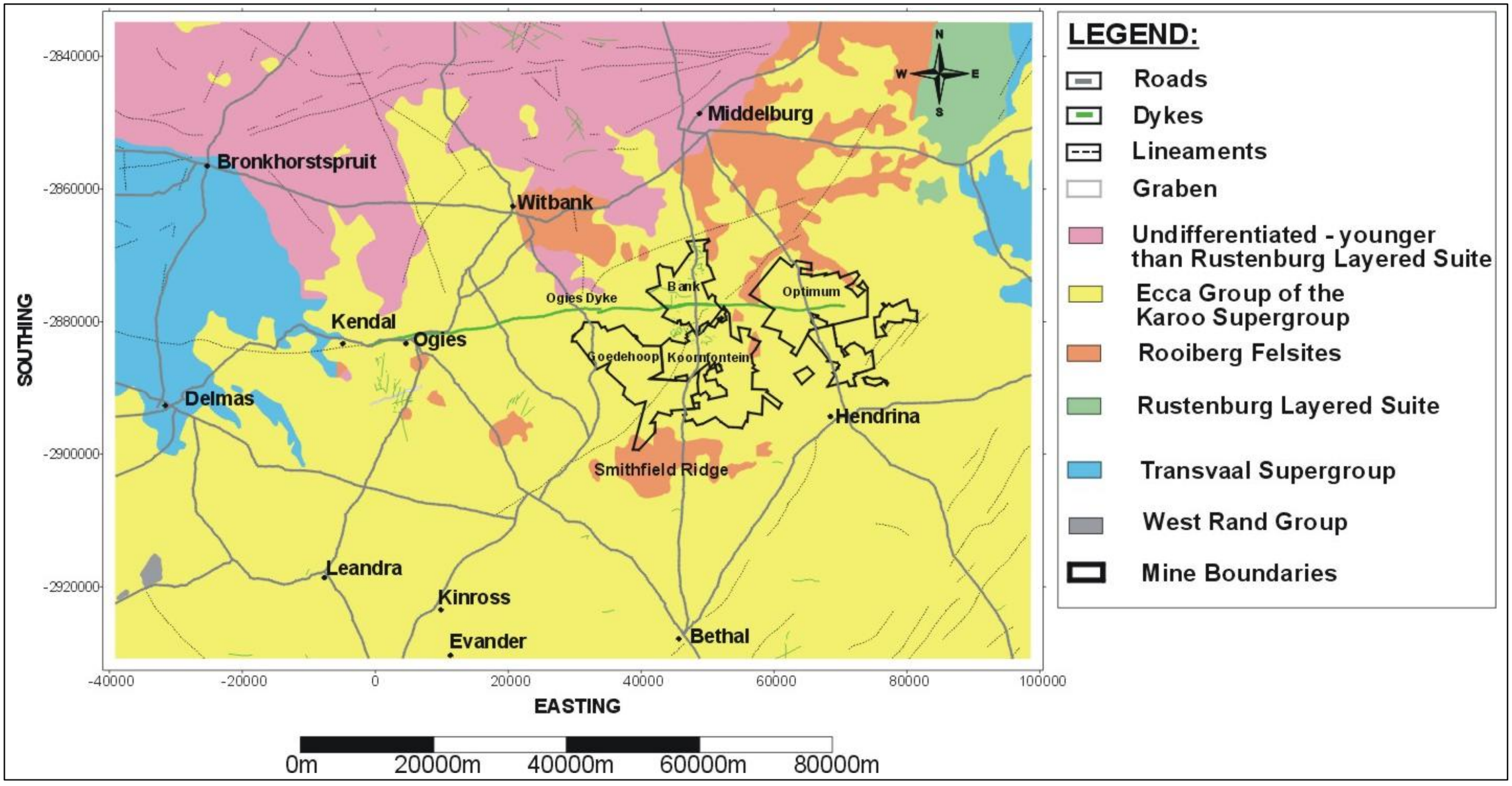

Figure 3.2: Regional scale geological map.

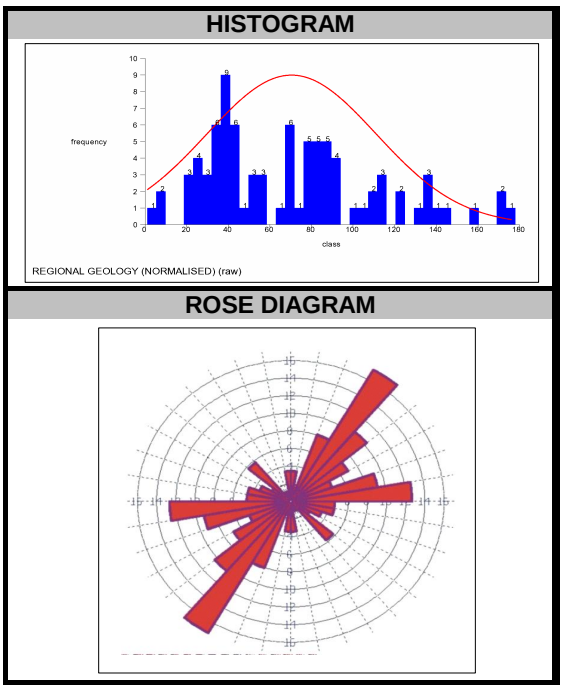

CLASSICAL STATISTICS	
VARIABLE	REGIONAL GEOLOGY (DATA >180deg NORMALISED TO 180deg RANGE)
NUMBER OF SAMPLES	87
MINIMUM VALUE	1
MAXIMUM VALUE	178
MEAN	70.39
VARIANCE	1657.84
STANDARD DEVIATION	40.72
COEFFICIENT OF VARIATION	0.58
SKEWNESS	0.70
KURTOSIS	2.86
TRIMEAN	66.06
BIWEIGHT	66.37
MAD	27.87
ALPHA	48.72
SICHEL-T	Not Calculated

Figure 3.3: ***Frequency of strike directions of lineaments from the regional scale geological map.***

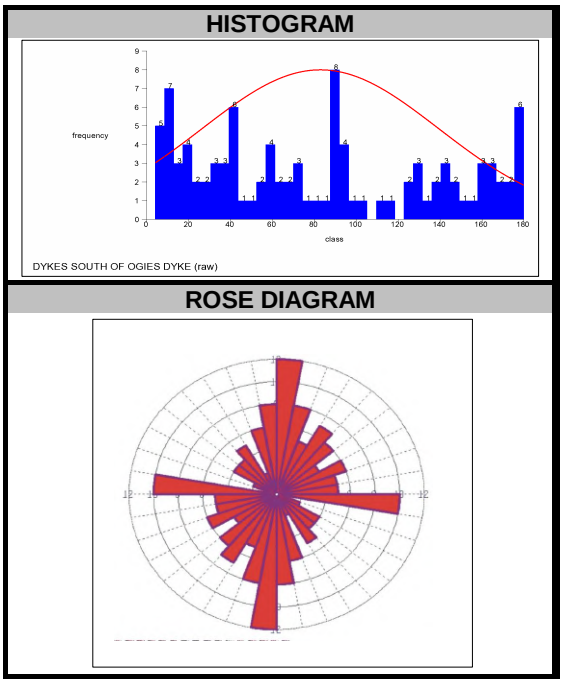

CLASSICAL STATISTICS	
VARIABLE	DYKES (DATA >180deg NORMALISED TO 180deg RANGE)
NUMBER OF SAMPLES	100
MINIMUM VALUE	4
MAXIMUM VALUE	180
MEAN	82.86
VARIANCE	3199.08
STANDARD DEVIATION	56.56
COEFFICIENT OF VARIATION	0.68
SKEWNESS	0.28
KURTOSIS	1.76
TRIMEAN	79.25
BIWEIGHT	80.63
MAD	51.00
ALPHA	137.61
SICHEL-T	Not Calculated

Figure 3.4: ***Strike frequency of dykes south of the Ogies Dyke.***

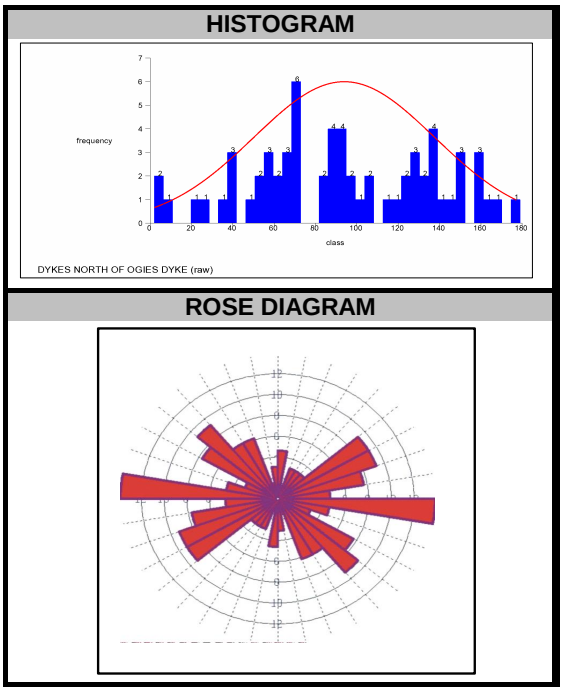

CLASSICAL STATISTICS	
VARIABLE	**DYKES (DATA >180deg NORMALISED TO 180deg RANGE)**
NUMBER OF SAMPLES	65
MINIMUM VALUE	2
MAXIMUM VALUE	179
MEAN	93.92
VARIANCE	1916.78
STANDARD DEVIATION	43.78
COEFFICIENT OF VARIATION	0.47
SKEWNESS	-0.08
KURTOSIS	2.18
TRIMEAN	94.38
BIWEIGHT	93.85
MAD	35.25
ALPHA	481.91
SICHEL-T	Not Calculated

Figure 3.5: Strike frequency of dykes north of the Ogies Dyke.

3.1.2.2 DISCUSSION AND INTERPRETATION

From the geological and basement maps it is clear that the Witbank Coalfield sedimentary strata have never been subjected to any obvious large scale structural events. NE striking lineaments in the Ecca rocks displayed in the lower right corner of Figure 3.2 coincide with the preferred Ventersdorp fabric. Propagation paths of some NE striking Witbank Coalfield dolerites were pobably controlled by this pre-existing fabric, resulting from the 2.7 Ga Ventersdorp rifting event (Uken and Watkeys, 1997).

Karoo-age intrusions in the Evander Goldfield and Secunda Coal Field, which are geographically not far apart, are similar in terms of relative age configurations with reference to the work undertaken by Van Niekerk (1995) on dolerites in the Secunda area. Yet no precise geochemical relationship between Karoo dolerites in the Witbank Coalfield and those occurring in the Secunda Coalfield have previously been established (pers. comm. J.J. du Plessis, 2001). However the chemical properties of the B8 dolerite sill (Van Niekerk, 1995) in relation to the ±20m thick main sill occurring in the southeastern part of the Witbank Coalfield reveal similarities. Van Niekerk (1995) concluded that the transgressive B8 sill intruded along very steep to vertical angles that mainly

follow the pre-existing regional joint pattern, with the exception of certain dolerites that intruded slightly oblique to the joint sets. Minor joint sets are intruded by NW trending dykes while NS and EW striking dolerites coincide with the prominent joints sets.

Previous observations on the Ogies dyke revealed that it has intruded into a zone of high, linear tectonic disturbance probably of pre-Karoo age (Smith, 1990). Basement geology at certain localities at Bank and Optimum Collieries, transected by the Ogies Dyke, constitutes pre-Karoo diabase. Major trends in the pre-Karoo diabase are NW, EW and NE (Uken and Watkeys, 1997). The EW pre-Karoo diabase trend is similar to the Bushveld Complex axis that is associated with a craton wide EW compression (Uken and Watkeys, 1997), which coincides with the EW Ogies Dyke suggesting that it probably intruded into a weak tectonic zone of pre-Karoo diabase. Karoo-age dyke trends, which are NNW, NE and NS along the northern and eastern margin of the Kaapvaal Craton (Uken and Watkeys, 1997) probably concludes that its intrusion was mainly controlled by this pre-Karoo weakness plane.

The geochemical and mineralogical fingerprinting of the Ogies Dyke, according to Du Plessis (pers. comm. 2001), are markedly different to other dyke and sill material in this area: this could be indicative of a relative age difference. No radiometric age determinations have been carried out on the Ogies Dyke to date. Sills would ideally intrude when the crust is in state of compression implying that the Ogies Dyke could have re-utilised a pre-Karoo diabase sill probably related to the EW Bushveld Complex compressional event (Uken and Watkeys, 1997).

Considering the observation by Smith (1990) that immediately north of the Ogies Dyke dolerite sills are not present whilst dykes appear to be a common feature, the Ogies Dyke could have played a critical role in determining the source of magma provision to sills in this region.

The sub-ordinate ENE trending dykes south of the Ogies Dyke could be related to the ENE Tuli-Soutpansberg troughs (Figure 3.6) representing a syn-Karoo graben as the result of right-lateral strike-slip movement along reactivated Archaean structures (Uken and Watkeys 1997). The erosion of the Drakenberg Escarpment is mainly controlled by these ENE trending dykes and fracture system. In addition, the WNW trending dykes could be associated with the WNW trending Okavango Dyke Swarm (Figure 3.6) representing the failed arm of a possible plume generated Karoo-age triple junction.

Intrusion of NS dykes north and south of the Ogies Dyke could reveal both local and distant influences. On a local scale these dykes probably intruded into cooling joints that developed

perpendicular to the Ogies Dyke as a result of its intrusion. However the influence of the NS trending Lebombo monocline intersecting the Okavango Dyke Swarm at ~120° in the Nuanetsi area (Figure 3.6) is considered to be likely (Uken and Watkeys, 1997). In addition, NS trending Karoo-age dolerite dykes are observed along the northern and eastern margin of the Kaapvaal Craton (op cit.).

EW striking dykes both north and south of the Ogies Dyke suggest that maybe the earlier Ogies Dyke related fracture fabric was intruded. These intruded fractures that parallel the Ogies Dyke might also be sheeting (pressure-release jointing) that developed parallel to its cooling surface and now are represented as magma filled cracks. EW striking lineaments (see Figure 3.2) occurring to the north of the study area parallel a similar Ogies Dyke trend and also correspond with the EW Bushveld Complex axis. The Ogies Dyke seems very different and therefore might pre-date its surrounding dolerite dykes and sills. However, Blignaut (1952) stated that in the Natal Coalfield, dolerite dykes represent the last phase of igneous activity, as the cooling and contraction created by the sills produced tensional stresses, which are preferred conditions for dyke intrusion.

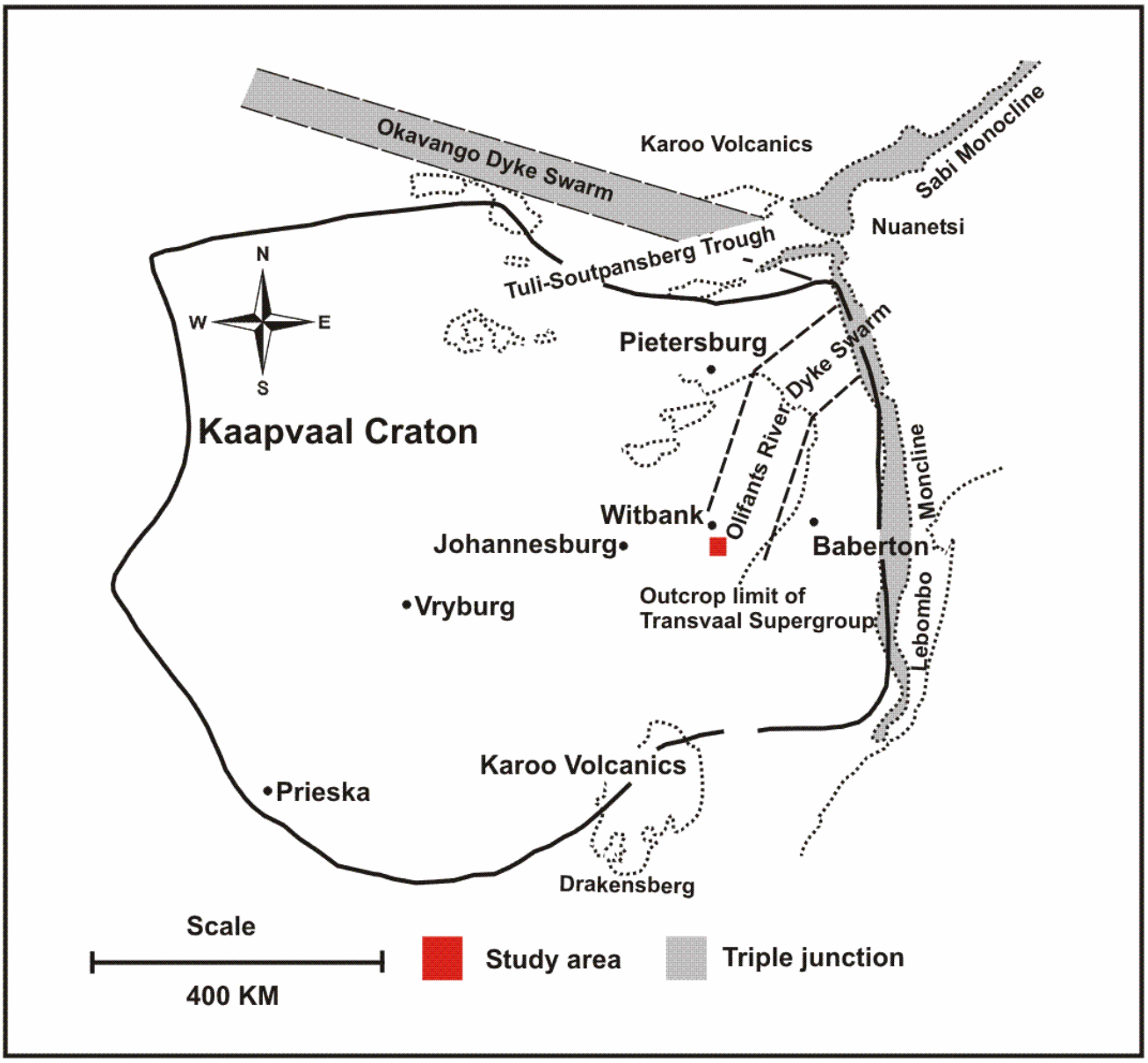

Figure 3.6: Mafic dyke swarms on the Kaapvaal Craton and Limpopo Belt (Uken and Watkeys, 1997).

3.1.3 LINEAMENTS

3.1.3.1 DATA PRESENTATION

Lineament data interpreted from the Aeromagnetic, Landsat TM and MSS maps were digitsed and their strike directions measured in order to assess the possibility of favoured intrusion directions. Landsat TM has a resolution of 30m and is able to sub-sample to 25m depths. Landsat TM comprises seven bands of which 1 to 3 are visible, 4 falls in the mid-infra red spectrum, 5 in the mid-infra red reflected, 6 in the emitted infrared and band 7 is an infrared reflected band. The Landsat MSS has an 80m resolution and is able to sub-sample to 60m depth. It consists of four bands of which 3 falls within the visible spectrum and the fourth within the mid-infrared part. Structure mapping with higher resolusion Landsat MSS images is comprehensive and more accurate as opposed to Landsat TM.

Lineaments interpreted from the Aeromagnetic image (Figure 3.7) reveal predominant NE strike directions and sub-ordinate NS, EW, NWN, WNW directions (Figure 3.8). Two preferred strike directions NE and NNE are recognised (Figure 3.10) interpreted from a Landsat TM image (Figure 3.9). Distinctive NNW and sub-ordinate NNE trending lineaments (Figure 3.12) are revealed by the Landsat MSS image (Figure 3.11).

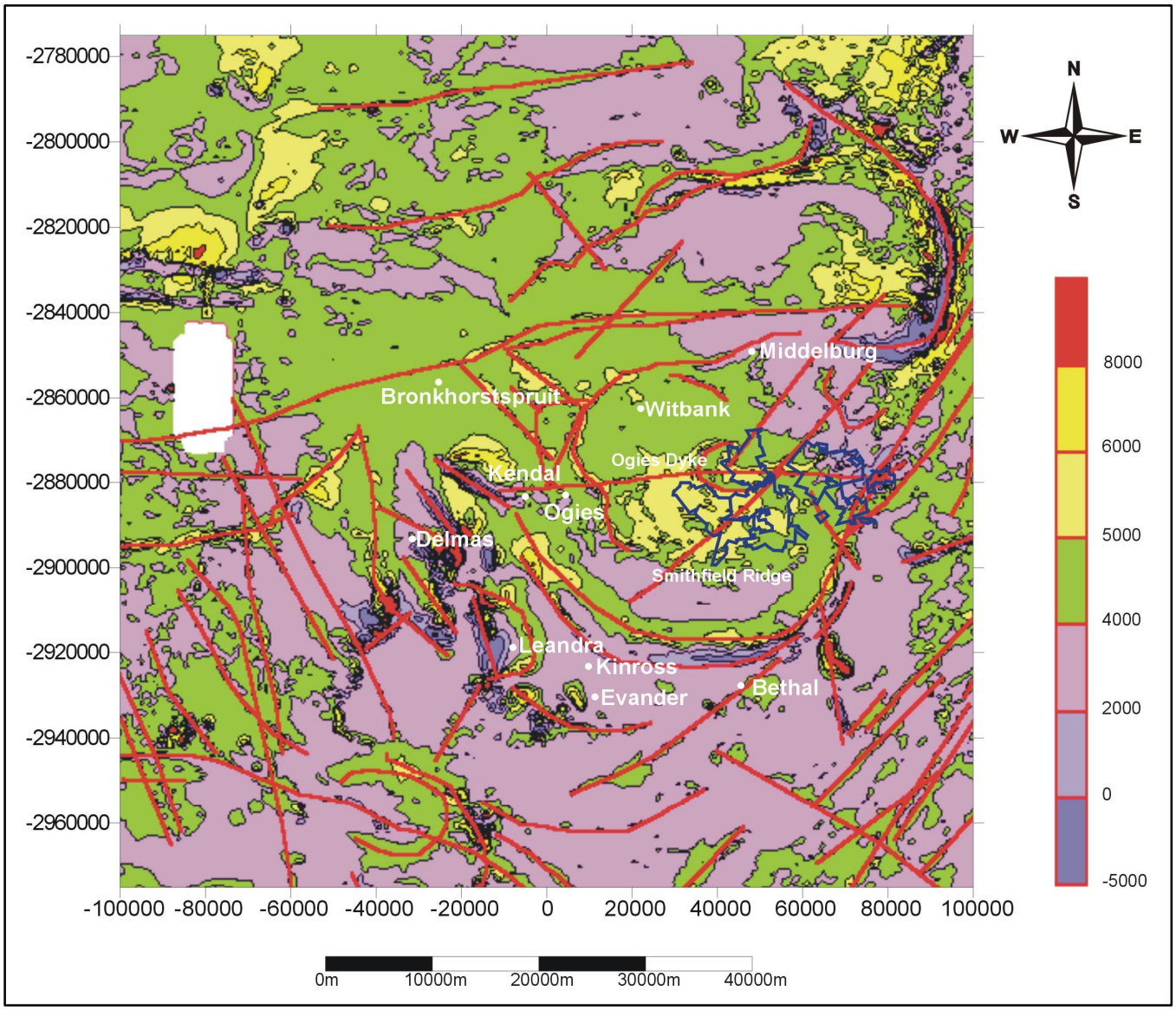

Figure 3.7: ***Lineaments interpreted from an Aeromagnetic image (pers. comm. Henckel, 2001). 1st Vertical Derivative of the Aeromagnetic Data. Values in nT.***

HISTOGRAM

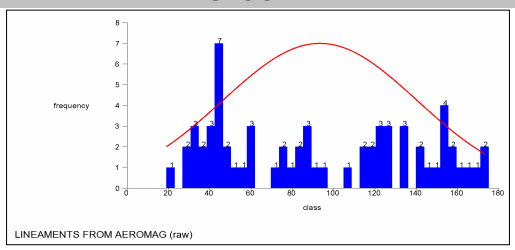

ROSE DIAGRAM

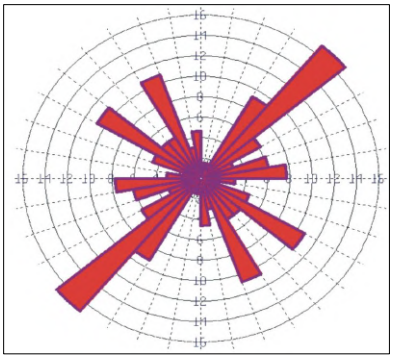

CLASSICAL STATISTICS	
VARIABLE	**AEROMAG LINEAMENTS (DATA >180deg NORMALISED TO 180deg RANGE)**
NUMBER OF SAMPLES	65
MINIMUM VALUE	19
MAXIMUM VALUE	175
MEAN	93.35
VARIANCE	2213.15
STANDARD DEVIATION	47.04
COEFFICIENT OF VARIATION	0.50
SKEWNESS	0.14
KURTOSIS	1.59
TRIMEAN	89.13
BIWEIGHT	92.30
MAD	47.05
ALPHA	99.51
SICHEL-T	Not Calculated

Figure 3.8: ***Strike frequency of lineaments interpreted from an Aeromagnetic image in Figure 3.6.***

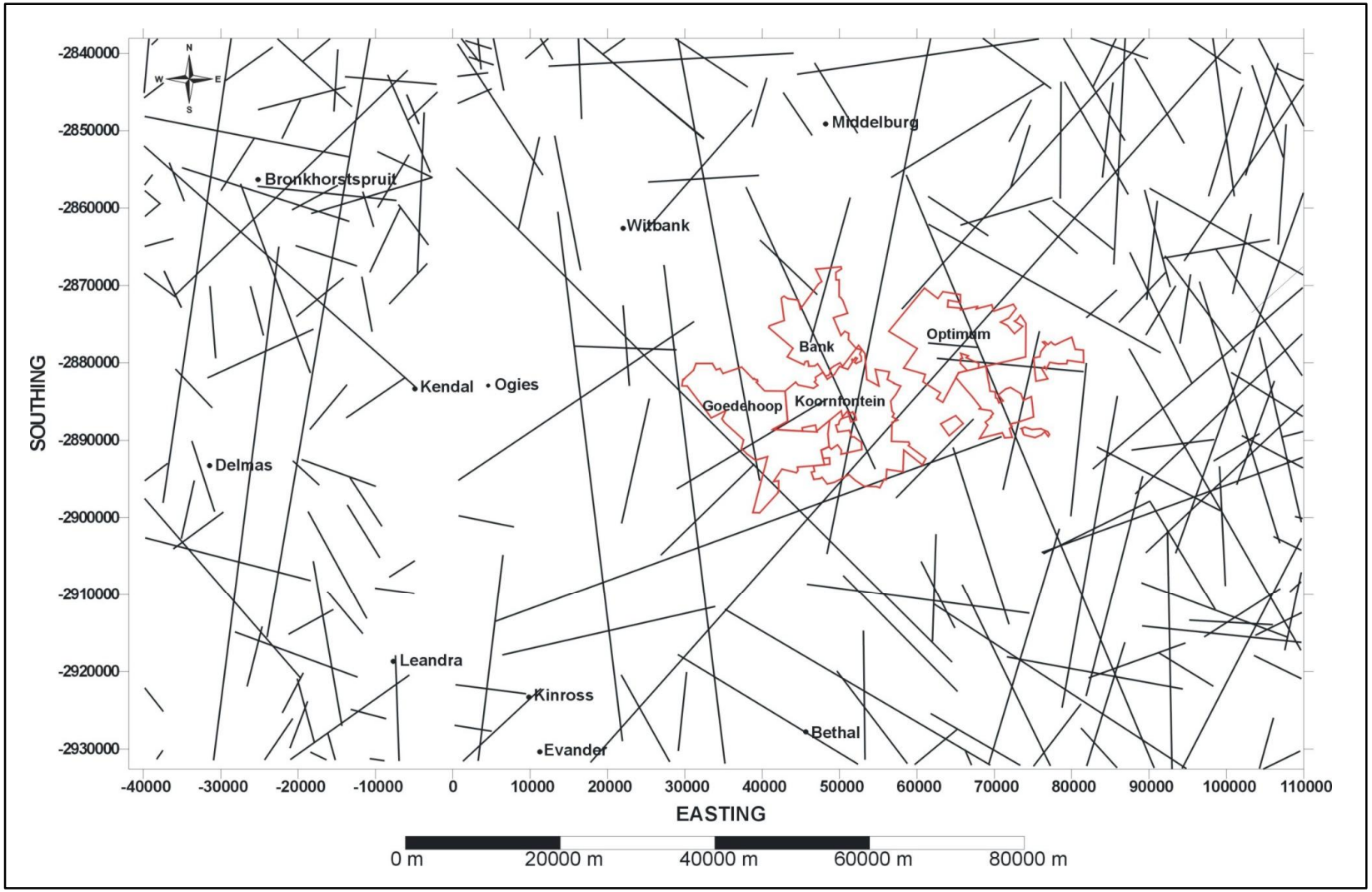

Figure 3.9: ***Lineaments interpreted from Landsat TM with the study area indicated in red demarcating the mine boundaries (after pers. comm. Henckel, 2001).***

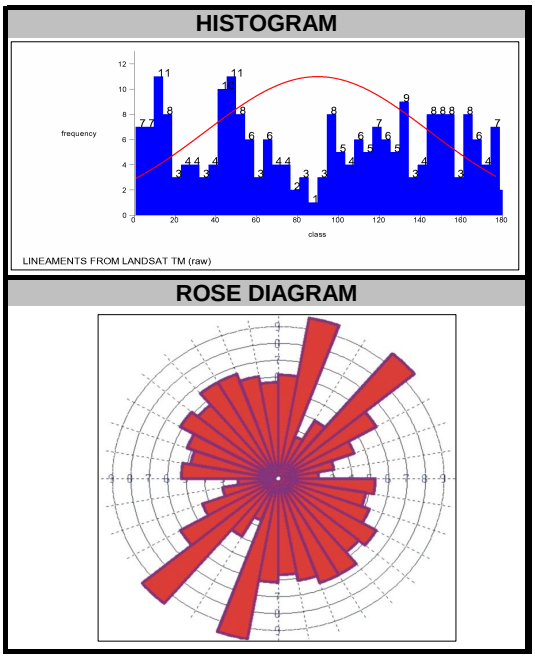

CLASSICAL STATISTICS	
VARIABLE	**LANDSAT TM LINEAMENTS (DATA >180deg NORMALISED TO 180deg RANGE)**
NUMBER OF SAMPLES	228
MINIMUM VALUE	1
MAXIMUM VALUE	179
MEAN	89.71
VARIANCE	2984.23
STANDARD DEVIATION	54.63
COEFFICIENT OF VARIATION	0.61
SKEWNESS	-0.02
KURTOSIS	1.65
TRIMEAN	93.75
BIWEIGHT	90.63
MAD	48.50
ALPHA	-0.74
SICHEL-T	Not Calculated

Figure 3.10: Strike frequency of lineaments interpreted from Landsat TM.

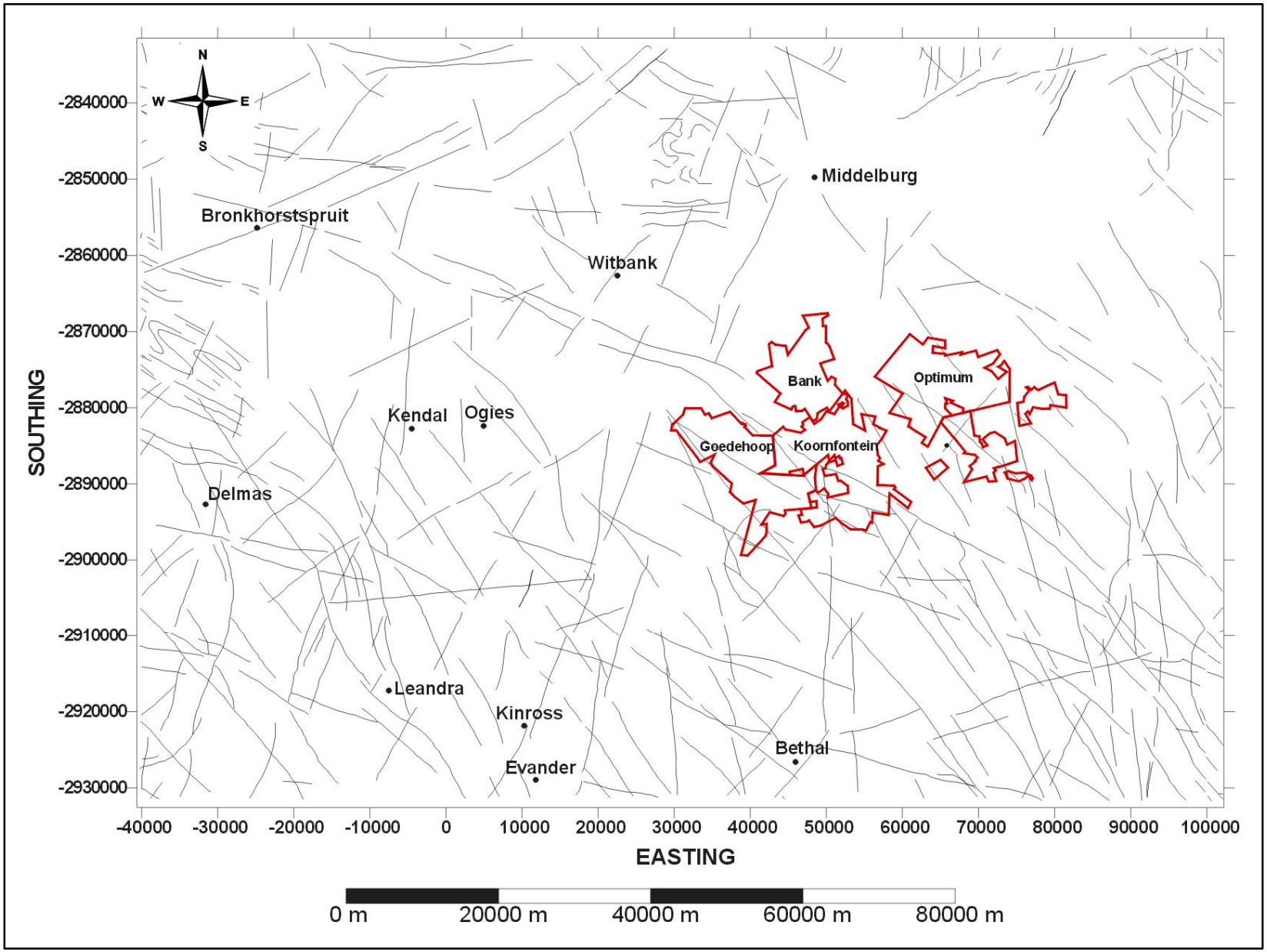

Figure 3.11: Lineaments interpreted from Landsat MSS with the study area indicated in red demarcating the mine boundaries (after pers. comm. Henckel, 2001).

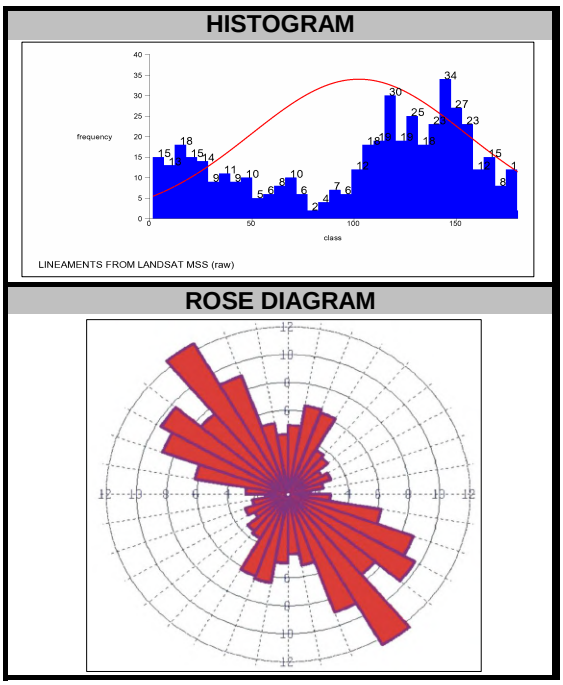

CLASSICAL STATISTICS	
VARIABLE	**LANDSAT MSS LINEAMENTS (DATA >180deg NORMALISED TO 180deg RANGE)**
NUMBER OF SAMPLES	466
MINIMUM VALUE	2
MAXIMUM VALUE	218
MEAN	102.31
VARIANCE	2777.29
STANDARD DEVIATION	52.70
COEFFICIENT OF VARIATION	0.52
SKEWNESS	-0.51
KURTOSIS	1.94
TRIMEAN	108.44
BIWEIGHT	106.63
MAD	40.75
ALPHA	-1.49
SICHEL-T	Not Calculated

Figure 3.12: Preferred strike directions of lineaments interpreted from Landsat MSS.

3.1.3.2 DISCUSSION AND INTERPRETATION

Predominant NE trending lineaments in Figures 3.8 and 3.3 respectively interpreted from the Aeromagnetic image (Figure 3.7) and depicted in Figure 3.2 coincide with the NE Ventersdorp basement fabric. In addition the NE Sabi monocline representing the third arm of a plume generated Karoo-age triple junction (op cit.) and NE striking Karoo-age dolerite dykes along the eastern and northern margin of the Kaapvaal Craton (op cit.) could also be revealed by this preferred lineament trend. Predominant lineament trends and Karoo-age dykes corresponding with the orientations of the triple junction probably conclude final Gondwana break-up between southern Africa and eastern Antarctica along the Lebombo and Sabi monoclines with the Okavango Dyke Swarm acting as the failed arm (Uken and Watkeys, 1997).

In Figure 3.13 a right-lateral east-west shear zone associated with the western Karoo dolerites is interpreted to be a failed transformed fault between an active rift system in the east and a zone of rift pre-weakening in the west (Chevallier and Woodford, 1999). Prominent NNE striking lineaments from the regional scale geological map could perhaps be extensional structures related to the NNE striking arm of an inferred triple junction (Figures 3.13 and 3.14) off the East Coast. These NNE trending structures intersect the present exposure of the Karoo volcanics in the central

Karoo and Nuanetsi in the north, following the NNE Olifants River Dyke Swarm and also coincide with the NNE axis of the main Karoo basin. These relationships re-emphasise that the Olifants River Dyke Swarm most probably acted as an important feeder system to Karoo sills and volcanics in the central Karoo basin (Uken and Watkeys, 1997).

The NE trending lineaments from the Landsat TM map coincide with the re-utilised basement trend (Uken and Watkeys, 1997) of the Olifants River Dyke Swarm south of the Tuli-Soutpansberg Trough and also tie in with the NE Karoo-age dolerite dyke trend as observed along the northern and eastern margin of the Kaapvaal Craton (op cit.). Further southwards the Olifants River Dyke Swarm changes strike direction to NNE, which coincides with NNE trending lineaments. These main Landsat TM lineament trends therefore probably represent the Olifants River Dyke Swarm.

Along the northern and eastern margin of the Kaapvaal Craton, NNW striking Karoo-age dykes have been recognised that are postulated to have accompanied the Mesozoic fragmentation of Gondwana (Uken and Watkeys, 1997). The distinctive NNW trending lineaments (Figure 3.12), interpreted from a Landsat MSS image (Figure 3.11), correlate with these dykes.

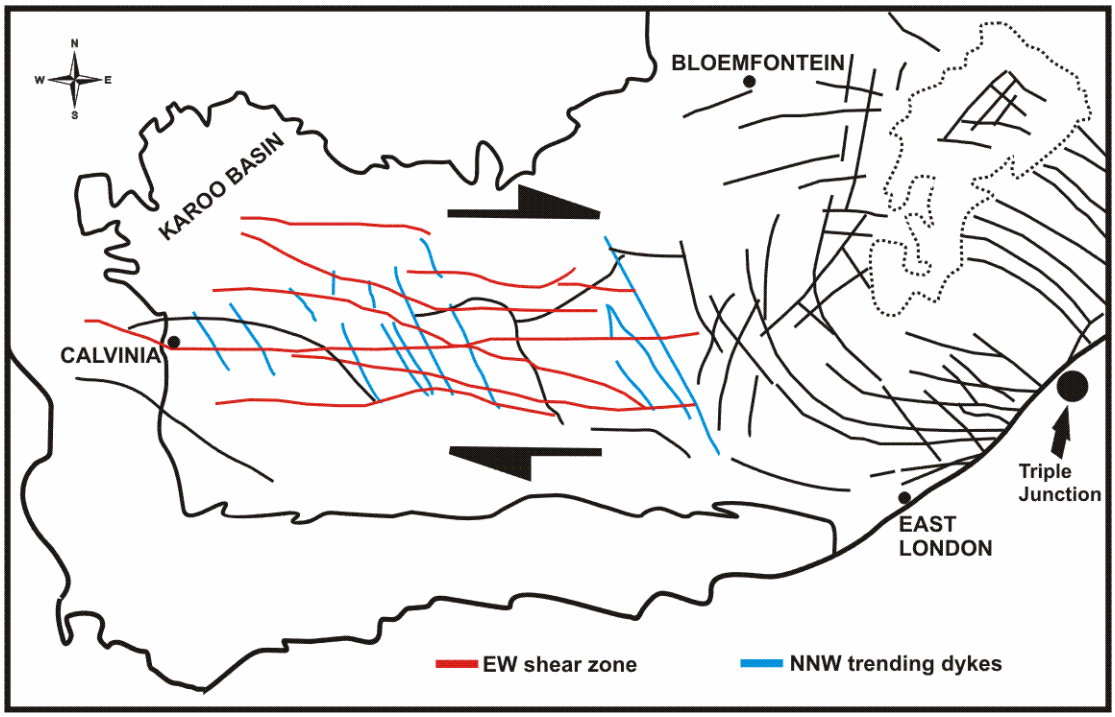

Figure 3.13: ***Simplified map showing the relation between the EW right lateral shear zone and the NNW trending dykes and also the position of a postulated triple junction off the East Coast (map is not to scale) (Chevallier and Woodford, 1999).***

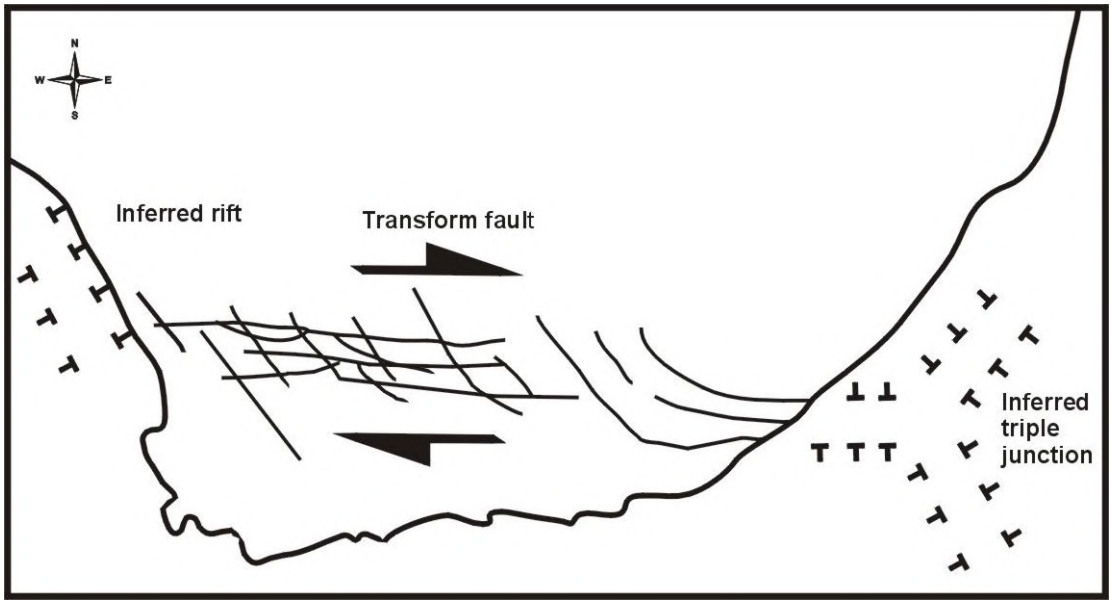

Figure 3.14: ***A geodynamic interpretation of the western Karoo dolerite structural set-up (Chevallier and Woodford, 1999).***

3.2 CONCLUSION AND SUMMARY

Table 3.1 summarises probable relationships between certain Karoo-age dyke, sill and lineament trends that are associated with the northern main Karoo basin and surroundings and could possibly provide insight into better understanding of the intrusion mechanism of dolerites in the south-eastern Witbank Coalfield. It is therefore probable that some of the Karoo-age intrusives in the south-eastern Witbank Coalfield followed older basement structures inherited by the Karoo strata and/or syn-tectonic structures related to Gondwana break-up which was synchronous with dolerite intrusion (Encarnación et al., 1996).

Table 3.1: Summary of the regional scale trend relationships possibly relating dykes, sills or lineaments in the Witbank Coalfield.

TREND	REGIONAL SCALE STRUCTURAL ASSOCIATION
NE	Karoo-age dolerite dykes
	Sabi monocline - 3rd arm of a plume generated Karoo-age triple junction
	Ventersdorp Fabric (2.7Ga rifting - extensional event) - strong aeromagnetic signature, Pre-Karoo diabase trend.
NS	Regional joints sets preferably favoured by the B8 dolerite sill in the Secunda Coalfield
	Lebombo monocline - part of Karoo age triple junction
	Karoo-age dolerite dykes
	Ventersdorp-age intrusives in the Evander Goldfield
NW	Regional joints sets preferably favoured by the B8 dolerite sill in the Secunda Coalfield
	Pongola fabric - aeromagnetically quiet
EW	Regional joints sets preferably favoured by the B8 dolerite sill in the Secunda Coalfield
	Karoo-age Ogies Dyke
	Pre-Karoo diabase
	Long axis of the Bushveld Complex
NNW	Karoo-age dolerite dykes
	Predominant lineament trend from Landsat MSS image
WNW	Okavango Dyke Swarm (failed arm of a Karoo-age triple junction)
ENE	Tuli-Soutpansberg troughs - syn-Karoo graben resulting from reactivated Archaean structures
	Retreat of Drakenberg Escarpment
NNE	Extensional structures of a Karoo-age triple junction off the East Coast
	Olifants River Dyke Swarm – important feeder to Karoo-age sills
	Axis of the main Karoo basin

The EW striking Ogies Dyke, which is the main structure in the Witbank Coalfield, most probably pre-dates its associated smaller scale dykes and sills. Conclusions for this relative age difference are summarised as being the following:

- Its association with EW basement Pre-Karoo diabase, which probably acted as a plane of weakness and might have triggered its earlier intrusion.
- Difference in geochemical and mineralogical characteristics.
- Absence of sills immediately to its north.
- Should the NS striking dykes north and south of the Ogies Dyke be favoured by cooling joints which developed as a result of its earlier intrusion, the age difference is evident.

CHAPTER 4

4. LOCAL STRUCTURE

4.1 EXPLORATION BOREHOLE DATA

4.1.1 DATA PRESENTATION

The original borehole database could not be included in the thesis due to the signed confidentiality agreements between all parties involved in COALTECH 2020 research program.

DATA INTERPRETATION

4.2 GEOLOGICAL CROSS-SECTIONS

4.2.1 INTRODUCTION AND METHODOLOGY

This section treats the two-dimensional dolerite sill interpretations using geological cross-sections; the criteria for interpretation entail a combination of observations during this study as well as observations from previous investigations in adjacent and other coalfields. Lithological and analytical coal information of 467 vertical exploration boreholes from Bank Colliery were utilised in this study. Geological cross-sections north-south, east-west and zig-zag were compiled over the principal study area. At least two geological cross-sections each in a different direction for every vertical borehole had to be constructed depending on the complexity of the dolerite. Ideally three cross-sections, each in a different direction through three closest vertical boreholes forming a triangle; or four sections in two different directions through four boreholes in the form of a square should be sufficient for dolerite interpretations.

Cross-section interpretations revealed the presence of a ± 20m thick, transgressive sill (main sill) as well as an upper ± 9m thick sill (occasionally > 15m thick); this rarely transgressing the No. 4L Coal Seam of which only remnants remain in the study area. Mineralogical and geochemical studies fingerprinted dolerite samples in a collaborative study carried out concurrently with this study. Those samples were collected from the underground mines in the study area, where the development excavations exposed the dolerite intersecting with the No. 2 Coal Seam.

It is well known that physical and chemical characteristics of individual sills are remarkably consistent for extensive distances (Blignaut, 1952). The geochemical and mineralogical data interpretations reveal the existence of two dolerite types which are the Ogies Dyke and the ± 20m thick main sill (pers. comm. J.J. du Plessis, 2001). The sill transgresses over a wide stratigraphic range, from Pre-Karoo basement and Dwyka Formation sedimentary rocks to the No. 5 Coal Seam and the present day erosion surface.

Negligible amounts of sedimentary material was assimilated by Karoo-age dolerites in the Natal Coalfield (Blignaut, 1952), as well as in the Secunda Coalfield (Van Niekerk, 1995). Similar observations pertain to the dolerite/sediment contacts in the Witbank Coalfield. The dolerite/sandstone contacts in Figure 4.1 are invariably sharp showing no assimilation of the host rock, but rather smooth contacts. The photograph in Figure 4.2 shows the intact dolerite and coal seam contacts with evidence of minimal assimilation of coal xenoliths on the contacts. It is evident from the photograph that the coal is *in-situ* and little dolerite was incorporated by the space available as provided by the coal to form a mozaic type of breccia on the contact. This phenomenon would not happen as a rule or on a larger scale as large open spaces in coal seams don't exist in this area. Also, no large chunks of country rock xenoliths have been reported in the dolerite or observed elsewhere in the Witbank Coalfield. It could therefore be interpreted with a reasonable level of confidence that the sediments had been consolidated at the time of the dolerite intrusion. This implies that the intrusion planes had to be pre-defined in that the space occupied by the sill was created by separation of the sedimentary rocks along the plane of intrusion. The likelyhood therefore exists for the smooth dolerite intrusion planes to represent pre-existing structures i.e. joints.

In underground mines, limited exposure of the dolerite contact with the interbedded strata is available for analysis. According to Blignaut (1952) the displaced and uplifted sedimentary rocks in the Natal Coalfield are not disturbed in a major way except for mild tilting near the contact. For a certain distance away from the contact between inclined dolerite sills and the country rock, intrusion related deformation structures are to be expected. Blignaut (1952) interpreted the force behind inclined dolerite sheets to not have been sufficient to push the strata horisontally apart to any significant extent. However, Van Niekerk (1995) reports on intrusion related macro-scale deformation structures in the host rock. High intrusion angles of the B8 dolerite sill in the Secunda Coalfield, in certain areas, had not uplifted the sedimentary rocks but rather laterally compressed the country rock resulted in shortening on either side of the intrusion in the form of faults and/or folds.

The degree and type of host rock deformation depends to some extent on the thickness of the intrusion: thicker intrusions have more severe influences than thin intrusions. Van Niekerk (1995) furthermore stated that in places sandstone, close to high angle intrusions shows deformation characteristics five times the thickness of the intrusion, whereas siltstones show bedding plane slip, bending and overthrusts closer to the contact. It was also noted that dolerite intrusions influence siliceous country rocks to a much larger extent as opposed to coal country rock.

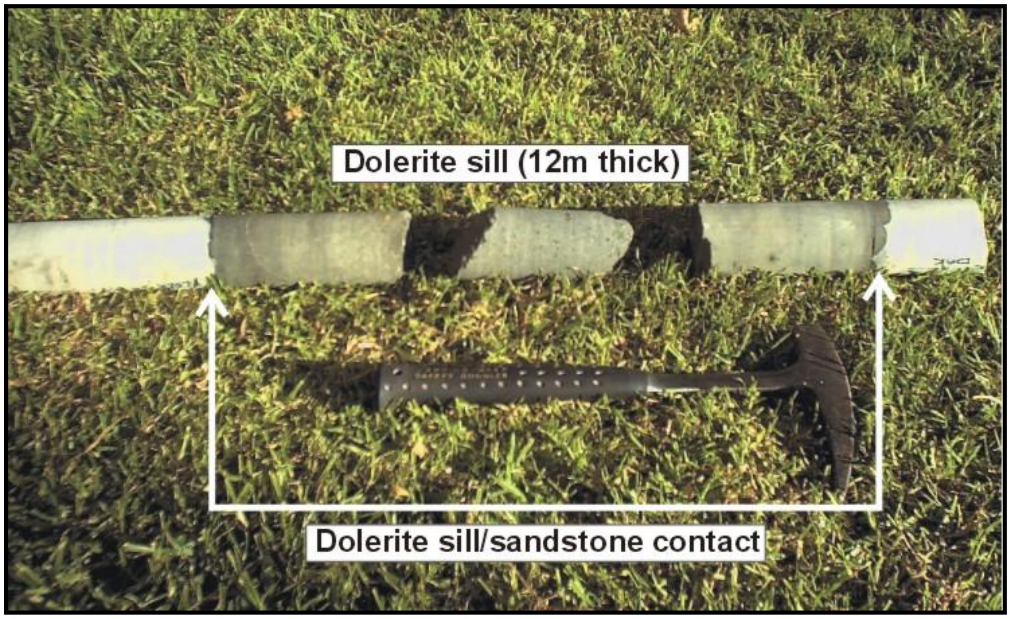

Figure 4.1: ***Photograph showing the very sharp and smooth contacts between a 12m thick dolerite sill and the sandstone host rock.***

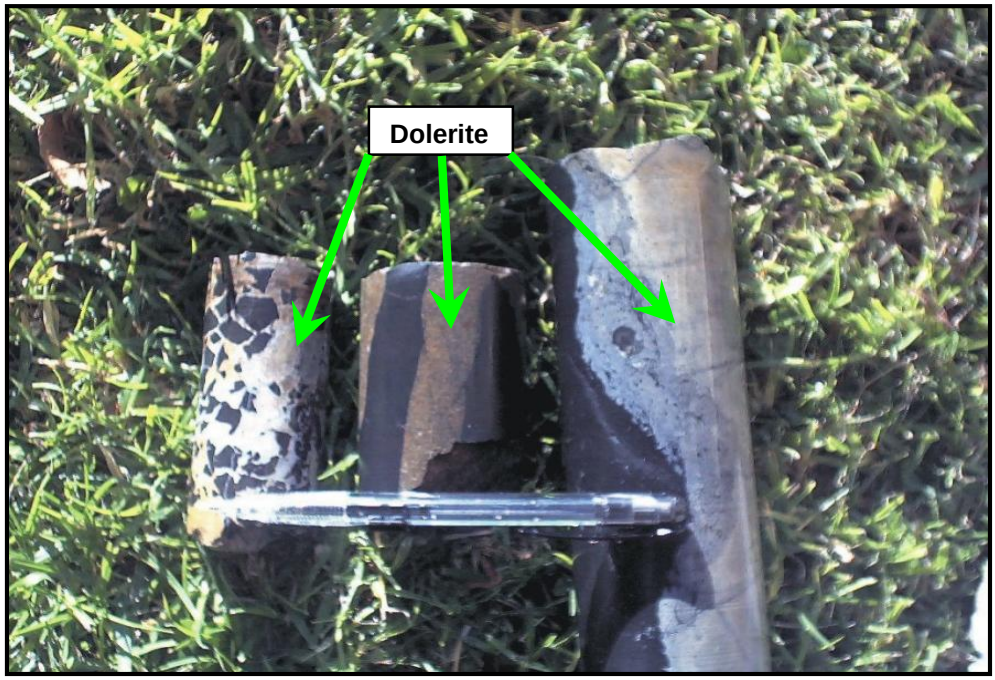

(*Note the coal in the left-hand side core sample shows in–situ breccia.)

Figure 4.2: ***Photograph showing dolerite in coal.***

The ± 20m thick sill (main sill) in the Witbank Coalfield is undulating, intruded transgressively and tends to bifurcate regularly forming offshoots or stringers that are up to 5m thick. After bifurcation, the offshoots rejoin the main sill thus maintaining a consistent thickness of ± 20m. However when the sill periodically intrudes to a higher stratigraphic level, the offshoots sometimes died out before they could rejoin the main sill, affecting the consistency of its thickness.

Van Niekerk (1995) referred to dolerite model A (Figure 4.3) of the Secunda Coalfield that assumes dolerite sills to have a constant width with a maximum variation of 15%; this implies that a larger variation would lead to the presence of an offshoot between the closest relevant boreholes. The accuracy of this method particularly for this study area is questioned in that offshoots of up to 5m occur that do not necessarily rejoin the main sill. However, in certain cases it was observed that this model has merit, depending largely on the borehole density and even more important the borehole depth; in other words, whether all doleritic material within the stratigraphic intrusion range were encountered during drilling.

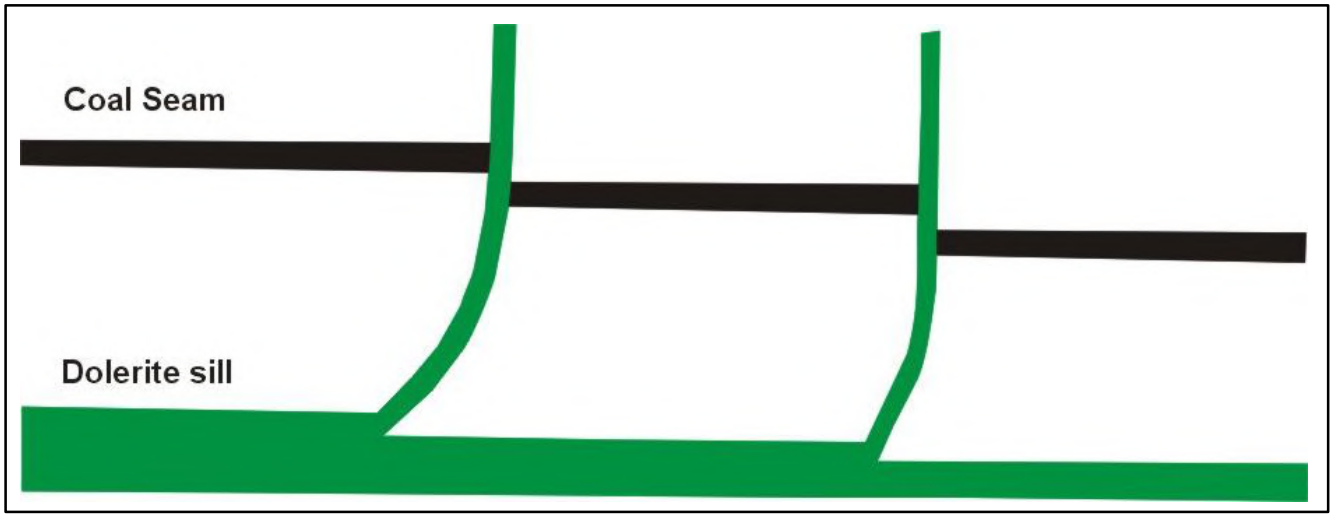

Figure 4.3: Proposed dolerite model A for the Secunda Coalfield (Van Niekerk, 1995).

The exact intersection positions of dolerite offshoots and coal seams between closest vertical boreholes are very difficult to establish. The confidence level in the interpretation of intersections between the highly unpredictable course of offshoots and coal seams is dependent on the borehole density as well as the borehole penetration depth. However, the ultimate way for determining their exact intersection positions would be angled drill holes, in-seam or directional drilling. However, both in-seam and directional drilling have major deficiencies and in-seam drilling is only valuable for short term mine planning (Saunderson and du Plessis, 2000).

The country rock occurring above the ± 20m thick sill and its associated offshoots particularly in the SE part of Witbank Coalfield was uplifted by an amount approximately equal to its width, depending on the intrusion angle. This statement however, implies that the sedimentary strata and pre-Karoo rocks below the sill remain *in-situ*. In places, the main sill tends to adopt a vertical dyke-like geometry, but there is always displacement associated with it and it always completes its circular domal or basin geometry irrespective of the degree of undulation.

The upper thinner sill of which only remnants remain is of less interest, as it infrequently intersects the coal seams and no exposure in underground mines was available for sampling nor could any drill core samples be found. In addition, verbal information from the mine was obtained in that this sill has undergone extensive weathering because of its proximaty to the present day erosion surface.

Parameters such as volatile matter content, calorific value (CV) and the ash content of coal were used to supplement the interpretation of dolerite structures. The volatile matter content of coal is calculated on a dry, ash-free basis (daf) using equation 1.

$$\textit{(1) \% volatile matter (daf)} = \frac{\textit{\% volatile matter (air-dried) x 100}}{\textit{100 - \%ash - \%moisture}}$$

In the proximity of dolerites, the calorific value (heat value) decreases rapidly from high values to very low values close to the dolerite; conversely ash values increase (Figure 4.4). Proximal to dolerites low volatile matter is observed, which is attributed to the attenuated loss of volatile constituents caused by heat emanated from the intrusion-related metamorphism (Du Plessis, J.J., 2001). Thermally affected coal seams should always be compared with un-affected coal seams, as the intra-seam sedimentological controls on coal seam quality vary significantly, especially within the No. 2 Coal Seam (Du Plessis, G.P. 2001).

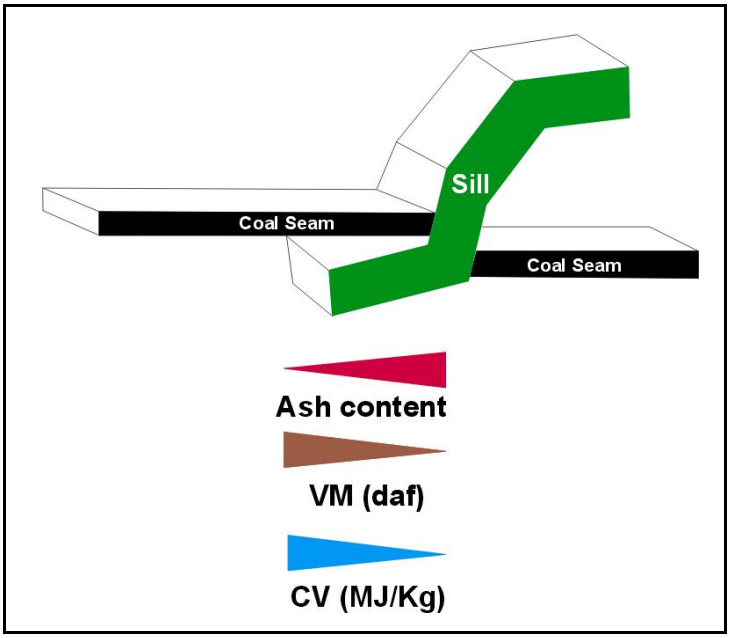

Figure 4.4: Summary of certain near dolerite affected parameters from the air-dried raw coal analyses that were used to assist dolerite interpretation.

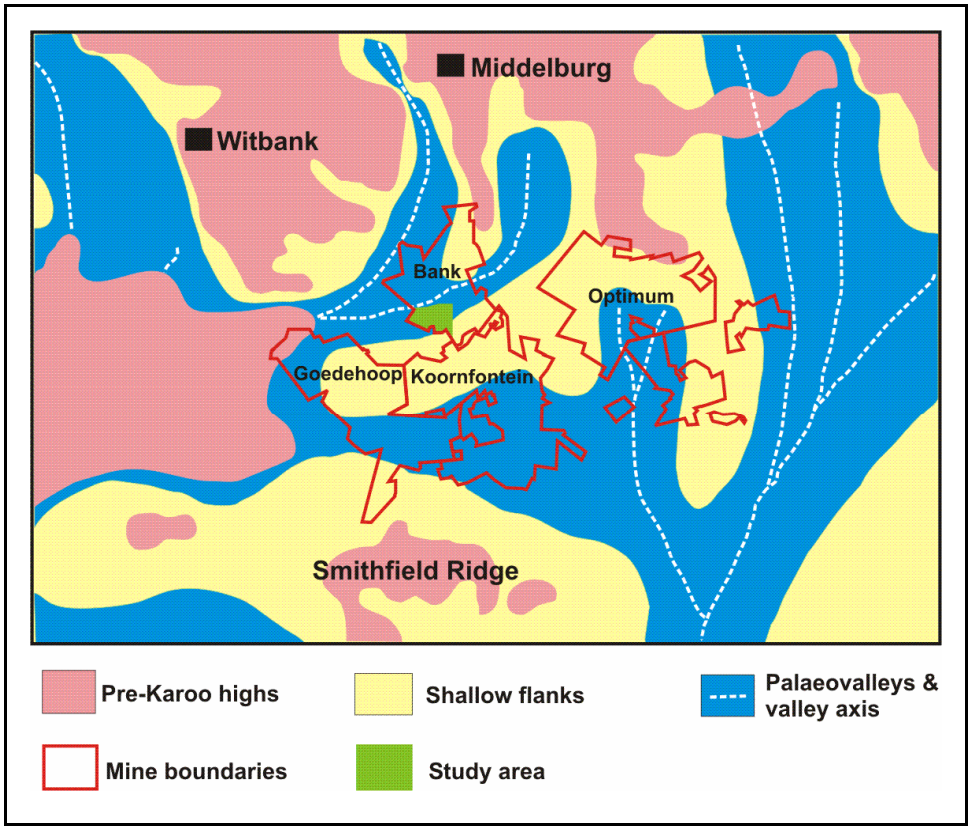

Figure 4.5: Palaeo-topography of the Pre-Karoo basement in the Witbank Coalfield (modified after Jeffrey, 2001).

The pre-Karoo basement topography exercised direct control on both the width and aerial distribution of the No. 1 and 2 Coal Seams, which are mainly confined to the predominant NS trending palaeo-valleys (Cairncross, 1989; Le Blanc Smith, 1980). The study area at Bank Colliery is situated close to the centre of a palaeo-valley (Figure 4.5) that is characterised by six stratigraphic bands within the No. 2 Coal Seam of alternating high and low quality coal. Coal quality is based on ash content as well as sedimentological controls (Jeffrey, 2001).

4.2.2 DATA INTERPRETATION

Dolerites are interpreted by the construction of numerous geological cross-sections in the principal study area at the Bank Colliery (Figure 4.6). Of all the sections that were compiled in this exercise, a representative set was selected for inclusion and discussion in the text (Figures 4.8 to 4.18). Information on the pre-Karoo basement is sparse as borehole penetration was terminated at the base of the coal seam of interest. Hence, there is a certain degree of uncertainty regarding the accuracy of the inference of the Dwyka Formation and the Pre-Karoo basement.

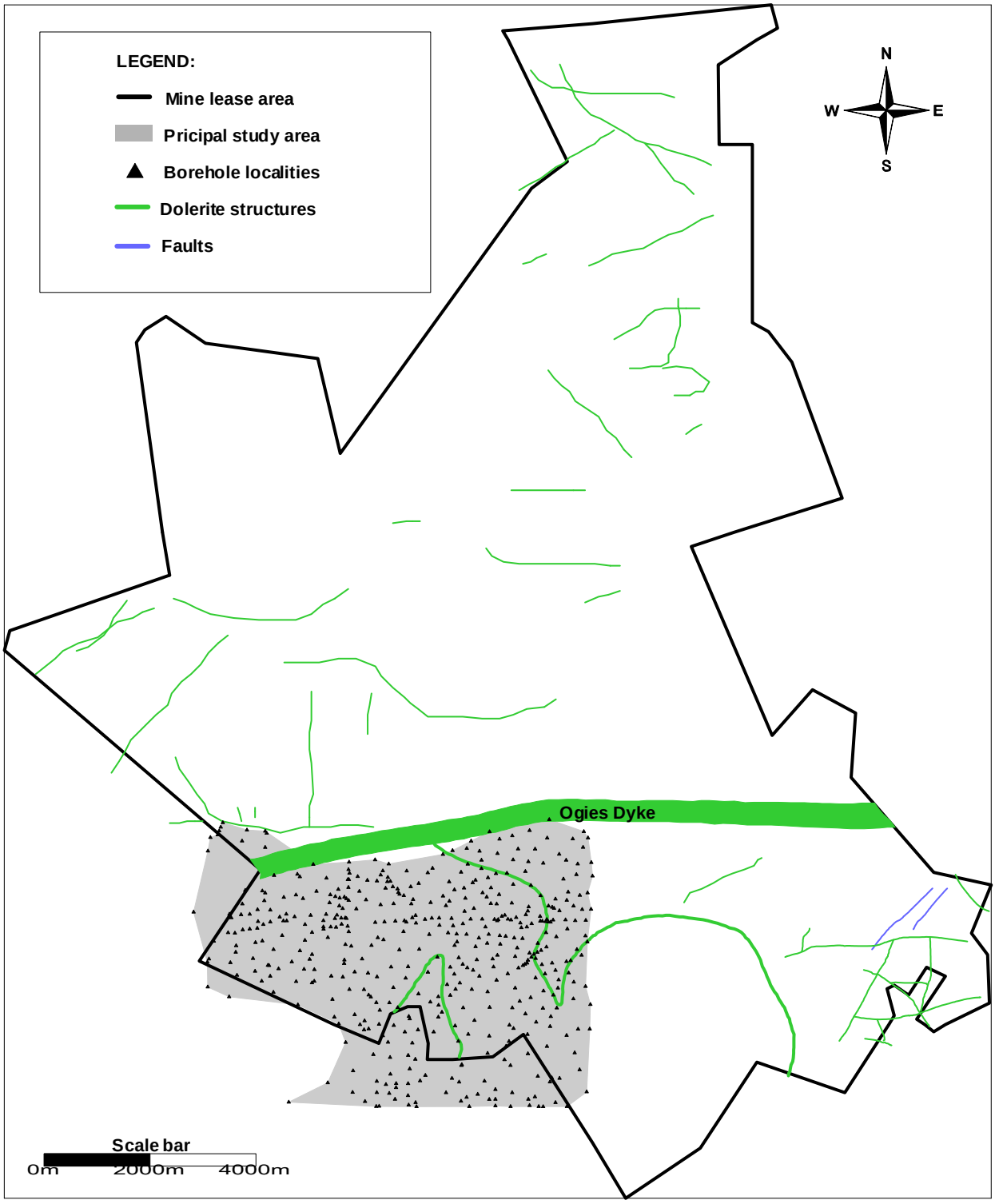

Figure 4.6: ***Map showing the mine lease area of Bank Colliery and the location of the principle study area with respect to dolerite structures digitised from mine plans.***

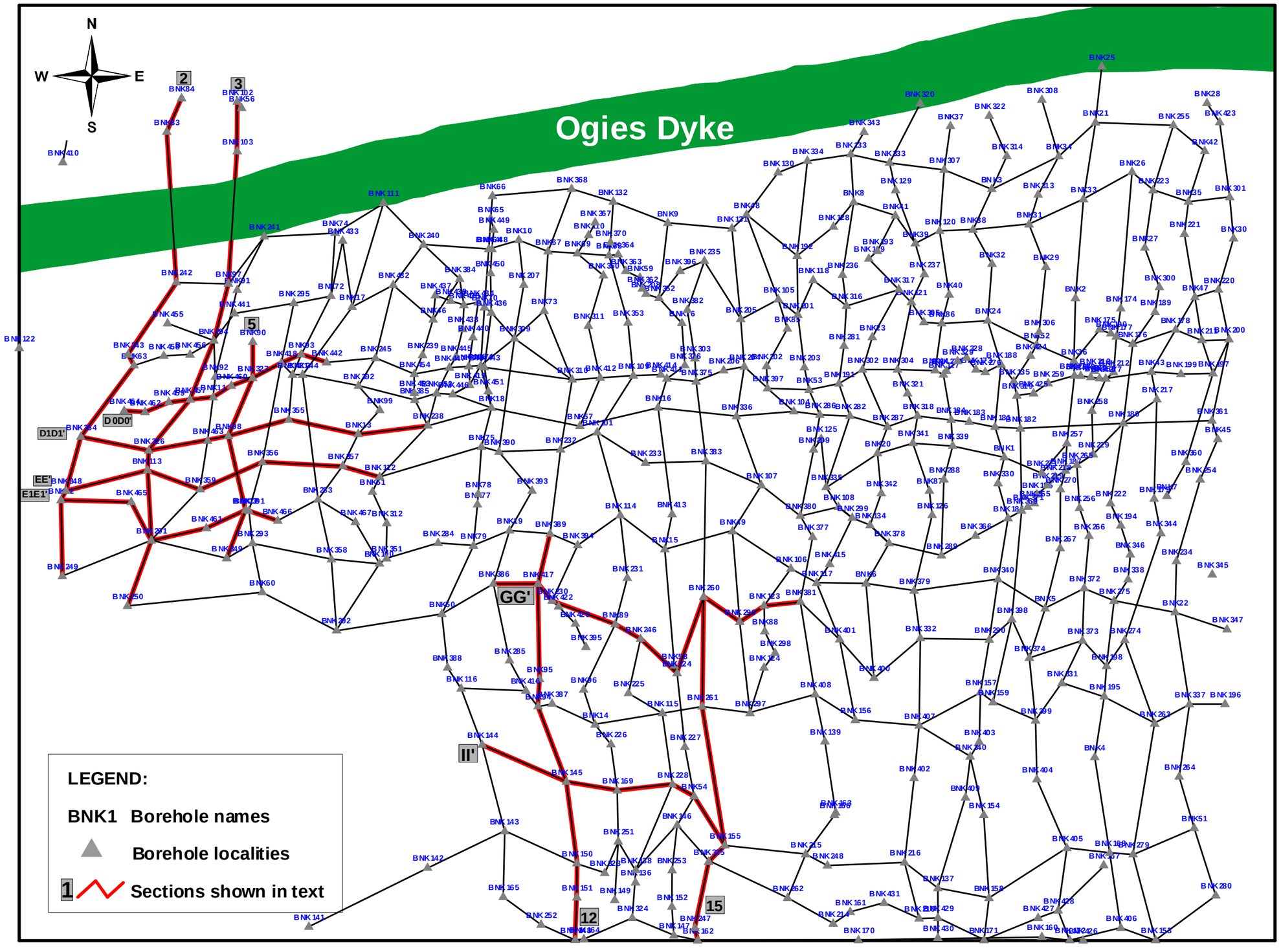

Figure 4.7: Geological cross-section lines (selected cross-section lines in red with their names attacthed to them are referred to in the text for discussion).

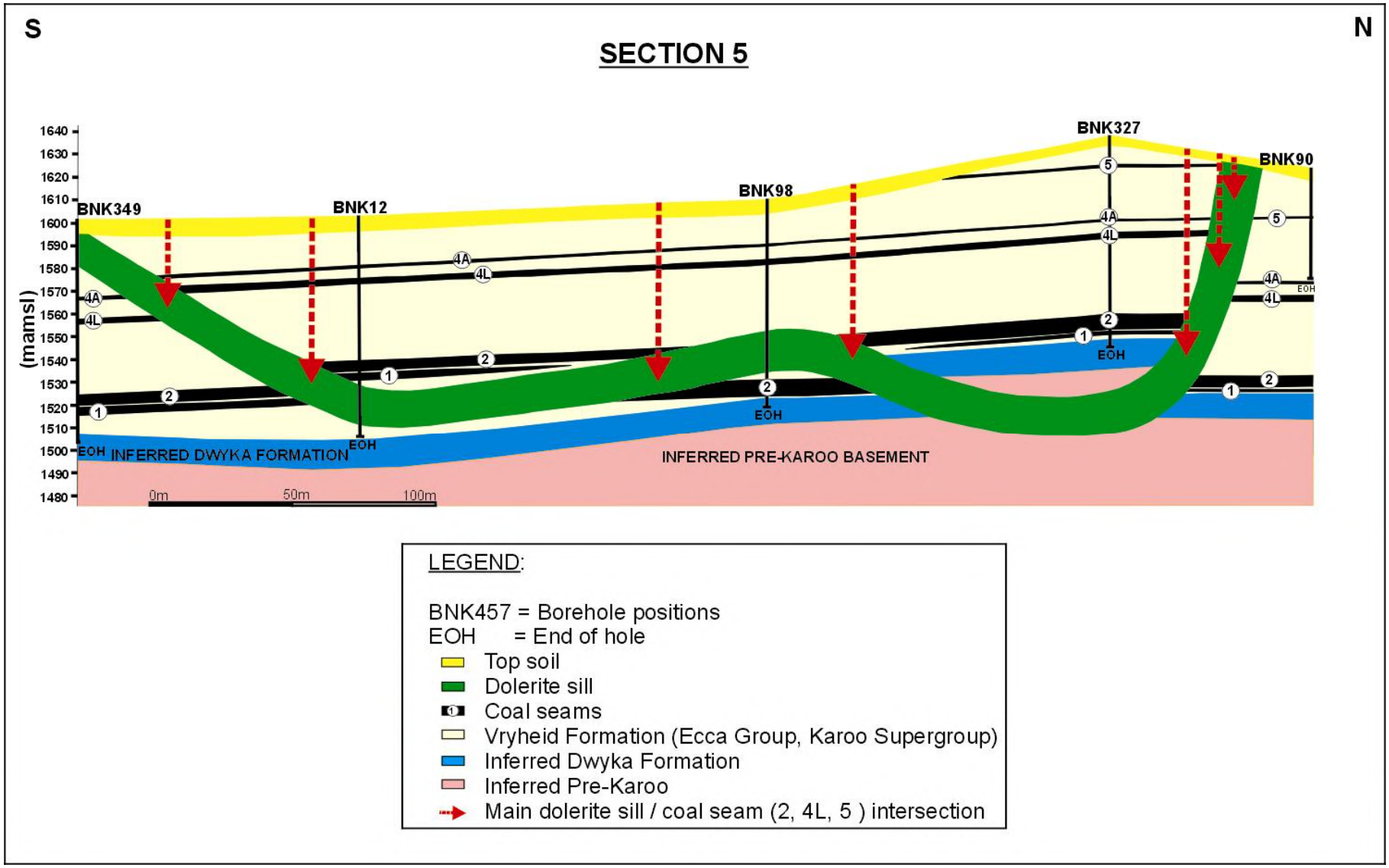

Figure 4.8: North-south geological cross-section 5 showing the main sill interpretation.

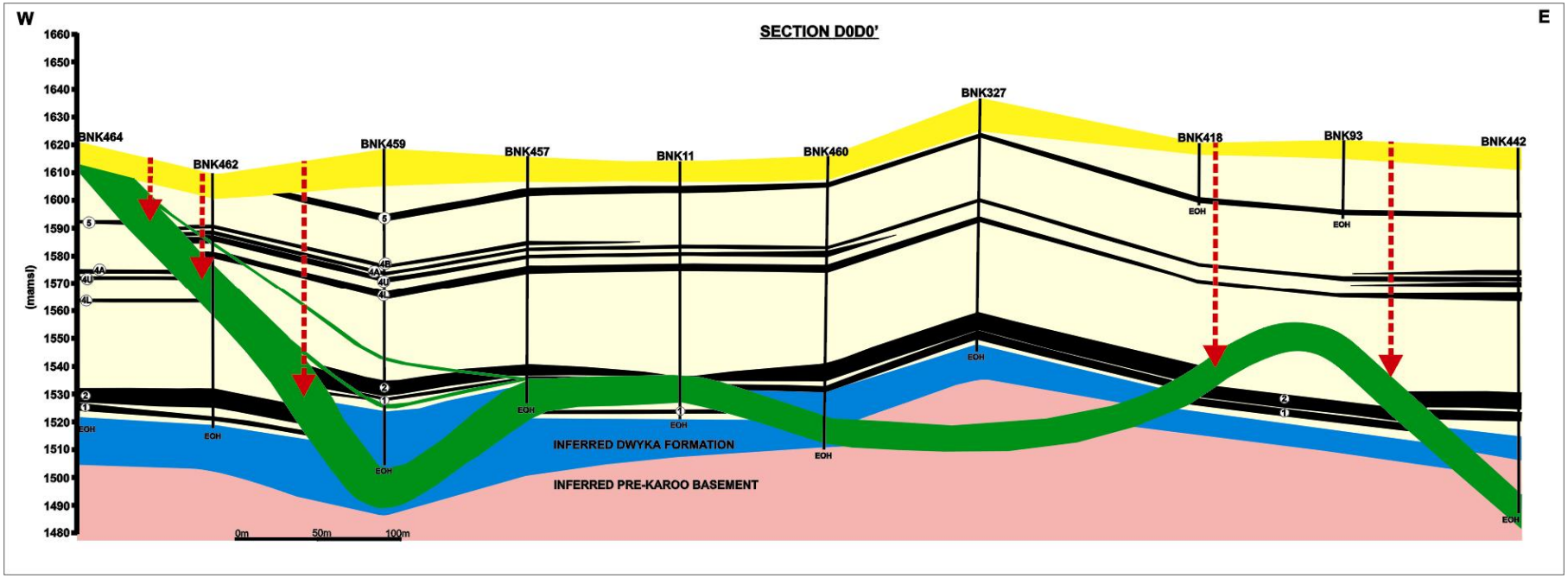

Figure 4.9: East-west geological cross-section D0D0' showing the main sill interpretation.

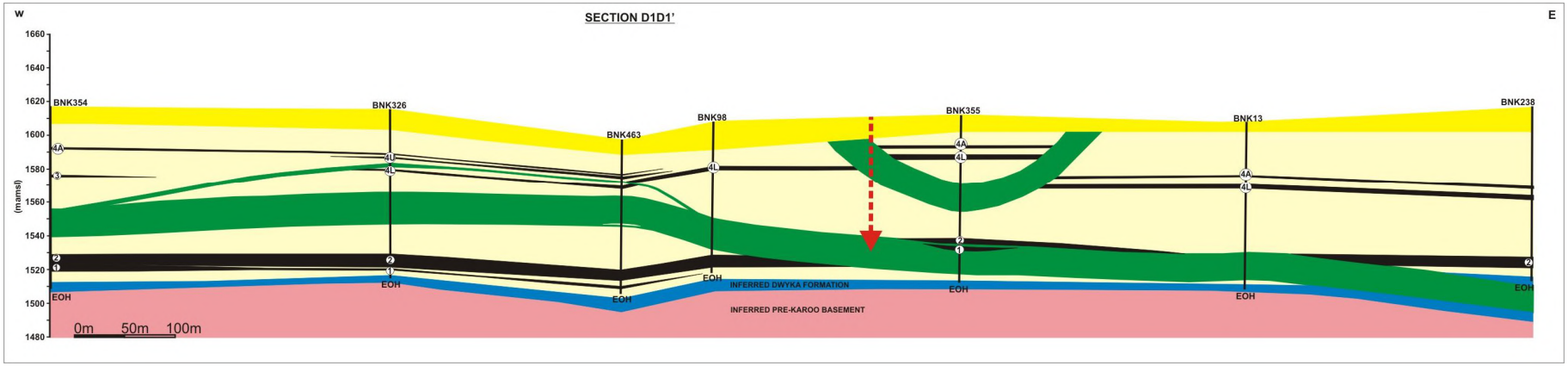

Figure 4.10: East-west geological cross-section D1D1' showing the main sill interpretation.

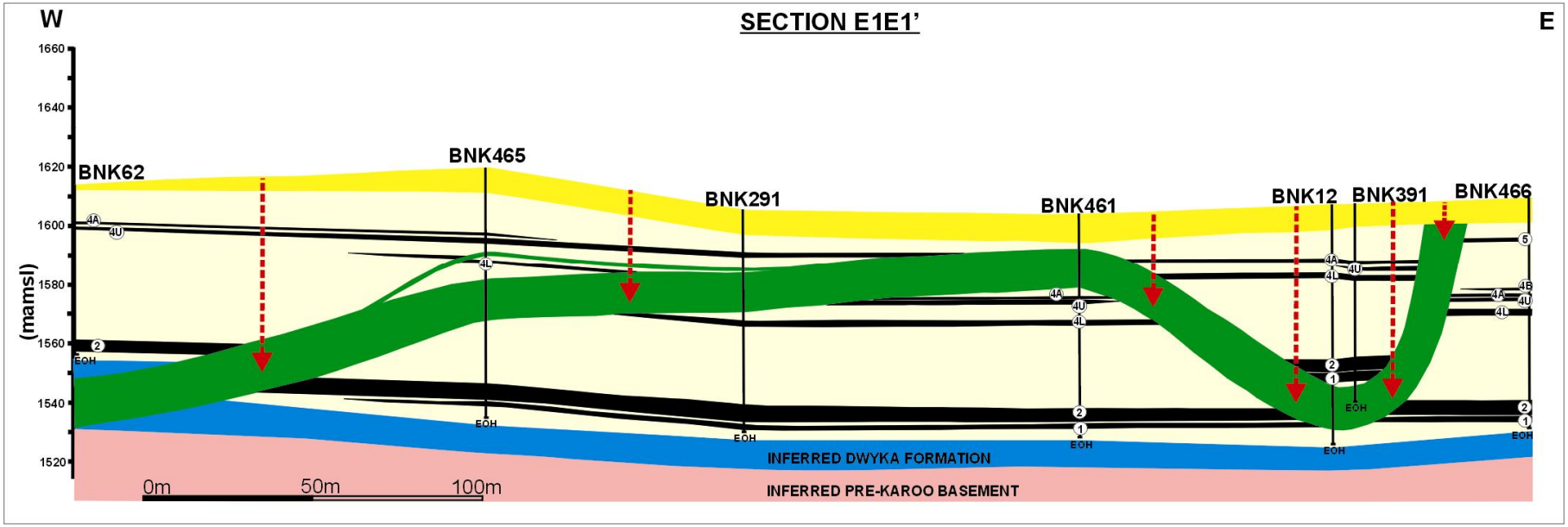

Figure 4.11: East-west geological cross-section E1E1' showing the main sill interpretation.

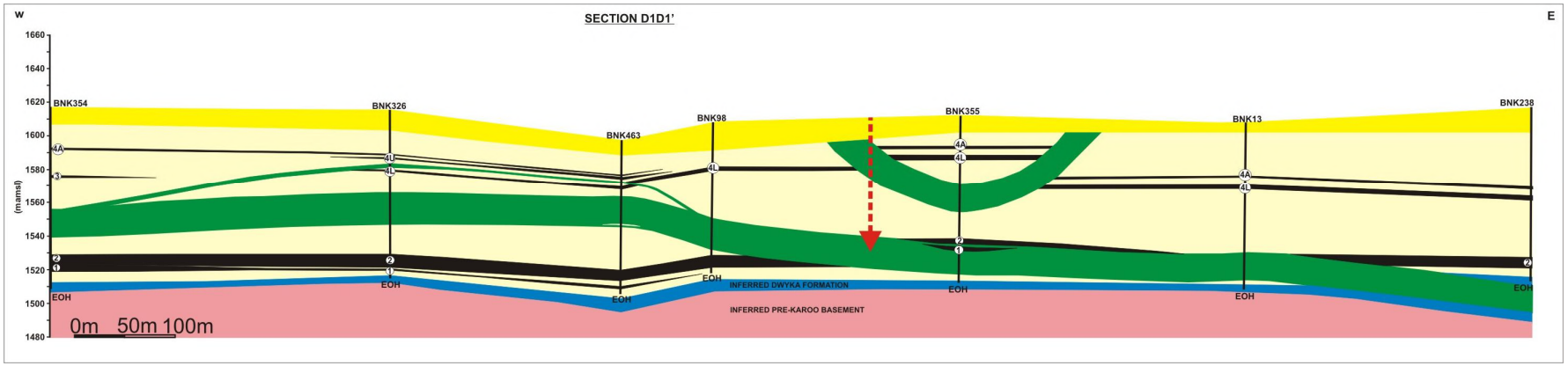

Figure 4.12: East-west geological cross-section EE' showing the main sill interpretation.

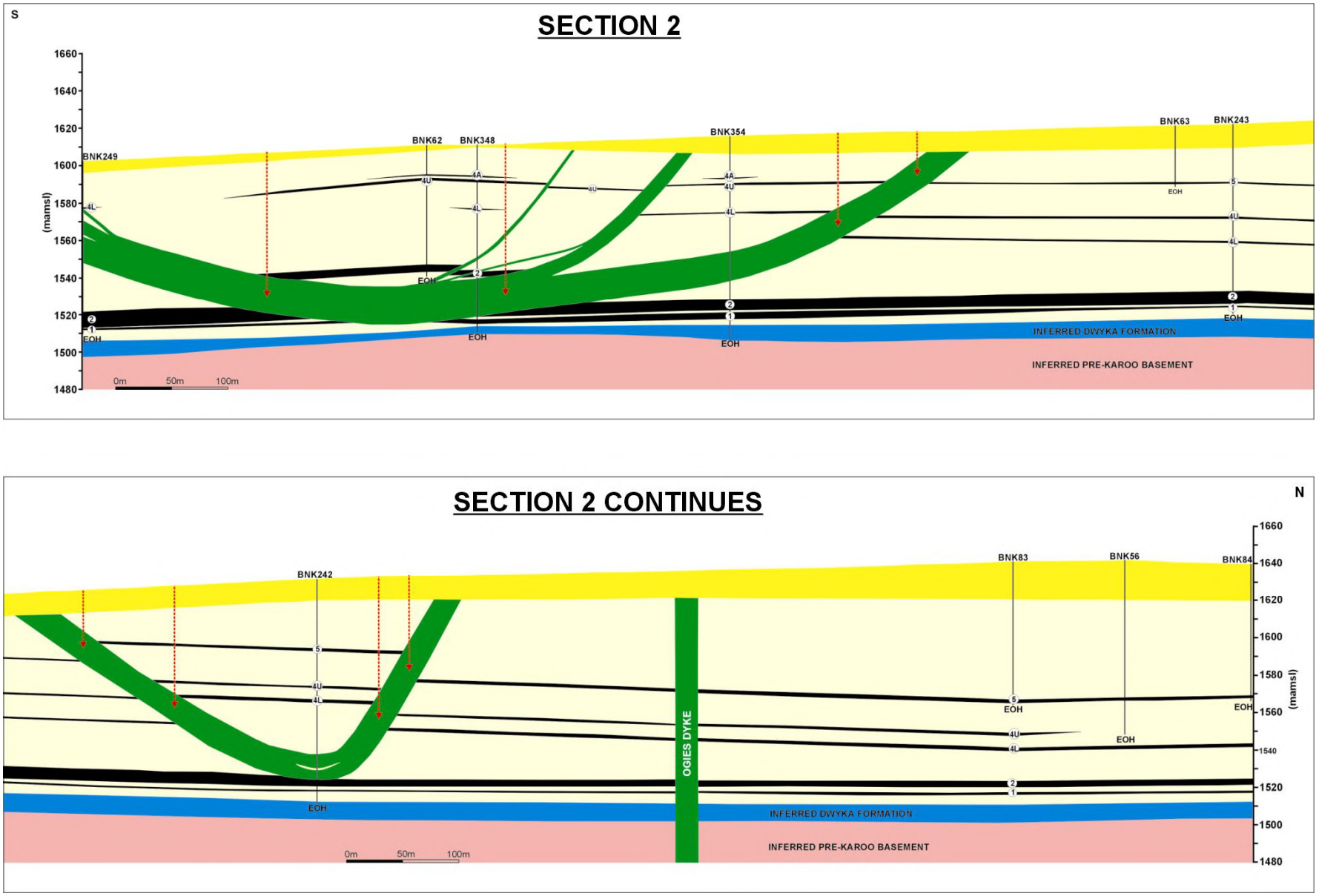

Figure 4.13: East-west geological cross-section 2 showing the main sill interpretation.

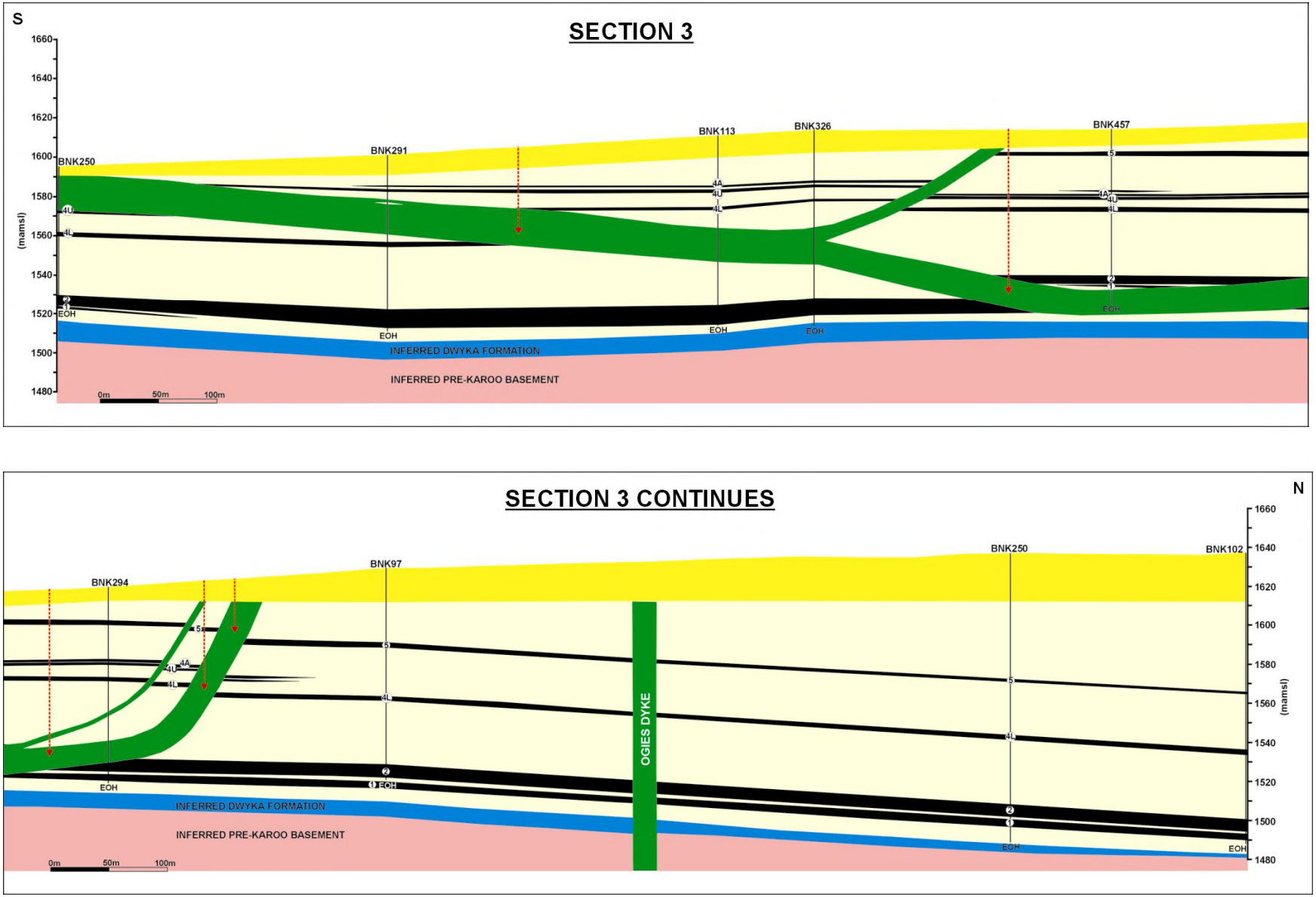

Figure 4.14: East-west geological cross-section 3 showing the main sill interpretation.

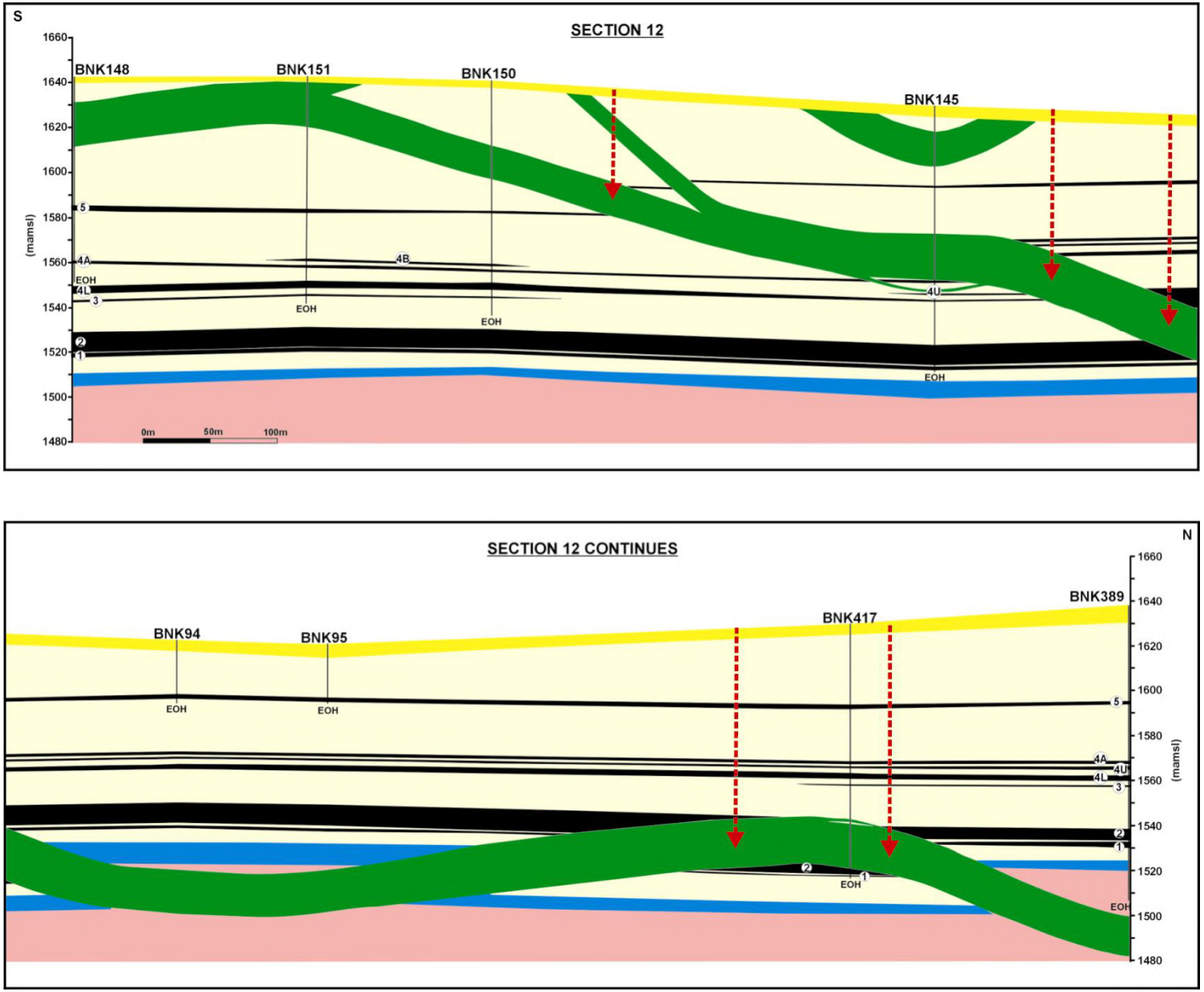

Figure 4.15: North-south geological cross-section 12 showing the main sill interpretation.

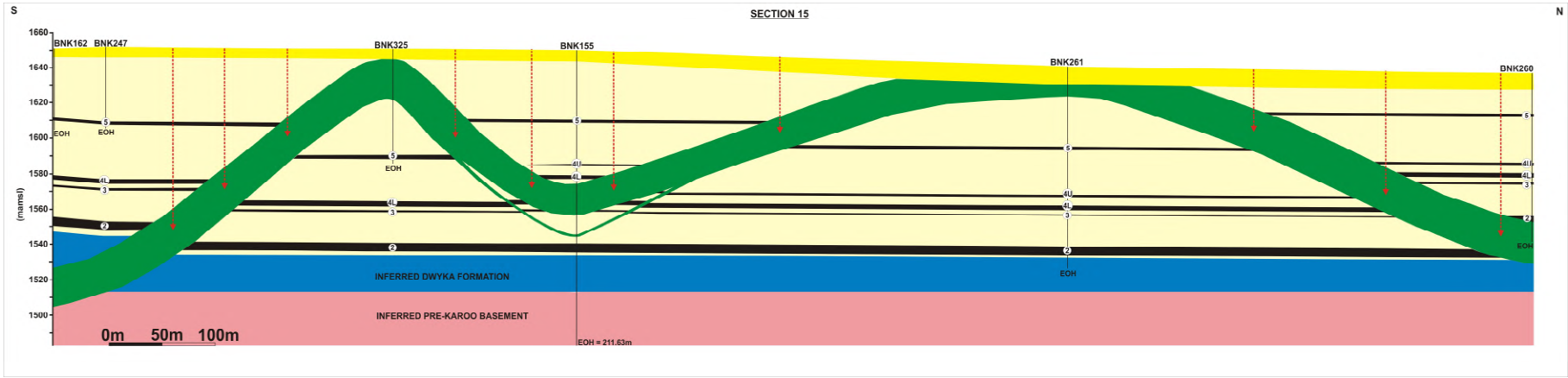

Figure 4.16: North-south geological cross-section 15 showing the main sill interpretation.

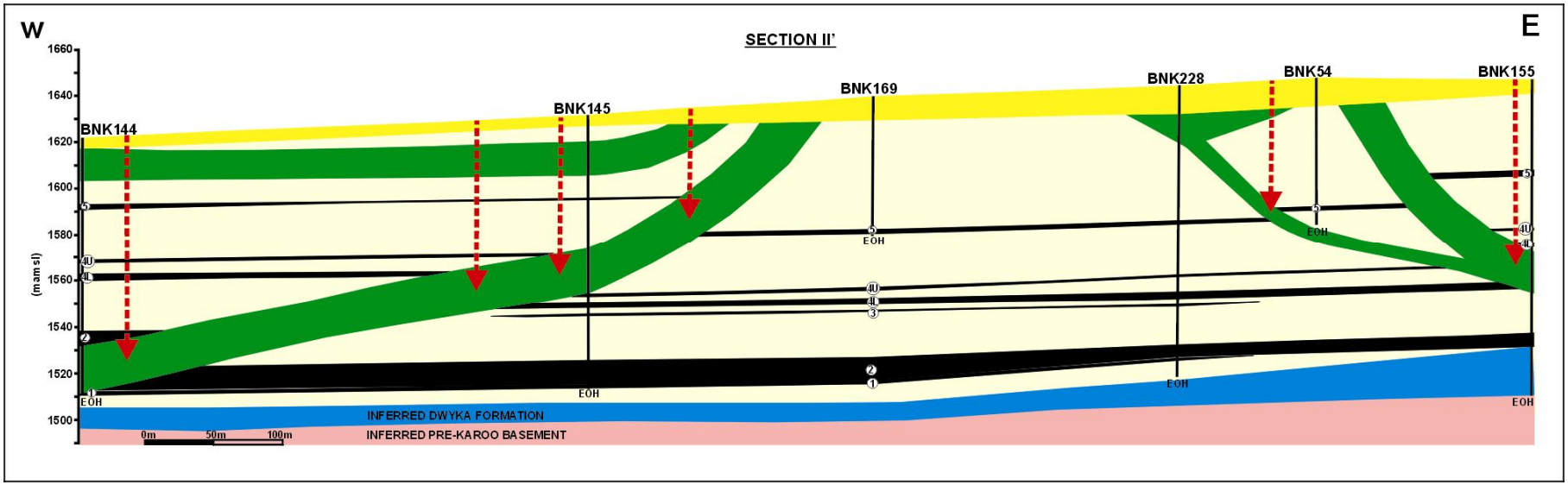

Figure 4.17: East-west geological cross-section II' showing the main sill interpretation.

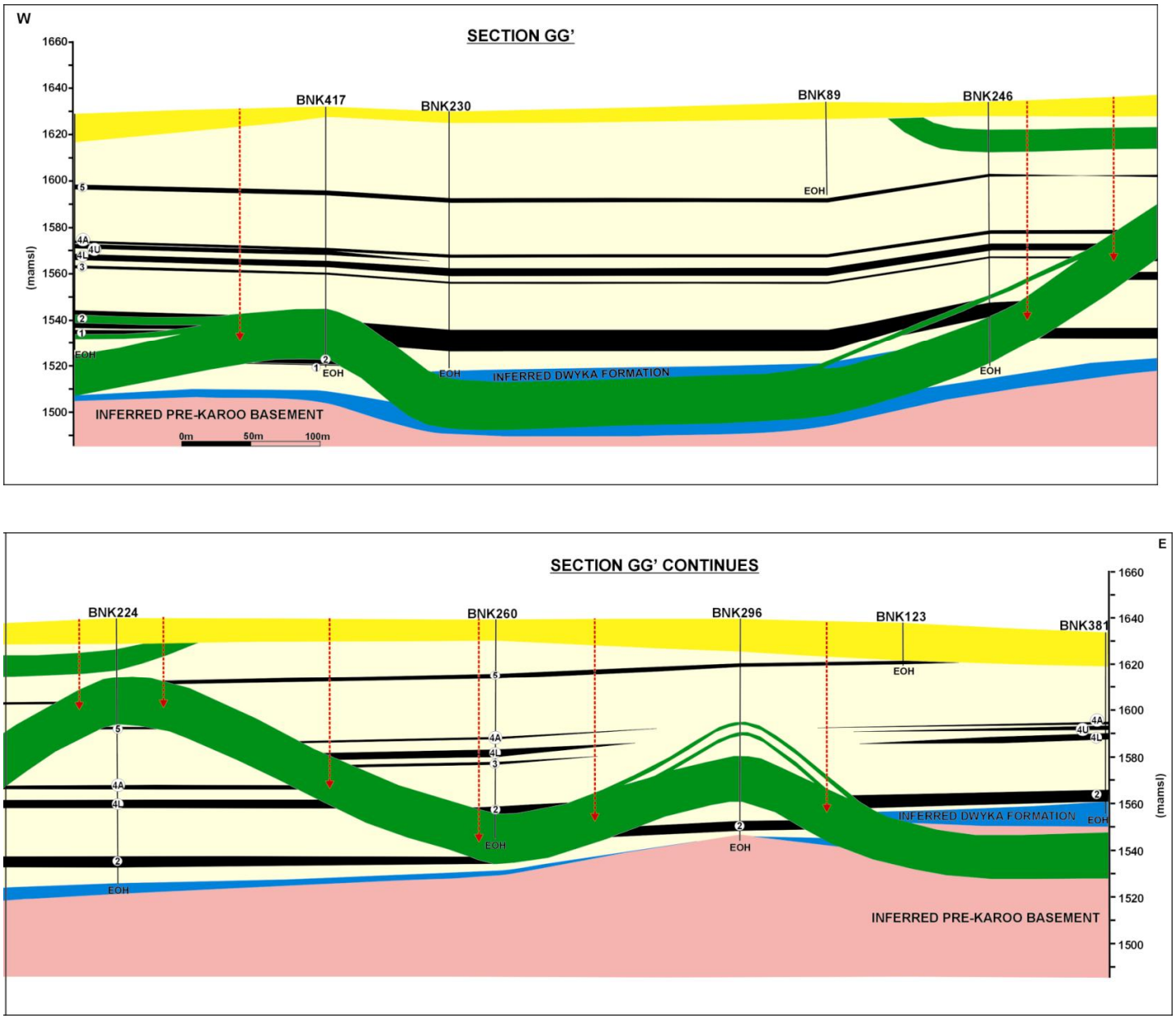

Figure 4.18: East-west geological cross-section GG' showing main sill interpretation.

4.2.3 SUMMARY AND CONCLUSIONS

Comparing the physical appearance of the ± 20m sill in the Witbank Coalfield with the B8 sill in the Secunda Coalfield, the two sills have a number of properties in common. However, these physical property comparisons are not precise and it is therefore suggested a detailed geochemical analysis focussing on the mineralogy, major and trace elements be undertaken.

Table 4.1: Analogy between the occurrence and properties of the main sill in the Witbank Coalfield and the B8 sill in the Secunda Coalfield (compiled from Van Niekerk, 1995).

PARAMETER	WITBANK COALFIELD (MAIN SILL)	SECUNDA COALFIELD (B8)
Width	±20m	4-26m
Consistancy	Bifurcates regularly, rejoining the main sill, <1m thick	Bifurcates regularly, rejoining the main sill, <1m thick
Behaviour/ geometry	Undulating – dome and basin geometry	Undulating – dome and basin geometry
Relation to Pre-Karoo topography and coal seams	Occasional relationship	Occasional relationship
Host rock assimilation	Minimal, remains *in-situ*, invariably sharp and smooth contacts	Minimal, remains *in-situ*, invariably sharp and smooth contacts
Intrusion angle	Moderate to very steep intrusion angles -dyke-like character	<60° occasionally, commonly 65°- 90° intrusion angles occur – dyke-like character
Coal contacts	Displaces rather than replaces the coal	Occasional irregularities, displaces rather than replace the coal
Host rock deformation structures	Not available for analysis	Variable: deformation depends on the host rock type and the intrusion thickness

4.3 GEOMETRY OF THE SILL

To better understand geological controls on dolerite intrusions, the scale and dimension of a study is critical. A slightly different approach was followed in this study compared with similar previous investigations (Van Niekerk, 1995; Blignaut, 1952; Chevallier and Woodford, 1999).

This section aims to establish the geometry of the sill. In addition, the structural analysis from digitised mine plans is included. Intersection positions between the main sill and the coal seams from the two-dimensional cross-sections were transferred onto a structure map (Figure 4.19). The apparent strike direction of the main sill was mapped and its direction of dip ascertained. The No. 5 Coal Seam is locally eroded preventing the mapping of the No. 5 Coal Seam intersection positions.

It is therefore possible to assess the relative position of the sill in relation to the pre-Karoo topography, coal seams and the inter-seam strata (Figure 4.19). In addition, this map provides the third dimension to the two-dimensional geological cross-section interpretations that is significantly useful in quantifying the metamorphic effect the sill had on the coal seams. Shaded areas on the map show where the sill uplifted and intruded underneath the No. 2 Coal Seam. Nearly 80% of the study area containing the most economical No. 2 Coal Seam was displaced and uplifted. The transgressive mode of the sill is well preserved in the country rock over much of the principal study area, except for several of its domal parts that had been eroded.

The sill/coal seam intersection map superimposed on a contour map of the main sill's floor elevation (Figure 4.20) evidently reveals its geometry and also represents the intrusion plane of the main sill. Approximation of the sill/coal seam intersection lines with straight lines is plotted on a rose diagram to assess its predominant strike of intrusion. The main sill most frequently intruded with strike directions of NNE, NS and ENE (Figure 4.23).

Dolerite offshoots from the main sill mostly occur in disarray and their propagation paths are chaotic. With a dolerite isolith map, it would be possible to map the amount of offshoots into which the main sill has bifurcated for a given set of boreholes in a specific area. However, there are significant amounts of doleritic material that is not encountered during drilling and the degree of uncertainty would lead to misinterpretation. Regardless of that, the main sill and dolerite offshoots are interpreted using cross-sections. Approximate positions where offshoots started bifurcating from and/or rejoining the main sill are plotted on the cross-section lines between adjacent boreholes in Figure 4.21. Where possible, those start or rejoin positions where offshoots bifurcated from the main sill between section lines were joined up using red dashed lines. It is therefore

conceivable that annotation of numbers to the amount of offshoots, a decrease by one would mean rejoining, whilst an increase by one would mean bifurcation between cross-section lines. It can so far be concluded that the main sill, with exception, bifurcated where it has changed its stratigraphic position either higher or lower, adopting a semi–vertical to vertical dyke-like character.

Dolerite offshoots and stringers in the No. 2 Coal Seam that were encountered as mining progressed were digitised from mine plans and measured to produce rose diagrams (Figures 4.22 and 4.24 respectively). It should be kept in mind that these dolerites are merely traces and do not necessarily represent their absolute orientation in space, but more importantly their intersection relationship with the No. 2 Coal Seam. The following definitive strike intersections with the No. 2 Coal Seam in descending frequency are revealed: EW, NW, WNW, NE, and NNW (Figure 4.24).

Also, fractures within the No. 2 Coal Seam were digitised and measured for adequate trend analysis. These fractures can, however, represent several structural domains. Firstly, they could reveal syn-depositional related structures as well as burial related jointing that preferably developed on the valley flanks of the palaeo-highs as a result of differential compaction and fracturing of the sedimentary rocks. Where these fractures occur close to dolerites they are intrusion related features, which are possibly either pressure-release and/or cooling joints. Furthermore, the EW striking Ogies Dyke intrusion undoubtedly has caused the coal seams to fracture for an unknown distance. Syn-tectonic structures contained within the Vryheid Formation i.e. lineaments associated with Gondwana break-up also could have produced large scale regional joint sets within the No. 2 Coal Seam.

Fractures within the No. 2 Coal Seam predominantly strike in two directions NS and ENE, consistent with the effect of the Ogies Dyke intrusion. This dyke seems to have had a large effect not only in controlling the dolerite intrusion, but also in significantly fracturing the No. 2 Coal Seam (Figure 4.25).

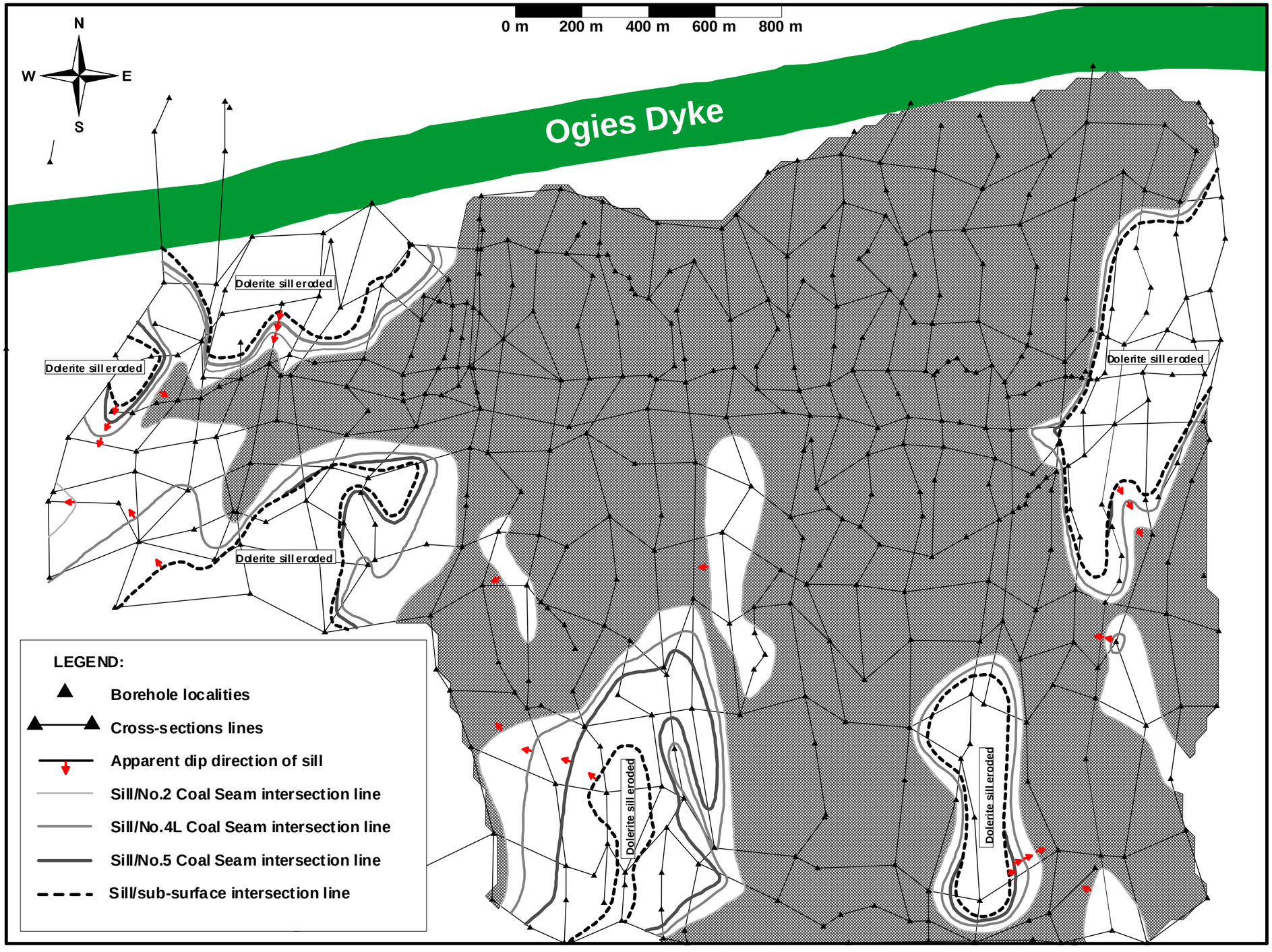

Figure 4.19: Sill/coal seam intersection map (intersection lines represent the apparent strike of the main sill with its associated dip direction. The hatched area shows where the sill is present below the No.2 Coal Seam. The thickness of the Ogies Dyke is no to scale.

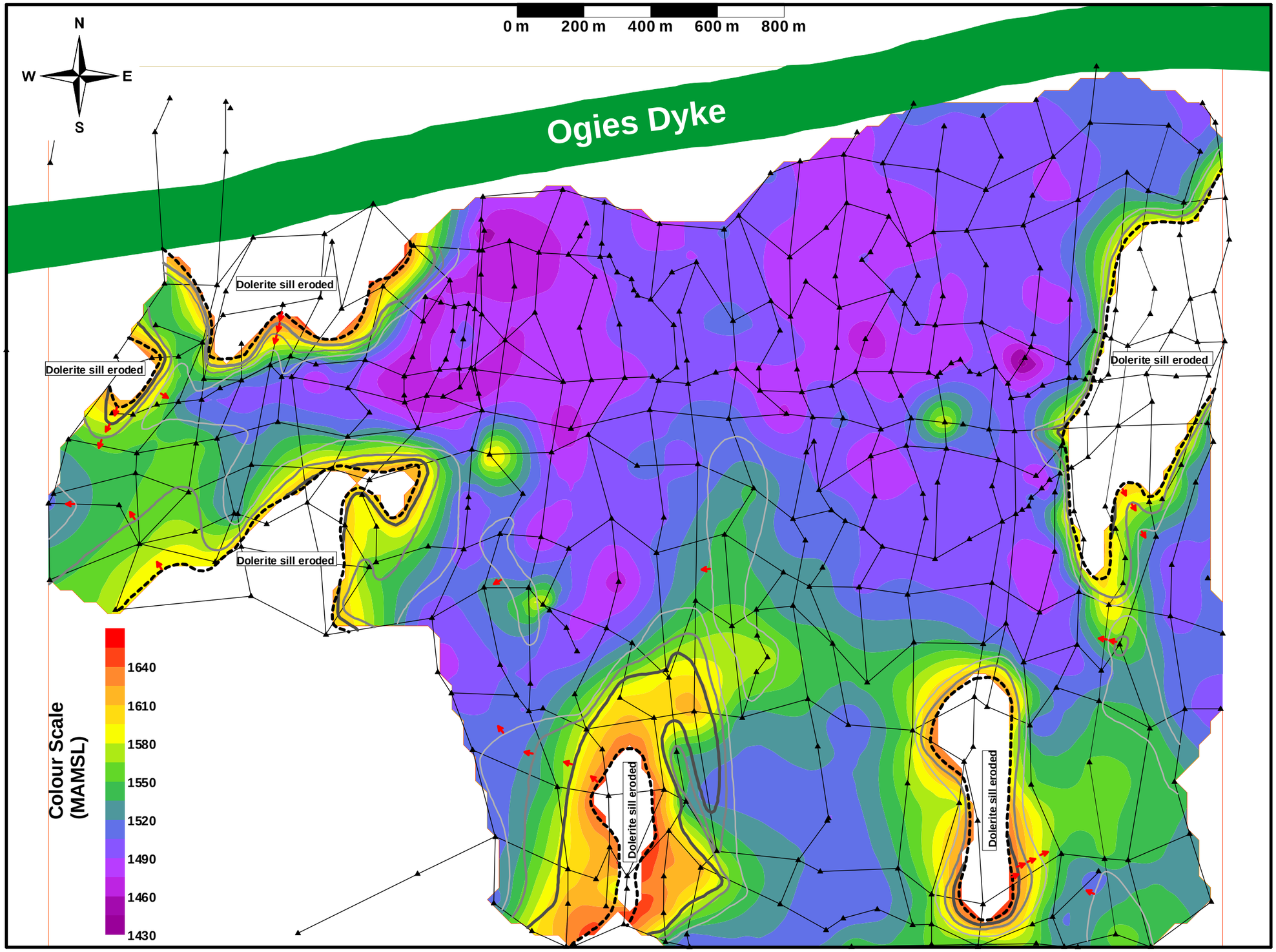

Figure 4.20: Sill/coal seam intersection map superimposed on the sill's floor elevation isopleth map (The floor elevation of the main sill represents its geometry and also the main intrusion plane).

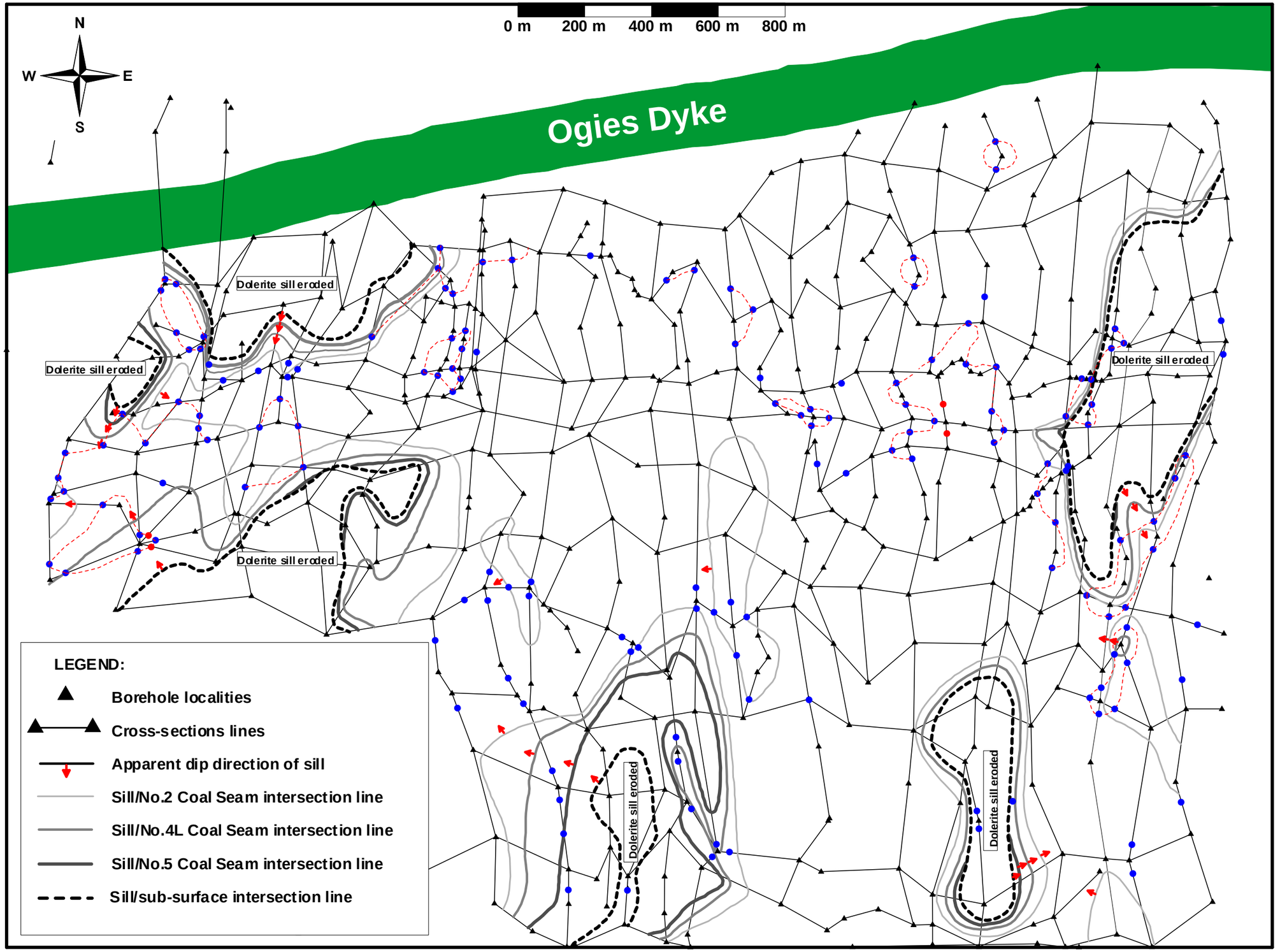

Figure 4.21: Dolerite bifucation map (The blue dots denote the interpreted starting and/or rejoining of the offshoots form the main sill. The red dashed lines show where these offshoots re-join).

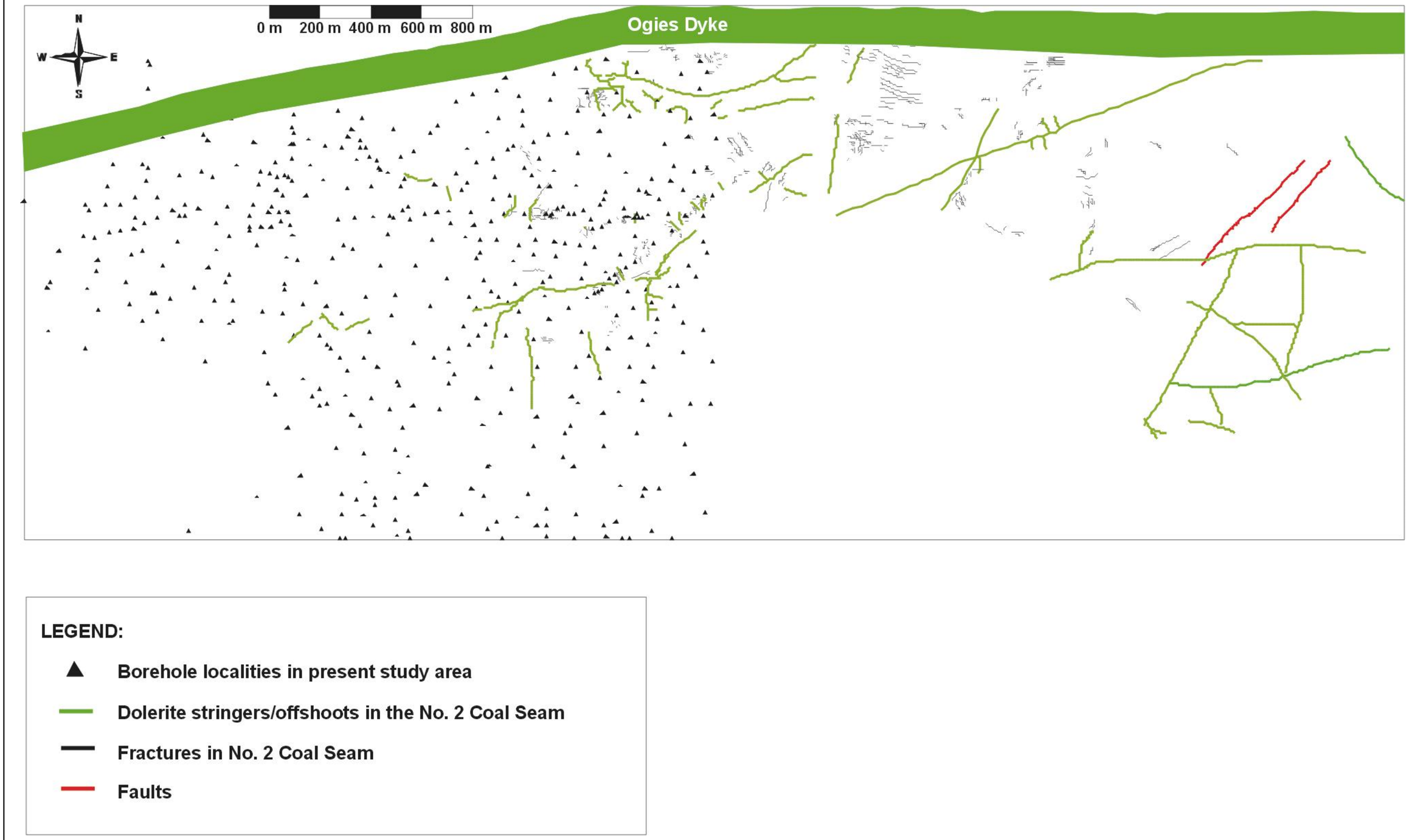

Figure 4.22: Dolerite dykes/offshoots (traces) and fractures within No. 2 Coal Seam.

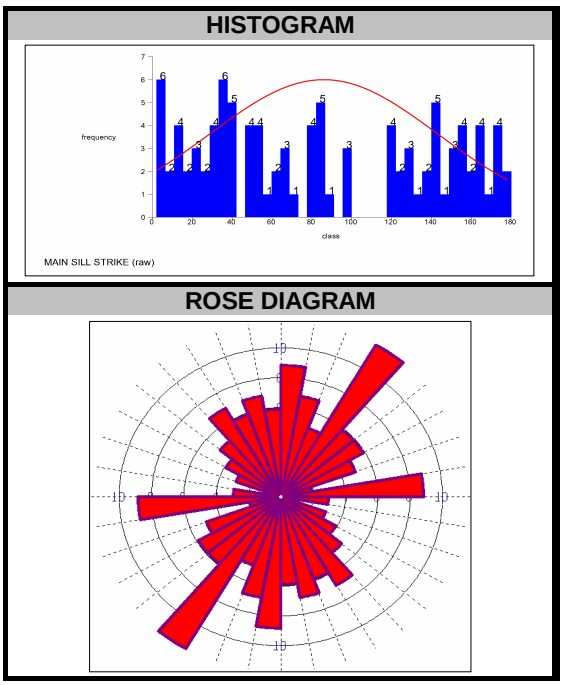

CLASSICAL STATISTICS	
VARIABLE	MAIN SILL STRIKE (DATA >180deg NORMALISED TO 180deg RANGE)
NUMBER OF SAMPLES	102
MINIMUM VALUE	2
MAXIMUM VALUE	180
MEAN	85.97
VARIANCE	3268.34
STANDARD DEVIATION	57.17
COEFFICIENT OF VARIATION	0.67
SKEWNESS	0.17
KURTOSIS	1.58
TRIMEAN	84.25
BIWEIGHT	84.64
MAD	53.14
ALPHA	231.18
SICHEL-T	Not Calculated

Figure 4.23: Strike directions preferably intruded by the main sill.

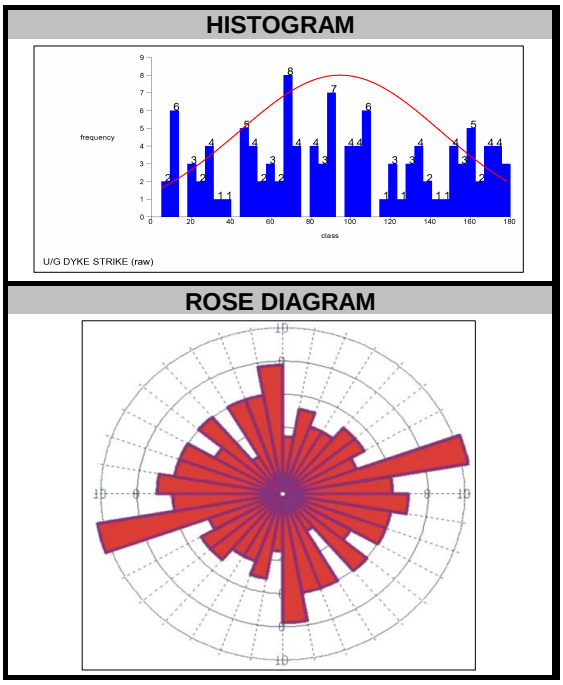

CLASSICAL STATISTICS	
VARIABLE	U/G DYKES (DATA >180deg NORMALISED TO 180deg RANGE)
NUMBER OF SAMPLES	116
MINIMUM VALUE	5
MAXIMUM VALUE	180
MEAN	94.58
VARIANCE	2533.21
STANDARD DEVIATION	50.33
COEFFICIENT OF VARIATION	0.53
SKEWNESS	0.01
KURTOSIS	1.93
TRIMEAN	92.75
BIWEIGHT	93.74
MAD	42.26
ALPHA	397.50
SICHEL-T	Not Calculated

Figure 4.24: Strike frequency of dykes and offshoots from sills as traces, encountered as mining proceeded.

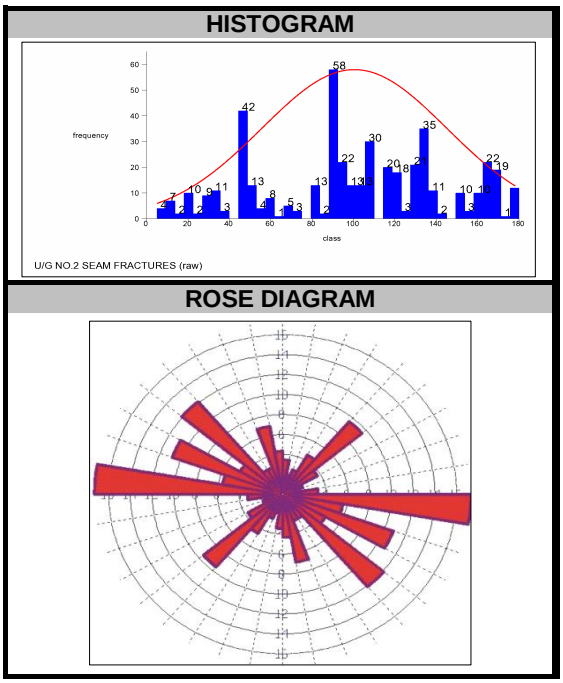

VARIABLE	FRACTURES IN NO.2 SEAM (DATA >180deg NORMALISED TO 180deg RANGE)
NUMBER OF SAMPLES	462
MINIMUM VALUE	5
MAXIMUM VALUE	180
MEAN	100.40
VARIANCE	1998.31
STANDARD DEVIATION	44.70
COEFFICIENT OF VARIATION	0.45
SKEWNESS	-0.18
KURTOSIS	2.19
TRIMEAN	100.00
BIWEIGHT	101.03
MAD	33.97
ALPHA	1243.33
SICHEL-T	Not Calculated

Figure 4.25: Strike frequency of fractures mapped in the No. 2 Coal Seam as mining proceeded.

4.4 RECONSTRUCTED SEDIMENTARY UNITS

4.4.1 INTRODUCTION

The sedimentary rocks of sequence of succession are reconstructed by removing the main sill from the stratigraphy. The reconstruction is aimed at determining if a spatial relationship exists between the coal seams, the intra-seam strata and the main sill prior to the intrusion event. Borehole information on the elevation of the pre-Karoo basement is sparse as borehole penetration was terminated at the bottom of the coal seam of interest. The removal of the dolerite convincingly reveals the pre-Karoo basement topography, palaeo-floor and -roof morphology, as well as the width distribution of the sedimentary units.

The following reconstructed sedimentary units were examined individually:

- No. 2 Coal Seam;
- Facies between the No. 2 Coal Seam and No. 4L Coal Seam;
- No. 4L Coal Seam;
- Facies between No.4L and No. 5 Coal Seam;
- No. 5 Coal Seam.

The examination process of the data of each unit starts with the statistical analyses thereof which includes histogram and probability plots of the palaeo floor, width and palaeo roof. A statistical report is completed for every unit and includes the following calculations:

- **MEAN**

  The MEAN is the arithmetic average of the data and is computed by dividing the sum of a set of data by the number of data points.

$$\bar{X} = \frac{1}{n}\sum X_i$$

- **VARIANCE**

  The VARIANCE describes the variability of the distribution or the spread of the data

$$S^2 = \frac{1}{n}\sum (X - \bar{X})^2$$

- **STANDARD DEVIATION**

The STANDARD DEVIATION is the square root of the variance.

- **SKEWNESS**

The SKEWNESS is a measure of the symmetry of the distribution. In a normal distribution, where the distribution is symmetric, the skewness is zero. The skewness is negative for distributions tailing to the left and positive for distributions tailing to the right.

- **KURTOSIS**

The KURTOSIS is a measure of how peaked the distribution is, or the steepness of ascent near the mode of the distribution. It has a value of zero in a normal distribution and so is a good test for distribution normality.

- **COEFFICIENT OF VARIATION**

The COEFFICIENT OF VARIATION is a measure of the relative variation of the data and is calculated by dividing the standard deviation by the mean of the distribution. It provides a very useful guide to the variability of the data and their subsequent suitability for use in geostatistics. As a general rule, those distributions with a coefficient of variation less than one should produce a reasonable variogram model; if the coefficient of variation is greater than one it implies that the data are quite variable and it is difficult to produce a good variogram model; if the coefficient of variation is greater than two there is virtually no chance of producing a good variogram model.

- **BIWEIGHT**

The BIWEIGHT is a measure of the central tendency of the distribution and is very resistant to outlier data.

- **TRIMEAN**

The TRIMEAN is the trimmed mean of the distribution and is also very resistant to outlier data.

- **MAD**

  The MAD or Median Absolute Deviation is the middle value of all the absolute deviations from the median and is also very resistant to outlier data.

- **ALPHA VALUE**

  The ALPHA value is the third parameter used in a 3-parameter log normal transformation and is sometimes called the location constant. It is calculated from the cumulative frequency distribution for untransformed data and so only has meaning for reports on raw data. A 3-parameter log normal transformation may be performed by specifying the alpha value for the raw data as the constant in a Natural Log (with constant) transformation.

- **SICHEL-T ESTIMATOR**

  The SICHEL-T estimator is a good estimator of the average of log normally distributed data and overcomes the tendency of the arithmetic mean to overestimate the average. It is a function of the mean, variance and number of samples of the log (base e) transformed data and thus has no meaning with any other transforms. It should be used with great care with geological data since even though they tend to show a highly skewed distribution they are rarely strictly log normal.

The statistical analysis is followed by contour plots of the interpolated data sets. The data is then further examined for possible relationships of the variables within the sedimentary units. This examination includes Quantile-Quantile plots (QQ-plots) and the determination of correlation coefficients by regession slope analysis.

4.4.2 NO. 2 COAL SEAM

4.4.2.1 CLASSICAL STATISTICS

Table 4.2: Classical Statistics of the No. 2 Coal Seam.

SEAM	NO.2 COAL SEAM			
VARIABLE	WIDTH	FLOOR	PALAEO-FLOOR	PALAEO-ROOF
NUMBER OF SAMPLES	333	333	333	333
MINIMUM VALUE	0.59	1487.28	1480.52	1492.31
MAXIMUM VALUE	13.77	1589.38	1574.66	1576.27
MEAN	6.97	1530.24	1519.23	1526.19
VARIANCE	5.46	223.16	238.26	202.85
STANDARD DEVIATION	2.34	14.94	15.44	14.24
COEFFICIENT OF VARIATION	0.34	0.01	0.01	0.01
SKEWNESS	0.07	0.42	0.53	0.53
KURTOSIS	2.70	4.13	3.95	4.01
TRIMEAN	6.88	1529.38	1518.16	1525.58
BIWEIGHT	6.90	1529.23	1518.03	1525.21
MAD	1.75	7.67	8.03	7.12
ALPHA	0.81	-1474.85	-1370.78	-1242.51
SICHEL-T	15788.50	Not Calculated	Not Calculated	Not Calculated

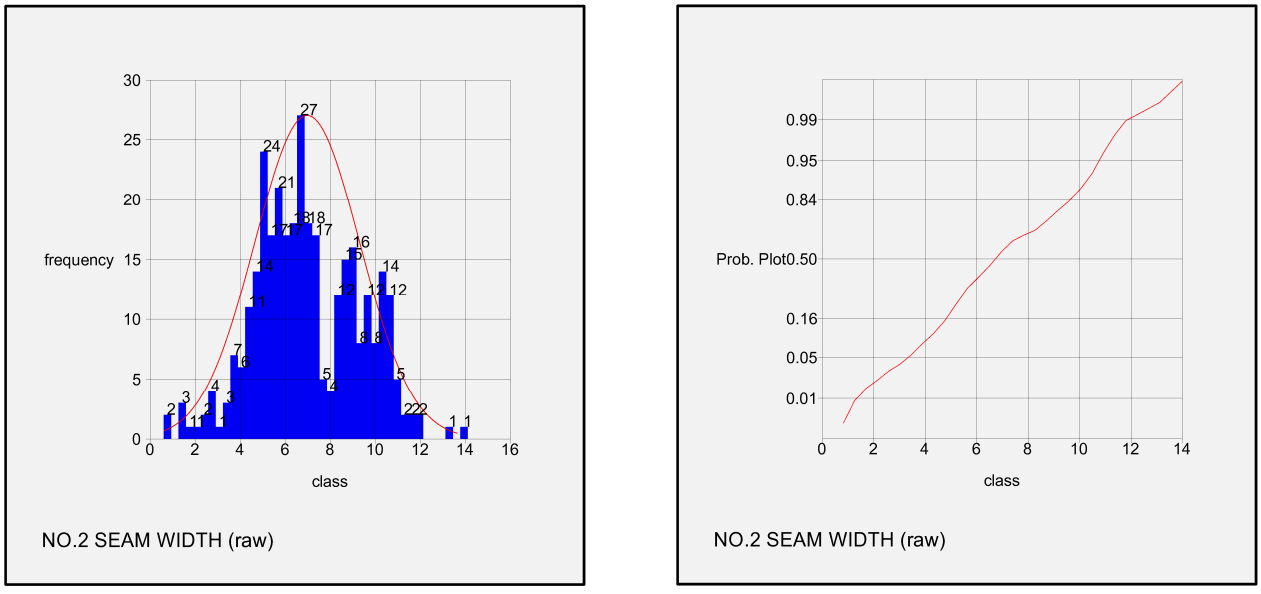

Figure 4.26: Histogram and probility plot of the No. 2 Coal Seam width.

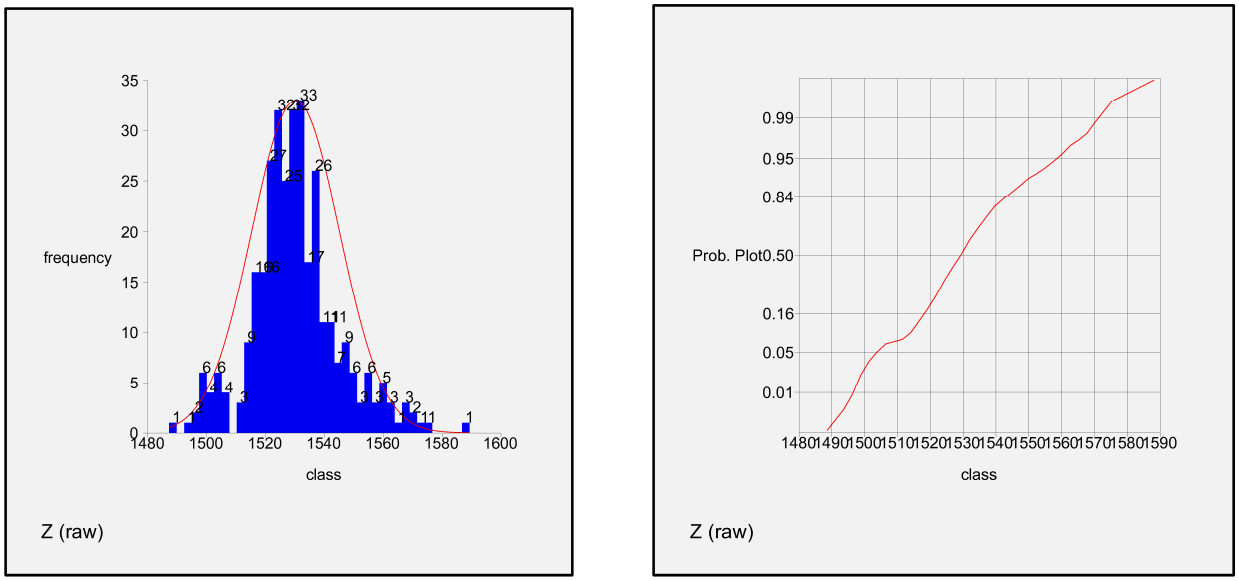

Figure 4.27: Histogram and probility plot of the No. 2 Coal Seam floor.

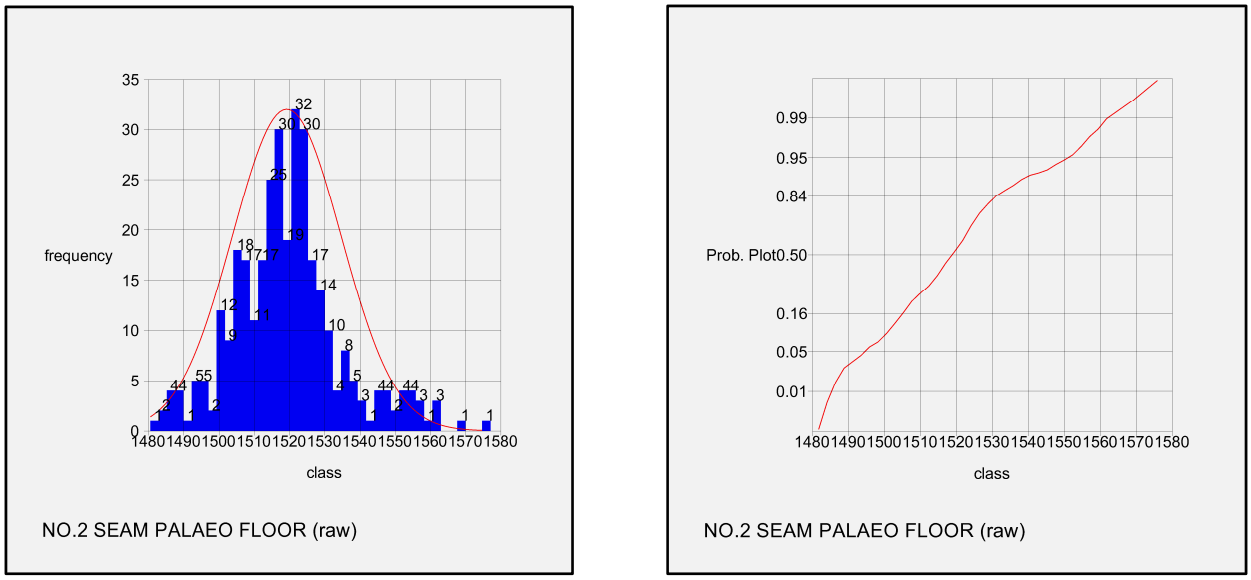

Figure 4.28: Histogram and probility plot of the No. 2 Coal Seam palaeo floor elevation.

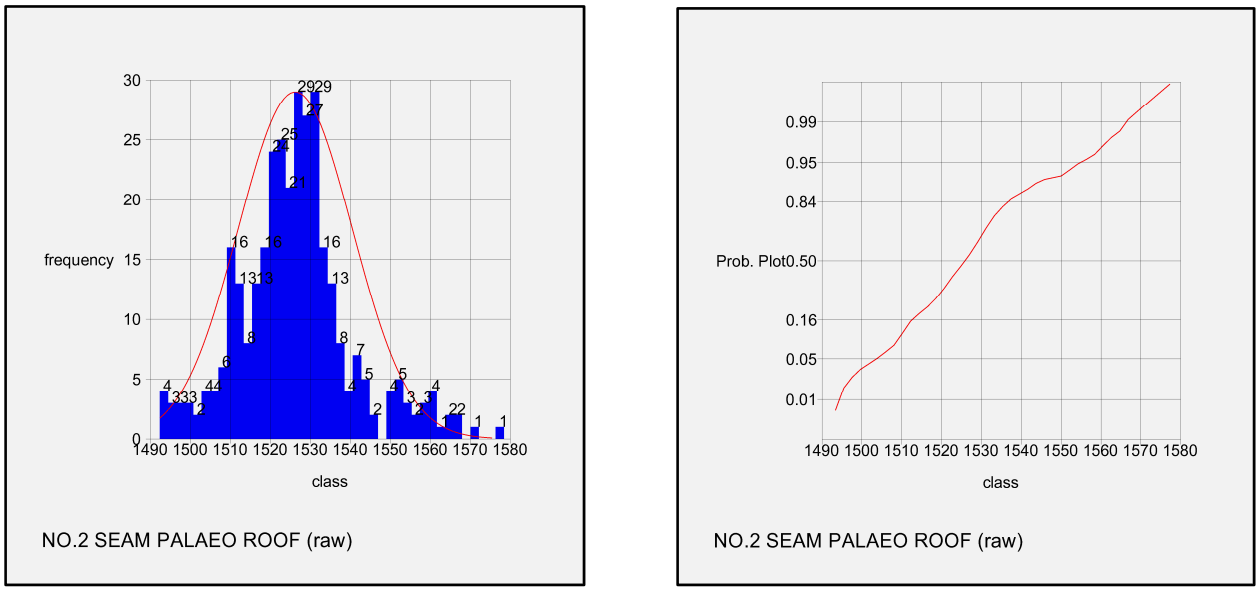

Figure 4.29: Histogram and probility plot of the No. 2 Coal Seam palaeo roof elevation.

4.4.2.2 DATA INTERPOLATION

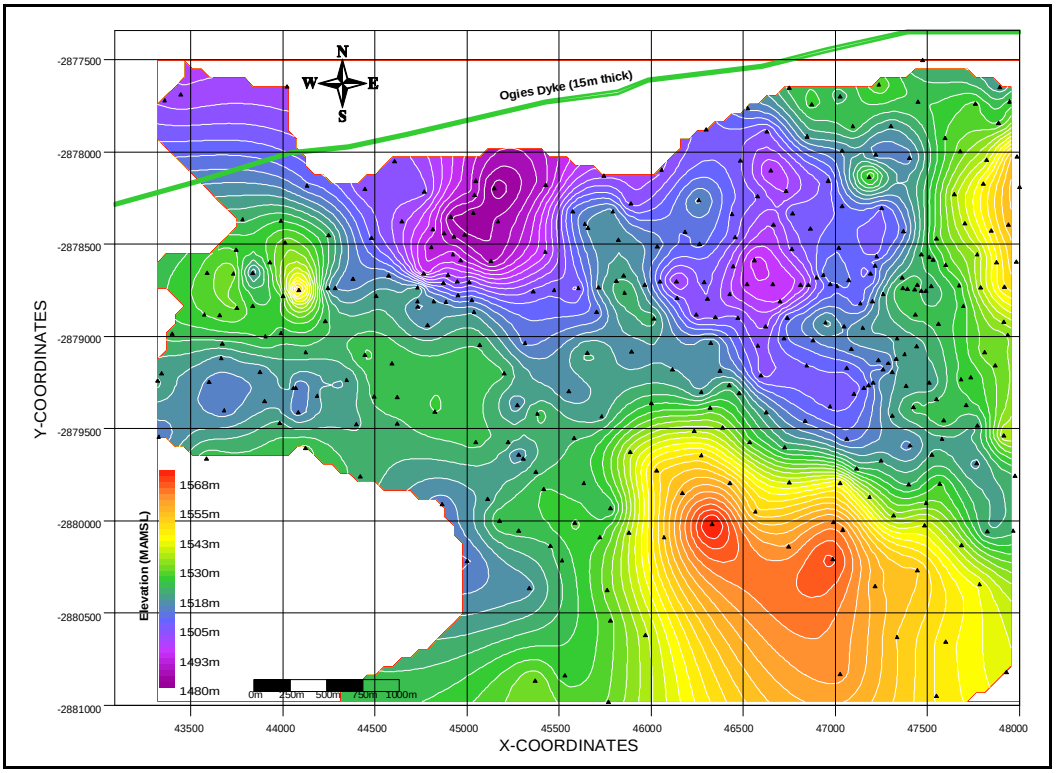

Figure 4.30: The No. 2 Coal Seam palaeo floor elevation.

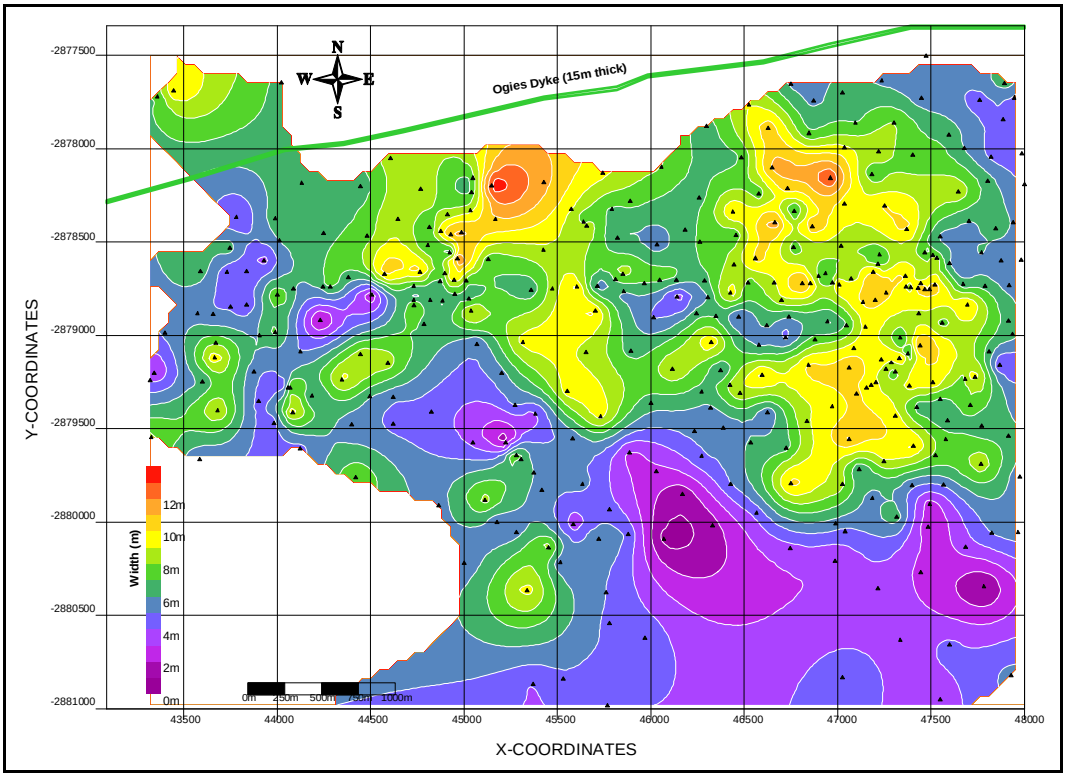

Figure 4.31: The No. 2 Coal Seam width.

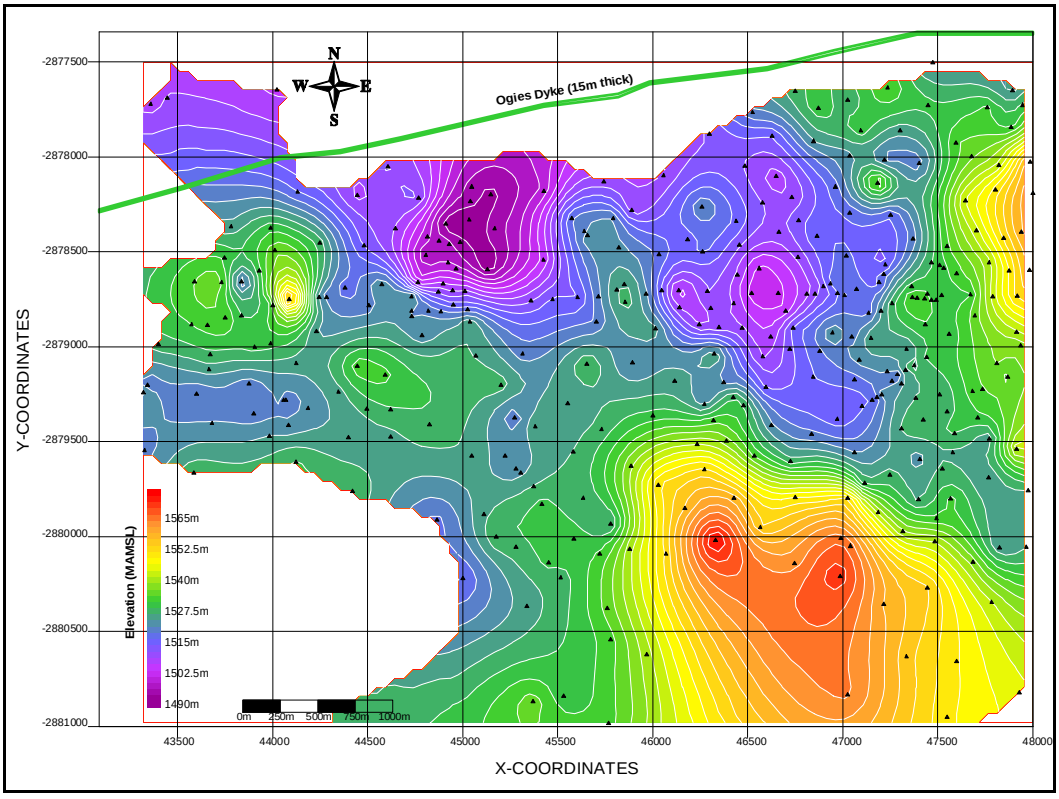

Figure 4.32: The No. 2 Coal Seam palaeo roof elevation.

4.4.2.3 DATA ANALYSIS

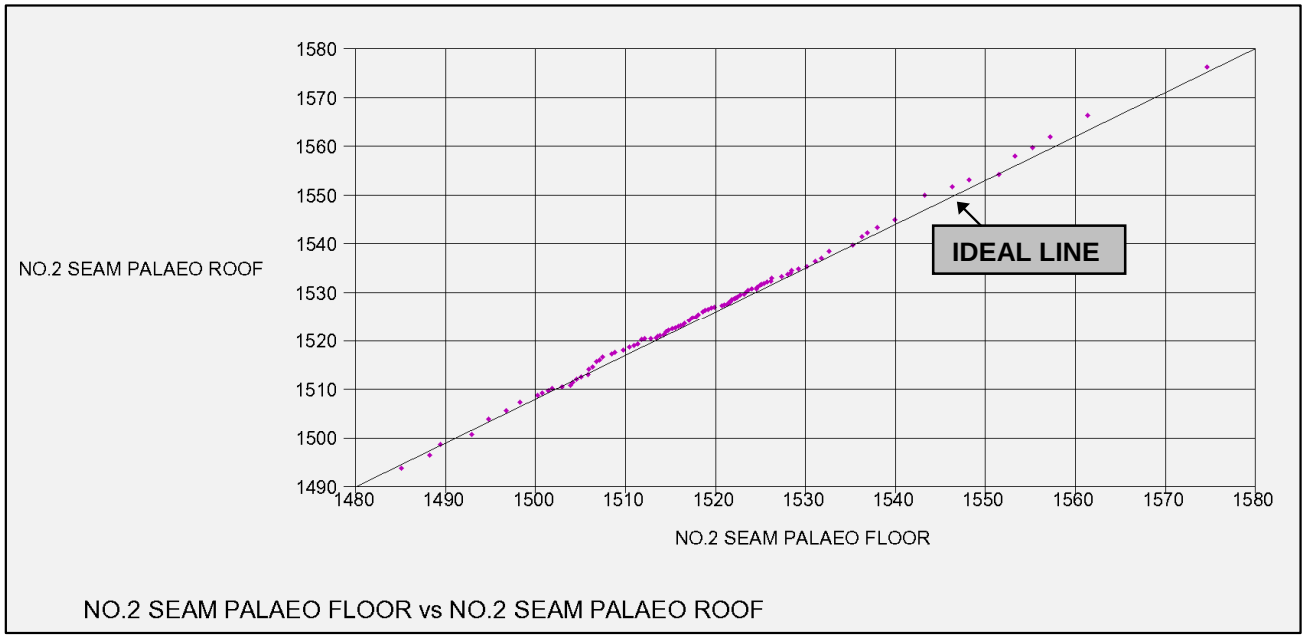

Figure 4.33: Quantile-Quantile plot of the No. 2 Coal Seam palaeo floor and roof elevations.

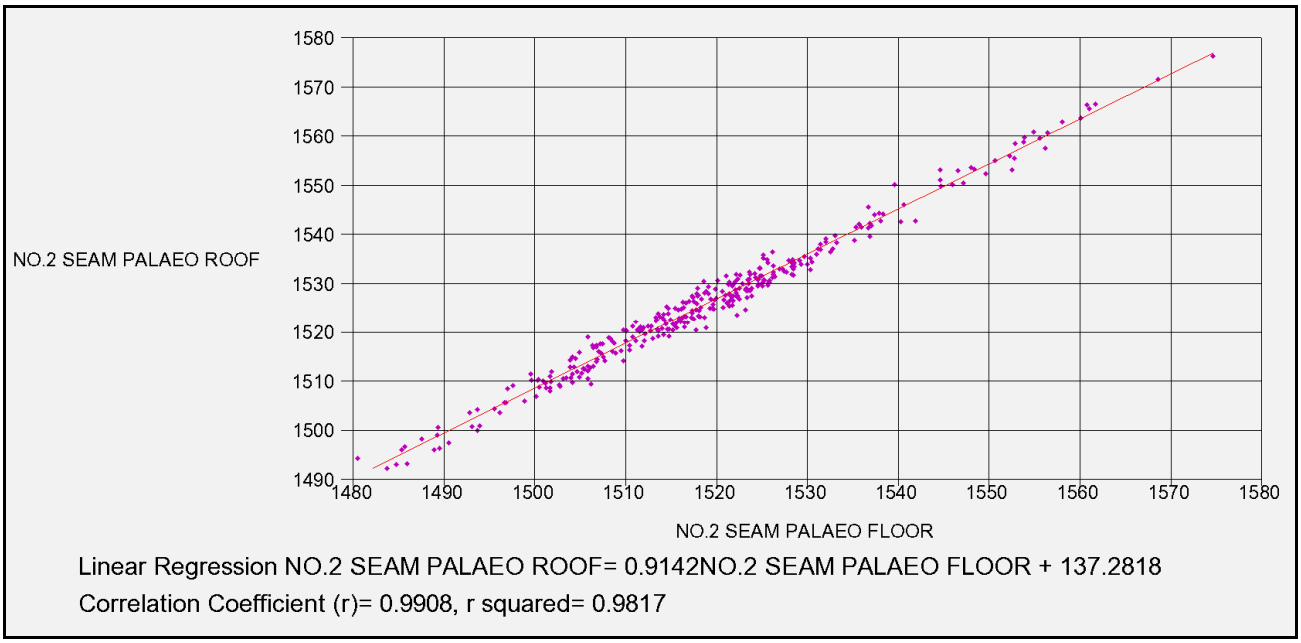

Figure 4.34: Correlation coefficient between the No. 2 Coal Seam palaeo floor and roof elevations.

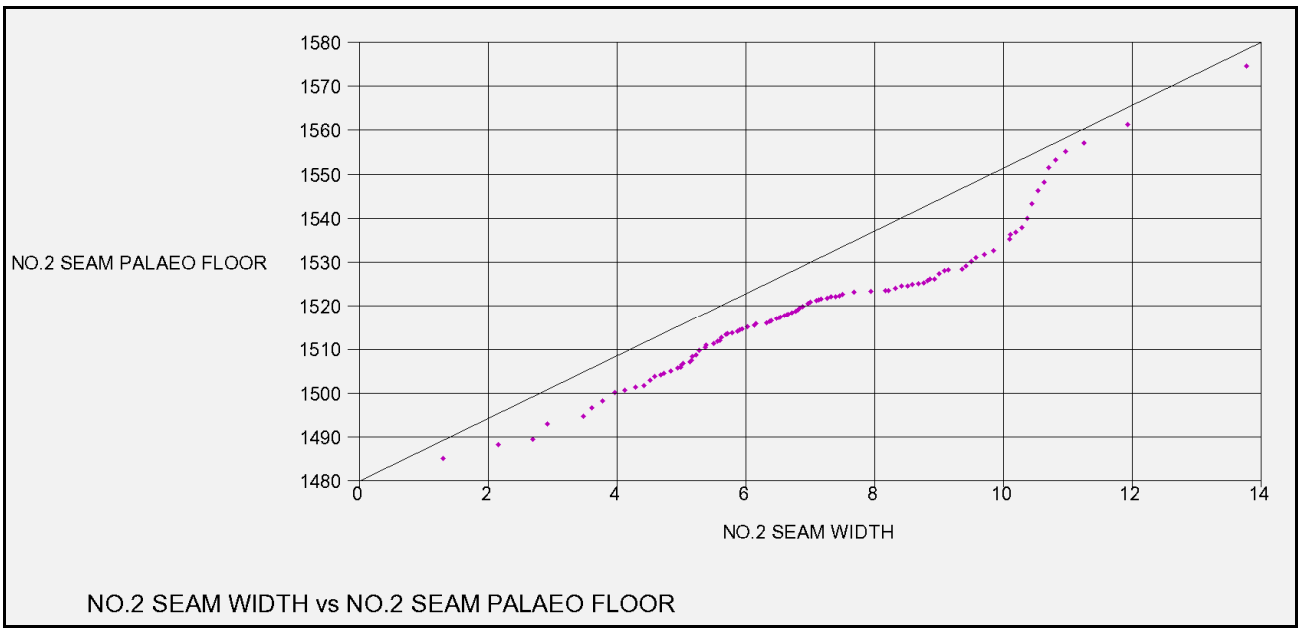

Figure 4.35: Quantile-Quantile plot of the No. 2 Coal Seam width and palaeo floor elevation.

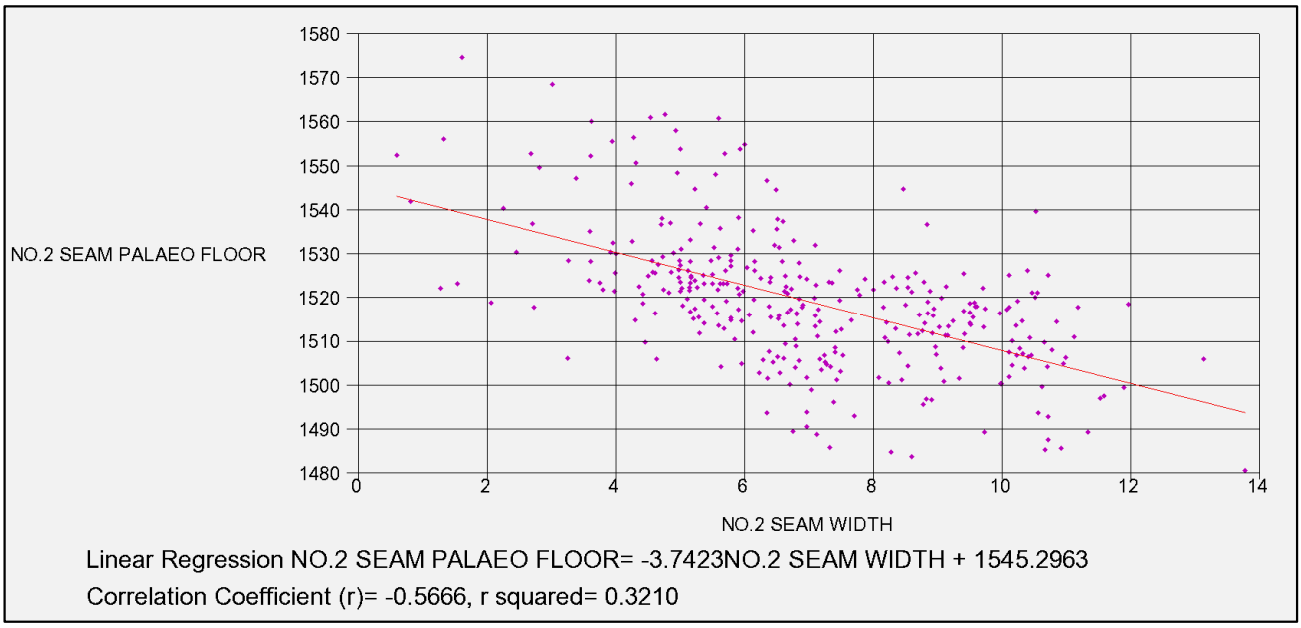

Figure 4.36: Correlation coefficient between the No. 2 Coal Seam width and its palaeo floor elevation.

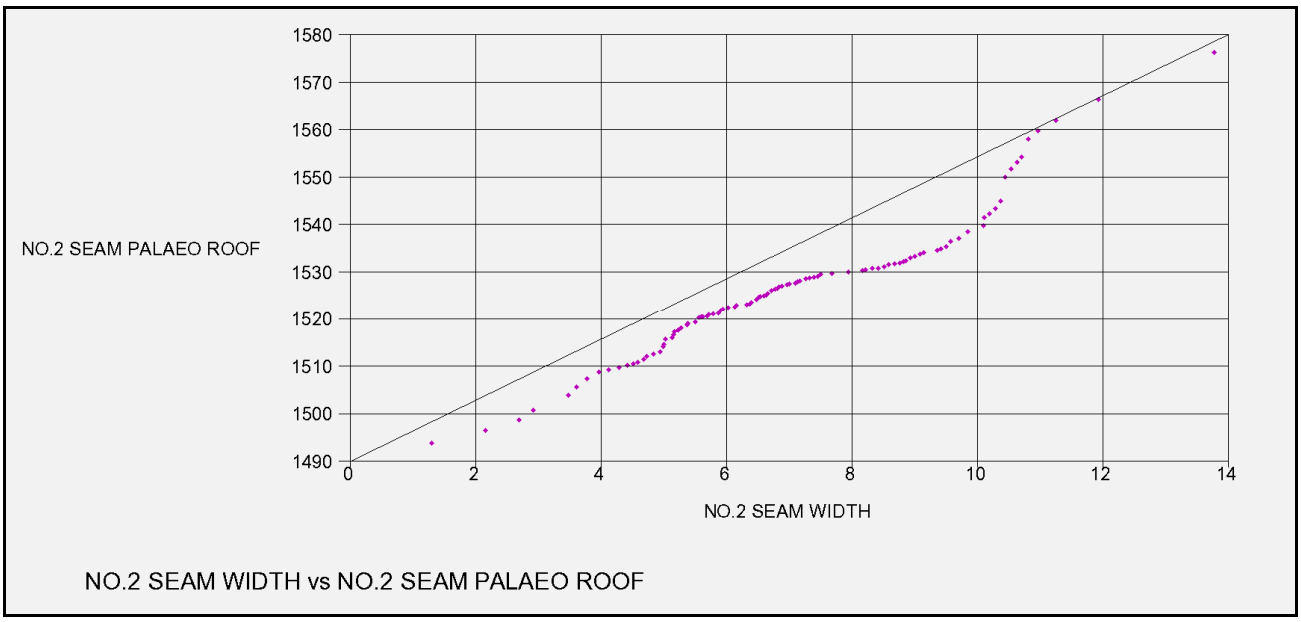

Figure 4.37: Quantile-Quantile plot of the No. 2 Coal Seam width and palaeo roof elevation.

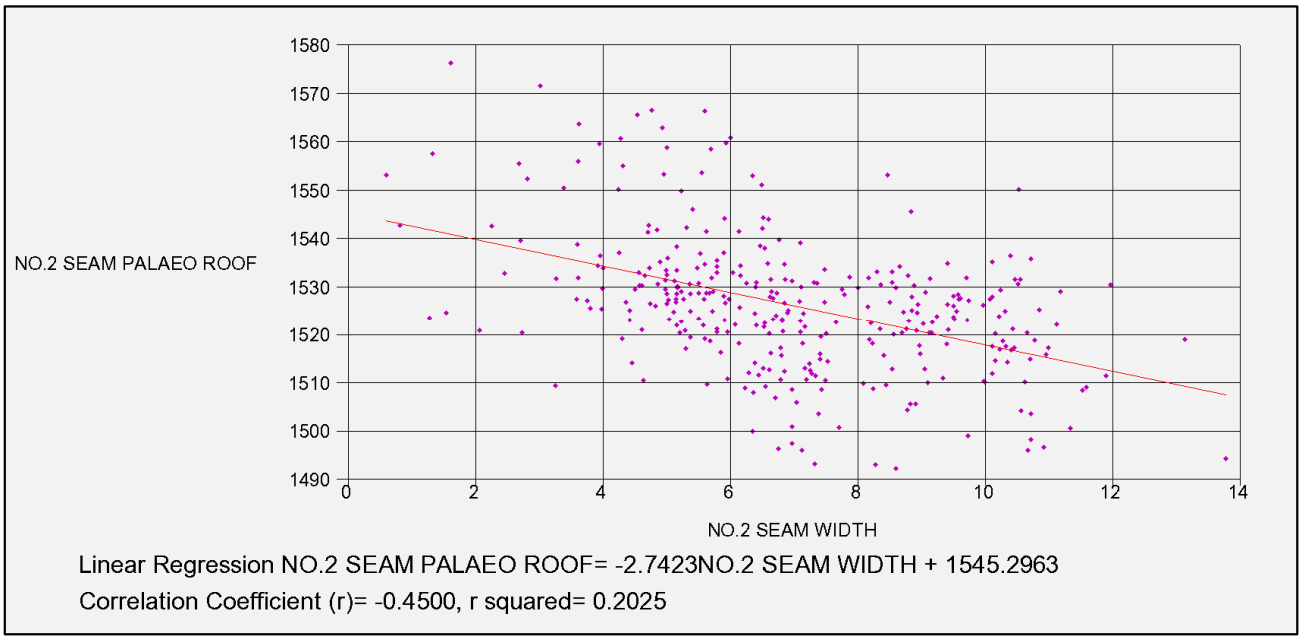

Figure 4.38: Correlation coefficient of the No. 2 Coal Seam width and its palaeo roof elevation.

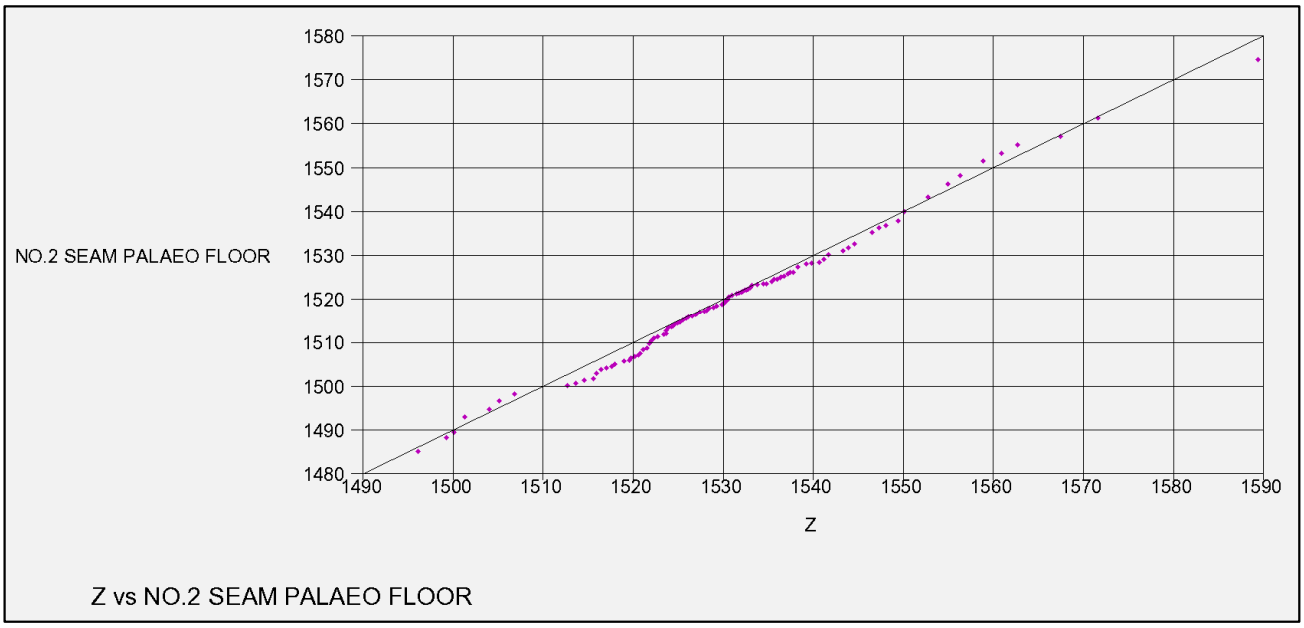

Figure 4.39: Quantile-Quantile plot of the No. 2 Coal Seam floor and palaeo floor elevation.

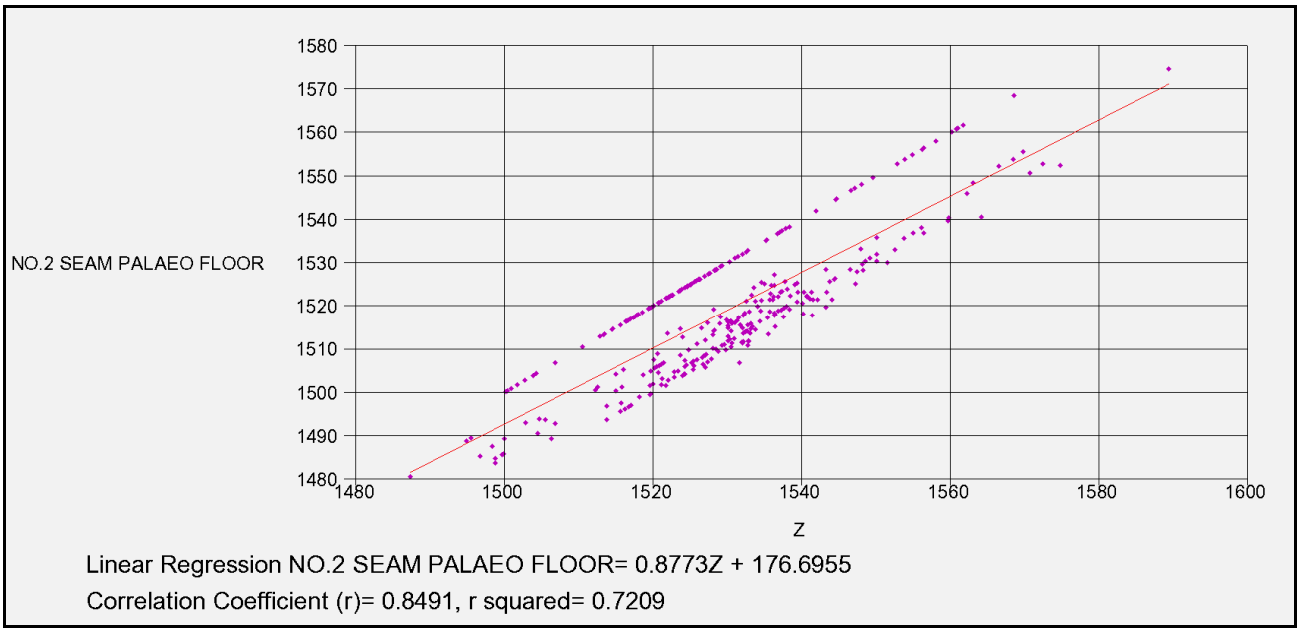

Figure 4.40: Correlation coefficient between the No. 2 Coal Seam floor and its palaeo floor elevation.

4.4.2.4 DISCUSSION AND INTERPRETATION

The No. 2 Coal Seam data set is supported by 333 samples which cover a surface area of 11,452,072m^2. The average sample spacing equates to 185m.

CLASSICAL STATISTICS

WIDTH

The histogram plot in Figure 4.26 reveals a normal distribution with a skewness of 0.07 (Table 4.2). The coefficient of variation of 0.34 indicates low variability in the data. Straightness of the probability curve in Figure 4.26 is reasonable and shows the normality in the data.

FLOOR

The histogram plot in Figure 4.27 is slightly positively skewed. The coefficient of variation of 0.01 indicates low variability in the data. The slightly skewed data set is revealed by the few kinks in the probability curve (Figure 4.27) that relates to the uplifted seam as a result of the sill intrusion.

PALAEO FLOOR

The histogram plot in Figure 4.28 is slightly positively skewed. The coefficient of variation of 0.01 indicates low variability in the data. The smoothness of the palaeo floor probability curve (Figure 4.28) is better in comparison to the floor data which is slightly lesser skewed (Figure 4.27). Smaller skewness in the uplifted floor in comparison to the palaeo floor is observed. The role of the uneven pre-Karoo basement in the differential compaction of the sedimentary rocks could be a result of the higher skewness. The degree of skewness of the palaeo floor data could be directly related the unevenness of the pre-Karoo basement topography and the compactibility of the coal and its underlying footwall sedimentary sequence.

PALAEO ROOF

A comparison between the coefficient of variation, skewness and kurtosis of the palaeo roof versus the palaeo floor (Table 4.2) show small differences which reveal the close similarity between the two data sets.

DATA INTERPOLATION AND ALALYSIS

Width distribution of the No. 2 Coal Seam is displayed in Figure 4.31. The most frequent width samples are between 6.5m and 7.0m (Figure 4.29), which occur on a range of elevations between 1490m and 1550m which is close to the range of the entire data set (Table 4.2).

The QQ-plot of the palaeo floor and roof data in Figure 4.33 shows a close relationship to the ideal line. The 0.99 correlation coefficient (Figure 4.34) and the visual comparison of the contour plots in Figures 4.30 and 4.32 is a confirmation of the tight linear relationship that exists between the palaeo floor and roof elevations. The QQ-plot (Figure 4.35) of the width and palaeo floor data with respect to the ideal line reveals an inverse relationship. This inverse relationship calculates a correlation coefficient of -0.57 (Figure 4.36) which effectively indicates that thicker coal is largely present in the lower lying areas and consequently thinner coal is draped over the palaeo highs.

A comparison of the curves resulted from the QQ-plots between the width and the palaeo floor (Figure 4.35) and roof (Figure 4.37), respectively confirm the similarity that exists. A correlation coefficient of -0.45 (Figure 4.38) between the width and the palaeo roof exhibits a poor relationship. In Figures 4.39 and 4.40 the quantity of palaeo floor data versus uplifted floor data is demonstrated.

4.4.3 NO.2-4L COAL SEAM FACIES

4.4.3.1 CLASSICAL STATISTICS

Table 4.3: Classical Statistics of the No. 2-4L Coal Seams.

FACIES	BETWEEN NO. 2-4L COAL SEAMS
VARIABLE	WIDTH
NUMBER OF SAMPLES	324
MINIMUM VALUE	2.8
MAXIMUM VALUE	37.84
MEAN	25.481
VARIANCE	26.934
STANDARD DEVIATION	5.19
COEFFICIENT OF VARIATION	0.204
SKEWNESS	0.331
KURTOSIS	3.185
TRIMEAN	24.771
BIWEIGHT	24.963
MAD	3.55
ALPHA	-2.772
SICHEL-T	4.65E+16

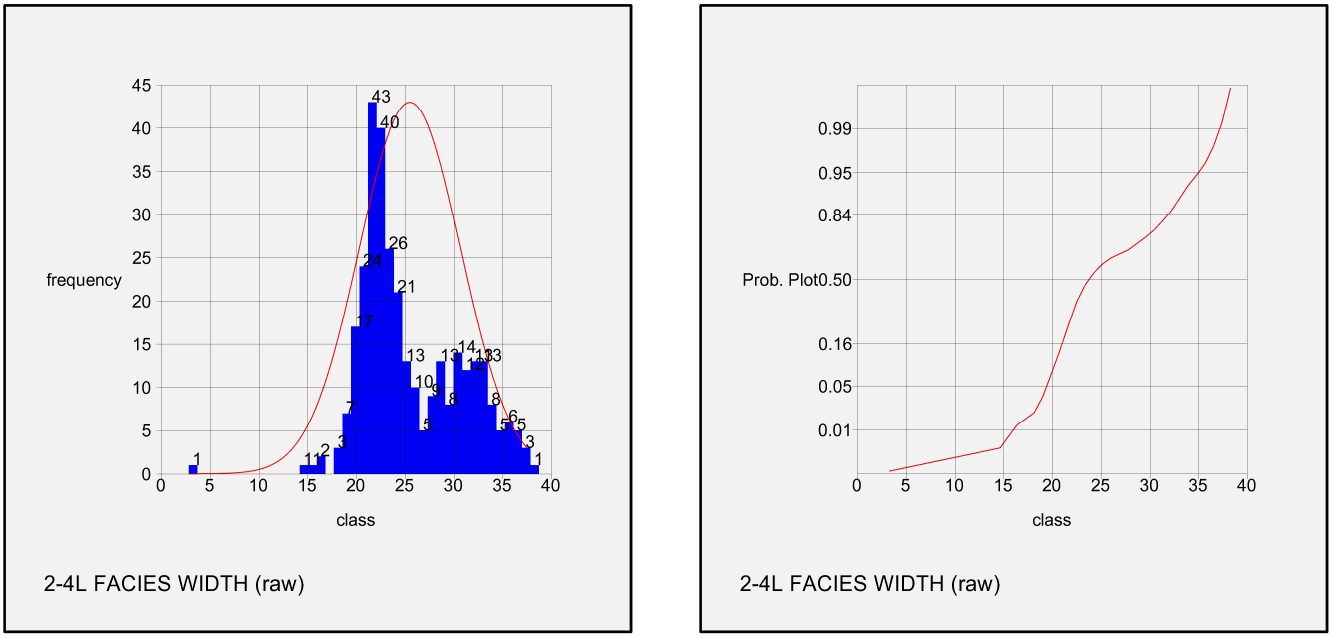

Figure 4.41: Histogram and probility plot of the net facies width between No. 2–4L Coal Seams.

4.4.3.2 DATA INTERPOLATION

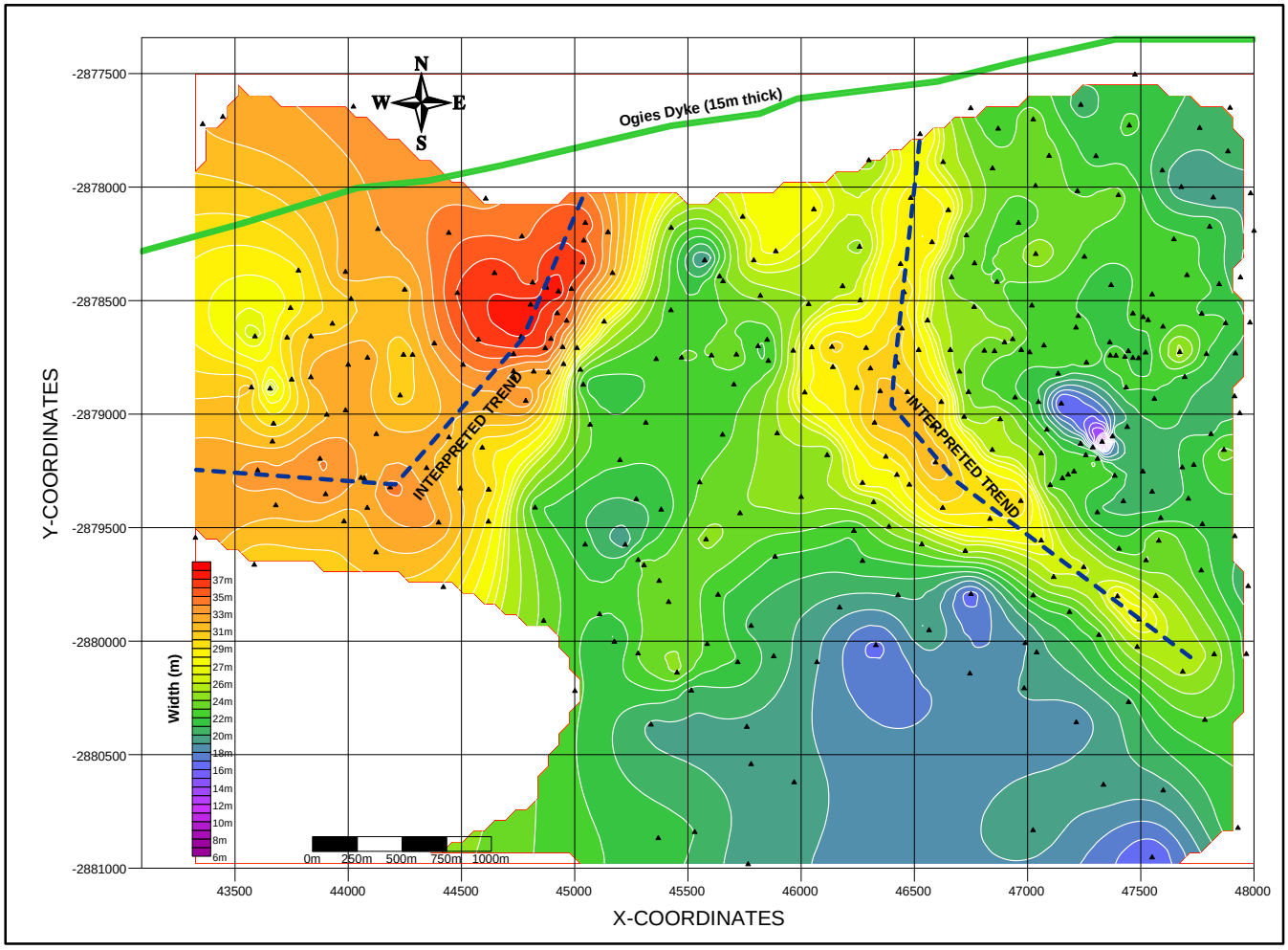

Figure 4.42: ***The net facies width between No. 2-4L Coal Seams. The interpreted trends show the axes of erosion channel bodies as blue stippled lines.***

4.4.3.3 DATA ANALYSIS

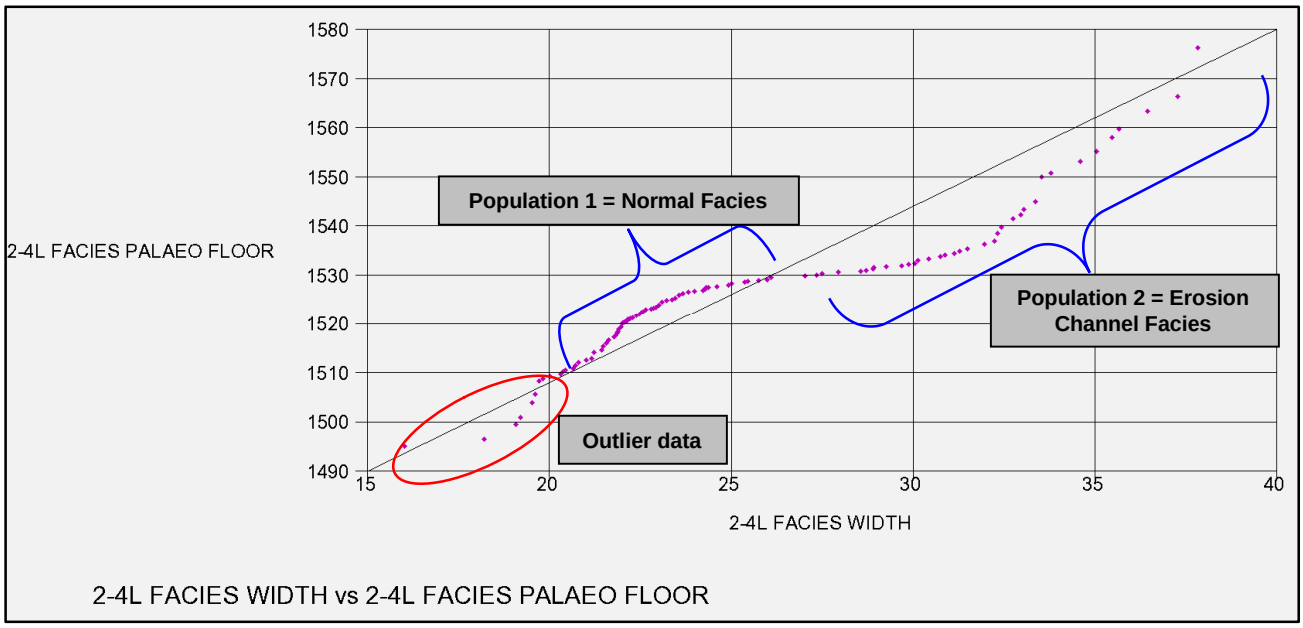

Figure 4.43: Quantile-Quantile plot of the net facies width between No. 2 and No. 4L Coal Seams and its palaeo floor elevation.

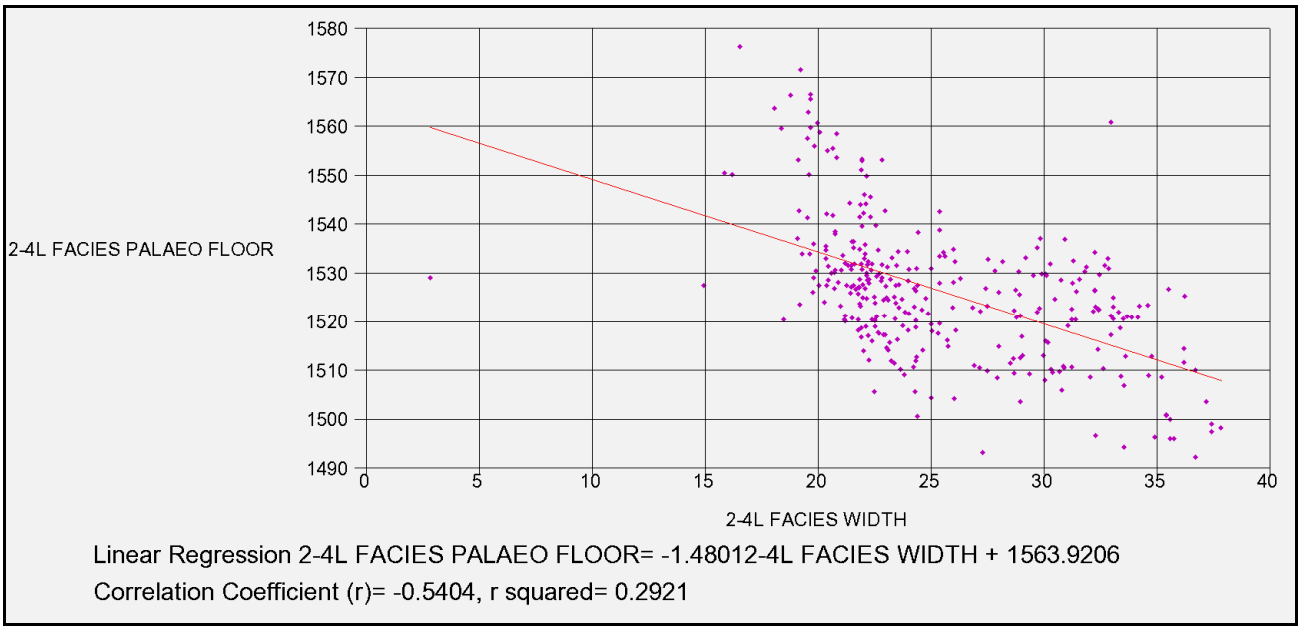

Figure 4.44: Correlation coefficient of the net facies width between No. 2 and No. 4L Coal Seams and its palaeo floor elevation.

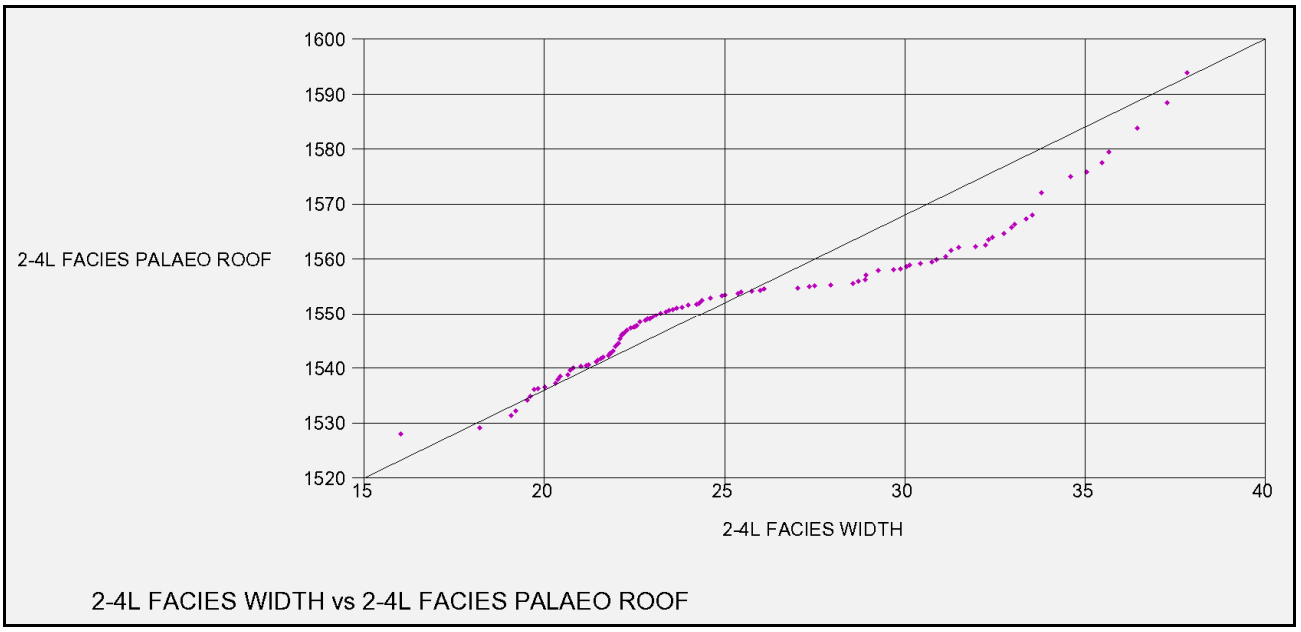

Figure 4.45: Quantile-Quantile plot of the net facies width between No. 2 and No. 4L Coal Seams and its palaeo roof elevation.

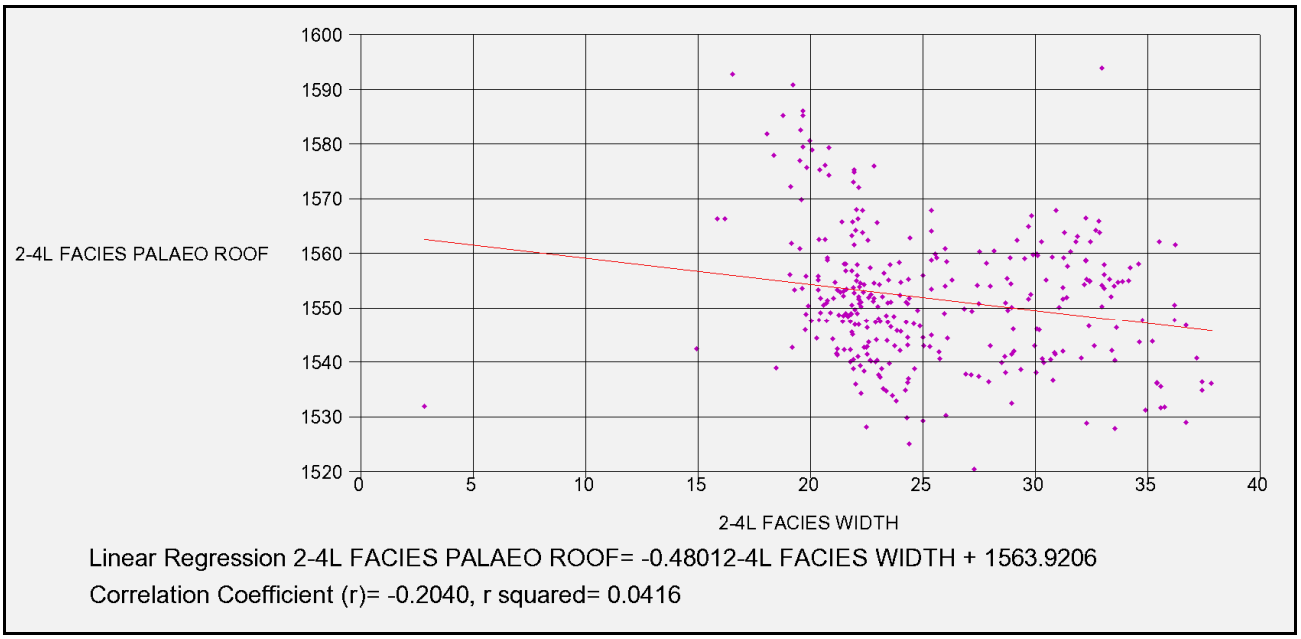

Figure 4.46: Correlation coefficient of the net facies width between No. 2 and No. 4L Coal Seams and its palaeo roof elevation.

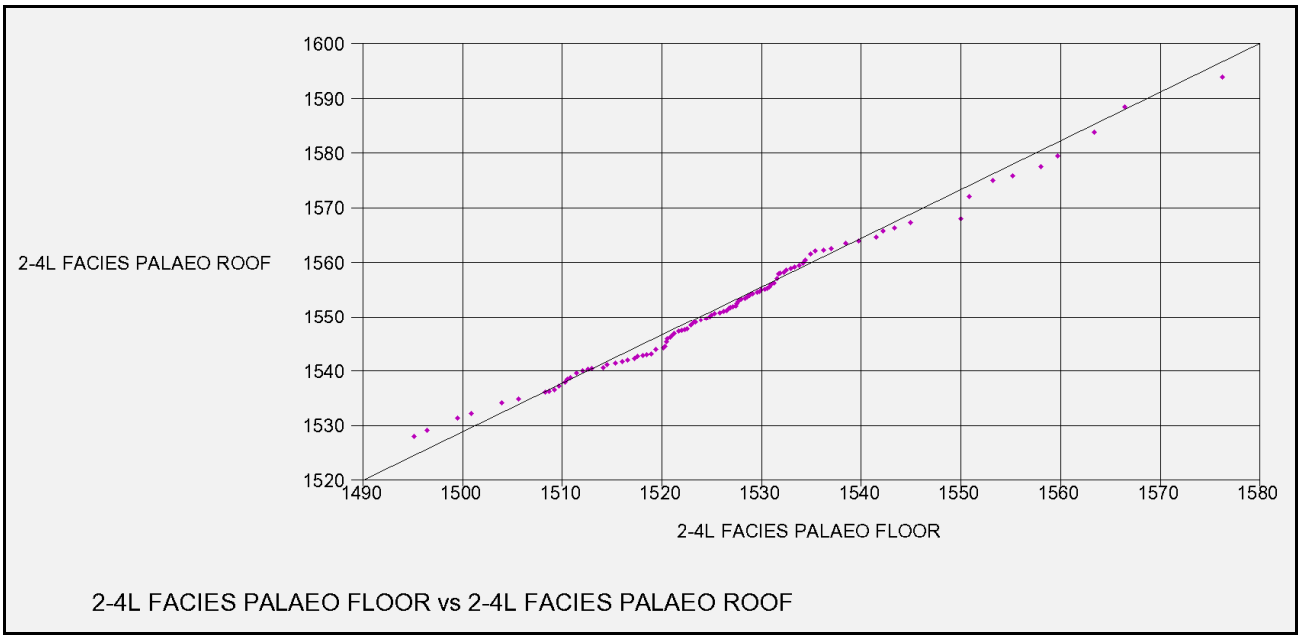

Figure 4.47: Quantile-Quantile plot of the palaeo floor and roof of the net facies width between No. 2 and No. 4L Coal Seams.

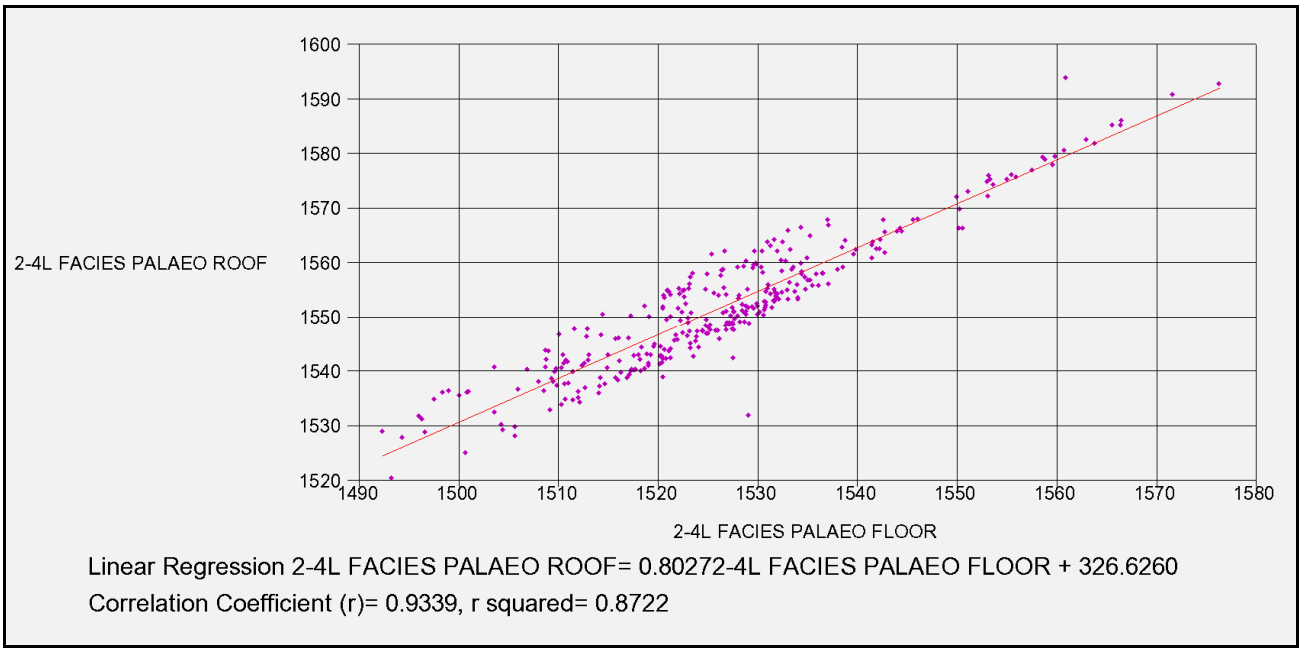

Figure 4.48: Correlation coefficient of the palaeo floor and roof of the net facies width between No. 2 and No. 4 L Coal Seams.

4.4.3.4 DISCUSSION AND INTERPRETATION

The net facies width between the No. 2 Coal Seam and No. 4L Coal Seam data set is supported by 324 samples which cover a surface area of 11,623,555m^2. The average sample spacing equates to 189m.

CLASSICAL STATISTICS

WIDTH

The histogram plot in Figure 4.41 reveals outlier data as well as a bimodal population which positively skews the distribution to a skewness of 0.33 (Table 4.3). The coefficient of variation of 0.20 indicates low variability in the data. Straightness of the probability curve in Figure 4.41 is influenced by the outlier data and the bimodal population.

DATA INTERPOLATION AND ANALYSIS

A net facies isopach map between the floor and roof of the No. 2 and 4L Coal Seams represents widths ranging between 2.80m – 37.84m (Figure 4.42). These facies contain clastic material of carbonaceous siltstone, bioturbated siltstone/sandstone, interlaminated siltstone as well as sandstone and coal (intermittently No. 3 Coal Seam). Cadle and Cairncross (1992) interpreted a braided/bed-load channel system deposited between the No. 3 and 4 Coal Seams. These channels incised through the underlying No. 3 Coal Seam and sometimes rest either close to or directly on the roof of No. 2 Coal Seam affecting its thickness. Texturally these sandbodies comprise coarse to very coarse-grained sandstone and granule-grade conglomerate and ranges in length between 1-12km and has a width range of 12m-22m.

Blue stippled lines depicted in Figure 4.42 delineate the axes of probably typical erosion channel bodies. The QQ-plot (Figure 4.43) exibits the outlier data as well as the two distinct populations that exist in the data set. These two distinct populations are provisionally defined in the QQ-plot as two separate sub-facies types and are hereinafter referred as the Normal (N-Facies) and Erosion Channel Facies (EC-Facies), respectively. Detail statistical analyses which assist with the definition of the facies are elaborated on in the section “Geozone Definition”.

In spite of the statistical relationships of the width data set, the correlation coefficient between the net facies width and the palaeo floor elevation shows an inverse relationship of -0.54 (Figure 4.44).

This relationship demonstrates however that generally the EC-Facies are present in the lower lying areas and the N-Facies are draped over the flanks and the palaeo highs.

The QQ-plot in Figure 4.45 reveals the relationship between the net facies width and the palaeo roof elevation which indicates a similar kind of relationship to the ideal line in Figure 4.43. A poor correlation coefficient of -0.20 is calculated between the palaeo roof and width of the net facies (Figure 4.46). In Figure 4.47 the QQ-plot reveals a remarkable correlation of the net facies palaeo floor and –roof with the ideal line. The linearity in the palaeo floor and roof curve of the net facies calculated a correlation coefficient of 0.93 (Figure 4.48).

GEOZONE DEFINITION

The geozone definition entails the exclusion of the outlier data and the individual examination of the statistical relationship of the N-Facies and EC-Facies. Table 4.4 summarises the classical statistics of the outlier data, N-Facies and EC-Facies. Coefficient of variation improved from 0.2 to 0.08 with the N-Facies definition. The histogram plot of the N-Facies (Figure 4.49) shows a symmetric distribution with a small positive skewness of 0.11 (Table 4.4). The straightness of the probability plot in Figure 4.49 is reasonable and shows the homogeneity of the data set. The QQ-plot (Figure 4.51) shows how the relationship between the width and palaeo floor of the N-Facies swerving from ideal line. An inverse relationship with a correlation coefficient of -0.52 is calculated (Figure 4.52).

A slight positive skewness of 0.31 (Table 4.4) for the EC-facies reveal a fairly normal distribution fit to the data set (Figure 4.50) and a reasonably straight probability curve (Figure 4.50) reveal good data coverage for the definition of the EC-Facies. Coefficient of variation improved from 0.2 to 0.09 with the EC-Facies definition. The QQ-plot (Figure 4.53) shows the existing relationship between the width and palaeo floor of the EC-Facies and the the curve's deviation to the ideal line. In comparison to the N-Facies a tighter relationship exists between the width and the palaeo floor. This poorer relationship is also revealed in the negative correlation coefficient of -0.34 (Figure 4.54).

The transition from the N-Facies to the EC-Facies is depicted by the 26.5m contour line in the width isopach map in Figure 4.55. This transition can be described as being abrupt, which is typical of the scouring effect that the erosion channel bodies have on the strata immediately to its footwall.

Table 4.4: Classical Statistics of the outlier data, N-Facies and EC-Facies.

VARIABLE	OUTLIER DATA	N-FACIES	EC- FACIES
NUMBER OF SAMPLES	6	205	116
MINIMUM VALUE	2.80	18.06	26.84
MAXIMUM VALUE	16.54	26.28	37.84
MEAN	13.80	22.36	31.65
VARIANCE	24.52	3.32	7.78
STANDARD DEVIATION	4.95	1.82	2.79
COEFFICIENT OF VARIATION	0.36	0.08	0.09
SKEWNESS	-1.74	0.11	0.31
KURTOSIS	4.11	2.55	2.31
TRIMEAN	15.87	22.27	31.40
BIWEIGHT	16.02	22.28	31.50
MAD	0.81	1.21	2.01
ALPHA	-2.77	-7.32	-14.58
SICHEL-T	320000000	26300000000	2.33E+15

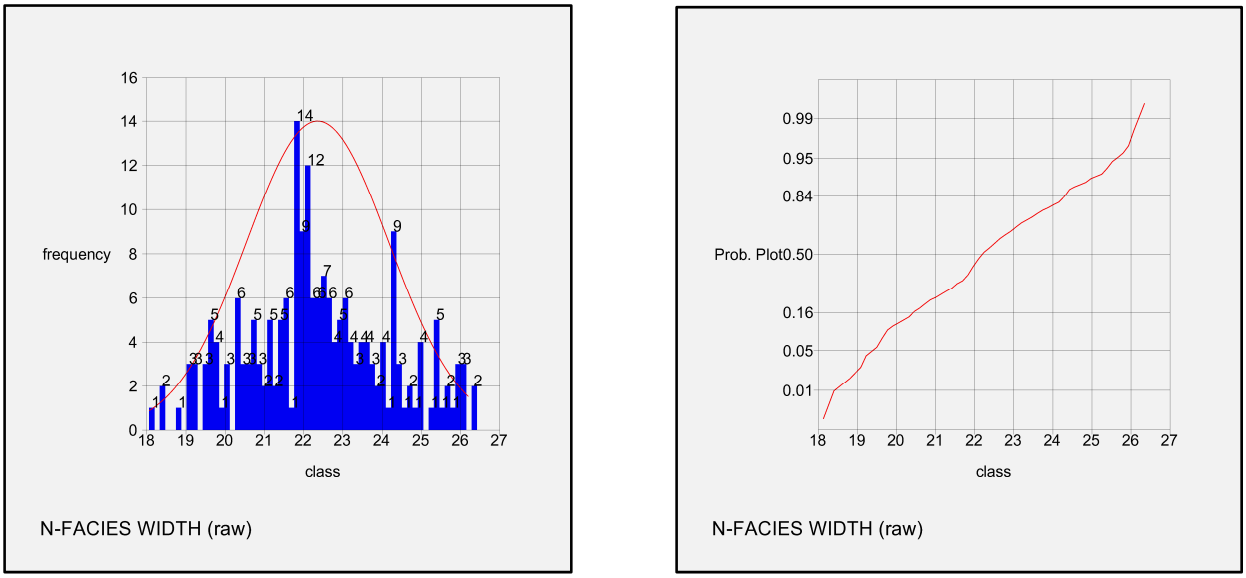

Figure 4.49: Histogram and probility plot of the N-Facies (>=17 and <=26.5) width between No. 2 – 4L Coal Seams.

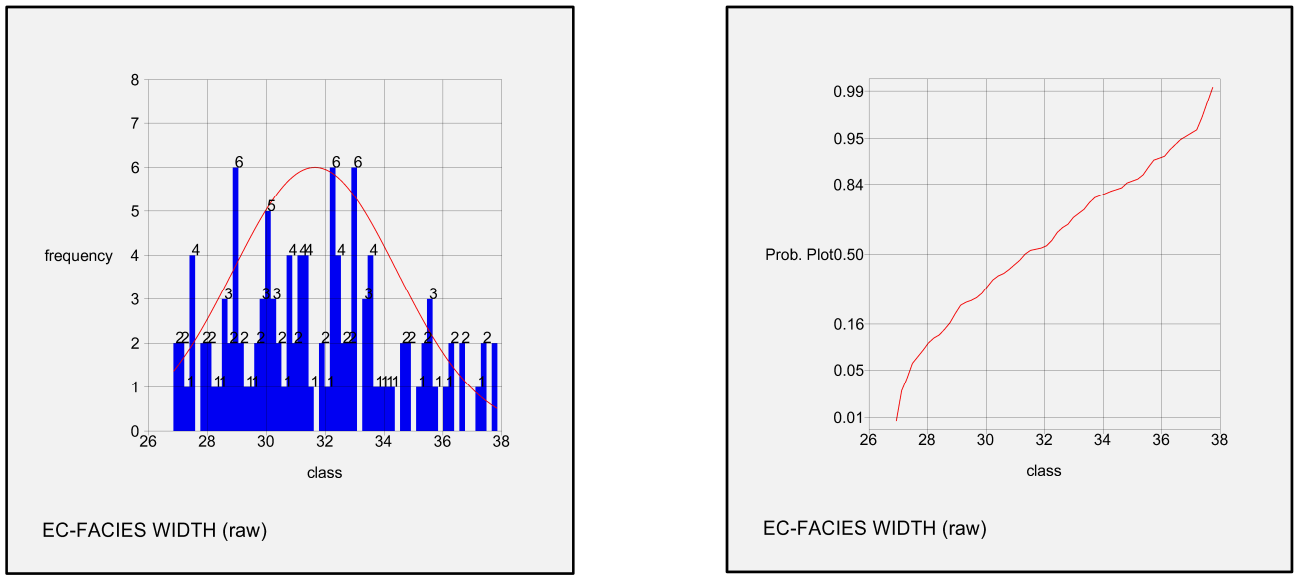

Figure 4.50: Histogram and probility plot of the EC-Facies (>26.5m) width between No. 2 – 4L Coal Seams.

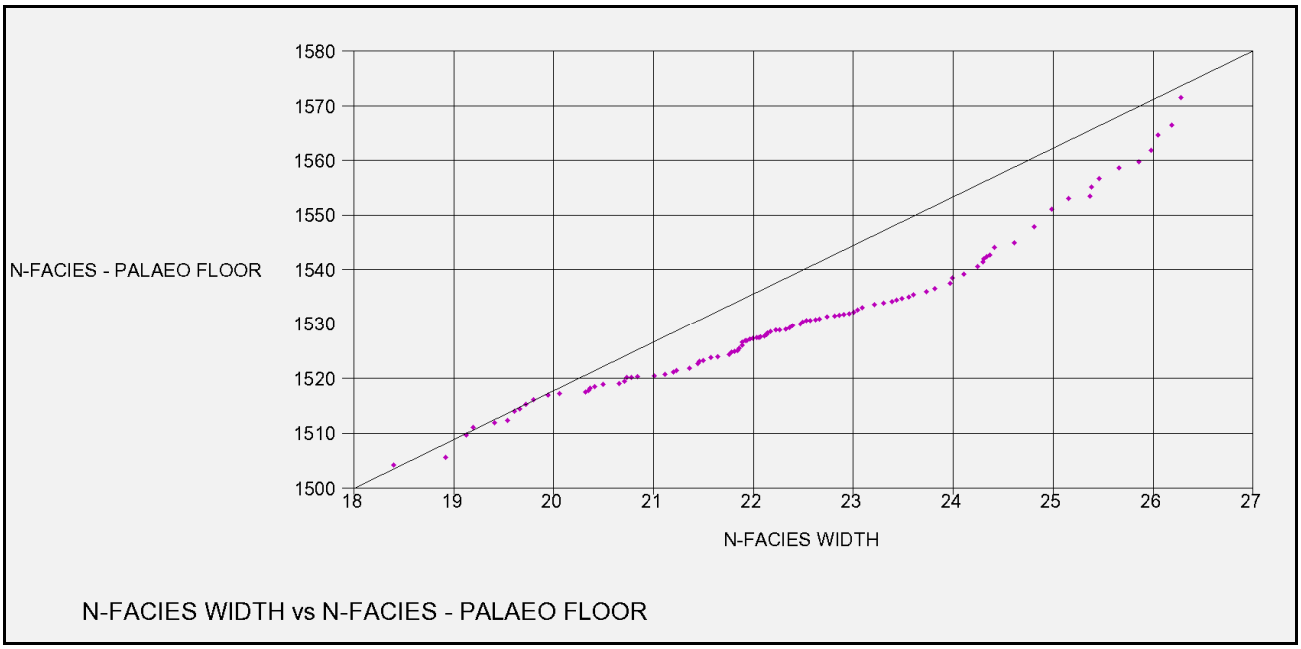

Figure 4.51: Quantile-Quantile plot of the palaeo floor of the N-Facies and the width of the N-Facies.

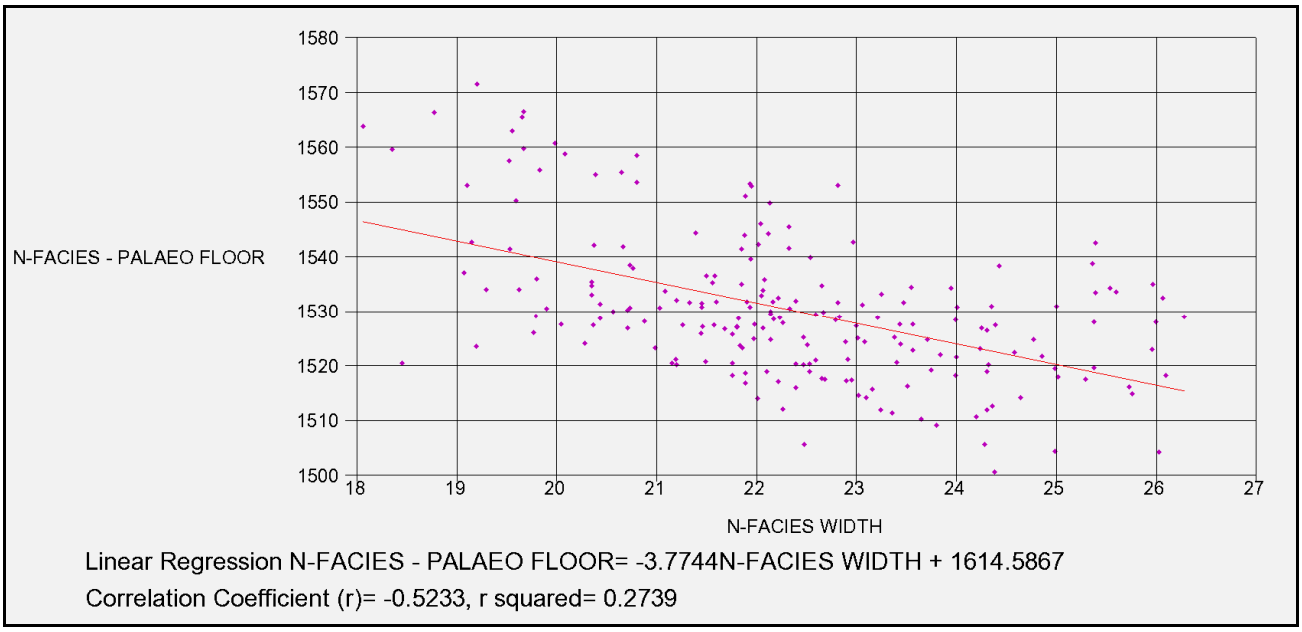

Figure 4.52: Correlation coefficient of the palaeo floor of the N-Facies and the width of the EC-Facies.

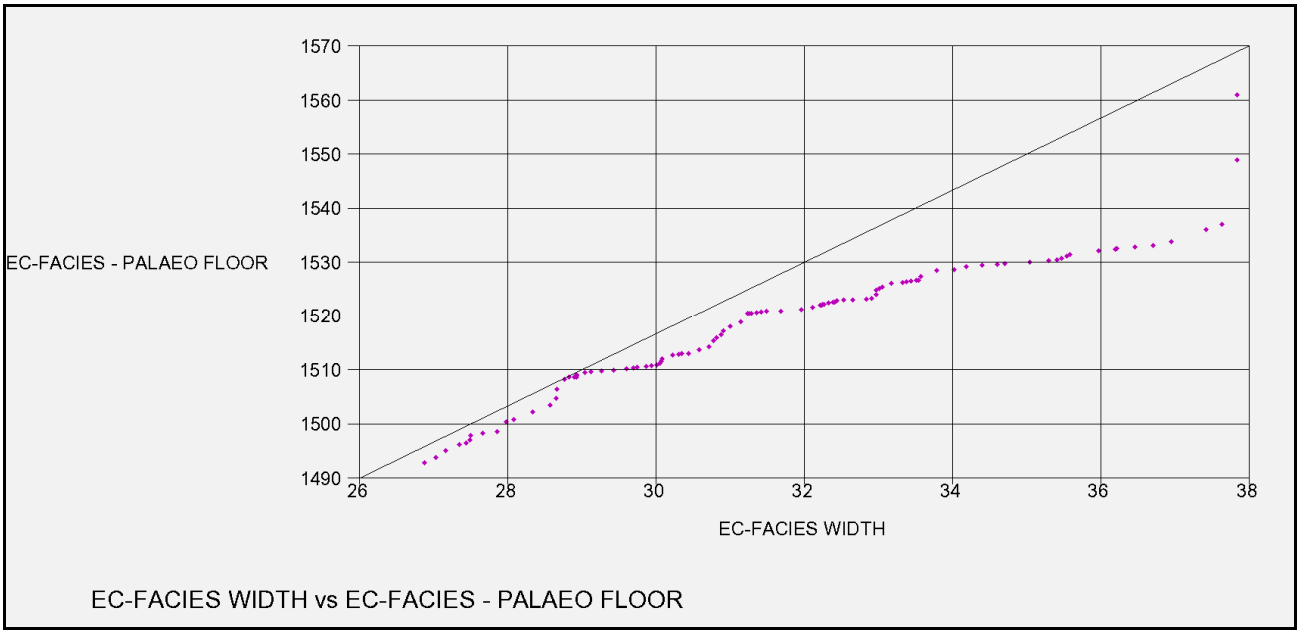

Figure 4.53: Quantile-Quantile plot of the palaeo floor of the EC-Facies and the width of the EC-Facies.

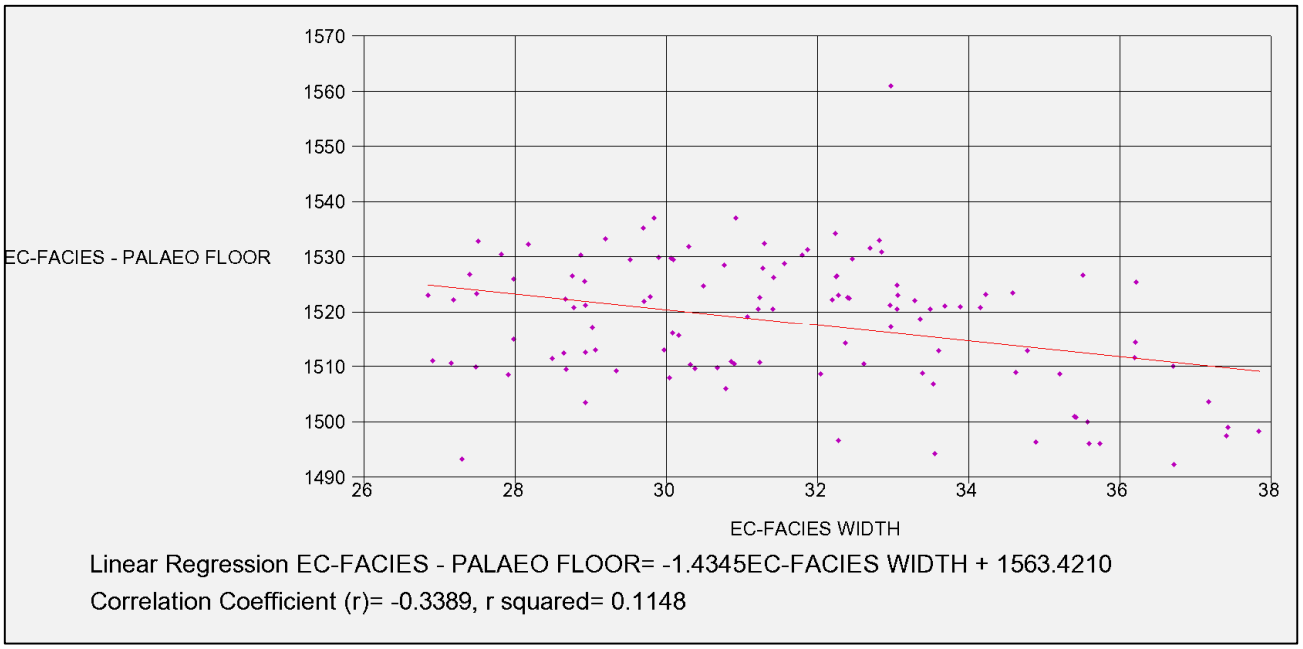

Figure 4.54: Correlation coefficient of the palaeo floor of the EC-Facies and the width of the EC-Facies.

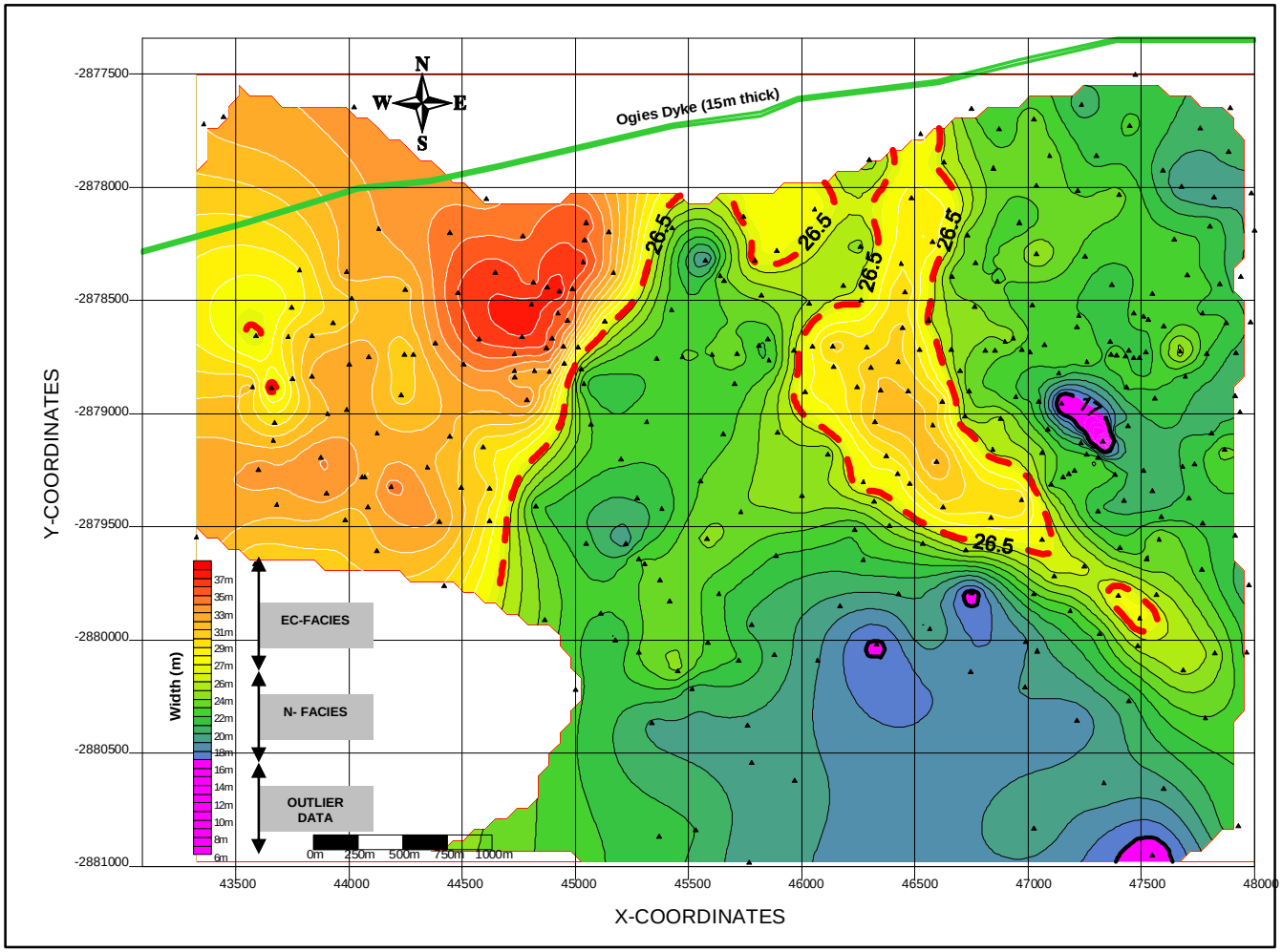

Figure 4.55: ***Width distribution of the outlier data, N-Facies and EC-Facies. Pink areas delineate the outlier data. The red stippled line shows the divide at 26.5m between the N-Facies and EC-Facies.***

4.4.4 NO.4L COAL SEAM

4.4.4.1 CLASSICAL STATISTICS

Table 4.5: Classical Statistics of the No. 4L Coal Seam.

SEAM	NO.4L COAL SEAM			
VARIABLE	WIDTH	FLOOR	PALAEO-FLOOR	PALAEO-ROOF
NUMBER OF SAMPLES	349	349	349	349
MINIMUM VALUE	0.31	1534.51	1493.94	1496.54
MAXIMUM VALUE	3.45	1610.02	1604.9	1607.3
MEAN	2.36	1564.78	1552.32	1554.68
VARIANCE	0.21	158.41	178.21	175.42
STANDARD DEVIATION	0.45	12.59	13.35	13.25
COEFFICIENT OF VARIATION	0.19	0.01	0.01	0.01
SKEWNESS	-1.38	0.89	0.52	0.53
KURTOSIS	5.94	4.18	4.95	5.02
TRIMEAN	2.43	1563.33	1551.17	1553.56
BIWEIGHT	2.45	1563.04	1551.13	1553.53
MAD	0.24	6.96	7.84	7.71
ALPHA	-0.31	-1525.80	-1488.79	-1489.43
SICHEL-T	11.79	Not Calculated	Not Calculated	Not Calculated

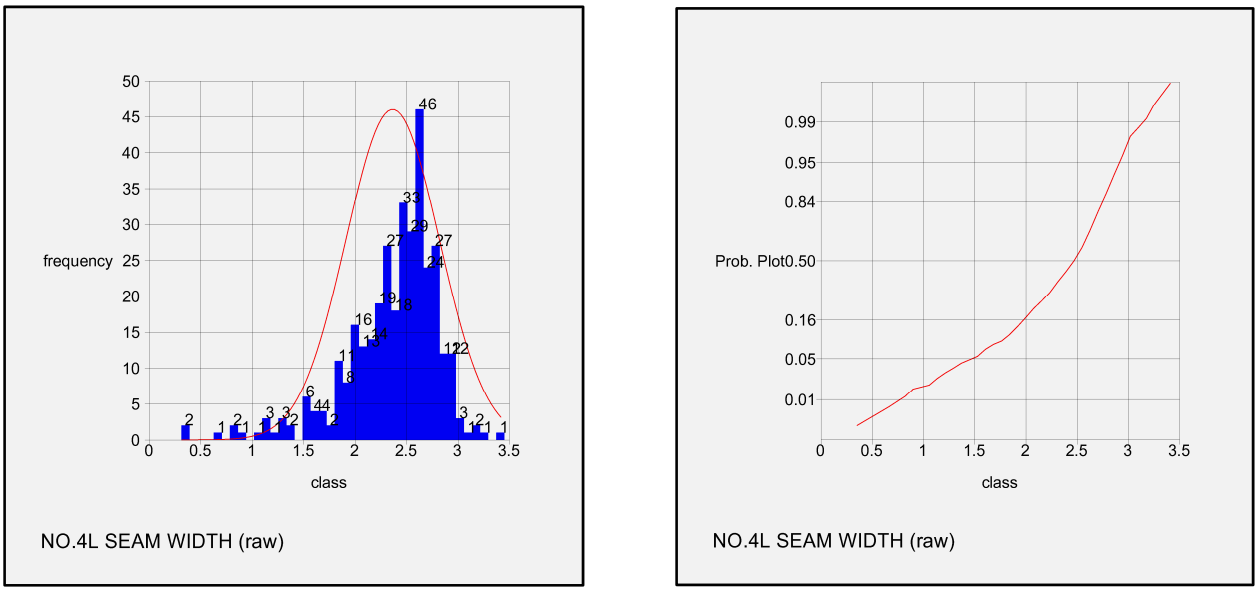

Figure 4.56: Histogram and probility plot of the No.4L Coal Seam width.

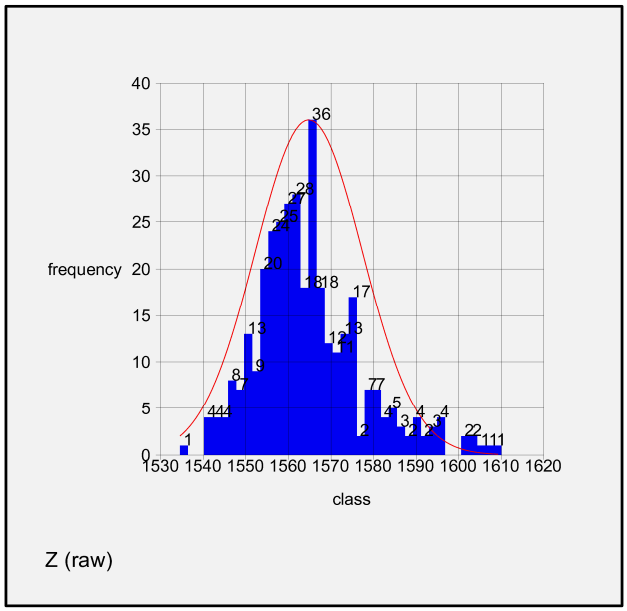

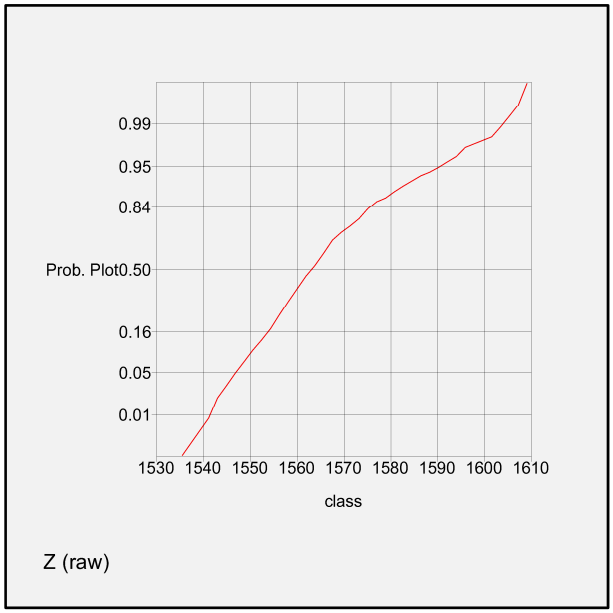

Figure 4.57: Histogram and probility plot of the No. 4L Coal Seam floor.

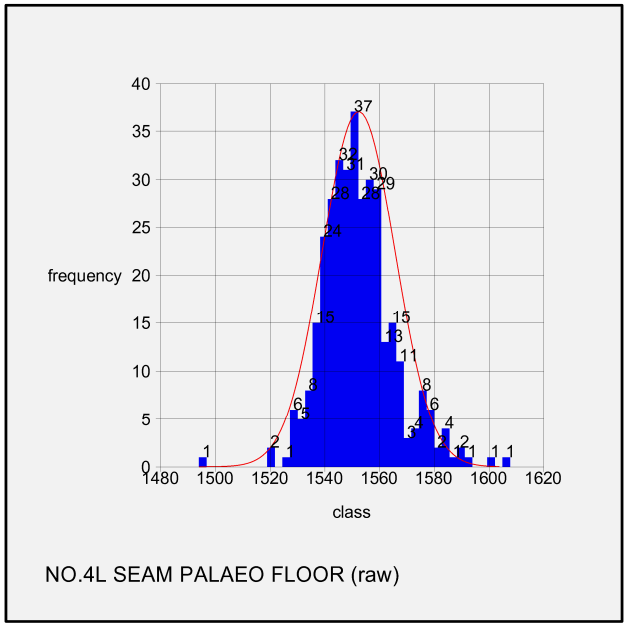

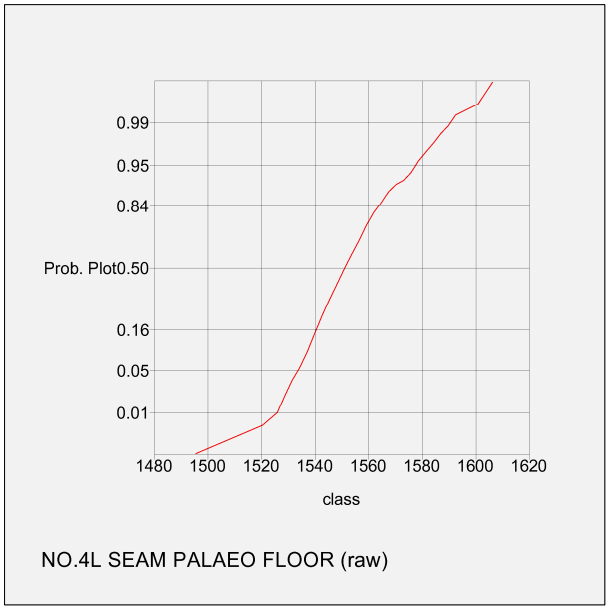

Figure 4.58: Histogram and probility plot of the No. 4L Coal Seam paleo floor elevation.

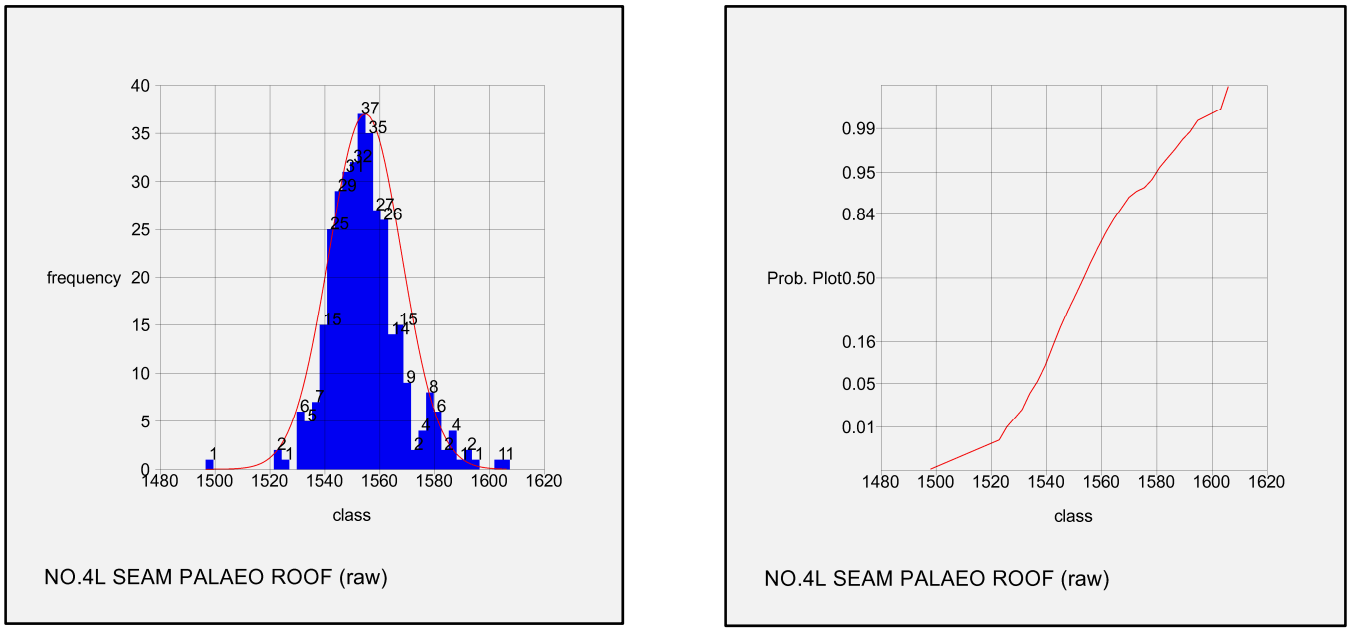

Figure 4.59: Histogram and probility plot of the No. 4L Coal Seam paleo roof elevation.

4.4.4.2 DATA INTERPOLATION

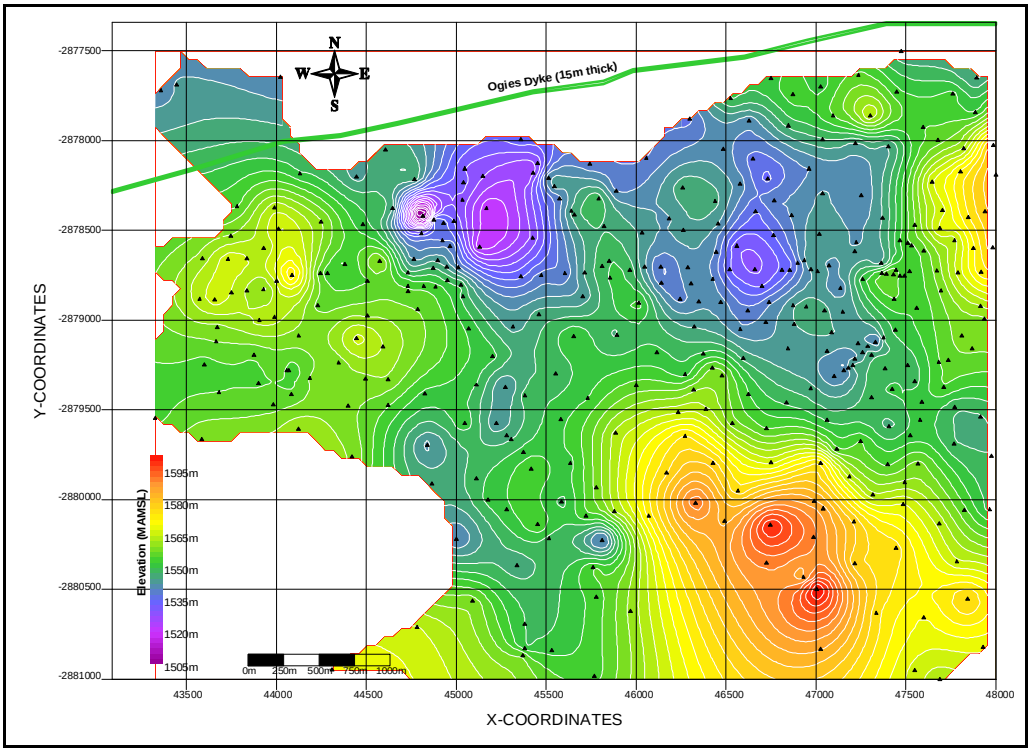

Figure 4.60: No. 4L Coal Seam palaeo floor elevation.

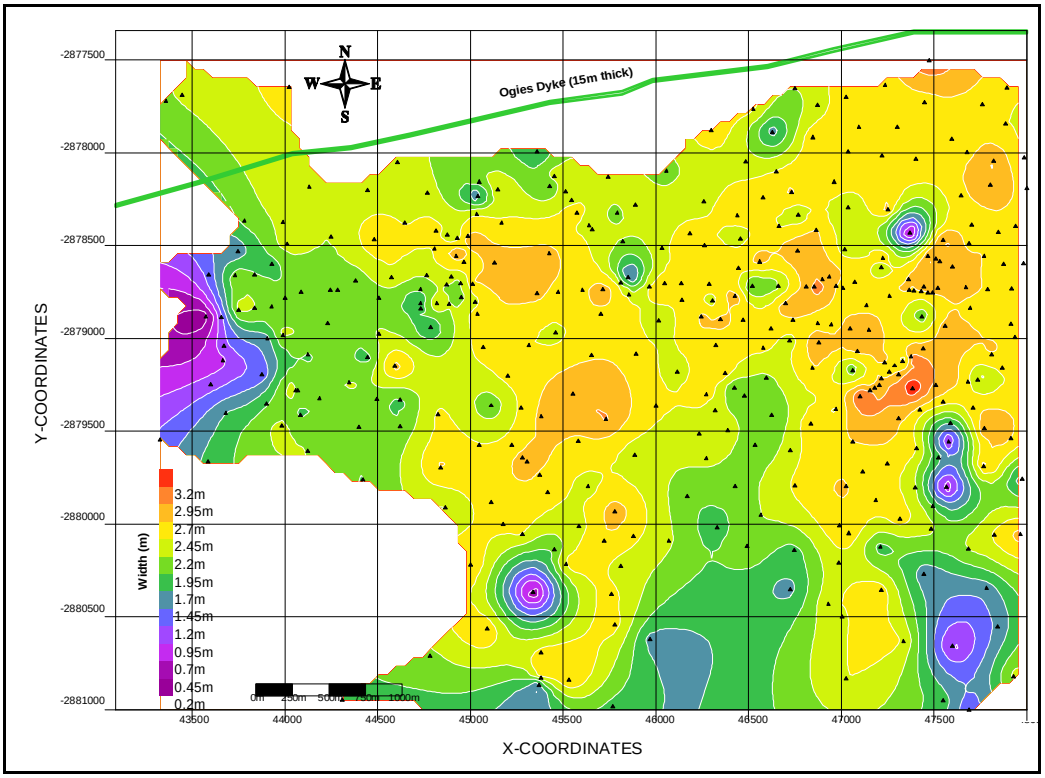

Figure 4.61: No. 4L Coal Seam width.

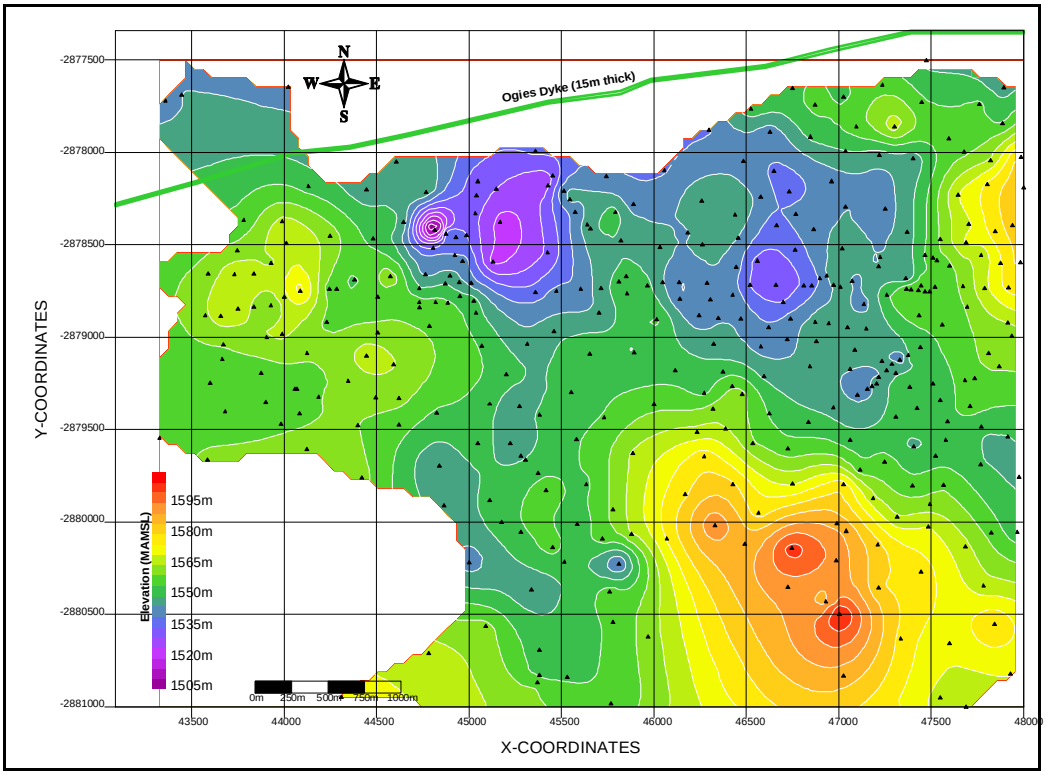

Figure 4.62: No. 4L Coal Seam palaeo roof elevation.

4.4.4.3 DATA ANALYSIS

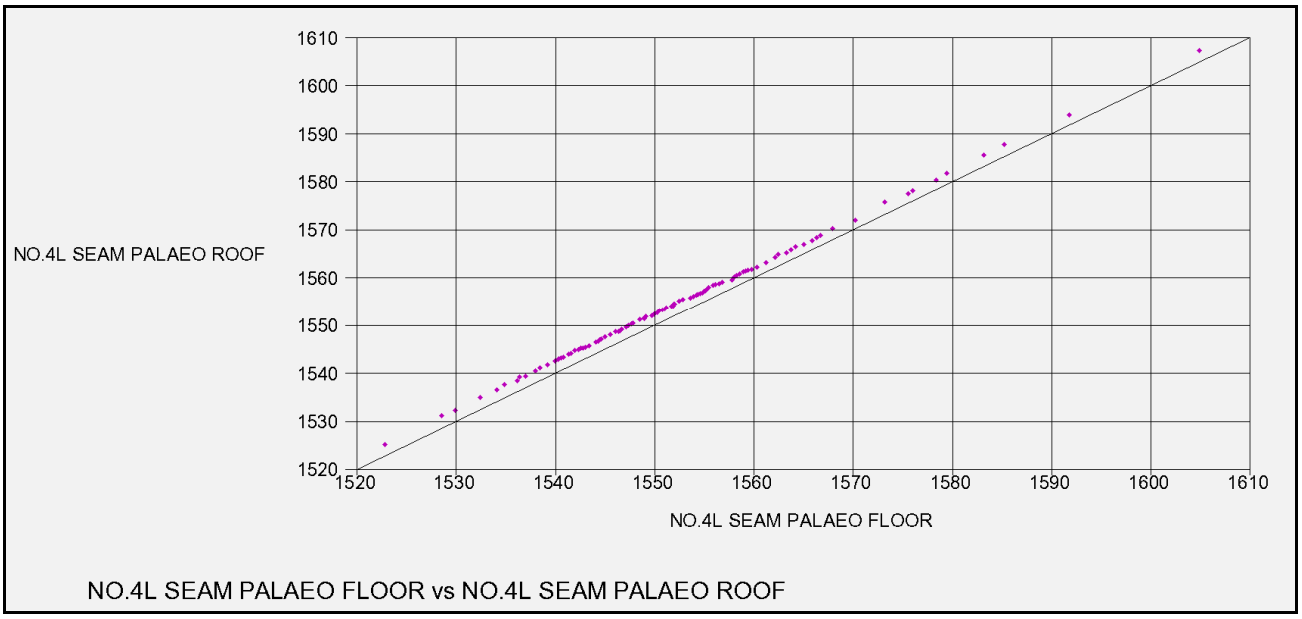

Figure 4.63: Quantile-Quantile plot of the No. 4L Coal Seam palaeo floor and roof elevations.

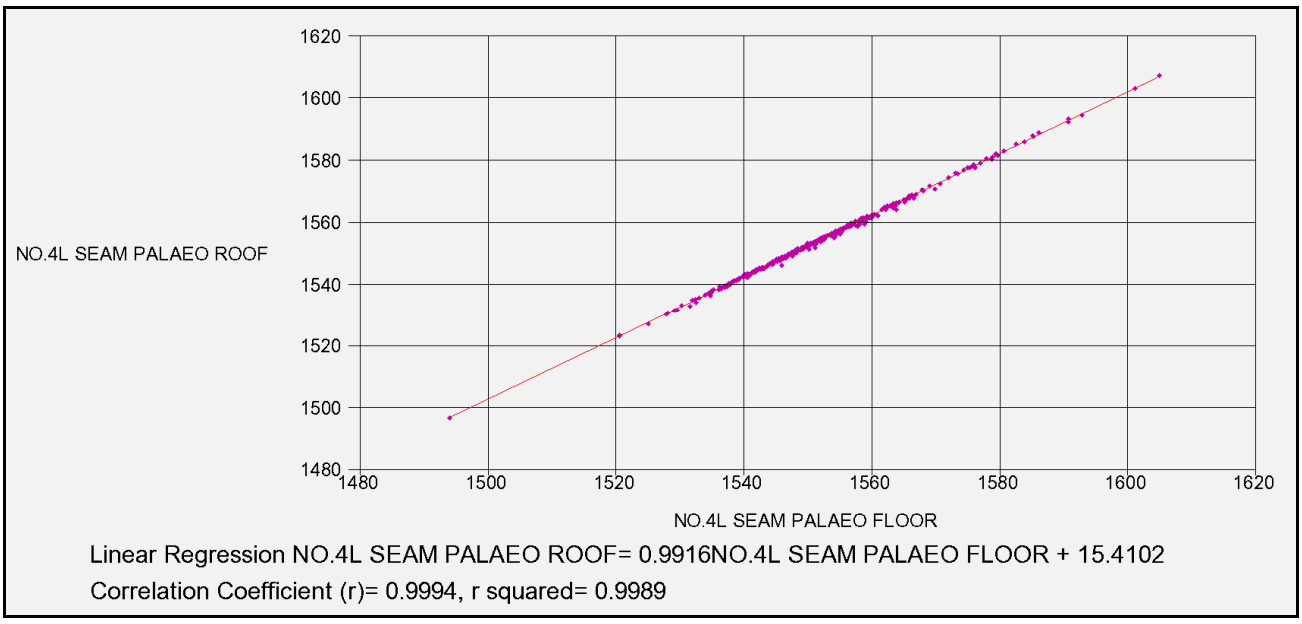

Figure 4.64: Correlation coefficient between the No. 4L Coal Seam palaeo floor and roof elevations.

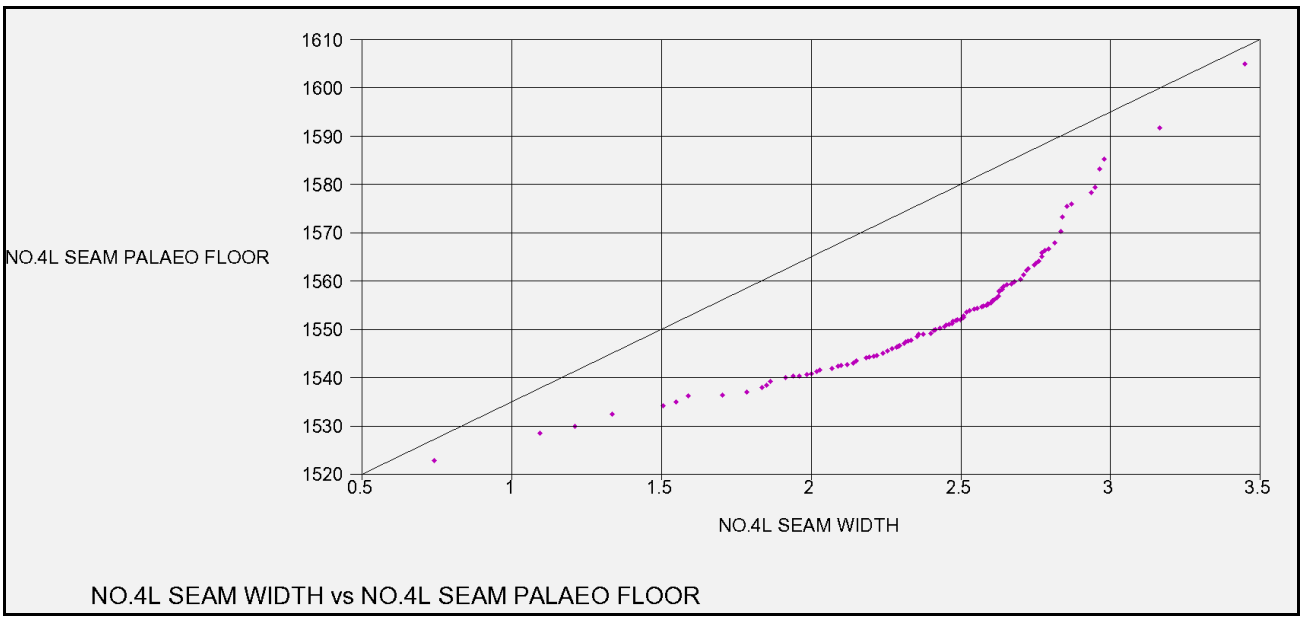

Figure 4.65: Quantile-Quantile plot of the No. 4L Coal Seam width and palaeo floor elevation.

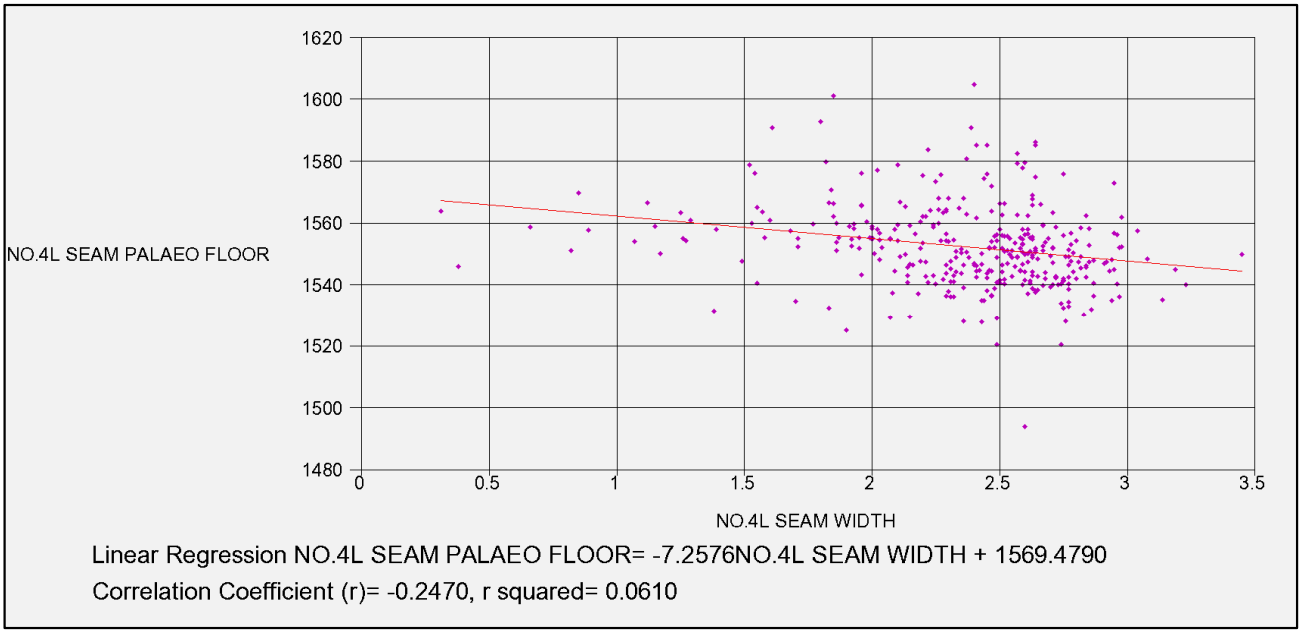

Figure 4.66: Correlation coefficient between the No. 4L Coal Seam width and its palaeo floor elevation.

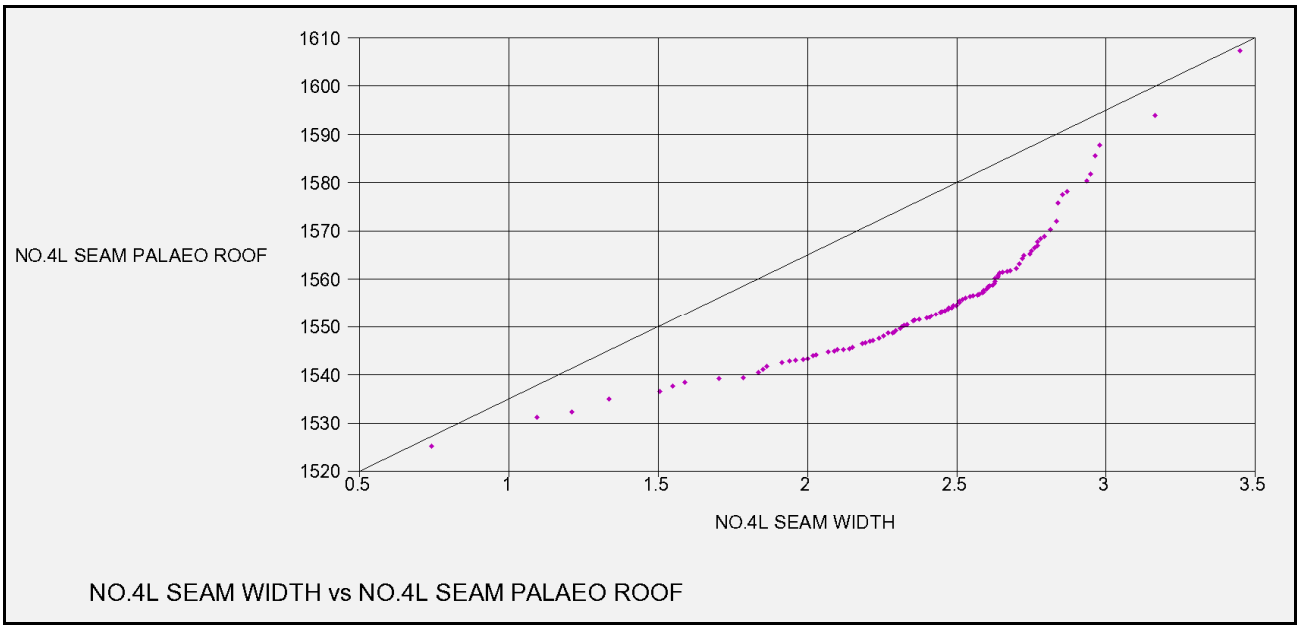

Figure 4.67: Quantile-Quantile plot of the No. 4L Coal Seam width and palaeo roof elevation.

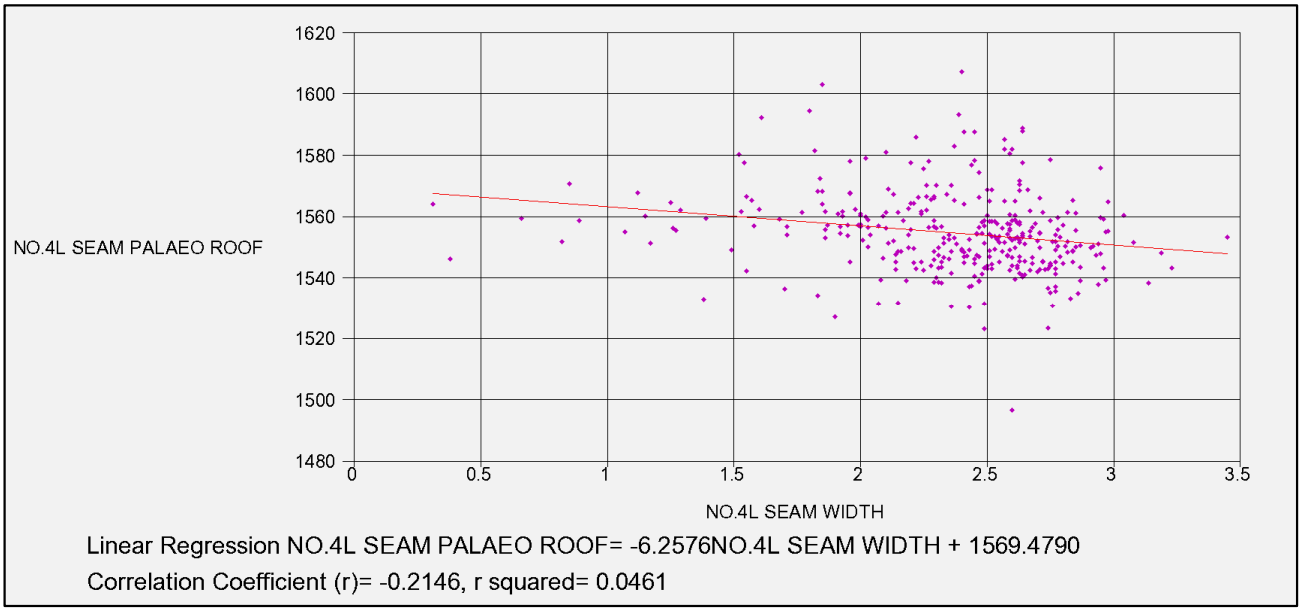

Figure 4.68: Correlation coefficient of the No. 4L Coal Seam width and its palaeo roof elevation.

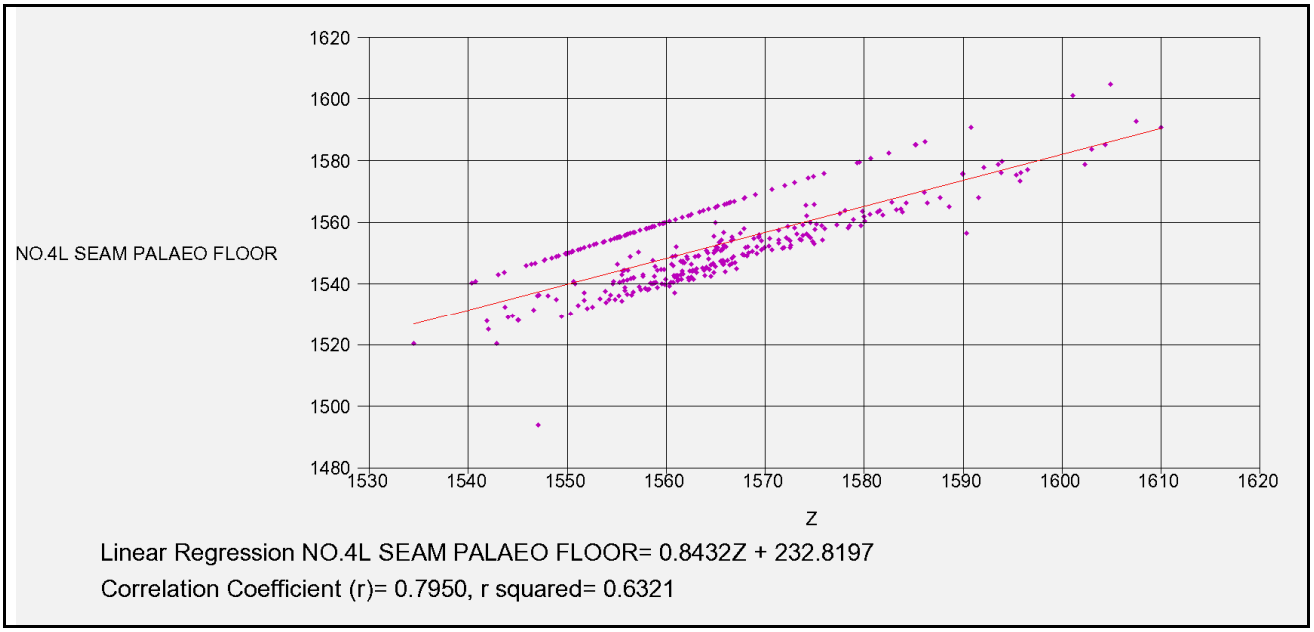

Figure 4.69: Quantile-Quantile plot of the No. 4L Coal Seam floor and palaeo floor elevation.

4.4.4.4 DISCUSSION AND INTERPRETATION

The No. 4L Coal Seam data set is supported by 349 samples which cover a surface area of 12,447,999m^2. The average sample spacing equates to 189m.

CLASSICAL STATISTICS

WIDTH

A negatively skewed distribution of -1.38 (Table 4.5) is revealed by the histogram plot in Figure 4.56. The coefficient of variation of 0.19 indicates low variability in the data. Deviation in the straightness of the probability curve in Figure 4.56 illustrates the skewness in the data set.

FLOOR

The histogram plot in Figure 4.57 is positively skewed by 0.89. Low variability in the data is confirmed by the coefficient of variation of 0.01. The slight skewness in the the data set is revealed by the probability curve in Figure 4.57.

PALAEO FLOOR

The histogram plot in Figure 4.58 is slightly negatively skewed by 0.52. The coefficient of variation is 0.01 which indicates low variability of the data. A few kinks in the probability curve (Figure 4.58) show the negative skewness. Similarly to the No. 2 Coal Seam the uneven pre-Karoo basement and its role in the differential compaction of the sedimentary rocks and coal could be related to the observed skewness.

PALAEO ROOF

The distribution of the palaeo roof data set (Figure 4.59) is similar to the distribution of the palaeo floor data set. A comparison between the coefficient of variation, skewness and kurtosis of the palaeo roof versus the palaeo floor (Table 4.5) show insignificant differences which reveal the close similarity between the two data sets.

DATA INTERPOLATION AND ANALYSIS

The width distribution of the No. 4L Coal Seam in Figure 4.61 is fairly consistent with the exception of a few isolated bulls-eyes. The QQ-plot of the palaeo floor and roof data in Figure 4.63 shows a tight relationship to the ideal line. The 0.99 correlation coefficient (Figure 4.64) and the visual

comparison of the contour plots in Figures 4.60 and 4.62 is a confirmation of the rigid linear relationship that exists between the palaeo floor and roof. The QQ-plot (Figure 4.65) of the width and palaeo floor data with respect to the ideal line reveals an inverse relationship. This inverse relationship calculates a poor correlation coefficient of -0.25 (Figure 4.67).

A comparison of the curves resulted from the QQ-plots between the width and the palaeo-floor (Figure 4.65) and roof (Figure 4.67), respectively confirm the similarity that exists between the two data sets. A correlation coefficient of -0.21 (Figure 4.69) between the width and the palaeo roof exhibits a poor relationship. In Figure 4.62 the quantity of the palaeo floor data versus uplifted floor data is demonstrated.

4.4.5 NO.4L-5 COAL SEAM FACIES

4.4.5.1 CLASSICAL STATISTICS

Table 4.6: Classical Statistics of the No. 4L-5 Coal Seams.

FACIES	BETWEEN NO. 4L-5 COAL SEAMS
VARIABLE	WIDTH
NUMBER OF SAMPLES	184
MINIMUM VALUE	5.24
MAXIMUM VALUE	39.8
MEAN	28.179
VARIANCE	14.148
STANDARD DEVIATION	3.761
COEFFICIENT OF VARIATION	0.133
SKEWNESS	-3.214
KURTOSIS	19.791
TRIMEAN	28.526
BIWEIGHT	28.58
MAD	1.445
ALPHA	-5.188
SICHEL-T	1.54E+15

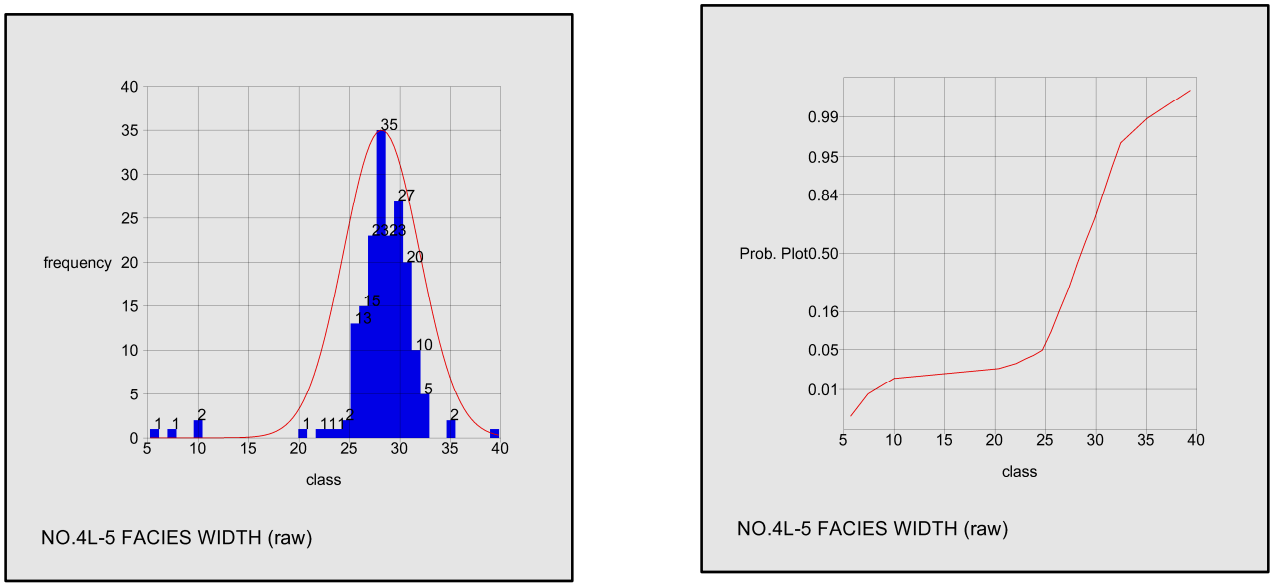

Figure 4.70: Histogram and probility plot of the net facies width between No. 4L–5 Coal Seams.

4.4.5.2 DATA INTERPOLATION

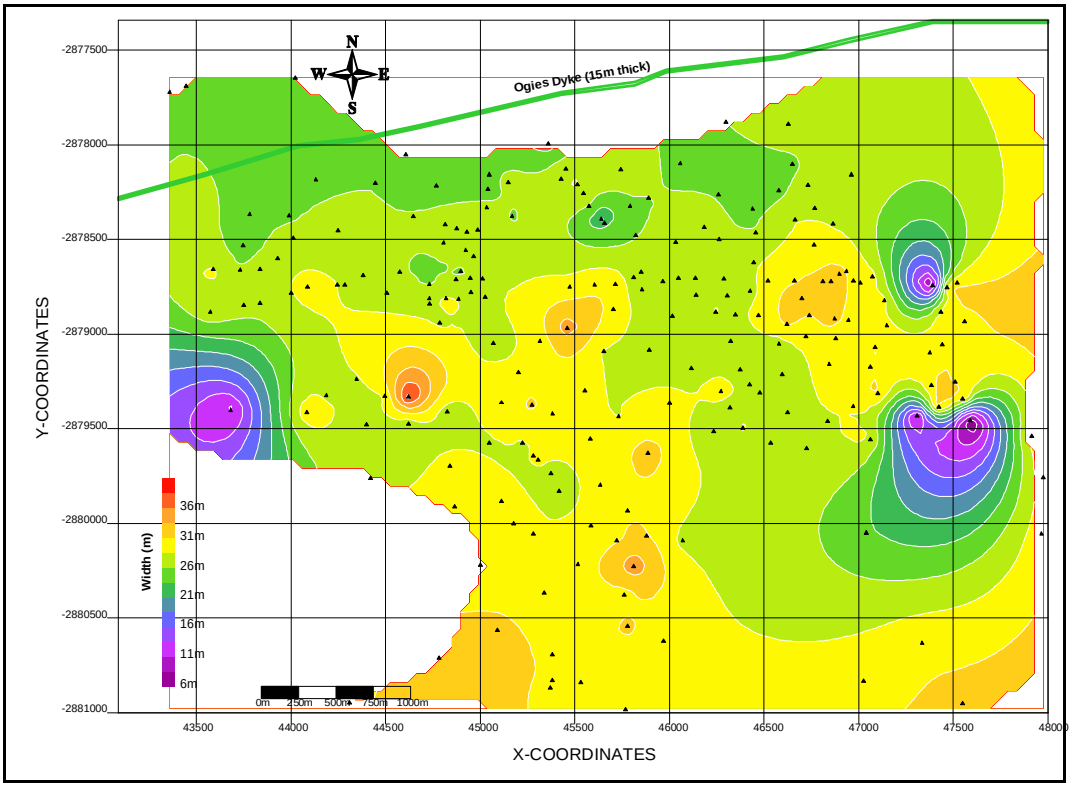

Figure 4.71: The net facies width between No. 4L-5 Coal Seams.

4.4.5.3 DATA ANALYSIS

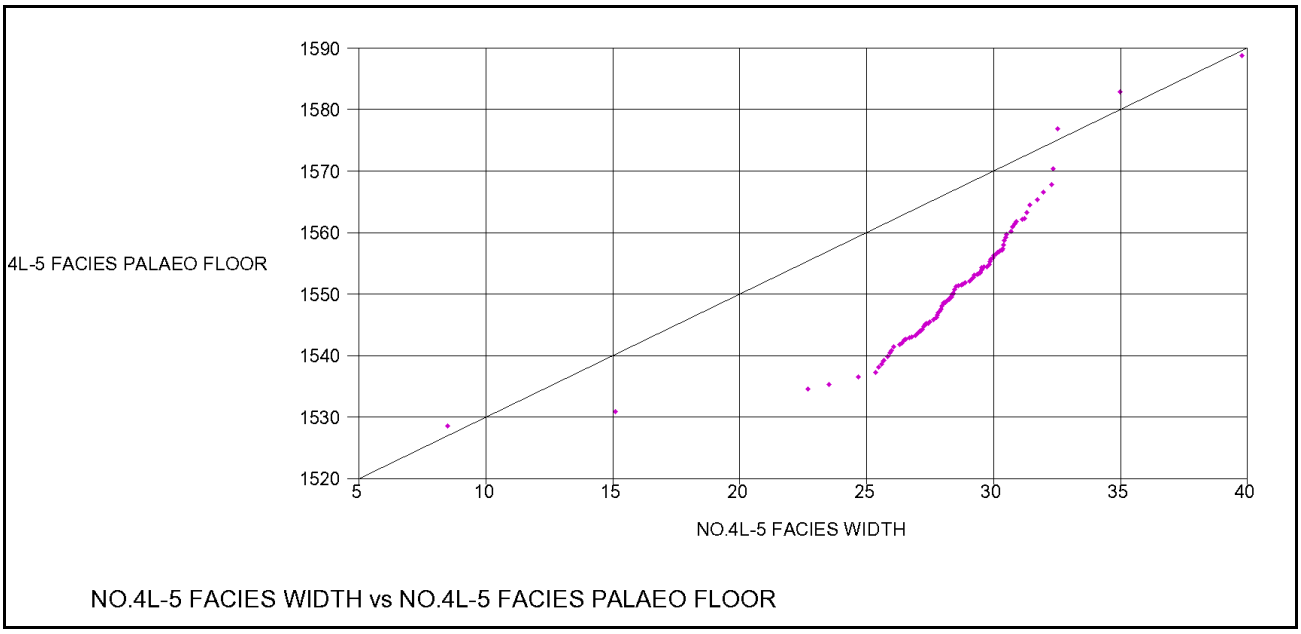

Figure 4.72: Quantile-Quantile plot of the net facies width between No. 4L and No. 5 Coal Seams and its palaeo floor elevation.

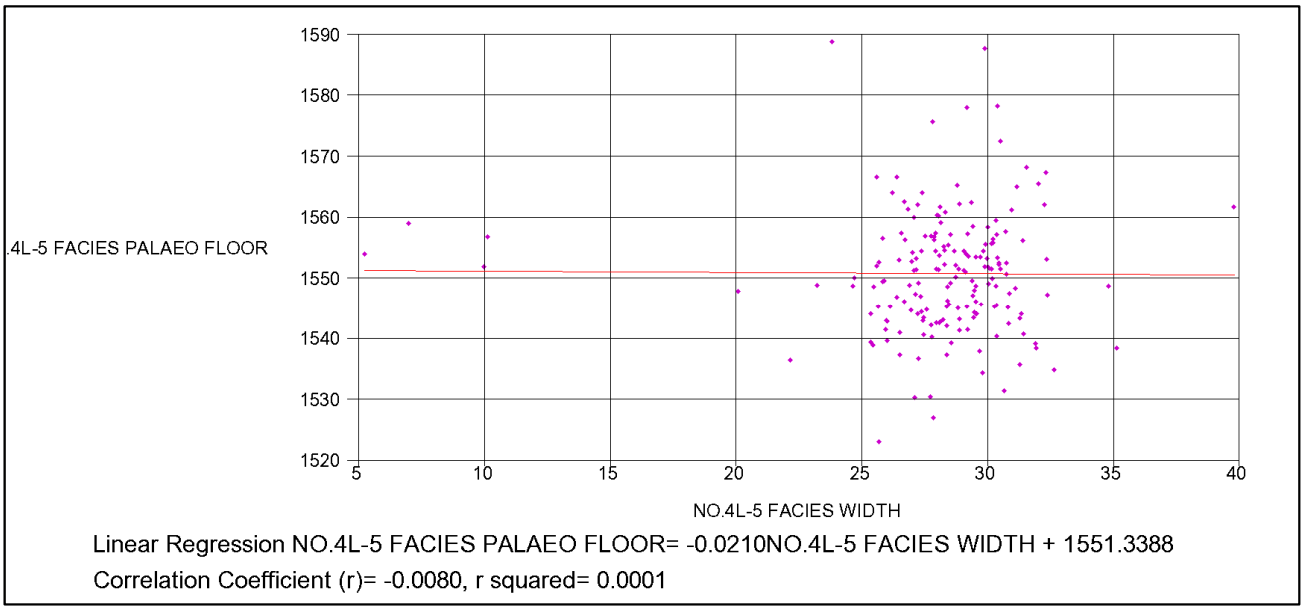

Figure 4.73: Correlation coefficient of the net facies width between No. 4L and No. 5 Coal Seams and its palaeo floor elevation.

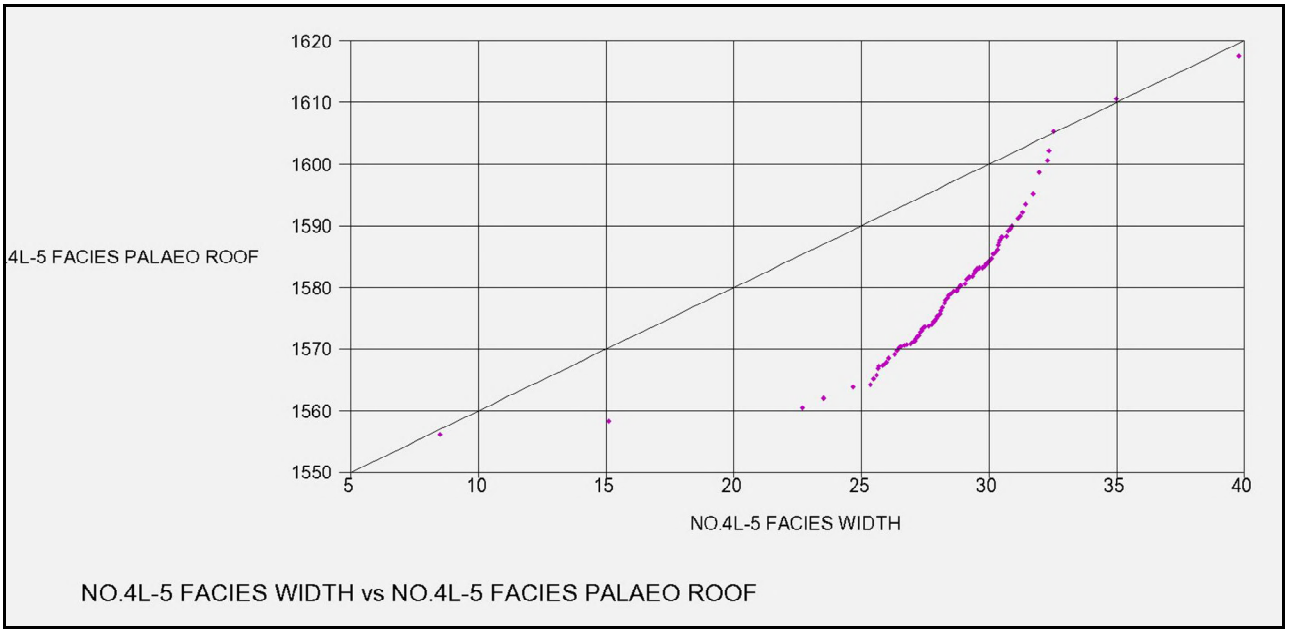

Figure 4.74: Quantile-Quantile plot of the net facies width between No. 4L and No. 5 Coal Seams and its palaeo roof elevation.

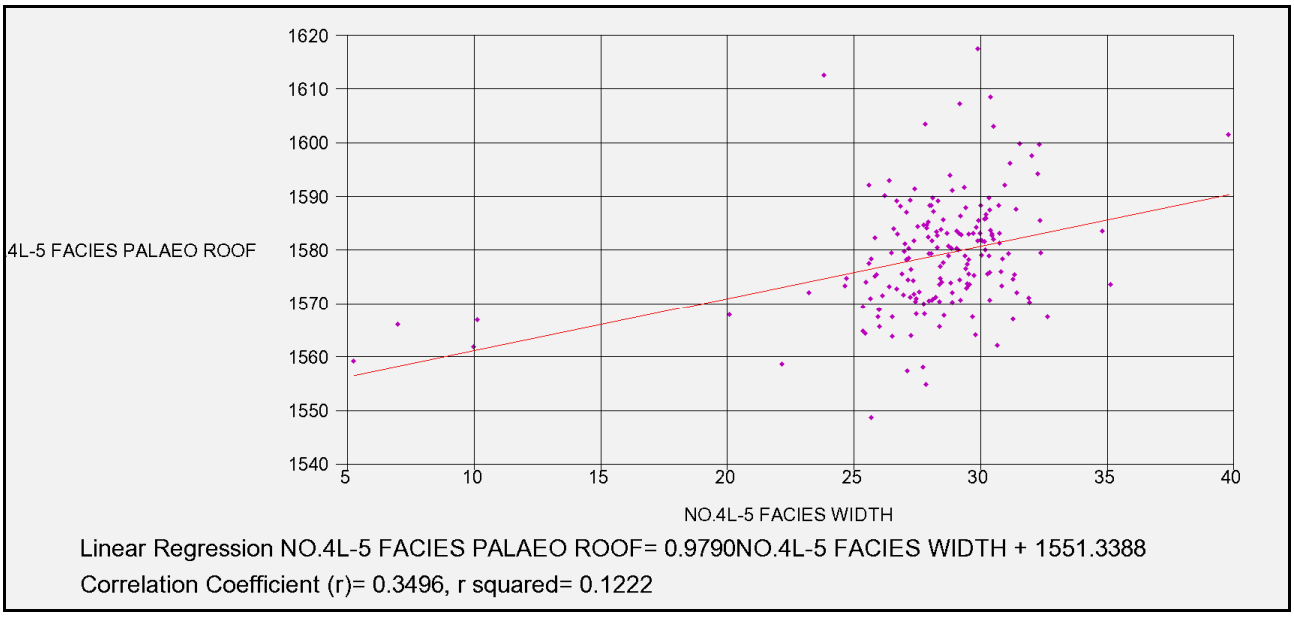

Figure 4.75: Correlation coefficient of the net facies width between No. 4L and No. 5 Coal Seams and its palaeo roof elevation.

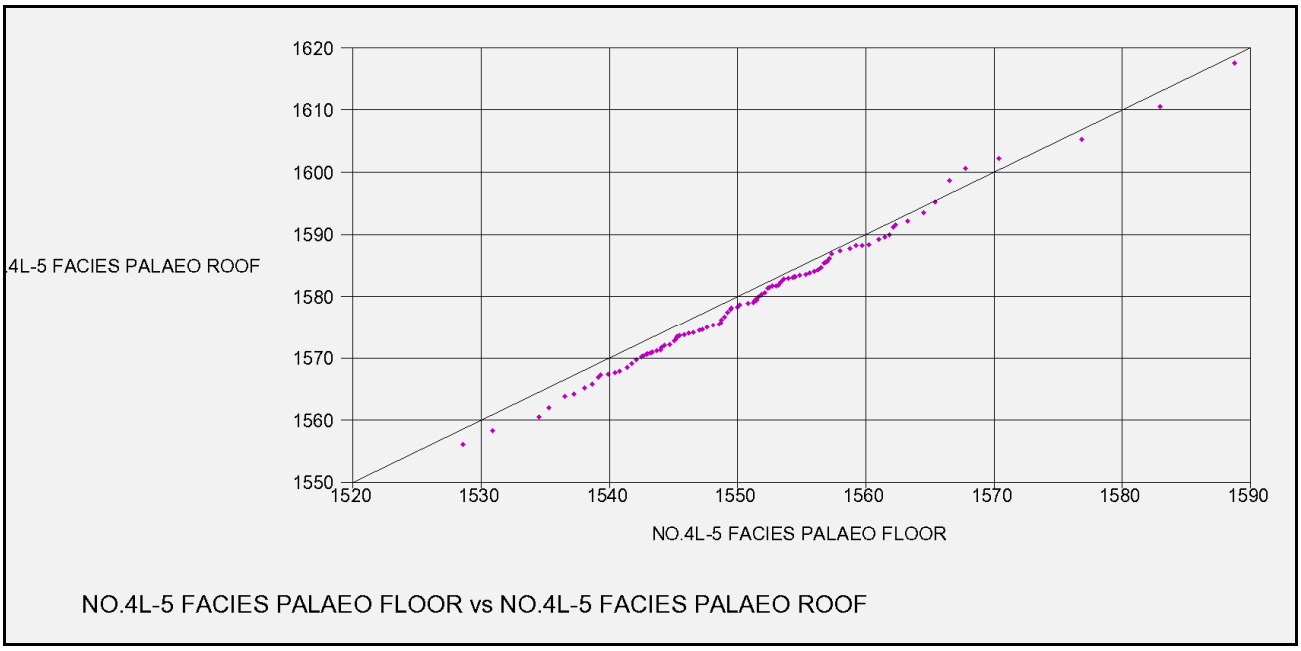

Figure 4.76: Quantile-Quantile plot of the palaeo floor and roof of the net facies width between No. 4L and No. 5 Coal Seams.

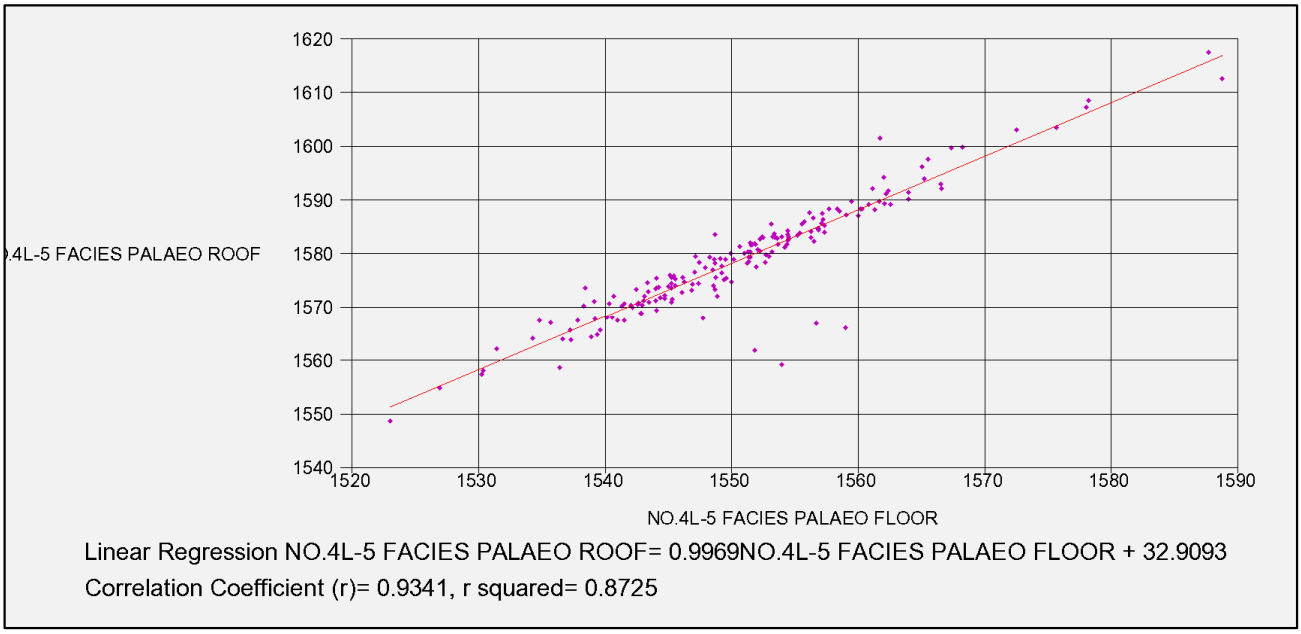

Figure 4.77: Correlation coefficient of the palaeo floor and roof of the net facies width between No. 4L and No. 5 Coal Seams.

4.4.5.4 DISCUSSION AND INTERPRETATION

The net facies width between No. 4L Coal Seam and No. 5 Coal Seam data set is supported by 184 samples which cover a surface area of 11,431,260m^2. The average sample spacing equates to 249m.

The histogram plot in Figure 4.70 is strongly negatively skewed by -3.21 (Table 4.6) as a result of the associated outlier data. The outlier data exists on both the low-end and top-end of the data range. Both the QQ-plots (Figure 4.72 and Figure 4.74) and regression curves (Figure 4.73 and Figure 4.75) reveal a poor, non-existing relationships between the net width and the palaeo floor and roof, respectively. However, the QQ-plot between the palaeo floor and roof has a close relationship with the ideal line (Figure 4.76). A direct relationship is confirmed with the correlation coefficient of 0.93 (Figure 4.77).

EXCLUSION OF OUTLIER DATA

The outlier data is examined through the calculation of one percent percentiles from 1 to 100. The percentile data graph is shown in Figure 4.78. The graph shows a sudden increase towards the 6th and the 98th percentile which represents values of 25.03m and 33.74m, respectively. Data above the yellow arrow line and below the red arrow line resulted in a symmetric histogram plot and a reasonably straight probability curve (Figure 4.79). The homogeinity in the data distribution is represented by an intergral part of the area.

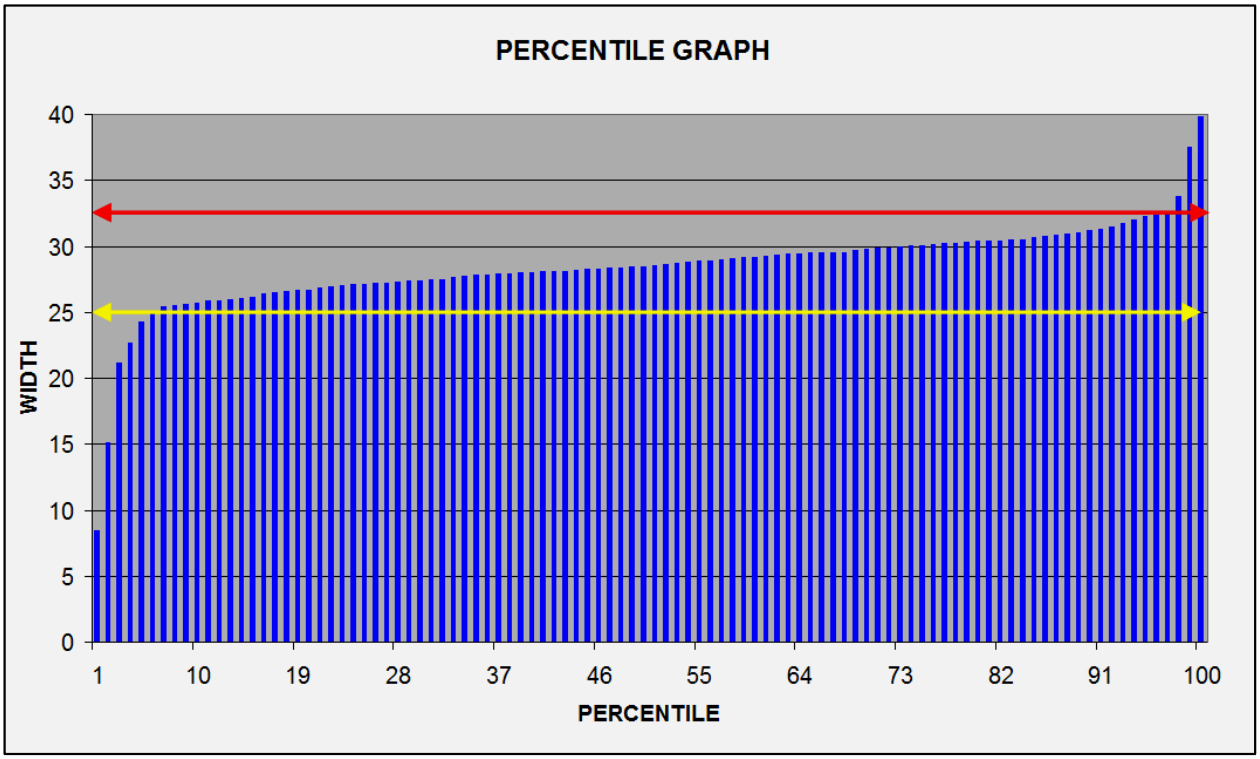

Figure 4.78: Percentile graph of the net facies width between the No.4L Coal Seam and the No. 5 Coal Seam.

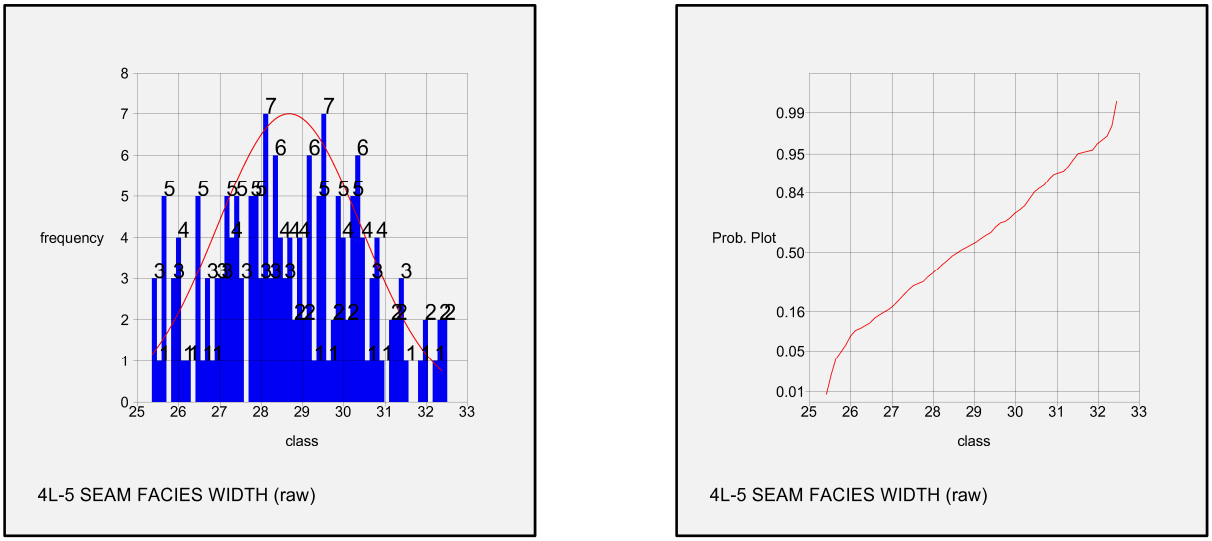

Figure 4.79: Histogram and probability plot of the facies width between No. 4L – 5 Coal Seam excluding the outlier data.

4.4.6 NO.5 COAL SEAM

4.4.6.1 CLASSICAL STATISTICS

Table 4.7: Classical Statistics of the No. 5 Coal Seam.

SEAM	NO.5 COAL SEAM			
VARIABLE	WIDTH	FLOOR	PALAEO-FLOOR	PALAEO-ROOF
NUMBER OF SAMPLES	310	310	310	310
MINIMUM VALUE	0.09	1544.09	1544.09	1545.81
MAXIMUM VALUE	2.37	1625.8	1625.64	1626.97
MEAN	1.42	1592.40	1580.04	1593.82
VARIANCE	0.11	165.11	159.74	164.48
STANDARD DEVIATION	0.34	12.85	12.64	12.83
COEFFICIENT OF VARIATION	0.24	0.01	0.01	0.01
SKEWNESS	-0.56	0.27	0.52	0.26
KURTOSIS	5.46	3.60	3.80	3.58
TRIMEAN	1.44	1591.79	1579.48	1593.04
BIWEIGHT	1.44	1591.37	1579.26	1592.72
MAD	0.16	6.54	8.08	6.70
ALPHA	-0.09	-1517.34	-1524.20	-1527.18
SICHEL-T	4.38	Not Calculated	Not Calculated	Not Calculated

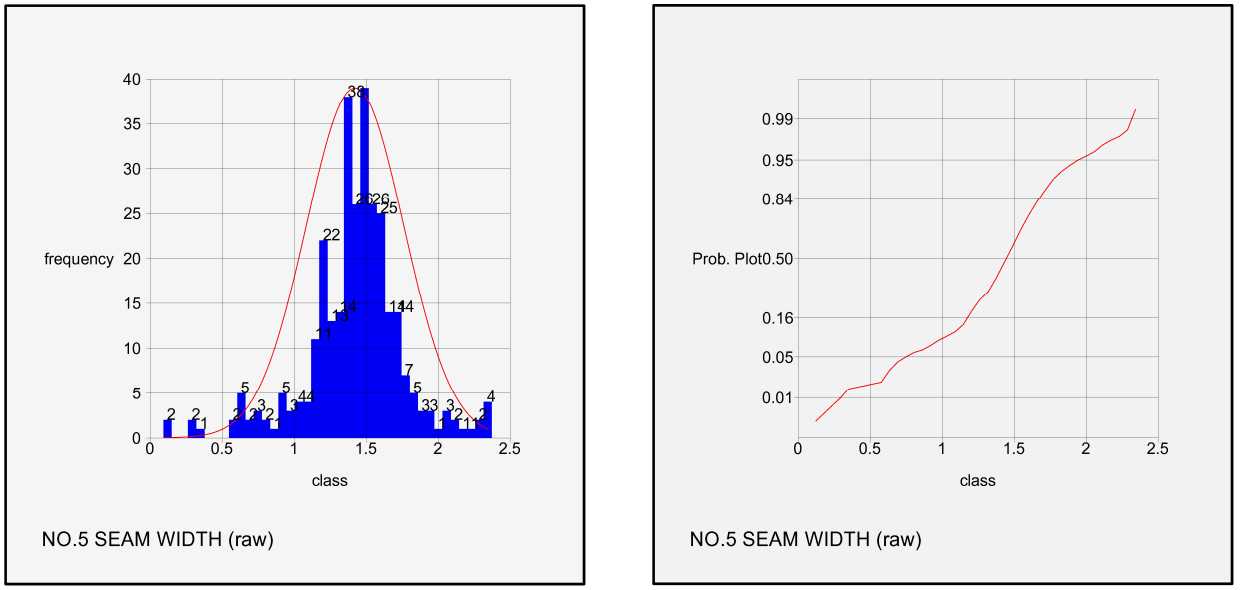

Figure 4.80: Histogram and probility plot of the No.5 Coal Seam width.

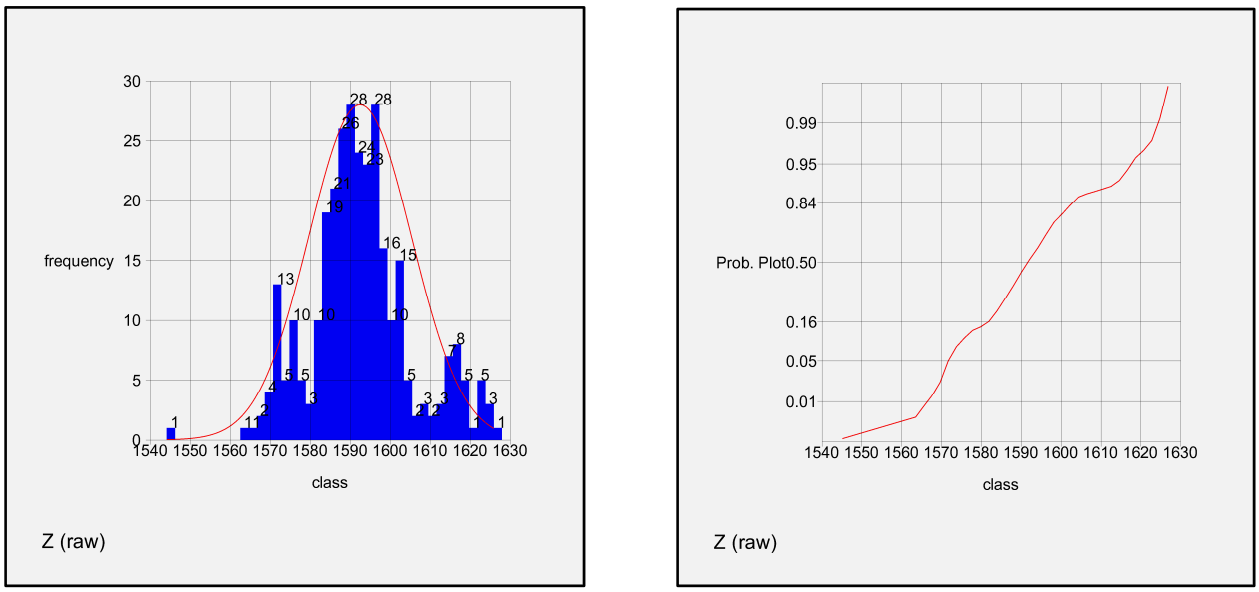

Figure 4.81: Histogram and probility plot of the No. 5 Coal Seam floor.

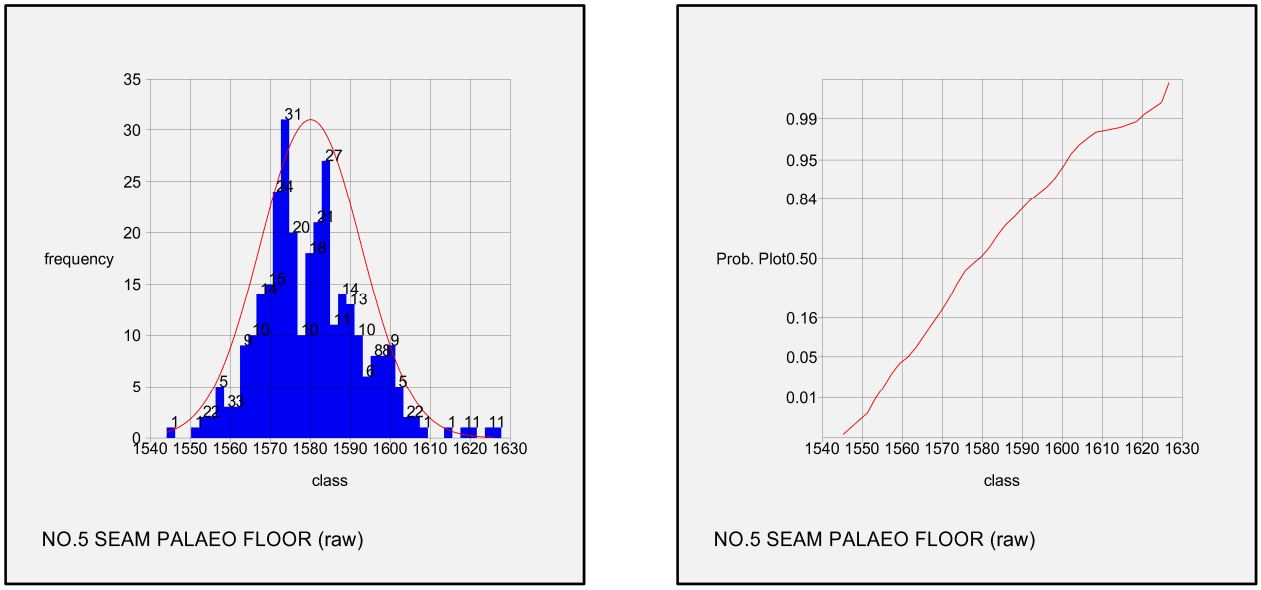

Figure 4.82: Histogram and probility plot of the No. 5 Coal Seam paleo floor elevation.

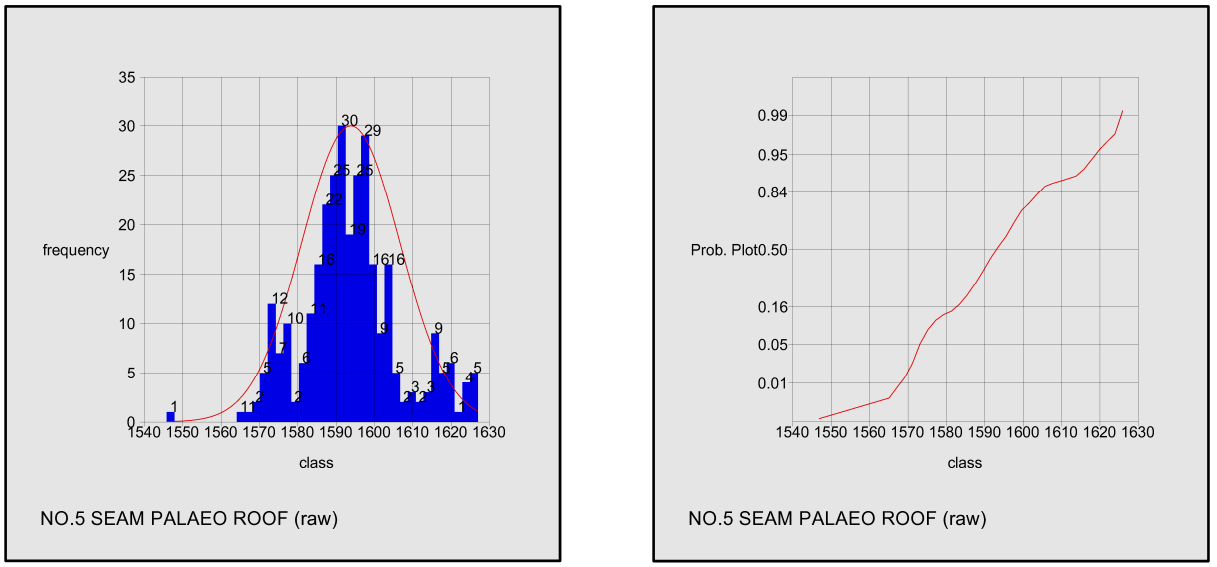

Figure 4.83: Histogram and probility plot of the No. 5 Coal Seam paleo roof elevation.

4.4.6.2 DATA INTERPOLATION

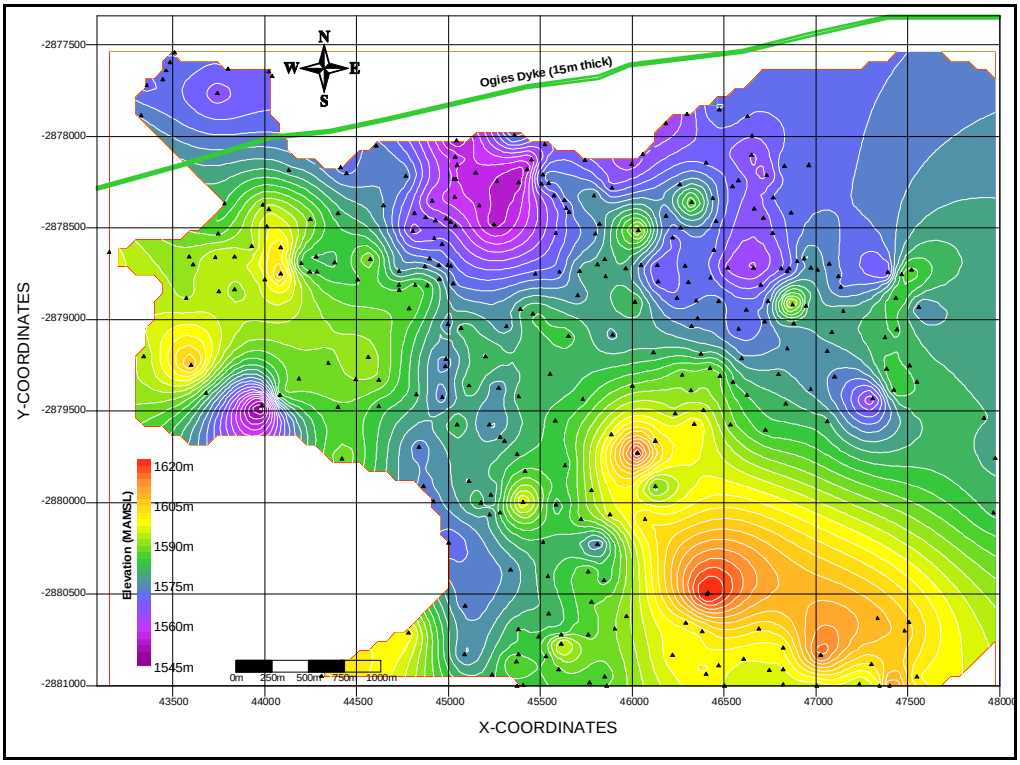

Figure 4.84: No. 5 Coal Seam palaeo floor elevation.

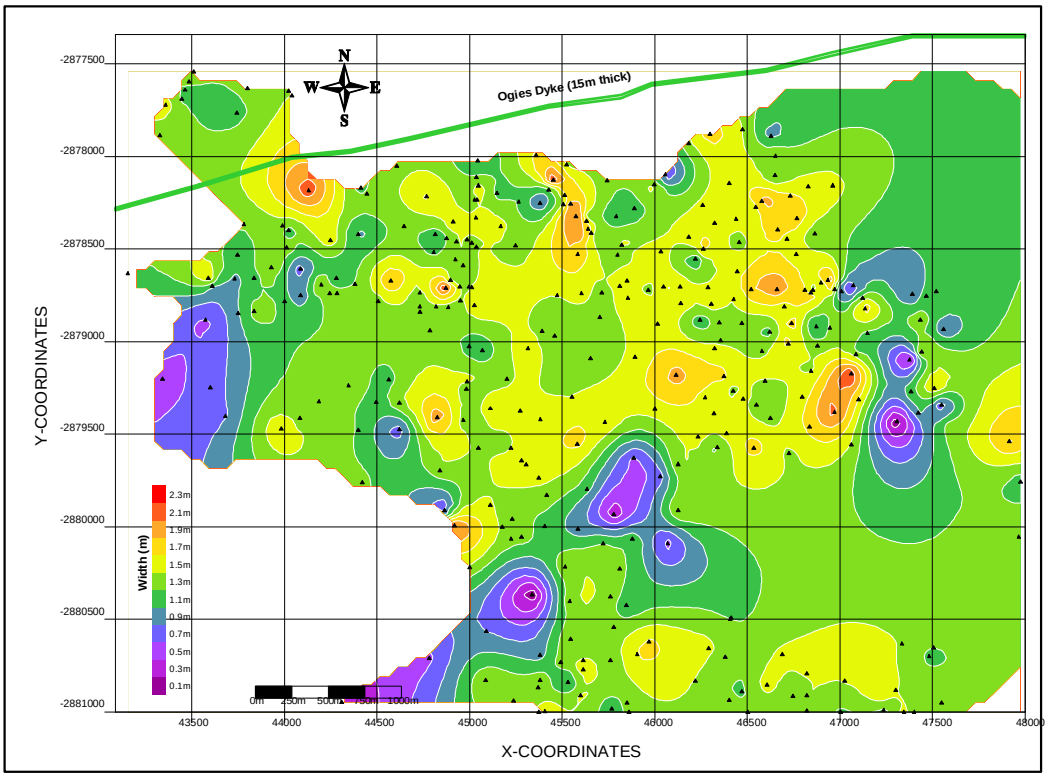

Figure 4.85: No. 5 Coal Seam width.

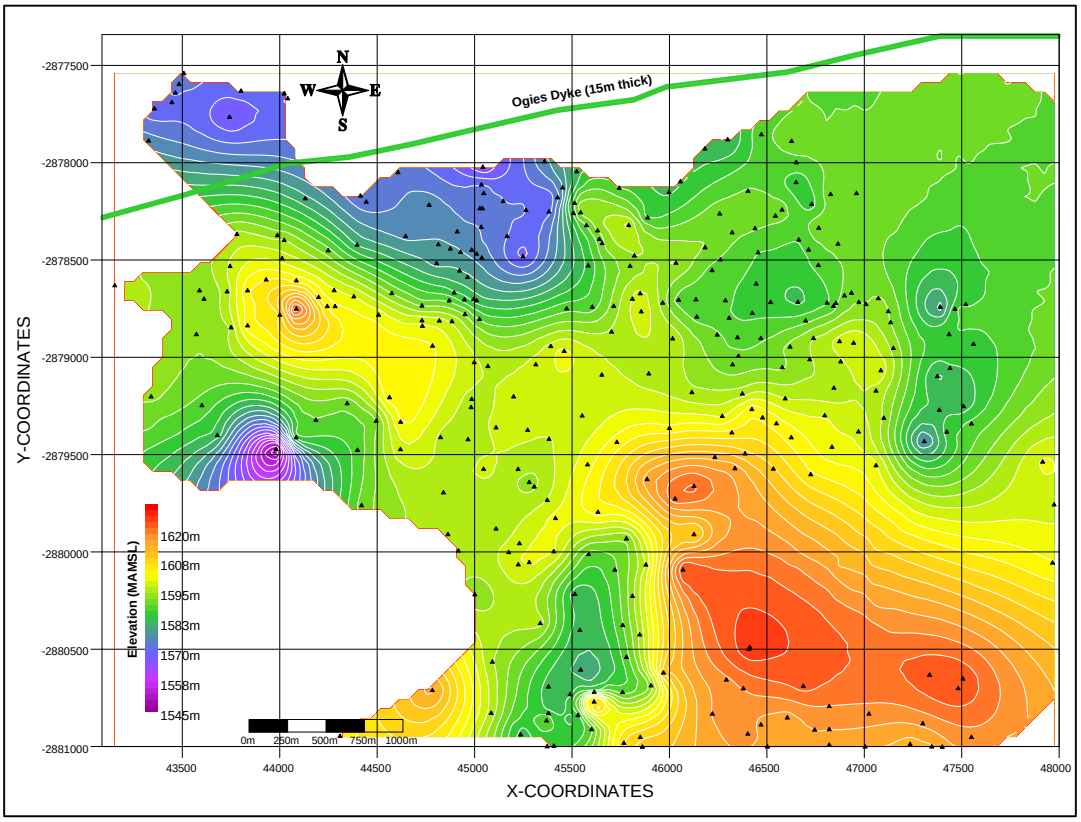

Figure 4.86: No. 5 Coal Seam palaeo roof elevation.

4.4.6.3 DATA ANALYSIS

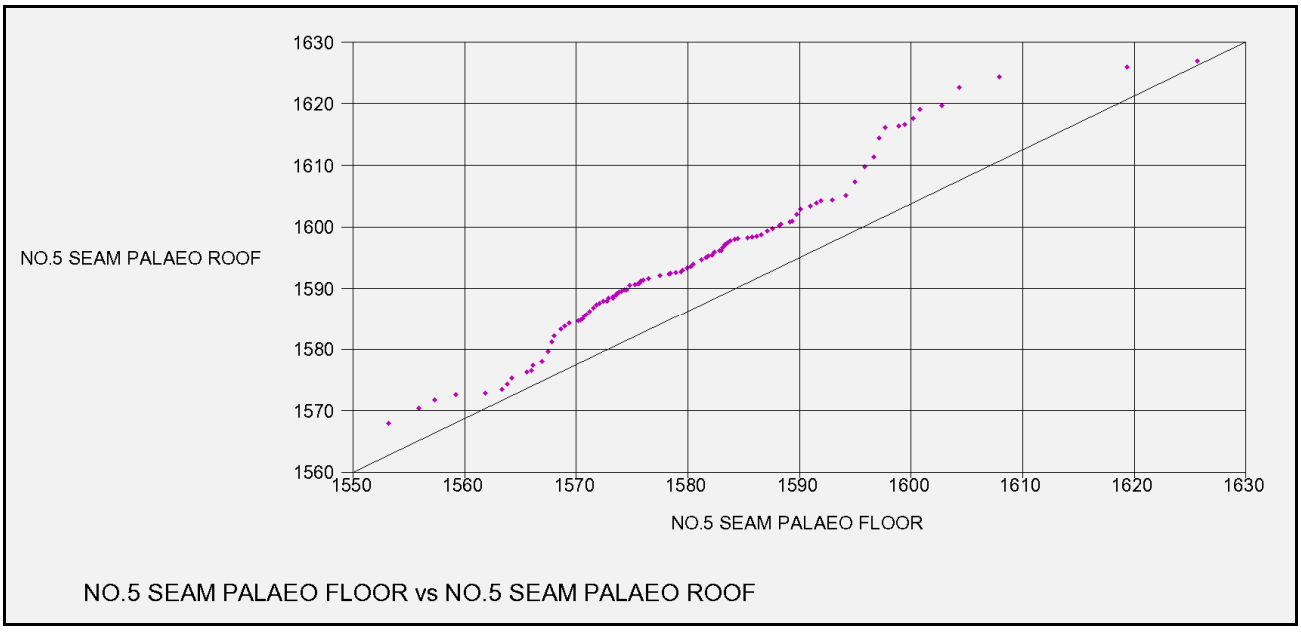

Figure 4.87: Quantile-Quantile plot of the No. 5 Coal Seam palaeo floor and roof elevations.

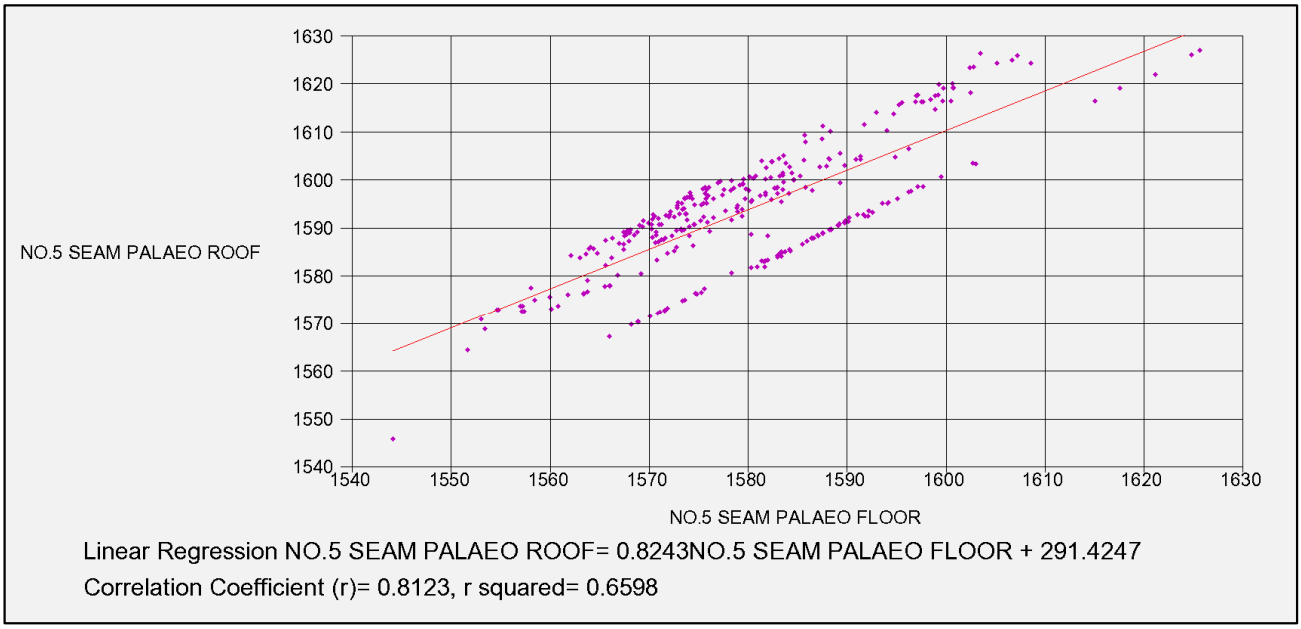

Figure 4.88: Correlation coefficient between the No. 5 Coal Seam palaeo floor and roof elevations.

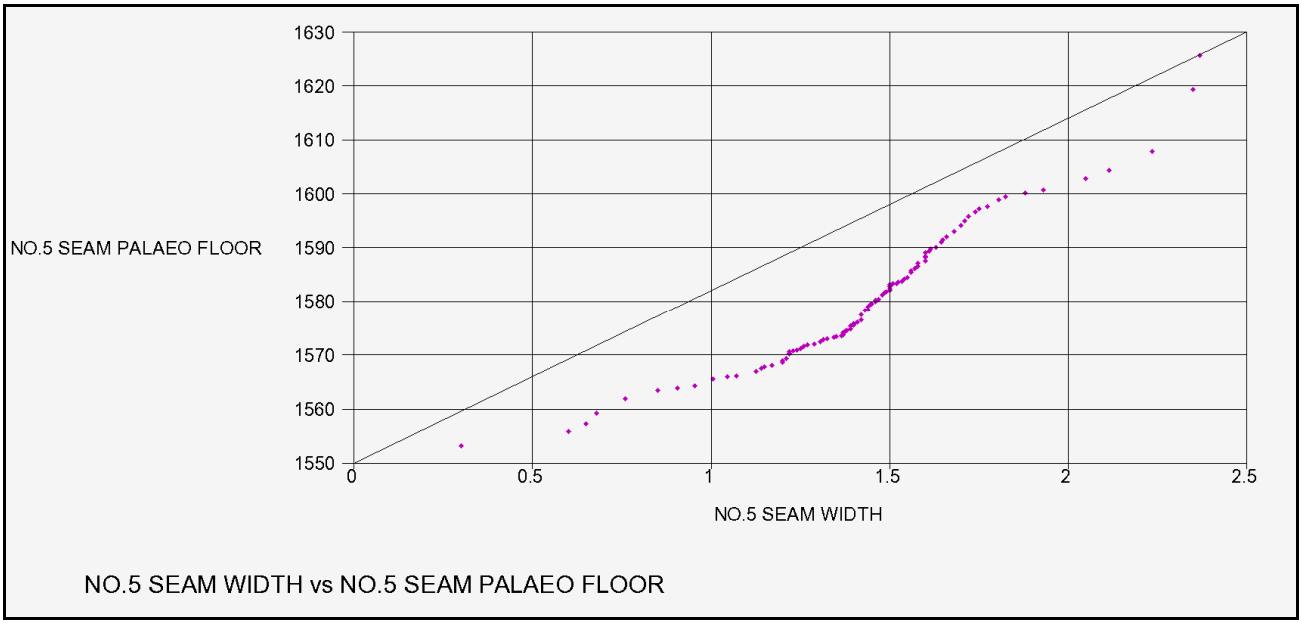

Figure 4.89: Quantile-Quantile plot of the No. 5 Coal Seam width and palaeo floor elevation.

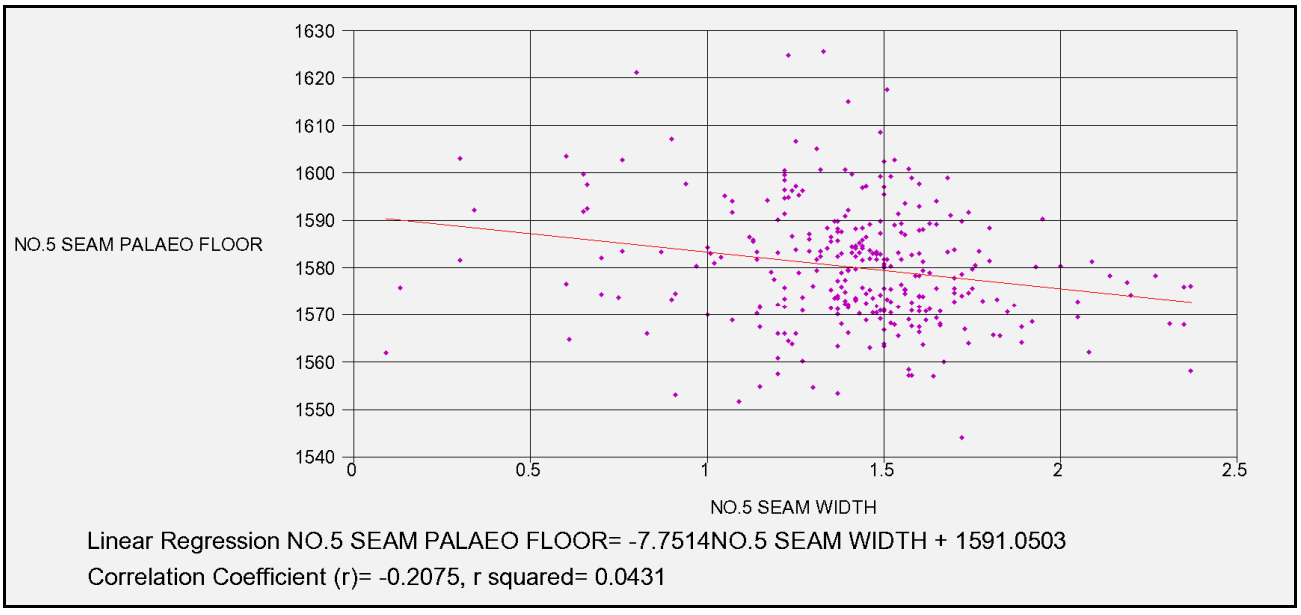

Figure 4.90: Correlation coefficient between the No. 5 Coal Seam width and its palaeo floor elevation.

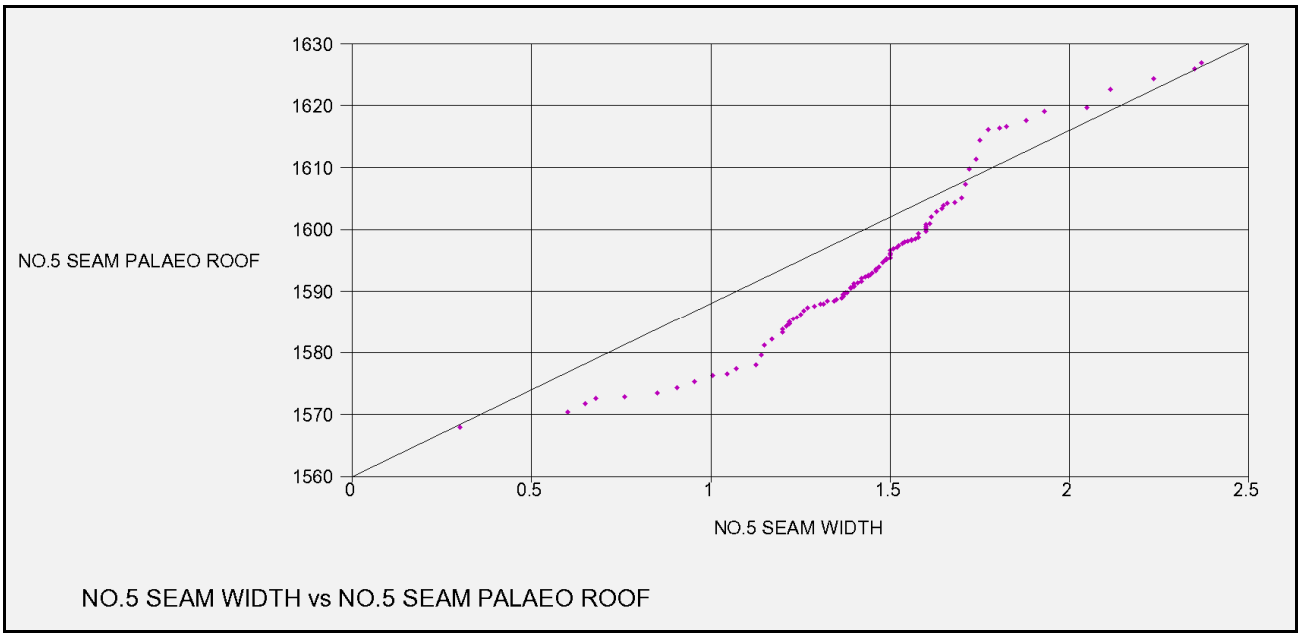

Figure 4.91: Quantile-Quantile plot of the No. 5 Coal Seam width and palaeo roof elevation.

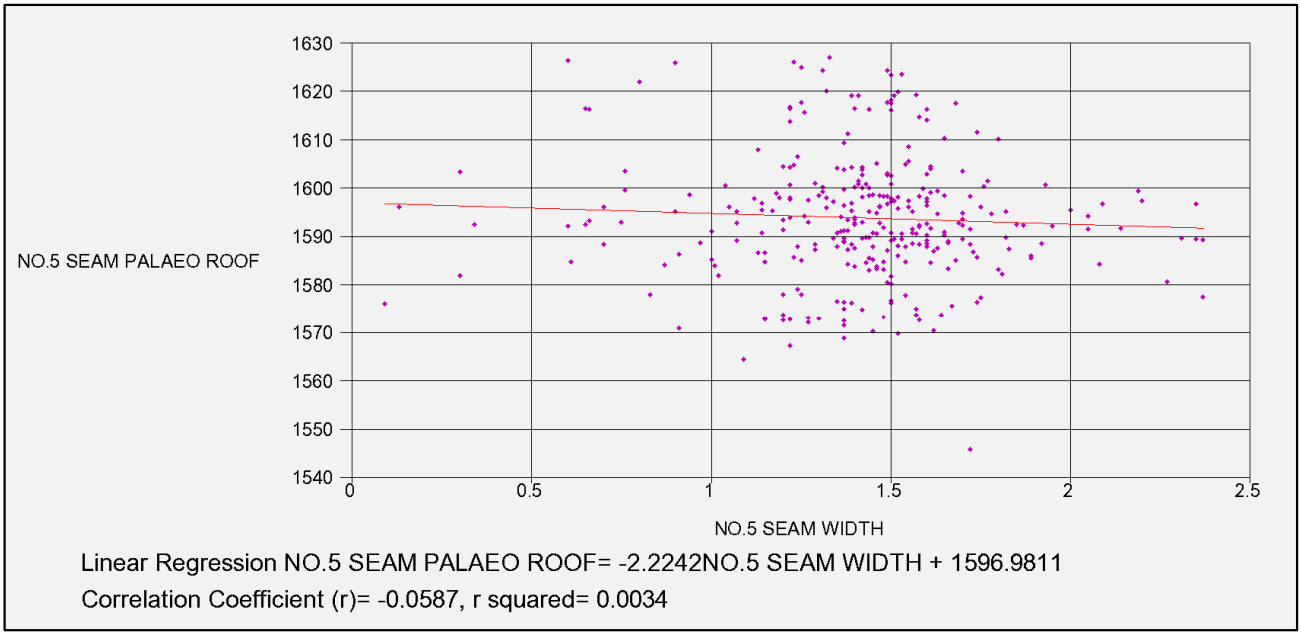

Figure 4.92: Correlation coefficient of the No. 5 Coal Seam width and its palaeo roof elevation.

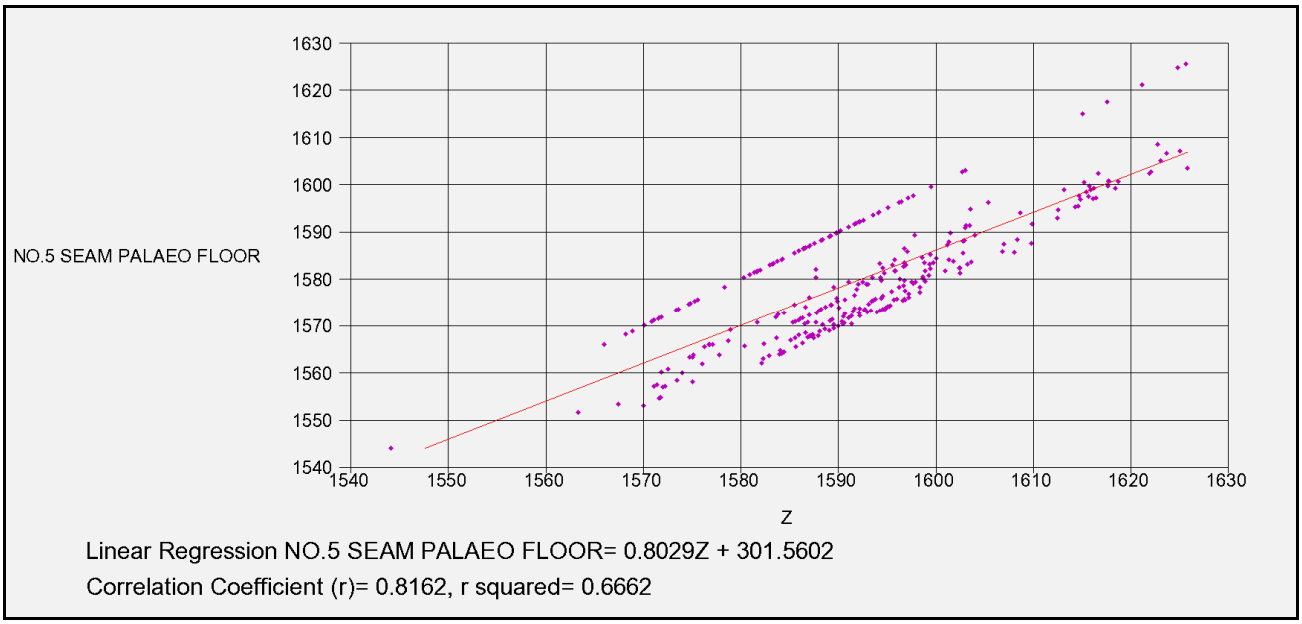

Figure 4.93: Correlation coefficient of the No. 5 Coal Seam floor and palaeo floor elevation.

4.4.6.4 DISCUSSION AND INTERPRETATION

The No. 5 Coal Seam data set is supported by 310 samples which cover a surface area of 11,556,985m^2. The average sample spacing equates to 193m.

CLASSICAL STATISTICS

WIDTH

A negatively skewed distribution of -0.56 (Table 4.7) is revealed by the histogram plot in Figure 4.80. This skewness is also illustrated in the deviation of the straightness of the probability curve in Figure 4.80. The coefficient of variation of 0.24 indicates low variability in the data.

FLOOR

The histogram plot in Figure 4.81 is negatively skewed by -0.56. The slight skewness in the data set is revealed by the probability curve in Figure 4.81. Low variability in the data is confirmed with the coefficient of variation of 0.01 (Table 4.7).

PALAEO FLOOR

The histogram plot in Figure 4.82 is slightly positively skewed by 0.52. The coefficient of variation is 0.01 which indicates low variability of the data. The probability curve (Figure 4.82) shows the slight positive skewness in the data set. Similarly to the No. 2 Coal Seam and 4L Coal Seam the the role of the uneven pre-Karoo basement in the differential compaction of the sedimentary rocks could be related to the observed skewness.

PALAEO ROOF

The distribution of the palaeo roof data set (Figure 4.83) is similar to the distribution of the palaeo floor data set. The coefficient of variation, skewness and kurtosis of the palaeo roof versus the palaeo floor (Table 4.7) show larger differences in comparison to the the No. 2 and 4L Coal Seam.

DATA INTERPOLATION AND ANALYSIS

The width distribution of the No. 5 Coal Seam in Figure 4.85 is fairly consistent for an integral part of the data coverage. A deviation from the ideal line is illustrated in the QQ-plot (Figure 4.87) between palaeo floor and roof data. The 0.81 correlation coefficient (Figure 4.88) and the visual comparison of the contour plots in Figures 4.84 and 4.86 portray the linear relationship that exists between the palaeo floor and roof. The QQ-plot (Figure 4.89) of the width and palaeo floor data with respect to the ideal line reveals a poor relationship. This poor relationship is confirmed by the correlation coefficient of -0.21 in Figure 4.90.

A correlation coefficient of -0.06 (Figure 4.92) between the width and the palaeo roof exhibits a poor relationship. This poor relationship could be a result of the close proximity of the No. 5 Coal Seam to the present day surface and the probable exposure to relatively higher degrees of weathering. In Figure 4.93 the quantity of palaeo floor data versus uplifted floor data is demonstrated.

4.5 SUMMARY AND CONCLUSIONS

A summary of the correlation coefficient values are shown in Table 4.8. The number of samples used to derive the correlation coefficients between any two variables depends on the number of boreholes that intersected both variables. As a result of the existing linearity between the palaeo floor and roof elevations the relationship between the floor elevations of the No.2, 4L and 5 Coal Seams was investigated. This investigation resulted in close to direct linear correlation curves (Figure 4.94) which disclose the existing relationships between the palaeo floor elevations of the No.2, No.4L and No.5 Coal Seams. Considering the range of correlation coefficient values of 0.81 to 0.99 for the palaeo floor elevations (Table 4.8) it convincingly reveal the co-existing relationship in the geometry of elevations throughout the entire stratigraphy of the sedimentary sequences.

Table 4.8: Correlation coefficients calculated for variables of the sedimentological units: widths, palaeo floor, and roof elevations.

	No. 5 Coal Seam : palaeo roof	No. 5 Coal Seam : width	No. 5 Coal Seam : palaeo floor	No. 4L - 5 Coal Seam: facies width	No. 4L Coal Seam: palaeo roof	No. 4L Coal Seam: width	No. 4L Coal Seam: palaeo floor	No. 2 - 4L facies width	No. 2 Coal Seam: palaeo roof	No. 2 Coal Seam: width	No. 2 Coal Seam: palaeo floor
No. 5 Coal Seam : palaeo roof	1.00										
No. 5 Coal Seam : width	**0.06**	1.00									
No. 5 Coal Seam : palaeo floor	**0.81**	**0.21**	1.00								
No. 4L - 5 Coal Seam: facies width	-	-	**0.35**	1.00							
No. 4L Coal Seam: palaeo roof	-	-	**0.93**	**-0.21**	1.00						
No. 4L Coal Seam: width	-	-	-	-	**-0.21**	1.00					
No. 4L Coal Seam: palaeo floor	-	-	**0.87**	-	**0.99**	**-0.25**	1.00				
No. 2 - 4L facies width	-	-	-	-	-	-	**-0.20**	1.00			
No. 2 Coal Seam: palaeo roof	-	-	-	-	-	-	**0.93**	**-0.54**	1.00		
No. 2 Coal Seam: width	-	-	-	-	-	-	-	-	**-0.45**	1.00	
No. 2 Coal Seam: palaeo floor	-	-	**0.85**	-	-	-	**0.86**	-	**0.99**	**-0.57**	1.00

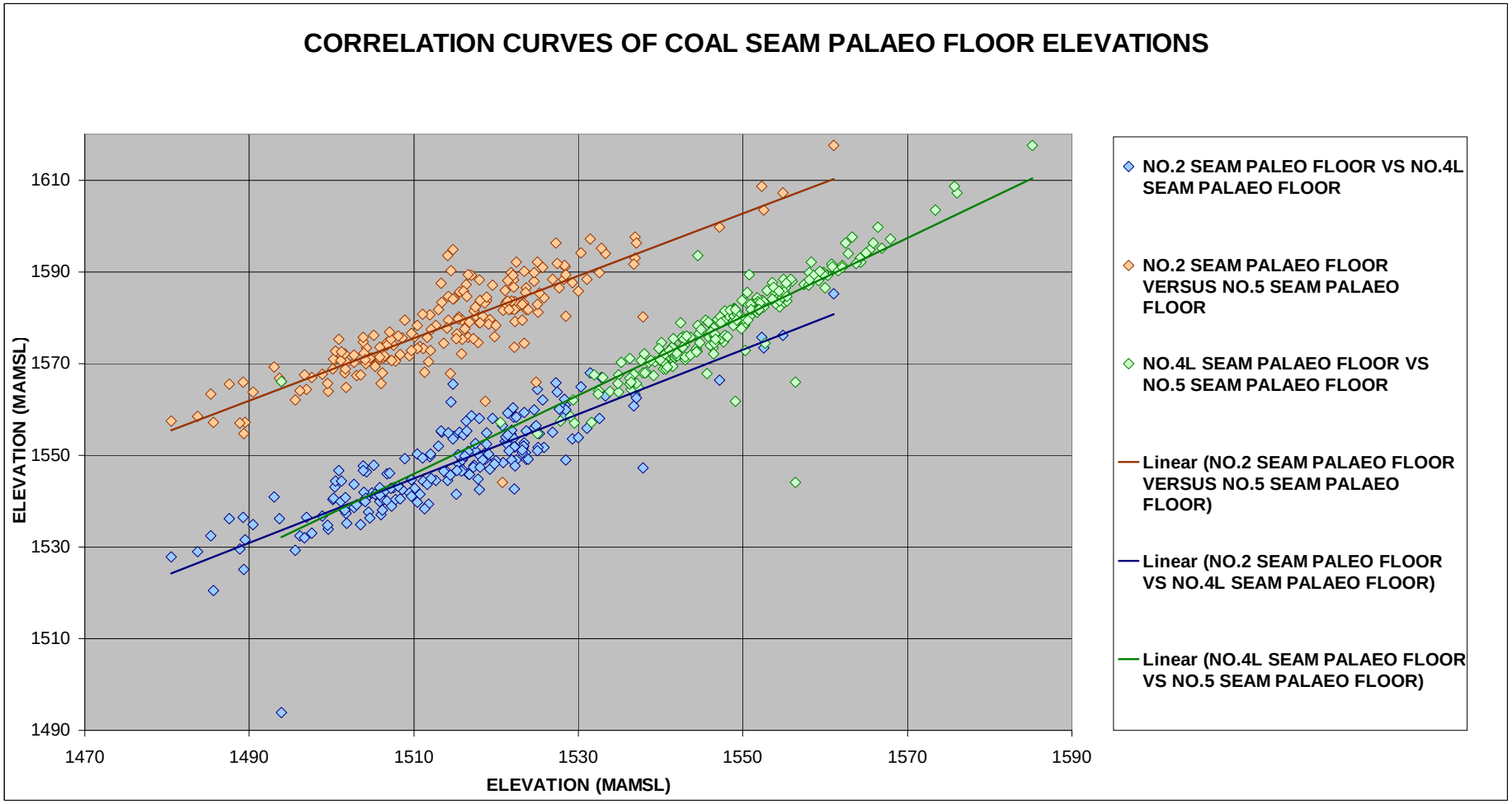

Figure 4.94: Correlation curves showing linear relationships of the palaeo floor elevations of the No.2, No.4L and No.5 Coal Seams.

Several factors contributed to the present day geometries and widths of coal and associated clastical sedimentary rocks of sequence of succession. Le Blanc Smith (1980) summarised five principal factors that affected coal distribution and width (Figure 4.95). Factors A, C and E are frequently recognised in the study area.

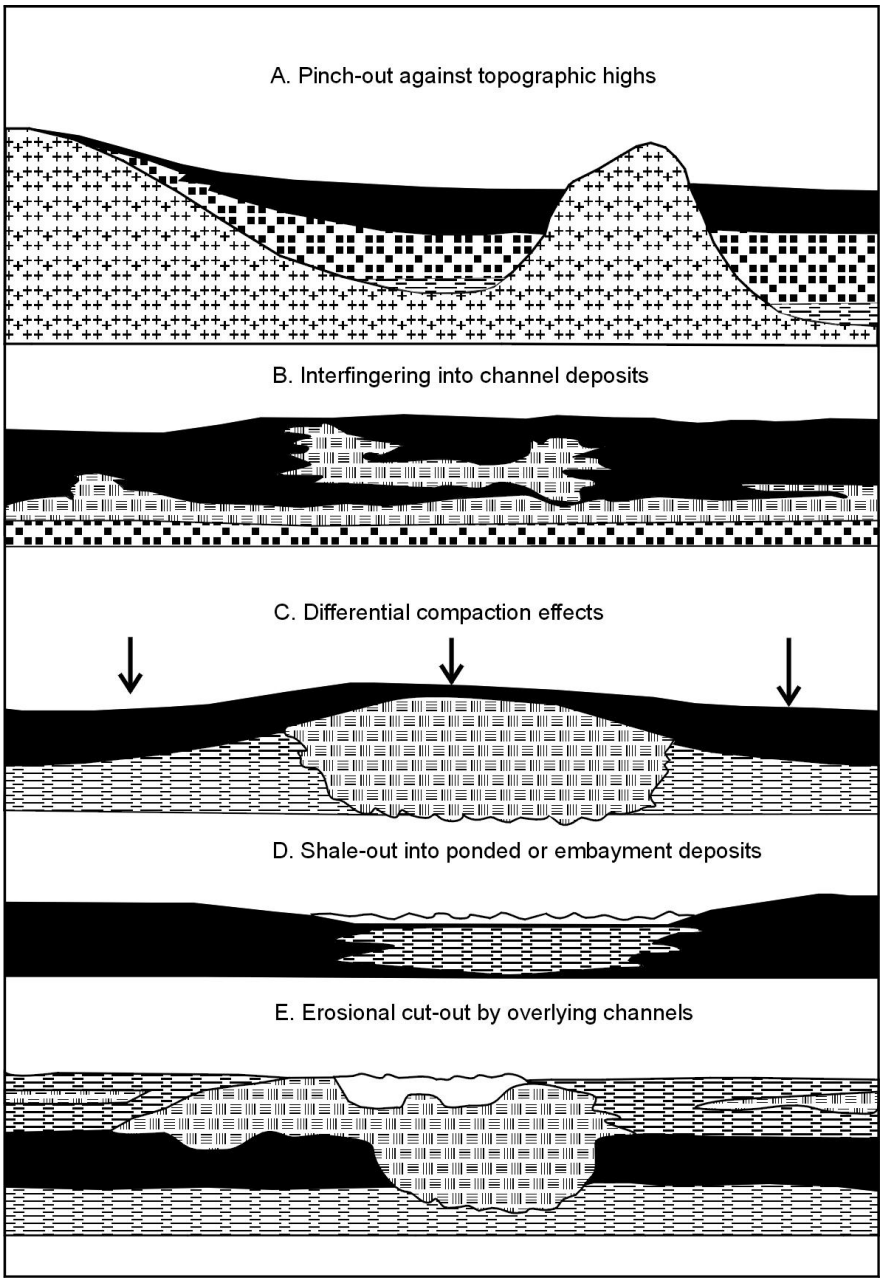

Figure 4.95: Schematic illustration of five principal factors affecting coal distribution and width (Le Blanc Smith, 1980).

The evidence in the relationship of the geometries of the palaeo floor and roof elevations concludes that irrespective of variable intra-seam strata and coal seam widths the pre-Karoo topography is reflected throughout the entire stratigraphic sequence. The nearly direct linear relationships could be evidence of lithification contemporaneous with basin development which resulted from reasonably uniform compaction rates. Significantly compacted sedimentary rocks over basement highs were recognised by Cairncross (1989). As a result of differential compaction both coal and clastic sedimentary rocks overlying valley-flanks would have slickensided and fractured to a degree depending on the gradient of the basement topography.

Prior to sediment burial, plant growth probably took place on similar structural relief with gentle attitudes. To conclude, a four-stage model (Figure 4.96) is proposed how burial could have influenced widths and aerial distribution of peat and intra-seam clastic sedimentary rocks. At the time of peat formation, the sediment sequences of succession had not yet undergone a great deal of lithification in that the floor structure of the peat might have been without undulations.

Therefore the present day coal and intra-seam strata are not displaying the syndepositional widths or aerial distribution, but rather reflect the result of subsidence which was probably contemporaneous with basin development. Hence the uneven, non-compactable pre-Karoo basement topography had a major influence in controlling the present day geometry of the coal and intra-seam strata.

The primary regional control on coal width is regarded as basin tectonics i.e. drowning of the peat swamps by basinal waters due to excessive subsidence postulated by Cadle et al. (1990). Furthermore, slow subsidence (Stratten, 1970) promoted the formation of inertinite rich Permian peat (70% compactability after Snyman 1998) as it has accumulated on the passive cratonic side of the Karoo foreland basin.

On the northern sector of the main Karoo basin the sediments probably reached a stage of maximum compaction and consolidation towards the end of the Karoo basin development which was halted by the intrusion event of the Karoo dolerites. Coal merely displays approximately 20% to 35% of its original width, depending on macaral composition. Clastic sedimentary rocks display only 60% to 90% of their original width, depending on grain size and clay content. These compactability variations of the different rock types and stratigraphic units are clearly illustrated in isopach maps presented in this study.

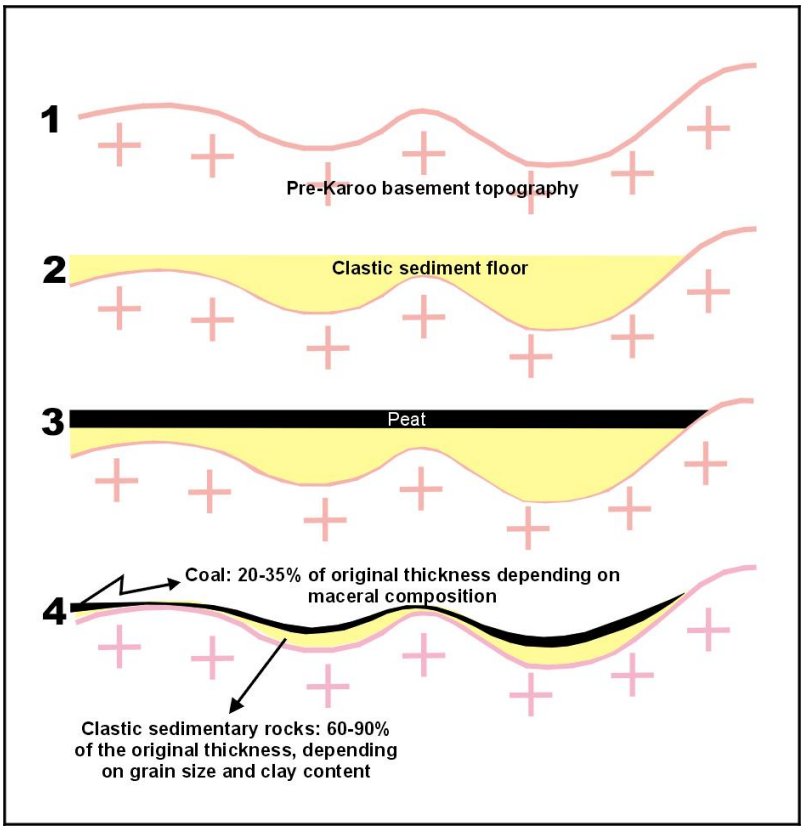

Figure 4.96: Four stages indicating how burial could have influenced width of peat and clastic sedimentary rocks.

In conclusion, a reasonable inverse relationship between the net width of the stratigraphic sequence from the palaeo floor of the No. 2 Coal Seam to the palaeo roof of the No.5 Coal Seam and the floor elevation of the main sill exists. Figure 4.97 shows the isopach map of the interpolated net width from the palaeo floor of the No.2 Coal Seam to the palaeo roof of the No.5 Coal Seam. A visual comparison with the dolerite floor elevation in Figure 4.98 discloses this inverse relationship.

Classical statistics of the two data sets are contained in Table 4.9. Normality in the two data sets, which are supported by 249 samples, is shown by the very small values in the coefficient of variation variable. The undulating nature of the main sill is revealed in the skewness of the histogram plot and the kinks in the probability curve as presented in Figure 4.99. The net width histogram plot (Figure 4.100) indicates a fair amount of negative skewness in the data. This negative skewness in the data is a result of the differentially compacted sedimentary rocks. The probability plot in Figure 4.100 reveals a consistently smooth curve which could be a result of the

geometrical relationship of the sedimentary rocks of sequence of succession with the pre-Karoo basement topography.

The QQ-plot in Figure 4.101 and the regression slope analysis plot in Figure 4.102 convincingly conclude the inverse relationship that exists between the the floor elevation of the main sill and the net with of the almost entire sedimentary rock sequence of succession. In this context the reasonable negative correlation coefficient of -0.57 is good.

This negative correlation implies that where the main sill is present in the lower stratigraphic levels it underlies thicker sedimentary sequences and conversely where the sill had stepped up to higher stratigraphic levels it underlies the thinner sedimentary sequences. In conclusion the differential compaction of the sedimentary strata was in the main controlled by the the Pre-Karoo basement topography. This in turn resulted in the fracturing and jointing of the sedimentary rocks over the flanks of the pre-Karoo basement topography which to a large extent controlled the propagation path of the main sill.

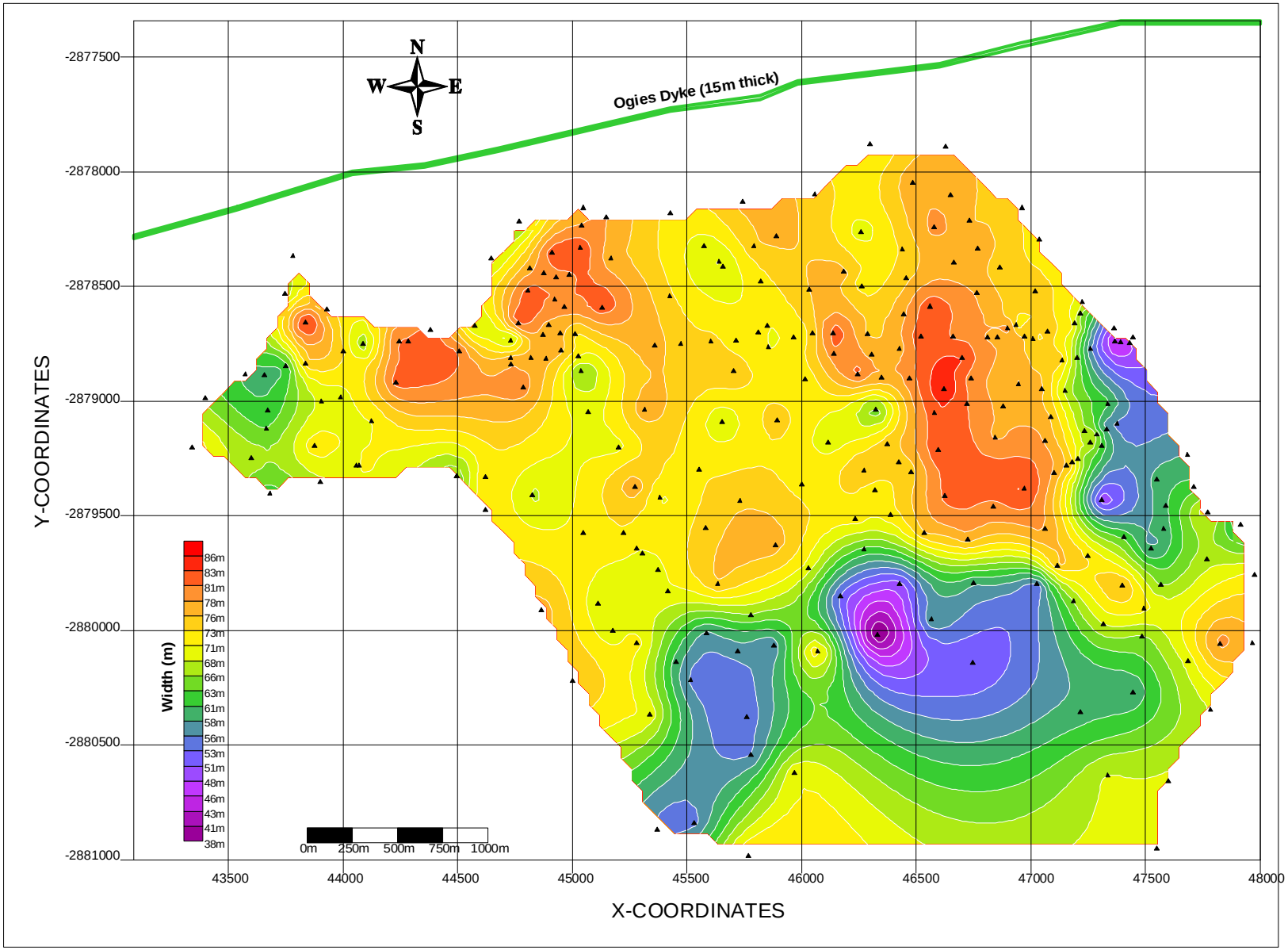

Figure 4.97: Net width between the No. 2 Coal Seam palaeo floor and the No. 5 Coal Seam palaeo roof.

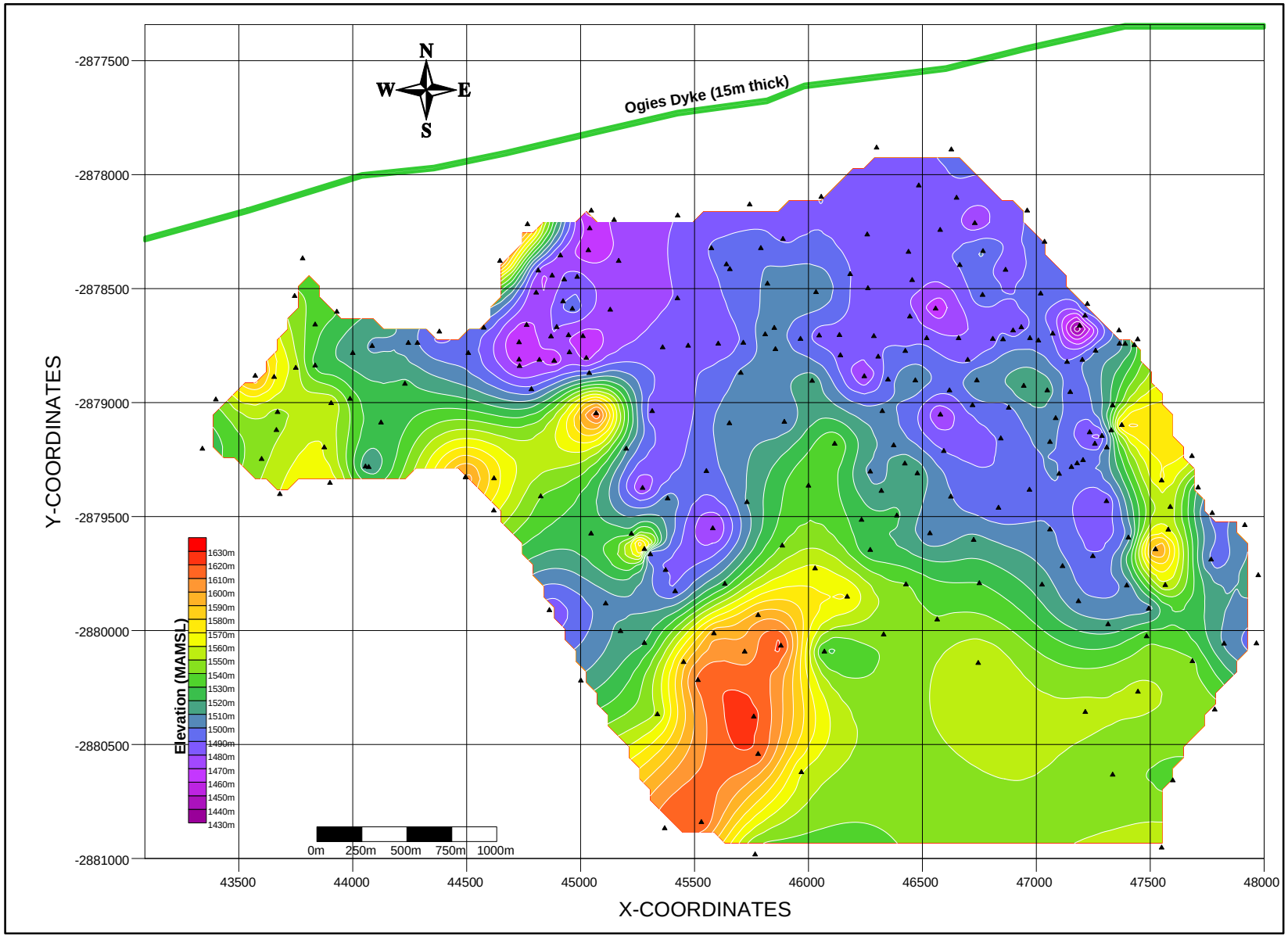

Figure 4.98: Main sill floor elevation.

Table 4.9: Classical Statistics of the main sill floor elevation and the net width between the No. 2 Coal Seam palaeo floor and the No. 5 Coal Seam palaeo roof.

VARIABLE	MAIN SILL FLOOR ELEVATION	NET WIDTH FROM NO. 2 SEAM FLOOR TO NO. 5 SEAM ROOF
NUMBER OF SAMPLES	249	249
MINIMUM VALUE	1418.40	36.69
MAXIMUM VALUE	1626.30	85.67
MEAN	1512.96	70.67
VARIANCE	1479.96	74.64
STANDARD DEVIATION	38.47	8.64
COEFFICIENT OF VARIATION	0.03	0.12
SKEWNESS	1.14	-0.99
KURTOSIS	4.00	3.90
TRIMEAN	1506.10	71.86
BIWEIGHT	1504.03	72.02
MAD	18.89	5.10
ALPHA	-1404.22	-36.32
SICHEL-T	Not Calculated	Not Calculated

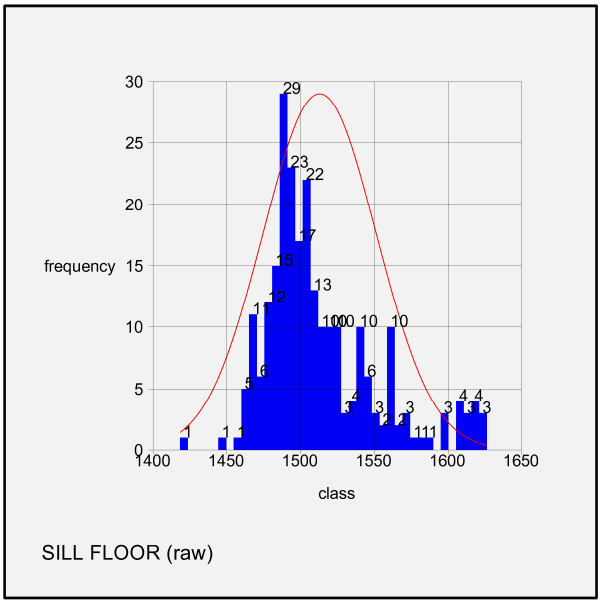

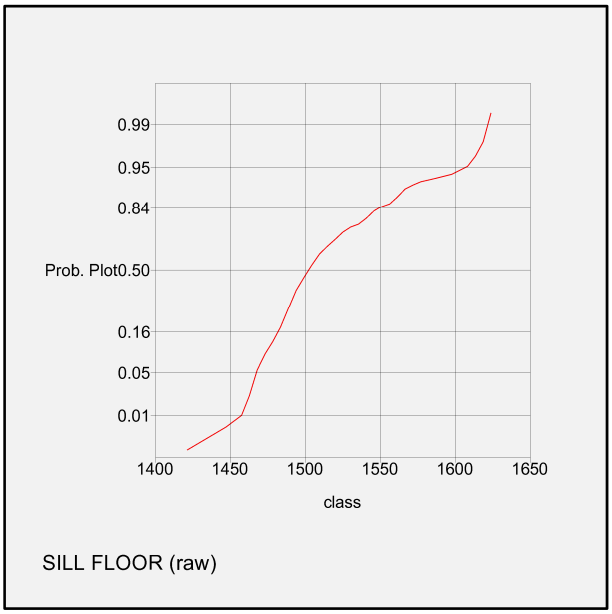

Figure 4.99: Histogram and probility plots of the main sill floor elevation.

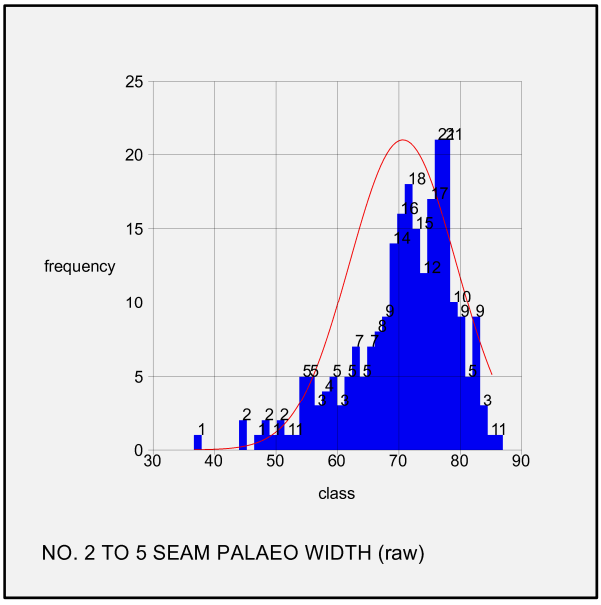

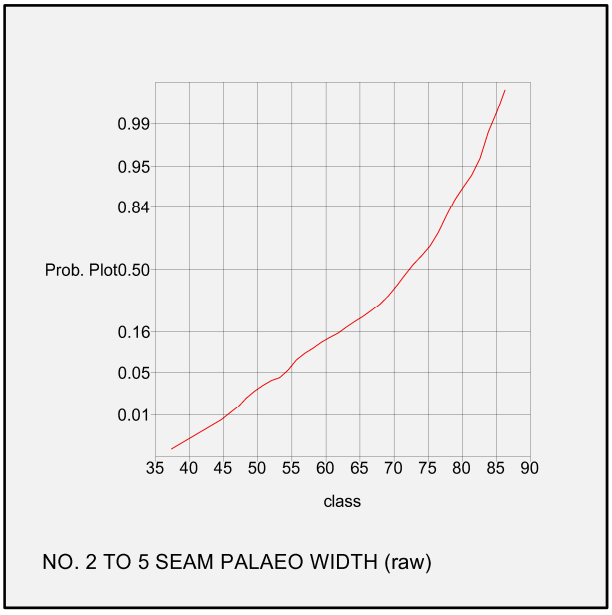

Figure 4.100: Histogram and probility plots of the net width between the No. 2 Coal Seam palaeo floor and the No. 5 Coal Seam palaeo roof.

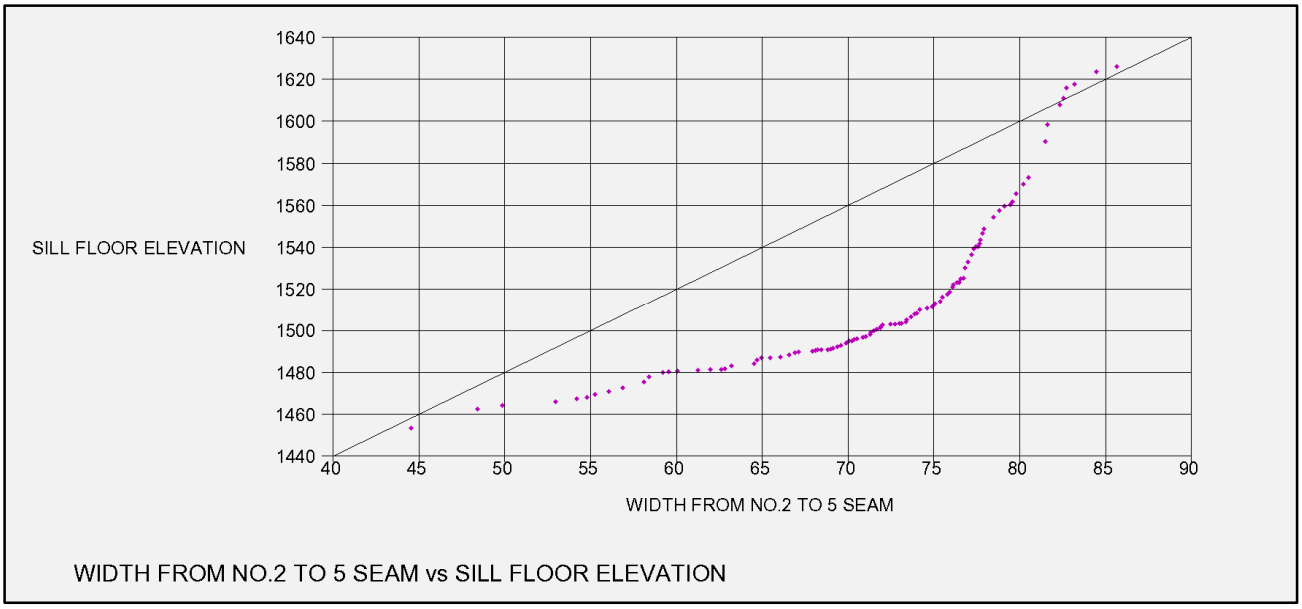

Figure 4.101: Quantile-Quantile plot of the net width between the palaeo floor of the No.2 Coal Seam and the palaeo roof of the No. 5 Coal Seam and the floor elevation of the main sill.

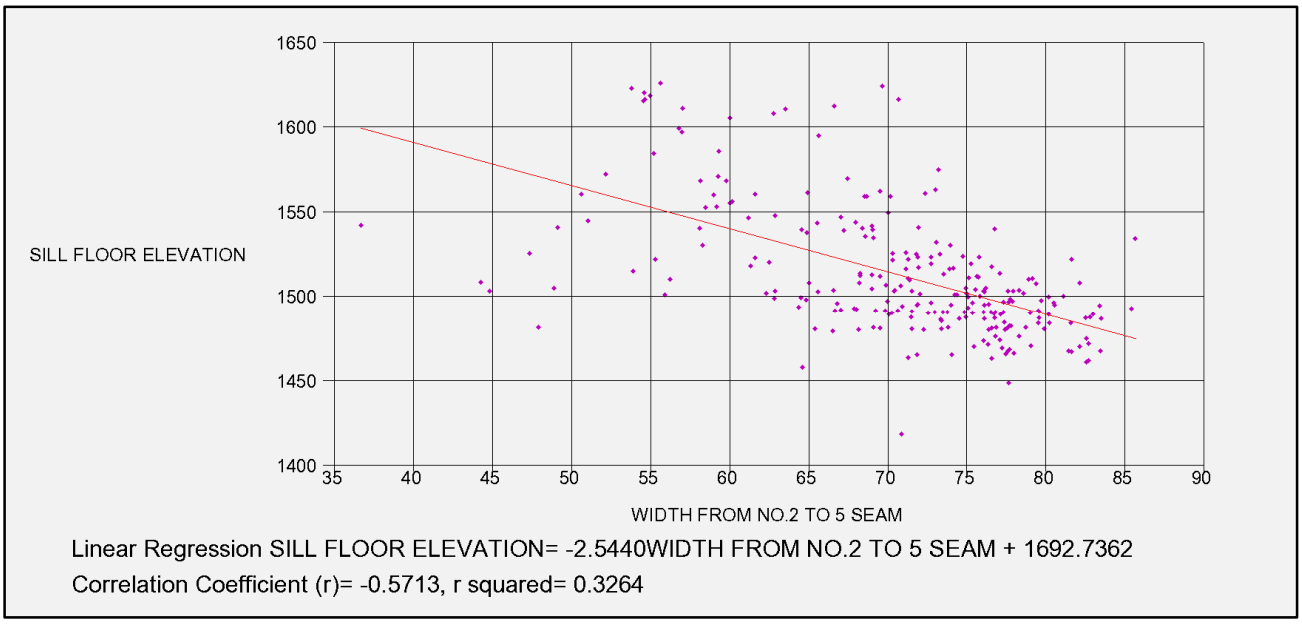

Figure 4.102: Correlation coefficient of the net width between the palaeo floor of the No.2 Coal Seam and the palaeo roof of the No. 5 Coal Seam and the floor elevation of the main sill.

CHAPTER 5

5. SUMMARY AND CONCLUSIONS

In conclusion, the controlling factors for the intrusion of dolerites in the south-eastern Witbank Coalfield are either principally regional scale structures or localised structures. The Witbank Coalfield on the northern main Karoo basin has been minimally affected by any large scale structural events due to its geographical location on the passive side of the Karoo foreland basin and the depositional style of the Ecca Group of rocks.

On a mine scale the structural disturbances mainly occurring in the study area are the transgressive ±20m thick main sill and the ±15m thick EW striking Ogies Dyke. The Ogies Dyke is interpreted to pre-date dolerite dykes and sills in its immediate vicinity, and its orientation probably controlled by EW striking pre-Karoo diabase intrusions.

The source of the magma for the sill formation could have been as far away as the NNE trending Olifants River Dyke Swarm, causing the magma to have been transported laterally within the sedimentary rocks of sequence of the succession over long distances. The timespan in which the regional scale structures could have developed to control the main sill's intrusion is limited due to the unconformable deposition of the glaciogene strata of the Dwyka Formation (285 Ma, after SACS, 1980) until shortly before the commencement of fragmentation of Gondwana (middle Jurassic times: after Storey and Kyle, 1997) which was synchronous with the emplacement of Karoo dolerites (Encarnación et al., 1996).

Considering both regional and local scale structures this study interprets the following factors to have controlled the propagation paths of the main sill and its associated offshoots:

BASIN TECTONICS

- Slow subsidence rates associated with the northern main Karoo basin development reached its maximum towards the commencement of Gondwana fragmentation. The fragmentation was accompanied by the outpouring of lava which was fed by abundant dykes that brought the sedimentation process to a stand-still. Topography of the non-compactable pre-Karoo basement provided the major control over the compaction of the sedimentary rocks as they are presented today. Differential compaction joints and fractures developed as a result of the unevenness of the pre-Karoo basement topography.

Van Niekerk (1995) used thin sections to investigate micro-scale deformation structures in the host rock up to 150m away from the intrusions. His investigation led to the detection of normal micro-faults associated with discernible slip, produced by lithostatic pressure due to compaction. Establishment of slip direction was found problematic, as displacement mainly took place along quartz grain boundaries. The influence of basin tectonics on dolerite intrusion in the southerly bounded Secunda Coalfield is well supported by Van Niekerk (1995).

- Even though the pre-Karoo basement topography is very well reflected by the overall structure of the coal seam floor and roof elevations and to some extent the inter-seam strata, their widths show a much more attenuated and slightly distorted form. That is due to difference in compactiblity of the intervening lithological units e.g. vitrinite precursors (about 90%), inertodetrinite precursors (about 70%), mud (about 50%), and sand (about 10%) (Snyman, 1998). Therefore within sedimentological units, less compactable channel fill sandstones situated adjacent to more compactable i.e. siltstone and shale facies from marine transgressions would have been differentially compacted and as a result developed fractures and joints in the associated transition zones. This concept is also applicable to the macaralogy of coal, as different macarals have variable degrees of compactability. The pre-existing jointing and fracturing of the sedimentary rocks occurring in these transition zones most probably were largely exploited by the intruding sill.

THE OGIES DYKE

- The Ogies Dyke fractured the sedimentary host rock both parallel and perpendicular to its orientation. Some of the fractures which parallel the Ogies Dyke might be a result of sheeting (pressure-release jointing) that developed parallel to its cooling surface. NS trending structures are probably cooling joints that developed perpendicular to the Ogies Dyke.

The Ogies Dyke intrusion seems to have played an important role in determining the emplacement mechanism of the offshoots from the main sill. EW striking dolerite offshoots from the main sill, intersected the No. 2 Coal Seam predominantly implies that pressure-release joints paralleling the Ogies Dyke, excersized some control. Both sub-ordinate ENE and NS strike directions for the main sill coincide with the dominant strike directions of fractures mapped in the No. 2 Coal Seam.

SYN-TECTONICS

- The synchronous emplacement of Karoo dolerites and early breakup of Gondwana (Encarnación et al., 1996) provided syn-tectonic structures in the form of i.e. regional scale lineaments which could have had potential control over the directions of dolerite emplacement. The main sill predominantly intruded with a NNE strike which appears to be coincidental with some regional scale trends. The prominent NNE striking lineaments are interpreted as extensional structures related to the NNE striking arm of an inferred triple junction off the East Coast. These NNE trending structures intersect the present exposure of the Karoo volcanics in the central Karoo and Nuanetsi in the north, following the NNE Olifants River Dyke Swarm and ultimately coincide with the NNE axis of the main Karoo basin. The role of the Olifants River Dyke Swarm as an important feeder system to Karoo sills and volcanics in the central Karoo basin (Uken and Watkeys, 1997) could be deduced from these relationships.

- The intersection relationship between dolerite offshoots detected in the No. 2 Coal Seam revealed preferred strike intersections which in descending frequency are: EW, NW, WNW, NE, NNW. The influence of the Ogies Dyke and its related joints sets had a marked influence on the strike intersections of dolerite offshoots with the No. 2 Coal Seam. However, several other sub-ordinate, but definite strike frequencies tie in with some regional trends. The NE trend could probably be related to the Sabi-monocline, the third arm of a plume generated Karoo-age triple junction. The NNW trend, which is regarded as a Karoo-age trend is also coincidental with NNW striking lineaments from a Landsat MSS image. It is inconceivable for the NW intersecting offshoots to tie-in with the NW Pongola fabric. The WNW trend of the Okanvango Dyke Swarm, corresponds with WNW intersecting offshoots with the No. 2 Coal Seam.

Evidence established in this study regards basin tectonics to be the overriding controlling factor for the stratigraphic position of the main sill in the Vryheid Formation sedimentary rocks of sequence of succession of the south-eastern Witbank Coalfield. Other factors i.e. the influence of the Ogies Dyke and syn-tectonic related regional scale structures seem to have had some control in the propagation paths of the associated offshoots of the main sill.

6. ACKNOWLEDGEMENTS

- COALTECH 2020 Steering Committee: Mr. Johan Dempers (Chairman of COALTECH 2020 and Chief Geologist of Eskom)

- Financial Sponsors: CSIR Miningtek, Coal Mining Industry, THRIP.

- Dr. Rudy Boer (Consultant), Prof. Willem van der Westhuizen (UFS), Dr. Hermann Praekelt (UFS), Dr. Schalk van der Merwe (Geological Consultant), Mr. Johan Loock (UFS).

- Mr. Mark Grodner (CSIR), Mrs. Lesley Jeffrey (CSIR), Dr. Jochen Schweitzer (CSIR), Mr. Johann Beukes (COALTECH 2020 Program Manager)

- Mr. Johan Veldsman, Mr. Gerrit Esterhuisen (SASOL)

- Mr. Coenie van Niekerk, Mr. Stoffel van der Merwe, Mr. Gerrit Cronje (BHP Billiton/Ingwe)

- Mr. Chris Goodale, Mr. Mufaro Chivasa, Mr. Frans Botes, Mr. Cliff Delaporte, Mr. Bert Schalekamp (Anglo Coal)

- Prof. Carel Snyman (University of Pretoria.)

- Mr. Henrique Pinheiro, Mrs. Vivian du Cann (SABS)

- Mr. Flip en Mrs. Charlè Opperman (Farm Welverdiend, Middelburg)

- Mr. Gideon and Mrs. Margot Albertyn (Saxonwold, Johannesburg)

7. REFERENCES

Blignaut, J.J.G. 1952. Field relationships of the dolerite intrusions in the Natal Coalfields. *Transactions of the Geological Society of South Africa, 55:19-31.*

Cadle, A.B. 1982. Controls on coal distribution. In: Cadle A.B. (Editor), *Coal Exploration, Economics and Assesment.* Short Course, University of the Witwatersrand, Johannesburg, 20-34.

Cadle, A.B. 1986. Coal depositional systems of the Transvaal Coalfields: Their influence on coal distribution and quality. Geocongress '86, Geol.Soc.S.Afr., Johannesburg, p 667-670.

Cadle, A.B., Cairncross B., Christie, A.D.M. & Roberts, D.L. 1990. The Permo-Triassic coal-bearing deposits of the Karoo Basin. *Economic Geology Research Unit, Information Circular no. 218:* University of the Witwatersrand, Johannesburg, ISBN 1 86814 159 4.

Cadle, A.B. & Cairncross, B. 1992. Lateral-accretion deposition in braided fluvial systems: a case study from the Karoo Sequence, South Africa. Economic Geology Research Unit, Information Circular no. 254: University of the Witwatersrand, Johannesburg, ISBN 1 86838 029 7.

Cairncross, B. 1980. Anastomosing river deposits: palaeoenvironmental control on coal quality and distribution, northern Karoo Basin. *Trans.geol.Soc.Afr.,* 83:327-332.

Cairncross, B. 1986. Depositional environments of the Permain Vryheid Formation in the East Witbank Coalfield, South Africa: A framework for coal seam stratigraphy, occurrence and distribution. Ph.D. Thesis. Johannesburg, University of the Witwatersrand, South Africa, 232p.

Cairncross, B. 1987. A genetic stratigraphy for the Permian coal-bearing Vryheid Formation in the east Witbank Coalfield, South Africa. *S.Afr.J.Geol.,* 90(3):219-230.

Cairncross, B. 1989. Paleodepostional environments and tectono-sedimentary controls of the post-glacial Permian coals, Karoo Basin, South Africa. International Journal of Coal Geology, 12:365-380.

Cairncross, B. and Cadle, A.B. 1988. Palaeoenvironmental control on coal formation, distribution and quality in the Permian Vryheid Formation, East Witbank Coalfield, South Africa. *International Journal of Coal Geology*, 9:343-370.

Cairncross, B., Hart, R.J. & Willis, J.P. 1990. Geochemistry and sedimentology of the coal seams from the Permian Witbank Coalfield, South Africa; a means of identification. *International Journal of Coal Geology*, 16: 309-325.

Chevallier, L. & Woodford, A. 1999. Morpho-tectonics and mechanism of emplacement of the dolerite rings and sills of the western Karoo. South *Africa. S.Afr.J.Geol.,*102(1):43-54.

Coffin, M.A. & Eldholm, O. 1994. Large igneous provinces: crustal structure, dimensions, and external consequences. *Rev. Geophys*., 32:1-36.

Cox, K.G. 1970. Tectonics and vulcanism of the Karoo period and their bearing on the postulated fragmentation of Gondwanaland. *In:* Clifford, T.N. & Gass, I.G. (Eds.), *African Magmatism and Tectonics*. Oliver & Boyed, Edinburgh, 211-235.

Cox, K.G. 1972. The Karoo volcanic cycle. *J.geol.Soc.Lond.*, 128: 311-336.

Delaney, P.T., Pollard, D.D., Siony, J.I. & McKee, E.H. 1986. Field relations between dykes and joints: emplacement processes and palaeostress analysis. *J.Geophys.Res.*, 91: 4920-4938.

Du Plessis, G.P. 2001. The relationship between geological structures and dolerite intrusions in the south-eastern part of the Witbank Coalbasin, South Africa. Proceedings of Coal Indaba, the 7th Coal Science and Technology Conference, Saxonwold, 28 – 30 August. Johannesburg: FFF, 10p.

Du Plessis, J.J. 2001. An investigation of the metamorphic influence of dolerite intrusions on coal in the south-eastern part of the Witbank Coalfield, South Africa. Proceedings of Coal Indaba, the 7th Coal Science and Technology Conference, Saxonwold, 28 – 30 August. Johannesburg: FFF, 9p.

Du Plessis, J.J. 2001. Personal communication on results of the geochemical and mineralogical analyses of dolerite samples from the Witbank Coalbasin. Department of Geology, University of the Free State, Bloemfontein, 9300.

Duncan, R.A., Hooper, P.R., Rehacek, J. Marsh, J.S., Duncan, A.R. 1997. The timing and duration of the Karoo igneous event, southern Gondwana. *Journal of Geophysical Research*, 12: 127-138.

Encarnación, J., Fleming, T.H., Elliot, D.H. & Eales, H.V. 1996. Synchronous emplacement of Ferrar and Karoo dolerites and the early breakup of Gondwana. *Geol*, 24: 535 - 538.

Falcon, R.M.S., 1981. The pertrographic characterisation of coals from the No. 2 seam, Witbank Coalfield. In: Bereau for Mineral Studies: Characterisation of South African. Rep. 6, 193pp.

Falcon, R.M.S., 1988. Characteristics of Southern African coals. *J.S.Afr.Inst.Min.Metall* (88)5: 145-161.

Falcon, R.M.S. 1989. Macro- and micro-factors affecting coal-seam quality and distribution in southern Africa with particular reference to the No. 2 seam, Witbank coalfield, South Africa. *International Journal of Coal Geology*, 12: 681-731.

Falcon, R.M.S. 1986. A brief review of the origin, formation, and distribution of coal in southern Africa. *In* Anhausser, C.R. and Maske, S. (Eds.) Mineral Deposits of Southern Africa – Volume II: 1879-1898.

Gold, D.P., Doden, A.G., Sicree, A.A. 2001. An enigma: thin dykes with mantle inclusions. Program and abstracts of the Fourth International Dyke Conference. Ithala Game Reserve, 26-29 June. Kwasulu-Natal, South Africa, p. 12.

Grodner, M.W. 2002. A regional, 3-D computer-based sedimentological model of the Permian Witbank Coalfield, South Africa. M.Sc. Thesis. Johannesburg: Rand Afrikaans University, 90p.

Henckel, H. 2001. Personal communication on the regional scale information of the Witbank Coalfield. CSIR Division of Mining Technology, Carlow Road, Auckland Park, Johannesburg, 2000.

Holland, M.J., Cadle, A.B., Pinheiro, R., Falcon, R.M.S. 1989. Depositional environments and coal petrography of the Permian Karoo Sequence: Witbank Coalfield, South Africa. *International Journal of Coal Geology*, 11: 143-169.

Jeffrey, L.S. 2001. Literature review: Intra-seam sedimentological controls on coal quality – No. 2 Seam, Witbank Coalfield. Subtask 1, 2001-0323, CSIR Mining Technology, 30p.

Le Blanc Smith, G. 1980. Genetic stratigraphy and palaeoenvironmental controls on coal distribution in the Witbank Basin Coalfield. Ph.D. Thesis. Johannesburg: University of the Witwatersrand, 242p.

Park, R.G. 1997. Foundations of Structural Geology. London: Chapman and Hall, 202p.

Rubin, A.M. 1995. Propagation of magma-filled cracks. *Annu. Rev. Earth Planet Sci*. 23: 287-336.

SACS (South African Committee for Stratigraphy), 1980. Stratigraphy of South Africa, Part I. Compiled by L.E. Kent. Lithostratigraphy of the Republic of South Africa, S.W.A./Namibia, and the Republics of Boputhatswana, Transkei and Venda. Handbook Geol. Surv. S. Afr. 8, 690p.

Saunderson, R.D. & du Plessis, S.J. 2000. The successful prediction of non-magnetic dykes using a dighem survey. Proceedings of Coal Indaba, the 6th Coal Science and Technology Conference, Fourways, 15 – 16 November. Johannesburg: FFF, 12p.

Selley, R.C. 1976. Subsurface environmental analysis of the North sea sediments. *Bull. Amer. Assoc. pertol. Geol.,* 60: 184-195.

Smith, J.S. 1990. Optimum Hendrina Life Extension Project. *Report on Geological Structure*. Optimum Colliery, 16p.

Smith, R.M.H., Errikson, P.G. & Botha, W.J. 1993. A review of the stratigraphy and sedimentary environments of the Karoo-aged basins of southern Africa. *J.Afr.Earth.Sci.*, 16: 143-169.

Snyman, C.P. 1998. Coal. *In* Wilson, M.G.C. and Anhausser, C.R. (Eds.) The Mineral Resources of South Africa – Sixth Edition, Handbook 16: 136-205.

Snyman, C.P. and Barclay, J. 1989. The coalification of South African coal. *Int. Journ. Coal Geol. 13: 375-390.*

Storey, B.C. & Kyle, P.R. 1997. An active mantle mechanism for Gondwana breakup. *S.Afr.J.Geol*., (100) 4: 283 – 290.

Stratten, T. 1970. Tectonic framework of sedimentation during the Dwyka Period in southern Africa. Second Gondwana Symposium, South Africa, 1970, p: 483-490. *International Union of Geological Sciences*, Pretoria, 1972.

Tokarski, A.K. 1990. Dyke swarms as stress indicators: two constraints. *(In: Parker, A.J., Rickwood, P.C., Tucker, D.H. (Eds.), Mafic dykes and emplacement mechanisms. Balkema, Rotterdam*, p. 101-106).

Tweedie, E.B. 1986. The Evander Goldfield. *In* Anhausser, C.R. and Maske, S. (Eds.) Mineral Deposits of Southern Africa – Volume I & II: 705 – 730.

Uken, R. and Watkeys, M.K. 1997. An interpretation of mafic dykes swarms and their relationship with major magmatic events on the Kaapvaal Craton and Limpopo Belt. *S.Afr.J.Geol.,* 4:341-348.

Van Niekerk, J. 1995. Geochemistry of dolerites and the intrusion mechanisms of two major sills in the Secunda Coalfield. M.Sc. dissertation. University of Stellenbosch, 111p.

Veldsman, J.H and Esterhuisen, G. 2000. Personal communication on dolerite interpretation and investigation method. Sasol Coal Rosebank, 1 Sturdee Avenue, Johannesburg, 2000.

White, R.S. 1997. Mantle plume origin for the Karoo and Ventersdorp flood basalts, South Africa. *S.Afr.J.Geol*., 100 (4): 271 – 282.

White, R.S. & Mkenzie, D. 1995. Mantle plumes and flood basalts. *J. Geophys. Res., 100:* 17543 – 17585.

Winter, M.F. 1985. Lower Permian Palaeoenvironments of the northern Highveld Coalfield and their relationship to the characteristics of coal seams. Ph.D. thesis. Johannesburg, University of the Wittwatersrand, 245p.